Novel Phosphonate containing Ligands for optimised targeted Radiotherapy of Neoplastic Bone Disease: using Animal Models and Scintigraphy

Irene C. Dormehl

B.Sc. (Physics, Mathematics), M.Sc. (Physics), D.Sc. (Nuclear Physics)

Thesis submitted in fulfilment of the requirements for the degree:

Philosophiae Doctor

in

Pharmacology

At the:

North-West University
Potchefstroom Campus

Promotor: Prof. Douglas W. Oliver
North-West University
Potchefstroom Campus

Co-promoter: Dr. Werner K.A. Louw
University of Pretoria

Novel Phosphonate containing Ligands for optimised targeted Radiotherapy of Neoplastic Bone Disease: using Animal Models and Scintigraphy

Irene C. Dormehl

Summary

This thesis covers research on radiotherapy of bone cancer using bone seeking radiopharmaceuticals i.v. applied. Such research generally has been confined to the treatment of bone pain in people with metastatic bone cancer but on occasion also for treating cases of osteosarcoma. It is typically used when there are multiple metastatic lesions in the skeleton, which makes local and focal treatment impractical and systemic treatment the alternative. The treatment is tumour specific since the radiopharmaceutical targets the area of increased mineral turnover. This allows selective uptake and prolonged radiopharmaceutical retention in these areas.

An ideal radiopharmaceutical for the treatment of neoplastic bone disease would be a radiolabelled compound, which would predominantly accumulate in the bone lesion with limited access to normal bone and other organs.

Criteria governing the selection of the radionuclide are particle range, physical half-life, gamma yield (for scintigraphic monitoring), chemistry and type of ligand. The most commonly used radionuclides at present are phosphorus-32, strontium-89, tin-117m, samarium-153, and rhenium-186/188.

Currently the available bone seeking agents which are phosphonate containing ligands tend to localize throughout the skeleton. This thesis focuses on methylenediphosphonic acid (MDP), 1- hydroxy-ethylenediphosphonic acid (HEDP), and the novel agent polyethyleneimine functionalised with methylene phosphonate groups (PEI-MP) from this laboratory, as well as the octa-anion ethylenediaminetetramethylphosphonate (EDTMP). MDP and HEDP are bisphosphonates, EDTMP a multidentate aminophosphonate. In targeted therapy EDTMP is used in combination with ^{153}Sm and might be binding to hydroxyapatite crystals in a different manner than HEDP.

^{186}Re-HEDP is used for palliation of bone pain to metastatic bone cancer. Complications known with ^{153}Sm-EDTMP and ^{186}Re-HEDP treatment are myelotoxicity and in some cases a transient increase in bone pain following treatment (flare response).

In contrast to this ^{188}Re-HEDP appears to fulfil the criteria of a good radiotherapeutic agent as it has a stronger β-emission than ^{153}Sm and ^{186}Re and a shorter physical and biological half-life which reduces myelotoxicity.

The aim of this research is to optimise and investigate novel bisphosphonate containing ligands for targeted radiotherapy of neoplastic bone disease using rodent and primate animal models and scintigraphy.

The successful outcome of these studies requires that the normal primate (*Papio ursinus*) with its in vivo bisphosphonate behaviour for purposes of scintigraphic monitoring, (using ^{99m}Tc-MDP), be validated as a useful model to interpret experimental results and extrapolate to man as was done successfully in the fracture healing experiments discussed here.

The pharmacokinetics of ^{153}Sm-EDTMP, the well known therapeutic radiopharmaceutical used for palliation in painful human skeletal metastases, was determined in normal primates by scintigraphic monitoring and compared with available human data in order once more to establish sufficient similarity of in vivo behaviour and thus direct the meaningful continuation of these biodynamic investigations.

A novel approach for ligand optimisation involving neoplastic tissue's abnormal blood supply (increased permeability) and lack of lymphatics (EPR effect) was investigated, whereby radiolabelled macromolecules accumulated selectively at the target site. The synthesis of the macromolecule polyethyleneiminomethyl phosphonic acid (PEI-MP), and its labelling with ^{99m}Tc, as well as quality control have been described in detail. Macromolecular sizes ranged from 3 to 300 kDa and the label ^{99m}Tc was selected to serve as tracer for the scintigraphic biodistribution studies performed in normal adult male primates. The results allowed the identification of a suitable size-fraction, i.e. 10-30 kDa of PEI-MP, as a bone-seeking ligand. Molecular sizing of the polymeric PEI-MP can drastically alter its pharmacokinetic properties.

To exploit these encouraging results, of organ sparing and speedy urine excretion a study of bone tumour accumulation of ^{99m}Tc-PEI-MP was done in five dogs with spontaneous occuring appendicular osteosarcomas. Mean tumour: background uptake of 4:1 was obtained with the molecular size fraction 10-30 kDa. To fulfil a therapeutic role the most suitable

ligand would have to form a stable and appropriate complex with one or more of the therapeutic radionuclides e.g. ^{153}Sm, ^{186}Re and ^{117m}Sn(II).

For informed selection of such a radionuclide which would be successfully complexed with the ligand PEI-MP for targeted delivery to osteosarcoma/metastatic bone tumours, metal ion speciation in blood plasma was used to predict the in vivo behaviour of the potential bone-seeking therapeutic radiopharmaceuticals. The blood plasma model ECCLES used here, included PEI-MP as ligand, and predicted good in vivo behaviour of ^{117m}Sn(II)-PEI-MP, but not so when complexed with ^{153}Sm and ^{166}Ho. Labelling of PEI-MP with ^{117m}Sn(II) and also with ^{186}Re was subsequently successfully achieved.

It is known that changing the radionuclide label of a particular ligand might change the resultant biodistribution. Therefore the biodistribution of variously molecular sized ^{117m}Sn(II)-polyethyleneiminomethyl phosphonate complexes were investigated in the normal primate model to establish their potential as selective therapeutic bone agents. The in vivo stability of ^{117m}Sn-PEI-MP, and reduced accumulation in the kidneys and normal bone observed from these biodistribution studies prompted the investigation of its potential to exploit the EPR effect due to its macromolecular nature, where bone malignancies are present. The tumour uptake of ^{117m}Sn-PEI-MP in different types of canine osteosarcoma induced into nude mice, was therefore studied.

The osteosarcoma model followed from subcutaneous injection of canine osteosarcoma cells with high lung metastatic capacity (HMPOS) in some mice, and without this capacity (POS) in another group. The former yielded faster growing non ossified tumours compared to slower growing tumours from POS cells, with ossified tissue, both observed histologically. The high accumulation of ^{117m}Sn-PEI-MP in the bladder wall is of great concern and a focus of continuing research.

There is however no doubt that the ligand PEI-MP exhibits promising characteristics for targeted delivery of therapeutic radionuclides to neoplastic bone lesions and essentially spares vital organs and normal bone.

The normal primate furthermore turned out to be a useful model from which to interpret scintigraphic results related to in vivo bisphosphonate behaviour, also for scintigraphic

monitoring of the pharmacokinetics and biodistribution of bone therapeutic radiopharmaceuticals.

Opsomming - Nuwe Fosfonaatbevattende Ligande vir die optimaal teikengerigte Radioterapie van Neoplastiese Beenletsels deur gebruik van Dier Modelle en Sintigrafie

Hierdie proefskrif handel oor navorsing in radioterapeutiese behandeling van beenkanker deur gebruik te maak van beensoekende radiofarmaseutika wat binneaars toegedien word. Oor die algemeen was sodanige navorsing dusver beperk tot die behandeling van beenpyn in persone met metastatiese beenkanker, maar by geleentheid ook vir die behandeling van gevalle van osteosarkoom. Dit word tipies gebruik waar daar veelvuldige metastatiese letsels in die skelet aanwesig is, wat plaaslike en fokale behandeling onprakties maak en sistemiese behandeling die alternatief is. Die behandeling is tumorspesifiek aangesien die radiofarmaseutika die area van vermeerderde mineraalomsetting as teiken het. Dit maak voorsiening vir selektiewe opname en verlengde radiofarmaseutiese retensie in daardie areas.

'n Ideale radiofarmaseutikum vir die behandeling van neoplastiese beenletsels sou 'n radioaktief gemerkte verbinding wees wat hoofsaaklik in die beenletsels akkumuleer met beperkte opname deur normale been en ander organe.

Kriteria wat die keuse van die radionuklied bepaal, sluit in die reikwydte van die partikels, fisiese halfleeftyd, gamma-lewering (vir sintigrafiese monitering), chemie en die tipe ligand. Die radionukliede wat tans die meeste gebruik word, is fosfor-32, strontium-89, tin-117m, samarium-153 en renium-186/188.

Die beensoekende middels tans beskikbaar, naamlik ligande wat fosfonate bevat, neig om deur die totale skelet te versprei. Hierdie proefskrif konsentreer op metileendifosfoonsuur (MDP), 1-hidroksie-etileendifosfoonsuur (HEDP) en 'n nuwe middel poli-etileenimien gefunksionaliseer met metileenfosfonaatgroepe (PEI-MP) (uit hierdie studie), asook die okta-anioon etileendiamientetrametielfosfonaat (EDTMP). MDP en HEDP is bisfosfonate, EDTMP is 'n multidentaataminofosfonaat. By teikengerigte terapie word EDTMP saam

met ^{153}Sm gebruik en sou moontlik bind aan hidroksiapatiet kristalle op 'n ander wyse as HEDP.

^{186}Re-HEDP word gebruik om beenpyn by metastatiese beenkanker te verlig. Bekende komplikasies, wat voorkom by ^{153}Sm-EDTMP en ^{186}Re-HEDP-behandeling, is miëlotoksisiteit en in sommige gevalle, 'n beenpyn van verbygaande aard wat ná behandeling aanwesig is (flare response). ^{188}Re-HEDP voldoen in 'n groter mate aan die kriteria van 'n goeie radioterapeutiese agent, in die lig van die sterker beta-uitstraling teenoor die van ^{153}Sm en ^{186}Re, asook 'n korter fisiese en biologiese halfleeftyd het, met gevolglike verminderde miëlotoksisiteit.

Die doel met hierdie navorsing is om nuwe ligande wat bisfosfonaat bevat te optimaliseer en hul aanwending te bestudeer by teikengerigte radioterapie van neoplastiese beenletsels deur gebruik te maak van sintigrafie en knaagdier- asook primaatmodelle.

Die suksesvolle uitkoms van hierdie studie sou vereis dat die in vivo bisfosfonaatgedrag in die normale gesonde primaat/Kaapse bobbejaan (*Papio ursinus*) vir doeleindes van sintigrafiese monitering, (deur gebruik te maak van ^{99m}Tc-MDP), bevestig moet word, om sodanig as 'n geskikte model te dien vir interpretering van eksperimentele resultate en vir ekstrapolering na die mens. In hierdie doel is suksesvol geslaag soos aangetoon deur fraktuurgenesingseksperimente.

As gevolg van abnormale bloedtoevoer (verhoogde permeabiliteit) na en gebrek aan limfvate in neoplastiese weefsel, sou radioaktief gemerkte makromolekules (bisfosfonate) selektief akkumuleer in die letsels.

Hierdie vorm dus die basis vir 'n nuwe benadering van ligand optimalisering. Die sintese van die makromolekuul poliëtileeniminometiel fosfoonsuur (PEI-MP) en die merking daarvan met ^{99m}Tc, sowel as kwaliteitskontrole word breedvoerig beskryf. Makromolekulêre groottes wat wissel van 3 tot 300 kDa en ^{99m}Tc is gekies as spoorder ('tracer') vir die sintigrafiese biodinamika studies uitgevoer op normale volwasse manlike primate. Die resultate maak die identifisering van fraksies met geskikte groottes, naamlik 10-30 kDa van PEI-MP, as 'n beensoekende ligand moontlik. Die grootte van die makromolekules van die polimeriese PEI-MP kan die farmakokinetiese eienskappe drasties verander.

In die lig van belowende resultate van orgaanbeskerming en snelle uitskeiding in urien is 'n ondersoek gedoen, t.o.v. beentumor akkumulasie van ^{99m}Tc-PEI-MP, in vyf honde met spontane appendikulêre osteosarkomas. Gemiddelde tumor tot agtergrond-opnames van 4:1 is verkry met molekulêre fraksie-grootte van 10-30 kDa. Om die terapeutiese doel te bereik, moet die mees geskikte ligand 'n stabiele en toepaslike verbinding vorm met een of meer van die terapeutiese radionukliedes, byvoorbeeld ^{153}Sm, ^{186}Re en ^{117m}Sn (II).

Vir die ingeligte keuse van so 'n radionuklied, wat suksesvol bind met die ligand PEI-MP, om die osteosarkoom / metastatiese beentumors te teiken, was metaalioon spesiëring in bloedplasma gebruik om die in vivo gedrag van die potensieel beensoekende terapeutiese radiofarmaseutika te voorspel. Die bloedplasma-model ECCLES wat hier gebruik is bevat PEI-MP as ligand en het goeie in vivo respons van ^{117m}Sn(II)-PEI-MP aangedui wat nie die geval was met ^{153}Sm en ^{166}Ho komplekse nie.

Merking van PEI-MP met ^{117m}Sn(II) en met ^{186}Re was daarna suksesvol uitgevoer. Dit is bekend dat die verandering van die merker (radionuklied) van 'n spesifieke ligand die biodistribusie moontlik kan verander. In die lig hiervan is die biodistribusie van verskeie molekulêre groottes van ^{117m}Sn(II)-poliëtileeniminometielfosfonaat verbindings ondersoek by die normale primaatmodel om die geskiktheid te bepaal as selektiewe terapeutiese beenmiddels. Die in vivo stabiliteit van ^{117m}Sn-PEI-MP en die verminderde akkumulasie in die niere en normale been soos uit hierdie biodistribusie studies waargeneem was, het as aansporing gedien om die potensiële toepassing te bestudeer van die EPR-effek (Verhoogde permeabiliteit en retensie effek) by been tumore a.g.v. die makromolekulêre eienskappe van die polimeer by die tumore. In die lig van die laasgenoemde was die tumor-opname ondersoek van ^{117m}Sn-PEI-MP in verskillende soorte honde-osteosarkomas, in muise geïnduseer.

Die osteosarkoommodel volg vanuit die subkutane inspuiting van die selle van honde-osteosarkoom met hoë longmetastatiese kapasiteit (HMPOS) in sekere muise en sonder hierdie kapasiteit (POS) in die ander groep. Eersgenoemde het snellergroeiende nie-ossifiserende tumore gelewer teenoor die stadigergroeiende tumore van POS-selle met histologies bevestigde ossifiserende weefsel. Die hoë voorkoms van ^{117m}Sn-PEI-MP in die blaaswand, is kommerwekkend en gevolglik ook 'n fokus van voortgesette navorsing.

Hierdie navorsing het duidelik aangetoon dat die PEI-MP-ligand belowende eienskappe toon vir teikengerigte lewering van terapeutiese radionukliedes aan neoplastiese beenletsels, sonder om lewensbelangrike organe en normale been te benadeel.

Die normale primaat blyk ook 'n geskikte proefdier te wees om sintigrafiese resultate van bisfosfonaatgedrag te interpreteer, asook vir sintigrafiese monitering van die farmakokinetika en biodistribusie van beenterapeutiese radiofarmaseutika.

Acknowledgements

I would like to sincerely thank the following persons for their respective contributions to the work presented here:

- Prof. Douglas Oliver, as promoter and valued collaborator, for his assistance and guidance towards compiling the data and information eminating from this extensive research into a volume which could widely serve to direct future similar investigations. He was an enthusiastic collaborator and participant in an even wider field of investigation for more than 15 years during which I could benefit from his considerable knowledge in his field of expertise and share and enjoy with him his dedication to science in general. It is also solely through his vigorous administrative efforts that this thesis at all came to be. For especially this, Douglas, words of thanks fail me.

- Dr. Werner Louw for his painstaking scrutiny of all the facts and figures which appear in this manuscript. As an important partner in these studies, he was not just the backroom boy in the radiochemistry laboratory, but rather the man behind new and innovative ideas. It was each time during many years an exciting experience to test yet another compound in vivo, and watch the intellectual reasoning become reality.

- Dr. Rowan Milner for kindly sharing his experience and expertise, especially in the treatment of canine osteosarcoma and developing of osteosarcoma cell lines for the rodent studies.

- Dr. Jan Rijn Zeevaart for modelling metal ion speciation in bloodplasma and for initiating and directing the investigations with ^{117m}Sn(II) obtained from the Netherlands.

- Dr. Frank Schneeweiss for enthusiastic international networking.

- Prof. Filomena Botelho for making facilities and staff available to continue with the rodent studies at IBILI, University of Coimbra. It is on her shoulders that the responsibilities for the future research will rest.

- Dr. Ralf Clauss for some clinical information.

- Me. Elmare Kilian for expert and dedicated technical assistance including caring and handling of the experimental animals, for many years.

- Prof. Antoine van Gelder for kindly taking care of the logistics which provided the infrastructure which for many years sustained the research and whose efforts also greatly supported the completion of this thesis.

- Me. Marianna Bergh for putting together so deftly all the scribbled pages of paper which became this book. That was the most difficult part. Marianna you are a star!

- Prof. Piet de Kock for translations.

Arranging the data and information from a near lifetime of research naturally brought with it moments of reflection. It was from these moments that I acutely recognized with humble gratitude and awe the hand that steered destiny for this, and much more, to fall into place, not only to produce a PhD thesis, but really to shape a life.

In this light I would like to dedicate this thesis to my mother who for all these years shared the woes, and savored the successes with me, and to Johann, my pillar of strength, who, when all else seemed to fail, made sanity prevail.

My thanks and appreciation to the following Institutions:

- University of Pretoria under the auspices of which the work was done

- University of North West for recent support

- University of Coimbra for support with the rodent studies

- Research Centre Jülich through support of Dr. Schneeweiss

- NECSA through support of Dr. Louw and Dr. Zeevaart

- NRF and the Bundesministerium Deutschland for bilateral travel funding between Germany and South Africa.

- Alexander van Humboldt Foundation, Bonn-Bad Godesberg, for sponsoring periods of research on many occasions.

- Volkswagen Foundation Hannover for sponsoring this research extensively for 3 years.

Table of Contents

Table of Figures

Chapter 1 - Introduction

1.1 Background

The field of research reported on in this thesis covers procedures of radiotherapy of bone cancer using bone seeking radiopharmaceuticals i.v. applied. To a large extent such research generally has been confined to the treatment of bone pain in people with metastatic bone cancer but on occasion also in cases of osteosarcoma (Goeckeler *et al.*, 1987; Holmes 1992; Bruland et al., 1996; Serafini, 2001). It is typically used when there are multiple metastatic lesions in the skeleton, which makes local and focal treatment impractical and systemic treatment an attractive alternative (Lewington, 1996). The treatment is tumour specific since the radiopharmaceutical targets the area of increased mineral turnover. This allows for selective uptake and prolonged radiopharmaceutical retention in these areas (Goeckeler *et al.*, 1987). It also suggests that treatment would be more effective in predominantly sclerotic lesions associated with brisk osteoblastic reaction than in destructive lesions. Since the treatment is localized to the active lesions in certain parts of the skeleton, toxicity is reduced minimising damage to healthy tissue. However this is not always the case as myelotoxicity occurs with high doses of radiopharmaceuticals (Lattimer *et al.*, 1990; Bayouth *et al.*, 1994; Milner *et al.*, 1998; Franzius *et al.*, 2002; Anderson *et al.*, 2002).

An ideal radiopharmaceutical for the treatment of neoplastic and inflammatory (benign) bone diseases would be a radiolabelled compound, which would predominantly accumulate in the bone lesions with limited access to normal bone and other organs. (Bouchet *et al.*, 2000)

Criteria governing the selection of the radionuclide are particle range, physical half-life, gamma yield (scintigraphic monitoring), chemistry and type of ligand. The most commonly used radionuclides at present are listed in Table 1-1 (Atkins, 1998; Liepe *et al.*, 2000; Body & Mancini, 2002).

Currently the available bone seeking agents which are phosphonate containing ligands tend to localize throughout the skeleton. This thesis focuses on methylenediphosphonic acid (MDP), 1- hydroxy-ethylenediphosphonic acid (HEDP), and a novel agent polyethyleneimine

functionalised with methylene phosphonate groups (PEI-MP), as well as the octa-anion ethylenediaminetetramethylenephosphonate (EDTMP). MDP and HEDP are bisphosphonates, EDTMP a multidentateaminophosphonate which tends to form a more stable chelate with fewer structural forms than HEDP (Lin, 1996). In targeted therapy EDTMP is used in combination with ^{153}Sm and might be binding to hydroxy-apatite crystals in a different way than HEDP. In a review by Serafini (2001) the effect of EDTMP on bone neoplasia was mentioned to require further investigation as it was thought that the ligand in itself may effect bone neoplasia. ^{186}Re-HEDP is used for palliation of bone pain to metastatic bone cancer. Complications known with ^{153}Sm-EDTMP and ^{186}Re-HEDP treatment are myelotoxicity and in some cases a transient increase in bone pain following treatment (flare response) (Farhanghi *et al.*, 1992; Brenner *et al.*, 2001; Liepe *et al.*, 2005). In contrast to this ^{188}Re-HEDP appears to fulfil the criteria of a good radiotherapeutic agent as it has stronger β-emission than ^{153}Sm and ^{186}Re and a shorter physical and biological half-life which reduces myelotoxicity (Palmedo *et al.*, 2000; Li *et al.*, 2001; Liepe *et al.*, 2003; Palmedo *et al.*, 2003).

Research currently focusses on optimisation of phosphonate containing ligands carrying therapeutic radionuclides. These are designed to reach a target area and be retained there as a radiopharmaceutical to achieve optimal therapeutic efficacy. Some of the ligands used in radioisotope therapy are themselves pharmacologically active agents and may even contribute to the function of the radiopharmaceutical (Klenner *et al.*, 1990; Body *et al.*, 1998; Diel, 2000; Body & Mancini, 2002). HEDP is known as etidronate and is used therapeutically in osteoporosis in humans where it inhibits bone resorption (Manolagas, 2000).

An alternative and novel approach for ligand optimisation is to use neoplastic tissues' abnormal blood supply leading to increased permeability, as well as lack of lymphatics, which will lead to selectively accumulated radiolabelled macromolecules at the target site (Seymour, 1992). This enhanced permeability and retention effects (EPR) (Maeda *et al.*, 2001) form the basis of the unique study presented here using various molecular sizes of the radiolabelled macromolecule ^{99m}Tc polyethyleneiminomethylphosphonate (written as ^{99m}Tc-PEI-MP) so as to increase selectivity by the ligand, of bone seeking radiopharmaceuticals. This effect is applicable only to macromolecules and lipidic particles, not to low-molecular-weight compounds, the category to which most drugs in use today belong (Maeda *et al.*, 2001). Low molecular weight compounds are distributed freely by diffusion to various tissues and organs; the compounds move against the concentration gradient until finally an equilibrium results.

Their concentration in tumours cannot be higher than in blood plasma, nor can they be retained at high concentrations in tumours for a significant time period because of rapid excretion (washout) into the bloodstream. The plasma concentration also diminishes rapidly as a result of efficient renal clearance via the urine (Maeda *et al.*, 2001). In contrast, macromolecules and polymeric drugs are retained in tumour tissue at a much higher concentration than in plasma (Maeda *et al.*, 2001). There is thus a great difference between low- and high-molecular-weight compounds in their intratumour accumulation. This phenomenon, *the Enhanced Permeability and Retention (EPR) effect*, is now recognized as a general characteristic of viable and rapidly growing solid tumours. Another general characteristic is the structural deficiencies of tumour blood vessels, which also cause enhanced leakiness (Maeda *et al.*, 2001).

Table 1-1: Physical Properties of Therapeutic Radionuclides

Nuclide	Half-life (days)	Range in tissue (mm)	Beta-emission E_{max} (MeV)	Gamma-emission (keV)	Abundance (%)
Phosphorus-32	14.3	8	1.7		
Strontium-89	50.5	7	1.46		
Tin-117m	13.6	0.3	Conversion electrons	158	87
Rhenium-186	3.8	2.5	1.07	137	9
Samarium-153	1.9	3.7	0.8	103	29
Rhenium-188	16.9 hours	11	2.1	155	15

Molecular sizing of polymeric PEI-MP can drastically alter the pharmacokinetic properties (Dormehl *et al.*, 2001), which can be exploited to suit different applications and targeting of specific organs, tissues and pathological affected areas. The localisation of PEI-MP is also essentially in the surface areas of bone tumours (Milner, personal communication). In order to obtain an optimal molecular size, which would largely exclude damage to normal bone and other organs, the pharmacokinetics, i.e. biodistribution of various ^{99m}Tc-PEI-MP size fractions could be investigated using various groups of experimental baboons (*Papio ursinus*). Once an

optimal molecular size is identified it could be used in rodent experiments eventually using osteosarcoma bearing nude mice. The murine model is a familiar approach and useful for development of tumour seeking ligands to enhance targeted radiotherapy (Pool *et al.*, 1988).

Information concerning the in vivo behaviour of drug formulations following administration to human subjects can be obtained from radionuclide imaging techniques in investigative procedures (Siegel *et al.*, 1999). In general the radiolabelling can be achieved with gamma-emitting radionuclides e.g. ^{99m}Tc as tracer and monitored using a gamma camera. The therapeutic isotopes ^{153}Sm, ^{186,188}Re can in low activity imaging dosages serve as its own tracer with the relevant accompanying ligands.

The non-human primate has always served as an extremely suitable animal model in drug development and analysis, even in the very complex field of neurology, where remarkable similarities to human anatomy and physiology exist (Connolly, 1950; Le Gros Clark, 1960; Fridman & Popova, 1988; Fridman & Popova, 1988; Louw *et al.*, 1991). The advantage of this model together with regular nuclear medical equipment for scintigraphy lies in its size which will allow flexibility in extrapolating raw data from images, as well as of evaluated data to man. Dosimetry is an example of where the primate model becomes very useful.

Before embarking on bone seeking drug development however the baboon and its bisphosphonate bone biodynamics had to be studied, i.e. in fracture healing experiments, where the pattern of bone healing could be scintigraphically monitored. The applicability of the results from ^{99m}Tc-MDP images thus obtained, to humans would encourage subsequent studies to establish the pharmacokinetics of ^{153}Sm-EDTMP in the normal primate. Since such data obtained from gamma camera scintigraphic monitoring are also available for humans, good agreement would validate the use of the primate model for future novel drug development.

An established primate model, would permit novel phosphonate ligands to be studied. The biodistribution of variously sized macromolecules of radiolabelled polyethyleneiminomethyl phosphonic acid as a selective bone seeker for therapy could thus be studied in the normal primate model, bearing in mind sparing the bone marrow, kidneys and liver from excessive radiation exposure.

Metal ion speciation in blood plasma could be used to predict the in vivo behaviour of the potential bone-seeking therapeutic radiopharmaceuticals. The object here is to construct a blood plasma model which includes PEI-MP (May *et al.*, 1977; Jarvis & Wagener, 1995). This would enable informed selection of the radionuclide for delivery to osteosarcoma and metastatic bone tumours by PEI-MP. This gives an indication of the ability of the radiopharmaceutical to survive competition for the radionuclide by other blood plasma ligands. Therapeutic β-particle emitting radionuclides under consideration are ^{153}Sm, ^{166}Ho, ^{89}Sr, $^{186/188}$Re, as well as the Auger electron emitter ^{117m}Sn.

To evaluate the therapeutic potential of suitably labelled PEI-MP the biokinetics of e.g. the 10-30 kDa fraction (in diagnostic activities of radionuclide) could conceivably be studied in canine osteosarcoma bearing nude mice (Balb C) (Kadosawa *et al.*, 1994). Osteosarcoma is the most common bone tumour in man and accounts for 20% of all bone malignancies. It furthermore resembles canine osteosarcoma in histological appearance and biological behaviour (Owen, 1976; Brodey, 1979; Knapp & Waters, 1997; Macewen, 1990; Hahn *et al.*, 1994). This accounts for the approach taken here to model bone neoplasia from naturally occuring canine osteosarcoma in rodents (Parodi, 1982; Pelfrene, 1985; Pool *et al.*, 1988). It is also the closest to modelling human metastatic bone cancer, although the process involved in the production of osteolytic and osteogenic metastases differs from the abnormalities, largely of chromosomal origin, in osteosarcoma cells. Diagnosis of metastatic disease is similar for osteosarcoma and include radiographs, CT, scintigraphy and MRI (Forrest *et al.*, 1992; Leibman *et al.*, 2001; Davis *et al.*, 2002; Wallack *et al.*, 2002). The therapy for both is commonly directed at palliation of bone pain, and the drugs generally used consist of non-steroidal anti-inflammatory drugs, narcotic analgesics and bisphosphonates also with radionuclides as in this study (Straw *et al.*, 1990; Milner *et al.*, 1998; Ramirez *et al.*, 1999; Tomlin *et al.*, 2000).

Synthetic polymers provide a broad technology platform for applications in the pharmaceutical sciences (Alexander, 2001). A variety of compounds can be coupled directly or with a selection of appropriate linkers to an amino group containing the ligand PEI-MP to form many different possible polymer-drug conjugates. In the area of drug delivery, especially to tumours and inflammatory areas, PEI-MP could have a unique and novel role to play also without a radionuclide label.

1.2 Aim and Objectives

In view of the discussion above the aim of this research was to investigate novel bisphosphonate containing ligands for targeted radiotherapy of neoplastic bone disease using rodent and primate animal models and scintigraphy. The success of the outcome sets very specific requirements for the sequence of investigation as is described in the section on experimental design (Chapter 3).

This required sequence directs the specific objectives of the study as follows:

(i) To validate the primate model for its bisphosphonate bone metabolism in fracture healing where the pattern of bone healing was scintigraphically monitored and compared to human images.

(ii) To establish the pharmacokinetics and biodistribution of the known therapeutic radiopharmaceutical agent ^{153}Sm-EDTMP scintigraphically in primates, compare it to human data and thus validate the primate model for this experimental approach.

(iii) To design a novel ligand with optimised tumour localisation potential sparing the other vital organs by making use of the EPR principle.

(iv) To confirm the in vivo characteristics of this novel ligand (PEI-MP) through biodistribution studies in the normal primate model as established above, using scintigraphy with ^{99m}Tc labelling of the ligand.

(v) To perform metal ion speciation in blood plasma (ECCLES model) to predict the in vivo behaviour of this novel potential bone-seeking therapeutic radiopharmaceutical, labelled with various therapeutic ß-emitting radionuclides in order to allow informed selection of the radionuclide delivered to a bone lesion.

(vi) To develop labelling techniques of the ligand with ^{186}Re, and/or ^{117m}Sn, in order to obtain the required therapeutic radiopharmaceutical.

(vii) To investigate the labelled ligand ^{117m}Sn-PEI-MP scintigraphically for suitable biokinetic and biodistribution properties of tumour targeting initially in the normal primate model.

(viii) To evaluate the potential therapeutic properties of ^{117m}Sn-PEI-MP, through biokinetic biodistribution studies in canine osteosarcoma bearing nude mice, and

to calculate the radiopharmaceutical uptake by various tumours. This would indicate the therapeutic potential of the labelled ligand.

1.3 Study Design

The procedures used in this investigation include the highly specialized techniques of isotope production in a nuclear reactor (Safari-1, NECSA, Pelindaba), and the associated radiochemistry of isotope separation, and preparation to deliver the radionuclide to be used in the radiopharmacy laboratory for labelling the ligand, which had been designed through various synthetic chemistry considerations.

In vivo studies of the labelled ligand using the non-human primate model and rodents (Wistar rats and Balb C mice) will be performed with scintigraphic procedures (gamma camera), and organ counting in a well counter (rodents). These biodistribution studies will take place with the animals under controlled anaesthesia. Theoretical mathematical modelling will provide information on appropriate radionuclide selection (ECCLES), dosimetry (MIRD) and compartmental distribution of the radiopharmaceutical.

These studies will be performed after approval by the Ethics Committee of the University of Pretoria, according to the guidelines of the National Code for Animal use in Research, Education and Testing of Drugs and Related Substances in South Africa. These guidelines are in line with international standards.

1.4 Presentation of Thesis

The reader is reminded that this thesis is presented in the format, whereby the methods, results and discussions relating to the various studies were incorporated into the ten papers (chapters 4-13, see 1-5). Attention is drawn to the fact that the ten papers have already been published internationally. Also note that the references to chapters 4-13 are presented as in the original publications.

1.5 Publications

Chapter 4: A Technique to Evaluate Bone Healing in Non-Human Primates Using Sequential ^{99m}Tc-Methylene diphosphonate Scintigraphy. *Nucl. Med.*21: 105-109. (1982)

Chapter 5: Evaluation of Samarium-153 and Holium-166-EDTMP in the Normal Baboon Model. *Nucl. Med. Biol. 23:*935-940. (1996)

Chapter 6: Uptake of Ethylenediamine Tetramethylene Phosphonic Acid in Normal Bone after Multiple Applications: A non-human primate study. *Arzneim.- Forsch./ Drug Res.* 48(4):408-414. (1998)

Chapter 7: Biodistribution and Pharmacokinetics of Variously Sized Molecular Radiolabelled Polyethyleneiminomethyl Phosphonic Acid as a Selective Bone Seeker for Therapy in the Normal Primate Model. *Arzneim.- Forsch/ Drug. Res.* 54: 258-263. (2001)

Chapter 8: Optimalisation of Radiolabelled Polymin-MP of Different Molecular Sizes as selective Bone Seeker for Therapy in Animal Models. *Physica Media* 17: 53-55. (2000)

Chapter 9: Metal ion Speciation in Blood Plasma Incorporating the Water-soluble Polymer, Polyethyleneimine Functionalised with Methylenephosphonate Groups, in Therapeutic Radiopharmaceuticals. *Radiochim. Acta.* 90: 237-246. (2002)

Chapter 10: ^{117m}Sn and ^{186}Re radiolabelling of polyethyleneiminomethyl phosphonic acid (PEI-MP), a potential selective therapeutic bone tumour seeker. *Nucl. Med. Comm.* 23: 1223-1224 (2002), presented at the 10th Biennual Congress of the South African Society of Nuclear Medicine, Stellenbosch, 4-7 Dec 2002.

Chapter 11: Biodistribution and pharmacokinetics of Variously Molecular Sized ^{117m}Sn(II)-Polyethyleneimonomethyl Phosphonate Complexes in the Normal Primate Model as Potential Selective Therapeutic Bone Agent. *Arzneim.- Forsch/ Drug res.* 54, No. 6, 340-347. (2004)

Chapter 12: ^{117m}Sn and ^{186}Re Radiolabelling of Polyetyleneiminomethyl Phosphonic Acid (PEI-MP), followed by In Vivo Targeting of Induced Osteosarcoma in Nude Mice. *Nucl. Med./Nukl. Med.* 42: 156-157 (2004), presented at Radio Isotopes in Clinical Medicine and Research, 26th International Symposium, Bad Gastein, Austria, 13-16 Jan 2004.

Chapter 13: Comparison of Tumour Uptake in Different Types of Osteosarcoma Mice as Studied with the Potential Bone-seeking Radiopharmaceutical, ^{117m}Sn(II)-PEI-MP. *World J. Nucl. Med.* 3: 237 (2004). International Congress of Radiopharmacy and Radiochemistry, Gdansk.

1.6 References

ALEXANDER, C. 2001. Synthetic polymer systems in drug delivery. *Expert. Opin. Emerging Drugs* 6(2): 345-363.

ANDERSON, P.M., WISEMAN, G.A., DISPENZIERI, A., ARNDT, C.A., HARTMANN, L.C., SMITHSON,W.A. *et al.* 2002. High-dose samarium-153 ethylene diamine tetramethylene phosphonate: low toxicity of skeletal irradiation in patients with osteosarcoma and bone metastases. *J Clin Oncol* 20(1):189-196.

ATKINS, H.L. 1998. Overview of Nuclides for Bone Pain Palliation. *Appl Radiat Isot* 49(4):277-283.

BAYOUTH, J.E., MACEY, D.J., KASI, L.P., FOSSELLA, F.V. 1994. Dosimetry and toxicity of samarium-153-EDTMP administered for bone pain due to skeletal metastases. *J. Nucl. Med.* 35(1):63-69.

BODY, J.J., BARTL, R., BURCKHARDT, P., DELMAS, P.D., DIEL, I.J., FLEISCH, H. *et al.* 1998. Current use of bisphosphonates in oncology. International Bone and Cancer Study Group. *J Clin Oncol* 16(12):3890-3899.

BODY, J.J., MANCINI, I. 2002. Bisphosphonates for cancer patients: why, how, and when? *Support Care Cancer* 10(5):399-407.

BOUCHET, L,G., BOLCH , W,E., GODDU, S.M., HOWELL, R.W., RAO, D.V. 2000. Considerations in the selection of radiopharmaceuticals for palliation of bone pain from metastatic osseous lesions. *J. Nucl. Med.*41(4):682-687.

BRENNER, W., KAMPEN, W.U., KAMPEN, A.M., HENZE, E. 2001. Skeletal uptake and soft-tissue retention of 186Re-HEDP and 153Sm-EDTMP in patients with metastatic bone disease. *J. Nucl. Med.* 42(2):230-236.

BRODEY, R.S. 1979. The use of naturally occurring cancer in domestic animals for research into human cancer: general considerations and a review of canine skeletal osteosarcoma. *Yale J Biol Med* 52(4):345-361.

BRULAND, O.S., SKRETTING, A., AAS, M. 1996. Targeted radiotherapy of osteosarcoma using 153 Sm-EDTMP. A promising approach. *Acta Oncol* 35:381-384.

CONNOLLY, C.J. 1950. In 'External morphology of the primate brain'. Charles C. Thomas Co., Springfield, USA, p. 3.

DAVIS, G.J., KAPATKIN, A.S., CRAIG, L.E., HEINS, G.S., WORTMAN, J.A. 2002. Comparison of radiography, computed tomography, and magnetic resonance imaging for evaluation of appendicular osteosarcoma in dogs. *J Am Vet Med Assoc* 220(8):1171-1176.

DIEL, I.J. 2000. Antitumour effects of bisphosphonates: first evidence and possible mechanisms. *Drugs* 59(3):391-399.

DORMEHL, I. C., LOUW ,W. K. A., SCHNEEWEISS, F. H. A., MILNER, R., SCHMITT, G., CROFT, S. A. 1998;Uptake of ethylenediamine tetra-methylene phosphonic acid in normal bone after multiple applications - A primate study. *Arzneim.- Forsch./ Drug Research* 48(4):408-414.

DORMEHL, I.C., LOUW, W.K.A., MILNER, R.J., KILIAN, E., SCHNEEWEISS, F.H.A. 2001. Biodistribution and pharmacokinetics of variously sized molecular radiolabelled polyethyleneiminomethyl phosphonic acid as a selective bone seeker for therapy in the normal primate model. *Arzneim.-Forsch./drug Res.* 51: 258-263.

FARHANGHI, M., HOLMES, R.A., VOLKERT, W.A., LOGAN, K.W., SINGH, A. 1992. Samarium-153-EDTMP: pharmacokinetic, toxicity and pain response using an escalating dose schedule in treatment of metastatic bone cancer. *J. Nucl. Med.* 33(8): 1451-1458.

FORREST, L.J., DODGE, R.K., PAGE, R.L., HEIDNER, G.L., MCENTEE, M.C., NOVOTNEY, C.A. *et al.* 1992. Relationship between quantitative tumor scintigraphy and time to metastasis in dogs with osteosarcoma. *J Nucl Med* 33(8):1542-1547.

FRANZIUS, C., SCHUCK, A., BIELACK, S.S. 2002. High-dose samarium-153 ethylene diamine tetramethylene phosphonate: low toxicity of skeletal irradiation in patients with osteosarcoma and bone metastases. *J Clin Oncol* 20(7):1953-1954.

FRIDMAN, E.P., POPOVA, V.N. 1988. Species of genus *Papio* (*Cercopithecidae)* as subjects of biochemical research: I. Biological basis of experiments on baboons. *J. Med. Primatol.* 17: 291-307.

FRIDMAN, E.P., POPOVA, V.N. 1988. Species of genus *Papio* (*Cercopithecidae)* as subjects of biochemical research: II. Quantitative characteristics of contemporary use of baboon species in medical and biological investigations. *J. Med. Primatol.* 17: 309-318.

GOECKELER, W.F., EDWARDS, B., VOLKERT, W.A., HOLMES, R.A., SIMON, J., WILSON, D. 1987. Skeletal localization of Samarium-153 chelates: Potential therapeutic bone agents. *J. Nucl. Med.*28:495-504.

HAHN, K.A., BRAVO, L., ADAMS, W.H., FRAZIER, D.L. 1994. Naturally occurring tumors in dogs as comparative models for cancer therapy research. In Vivo 8(1):133-143.

HOLMES RA. 1992. [153Sm]EDTMP: a potential therapy for bone cancer pain. *Semin Nucl Med* 22(1):41-45.

JARVIS, N.V., WAGENER, J.M. 1995.Mechanistic studies of metal ion binding to water soluble polymers using potentiometry. *Talanta* 42: 219-226.

KADOSAWA, T., NOZAKI, K., SASAKI, N., TAKEUCHI, A. 1994. Establishment and characterization of a new cell line from a canine osteosarcoma. *J Vet Med Sci* 56(6):1167-1169.

KLENNER, T., WINGEN, F., KEPPLER, B.K., KREMPIEN, B., SCHMAHL, D. 1990. Anticancer-agent-linked phosphonates with antiosteolytic and antineoplastic properties: a promising perspective in the treatment of bone-related malignancies? *J Cancer Res Clin Oncol* 116(4):341-350.

KNAPP, D.W., WATERS, D.J. 1997. Naturally occurring cancer in pet dogs: important models for developing improved cancer therapy for humans. *Mol Med Today* 3(1):8-11.

LATTIMER, J.C., CORWIN, L.A., JR., STAPLETON, J., VOLKERT, W.A., EHRHARDT, G.J., KETRING, A.R. *et al.* 1990. Clinical and clinicopathologic effects of

Samarium-153-EDTMP administered intravenously to normal Beagle dogs. *J. Nucl. Med.*31:586-593.

LE GROS CLARK, W.E. 1960. In 'The antecedents of man: an introduction to the evolution of primates'. Quandrangle Books, Chicago, USA, p. 262.

LEIBMAN NF, KUNTZ CA, STEYN PF, FETTMAN MJ, POWERS BE, WITHROW SJ *et al.* 2001. Accuracy of radiography, nuclear scintigraphy, and histopathology for determining the proximal extent of distal radius osteosarcoma in dogs. *Vet Surg* 30(3):240-245.

LEWINGTON, V.J. 1996. Cancer therapy using bone-seeking isotopes. *Phys Med Biol* 41(10):2027-2042.

LI, S., LIU, J., ZHANG, H., TIAN, M., WANG, J., ZHENG, X. 2001. Rhenium-188 HEDP to treat painful bone metastases. *Clin Nucl Med* 26(11):919-922.

LIEPE K, KROPP J, RUNGE R, KOTZERKE J. 2003. Therapeutic efficiency of rhenium-188-HEDP in human prostate cancer skeletal metastases. *Br J Cancer* 89(4):625-629.

LIEPE, K., FRANKE, W.G., KROPP, J., KOCH, R., RUNGE, R., HLISCS, R. 2000. [Comparison of rhenium-188, rhenium-186-HEDP and strontium-89 in palliation of painful bone metastases]. *Nucl. Med./Nukl. Med* 39(6):146-151.

LIEPE, K., RUNGE, R., KOTZERKE, J. 2005. The benefit of bone-seeking radiopharmaceuticals in the treatment of metastatic bone pain. *J. Cancer Res. Clin. Oncol.* 131(1): 60-66.

LIN, J.H. 1996. Bisphosphonates: a review of their pharmacokinetic properties. *Bone* 18(2):75-85.

LOUW, W.K.A., VAN RENSBURG, E.J., IZATT, H., ENGELBRECHT, R.I. 1991. Nucleoid sedimentation analysis of DNA superstructure, gamma-radiation-induced damage and repair in human and chacma baboon (*Papio ursinus)* peripheral lymphocytes. *Int. J. Radiat. Biol.* 59:951-962.

MACEWEN, E.G. 1990. Spontaneous tumors in dogs and cats: models for the study of cancer biology and treatment. *Cancer Metastasis Rev* 9(2):125-136.

MAEDA, H., SAWA, T., KONNO, T. 2001. Mechanism of tumour-targeted delivery of macromolecular drugs, including the EPR effect in solid tumor and clinical overview of the prototype polymeric drug SMANCS. *J. Controlled Release* 74: 47-61.

MANOLAGAS, S.C. 2000. Birth and death of bone cells: basic regulatory mechanisms and implications for the pathogenesis and treatment of osteoporosis. *Endocr Rev* 21(2):115-137.

MAY, P.M., WILLIAMS, D.R., LINDER, P.W. 1977. Computer simulation of metal ion equilibria in biofluids; Models of low-molecular-weight complex distribution of calcium (II), magnesium (II), manganese (II), Iron (III), Copper (II), Zn(II), Pb (II) ions in human blood plasma. *J. Chem. Soc., Dalton Trans.* 588 - 595.

MILNER, R.J. Personal Communication.

MILNER, R.J., DORMEHL, I., LOUW, W.K., CROFT, S. 1998. Targeted radiotherapy with Sm-153-EDTMP in nine cases of canine primary bone tumours. *J S Afr Vet Assoc* 69(1):12-17.

OWEN, L.N. 1976. Osteosarcoma in the dog. *Proc R Soc Med* 69(8):546-547.

PALMEDO, H., GUHLKE, S., BENDER, H., SARTOR, J., SCHOENEICH, G., RISSE, J. *et al.* 2000. Dose escalation study with rhenium-188 hydroxyethylidene diphosphonate in prostate cancer patients with osseous metastases. *Eur. J. Nucl. Med* 27(2):123-130.

PALMEDO, H., MANKA-WALUCH, A., ALBERS, P., SCHMIDT-WOLF, I.G., REINHARDT, M., EZZIDDIN, S. *et al.* 2003. Repeated bone-targeted therapy for hormone-refractory prostate carcinoma: randomized phase II trial with the new, high-energy radiopharmaceutical rhenium-188-hydroxyethylidenediphosphonate. *J. Clin. Oncol.* 21(15):2869-2875.

PARODI, A.L. 1982. Canine osteosarcoma as a model in comparative oncology. *Sem Hop* 58(30-31):1731-1735.

PELFRENE, A.F. 1985. A search for a suitable animal model for bone tumors: a review. *Drug Chem Toxicol* 8(1-2):83-99.

POOL, B.L., BERGER, M., SCHLEHOFER, J.R., WINGEN, F. 1988. In vivo and in vitro investigations on biological effects of aromatic bis-(2-chloroethyl)amino-bisphosphonic acids, new agents proposed for chemotherapy of bone tumors: cytostatic activity in rat osteosarcoma; toxicity and genotoxicity in liver and bone marrow; mutagenicity in S. typhimurium. *Invest New Drugs* 6(2):67-78.

RAMIREZ, O., DODGE, R.K., PAGE, R.L., PRICE, G.S., HAUCK, M.L., LADUE, T.A. *et al.* 1999. Palliative radiotherapy of appendicular osteosarcoma in 95 dogs. *Vet Radiol Ultrasound* 40(5):517-522.

SERAFINI, A.N. 2001. Therapy of metastatic bone pain. *J. Nucl. Med.* 42(6):895-906.

SEYMOUR, L.W. 1992. Passive tumor targeting of soluble macromolecules and drug conjugates. CRC *Crit. Rev. Ther. Drug Carrier Syst.*, 9: 135-187.

SIEGEL, J.A., THOMAS, S.R., STUBBS, J.B., STABIN, M.G., HAYS, M.T., KORAL, K.F. *et al.* 1999. MIRD pamphlet no. 16: Techniques for quantitative radiopharmaceutical biodistribution data acquisition and analysis for use in human radiation dose estimates. *J. Nucl. Med.* 40(2):37S-61S.

STRAW, R.C., WITHROW, S.J., POWERS, B.E. 1990. Management of canine appendicular osteosarcoma. *Vet Clin North Am Small Anim Pract* 20(4):1141-1161.

TOMLIN, J.L., STURGEON, C., PEAD, M.J., MUIR, P. 2000. Use of the bisphosphonate drug alendronate for palliative management of osteosarcoma in two dogs. *Vet Rec* 147(5):129-132.

WALLACK, S.T., WISNER, E.R., WERNER, J.A., WALSH, P.J., KENT, M.S., FAIRLEY, R.A. *et al.* 2002. Accuracy of magnetic resonance imaging for estimating intramedullary osteosarcoma extent in pre-operative planning of canine limb-salvage procedures. *Vet Radiol Ultrasound* 43(5):432-441.

Chapter 2 - Literature Review on the Research and Development Models of Phosphonate containing Ligands to target bone Tumours for Radiotherapy

In this chapter the scientific background and latest developments, also our own work, associated with all the concepts involved in the investigations covered in this thesis are discussed, as well as the rationale behind the experimental design and the procedures performed. The concepts of interest would clearly include aspects of bone physiology and pathology, in humans and animal models, the role of bisphosphonates in bone metabolism, and together with radionuclides in diagnostic scintigraphy and radiotherapy, the relevant instrumentation, computational procedures as well as mathematical models from which to obtain biokinetic data which could pronounce on therapeutic efficacy and dosimetry

2.1 Bone

2.1.1 Bone Physiology

Bone consists of three types of cells viz. osteoblasts, osteocytes and osteoclasts. Osteoblasts are responsible for the production of osteoid (protein matrix), which becomes mineralised. Mineralisation is under control of the osteoblast during which time local conditions of calcium and phosphate are regulated to promote hydroxy apatite formation (Manolagas, 2000; Rodan & Martin, 2000). The major product produced by osteoblasts is collagen type-1 which undergoes further extracellular processing to form collagen fibrils. Osteoblasts end up either being incorporated into bone and transform into osteocytes or form lining cells which are on the surface of quiescent bone (Shane & Bilezikian, 1995; Rodan & Martin, 2000). Osteoblasts express high amounts of alkaline phosphatase which is anchored to the external surface of the plasma membrane (Shane & Bilezikian, 1995; Rodan & Martin, 2000). Osteocytes, osteoblasts, bone marrow stromal cells and endothelial cells communicate with each other and form a functional syncytium (Grigoriadis *et al.*, 1996). The

osteocyte is postulated to function as a mechanosensory cell which is then responsible for the initiation of modelling or remodelling activity of bone (Grigoriadis *et al.*, 1996; Marcus 1996). Osteoclasts cannot bind directly to collagen layers covering bone and require lining cells to release collagenase and remove the protein matrix (Shane & Bilezikian, 1995). It is postulated that the lining cells give the homing signal to osteoclasts that initiates bone resorption (Shane & Bilezikian, 1995).

Morphologically osteoclasts are recognized as multinucleated cells with abundant mitochondria, lysosomes and free ribosomes. The most remarkable feature is the ruffled border which is surrounded by a clear zone. The clear zone delineates the area of attachment to bone and seals off a distinct area of bone. The area below the osteoclast allows for a microenvironment suitable for bone resorption (Manolagas, 2000). The osteoclasts secrete hydrogen ions via an ATPase proton pump and proteolytic enzymes to accomplish a resorptive process. Proteolytic enzymes such as matrix metalloproteinase and cathepsin K, B and L are secreted by the osteoclast. Osteoclasts also contain high levels of a phosphohydrolase enzyme, tartrate-resistant acid phosphatase (TRAPase). Systemic hormones such as parathyroid hormone (PTH) and vitamin D_3 and calcitonin exert a significant effect on osteoblasts and osteoclasts. PTH and vitamin D_3 are potent initiators of osteoclast formation. Calcitonin inhibits osteoclast development and promotes osteoclast apoptosis. Other hormones that have significant metabolic affects on bone are sex hormones, glucocorticoid and thyroid hormones (Manolagas, 2000).

The physiological process of bone formation and resorption involved in remodelling are considered as a unique temporary structure known as a basic multicellular unit (BMU) (Grigoriadis *et al.*, 1996). The BMU consists of a cluster of osteoclasts in the front and osteoblasts in the rear, a central vascular capillary, a nerve supply and associated connective tissue (Grigoriadis *et al.*, 1996). Each BMU travels from a point of origin to the target and in some cases beyond until termination. In cortical bone BMUs excavate a tunnel which is replaced by remodelled bone. In the case of trabecular bone a trench is excavated and replaced. In humans about 1 million BMU's are active at any one moment (Grigoriadis *et al.*, 1996; Marcus, 1996).

This remodelling process will slow down in normal and physiologic conditions, settling to an approximate rate of 5 percent annually during adulthood. Of course, this rate of renewal can vary greatly when increased demand for bone turnover is present, be it from chemical, endocrine, mechanical, neoplastic, or other etiology. A balance between bone formation and bone resorption is always attempted and in progress in the skeleton. This mechanism has been elegantly explained in relation to the osseous remodelling occuring at the site of osteoblastic and/or osteolytic bone metastasis. It has been called carcinomatous osseous dysplasia (Burkhardt *et al.*, 1982). This concept explains the true development of an osseous shell around a primary bone tumour, with very active and fast resorption and formation of bone occurring on the periphery of the tumour, probably by very accelerated periosteal bone deposition.

Another well known example of accelerated bone remodelling is seen during the healing stage of a fracture, when the periosteum develops frantic osteogenic activity in producing callous. This healing process, sometimes not detected by radiographs, is a brilliant indication for a nuclear bone scan, which may demonstrate healing stress fractures in adults and infants (Mettler, 1988).

2.1.2 Bone Anatomy

Once bone has completed its growth and has stabilized in a more or less permanent size and shape, a state of biodynamics is established with the ultimate purpose of homeostasis. Bone is a remarkable configuration of mesenchymal tissue, serving essential mechanical functions of support for soft tissue and for protection (cranium and vertebral column) and also plays an essential role for storage of calcium and phosphorus.

The vehicle to transport all the nutrients, hormones, oxygen, minerals, and metabolic waste disposal in and out of bone is the circulating blood. The volume of blood flow is a principal determinant in the image formation of a nuclear bone scan. Radiographs, of course, only show the inert component of bone, the mineral framework mostly of calcium apatite, enclosing a large radiolucent space.

Variations in bone density give a general idea of the blastic or clastic activity, expressing the degree of deviation from a homeostatic bone balance state. This method of demonstrating resorption or formation of bone has a greater radiographic specificity than is available from a nuclear bone scan, due to the ability of radiograph imaging to show patterns of calcification or lysis with greater resolution. Unfortunately sensitivity is much lower than that of the nuclear bone scan. It is a well-known fact that lytic destruction of trabecular bone by a neoplastic process must reach between 30 and 50 percent of the bone mass before it can be detected as a density deficit in a radiograph.

The empty or radiolucent spaces seen on a radiograph of bone indicate the site where the highly vascular mesenchymal parenchyma is located. This soft tissue is formed by marrow and afferent and efferent blood vessels. There is a very rich capillary sinusoidal network located in the marrow and in the trabecular and cortical bone that reaches the haversian systems through the Volkman's canals. This rich circulatory network is organized in nutritional circulatory fields (Allman & Brower, 1981). A nutritional circulatory field is a unit of territory with special behaviour patterns. This concept of nutritional circulatory fields is quite important for the understanding of the meaning of the uptake patterns in the nuclear bone scan.

There are three well-defined nutritional circulatory fields that are freely anastomosed by a rich network of adjacent arteries. They are the following:

1. The nutrient system arteries, consisting of the nutrient artery entering the diaphysis and branching to both ends of the bone, supplying the marrow and inner bone surfaces.
2. The periosteal-cortical system arteries, originating in the periosteum and entering perpendicular to the cortex, supplying the haversian systems and osteocytes through the Volkman's canals.
3. The epiphyseal-metaphyseal system arteries, arising from periarticular soft tissues. They remain as separated fields until the closure of the growth plate, when they form a unit.

The osseous circulatory system described above carries the radiopharmaceutical to the bone, where other physiologic mechanisms of physical and chemical nature will take place, determining the appearance of the final image of the nuclear bone scan. The important key factors here are (Silberstein, 1984):

1. Size of radiopharmaceutical molecule
2. Capillary wall permeability
3. Capillary diffusion
4. Rate of radiopharmaceutical extraction per pass
5. Radiopharmaceutical dispersion in extracellular fluid
6. Bone mineral surface
7. Kinetics of bone uptake

On the three-phase nuclear scan, the "blood pool" image corresponds to the configuration of the nutritional circulatory fields and the delayed phases (at 3 to 4 hours) generally correspond to bone uptake.

2.1.3 Bone Metabolism

Bone is the result of a very specialized configuration of mesenchymal tissue serving the two main missions of support and storage. Support function is met by the ground substance of the matrix formed mostly by collagen fibres. These collagen fibres are composed of periodic segments repeating every 640 Å, arranged or lined up end-to-end and overlapping side-to-side, like bricks on a wall. This organic protein of collagen fibres forms 90 to 95 percent of the bone matrix and is arranged also along lines of stress, providing the great tensile strength characteristic of bone. (Mathews, 1975; Nimni, 1975). The remaining 5 to 10 percent of the ground substance is formed by extracellular fluid and proteoglycans, especially hyaluronic acid and chondroitin sulfate.

The storage function is fulfilled by the mineral phase of bone – mainly bone salts. These crystalline deposits are composed principally of calcium and phosphate, forming the major crystalline salts known as hydroxyapatites. Other ions also intervene in the composition of

these salts, such as magnesium, sodium, potassium, and carbonate. Each bone salt crystal, shaped like a long, flat plate, measures 400 Å in length and 100 Å in width, and it is between 10 and 30 Å thick. Hydroxyapatite crystals have the ability to conjugate with different ions, and some of them may be foreign to bone, such as lead. The bony uptake may be very rapid, and when combined with the generous blood flow through the bone, up to 200 to 400 ml/min, the uptake acquires the characteristics of a detoxifying mechanism, removing foreign ions from the circulating blood, therefore relieving toxic manifestations. This ability is responsible for the uptake of fluoride (fluoridation-fluoridosis).

This uptake allows the performance of bone scans in the diagnostic range, but, unfortunately, the same uptake occurs with thorium, strontium, uranium, plutonium and other transuranic elements, gold, and lead and other heavy metals. These long-lived radionuclides conjugate with hydroxyapatite crystals in bone and cause prolonged radiation of bone tissues with possible induction of osteogenic sarcoma.

Hydroxyapatite has mechanical characteristics resembling those of marble and provides significant compressional strength. The crystals lie adjacent to the collagen fibres, and this intimate bonding provides high resistance to shear. This combination of organic and mineral phases of bone strongly resembles the structure of reinforced concrete, and actual measurements of tensile and compressional strength of bone equal or surpass that of reinforced concrete (Carter & Hayes, 1977). The initial formation of hydroxy apatite crystals, called crystal seeding or nucleation (Guyton, 1986) is not in the form of geometric crystals but rather of amorphous compounds (noncrystalline) (Fig. 2-1). Approximately 20 to 30 percent of bone salt may be found permanently in this configuration as amorphous compounds. These compounds form very small molecules with a very large combined surface. This is very important, because these salts ean be absorbed very rapidly when there is need for supplementary calcium in the extracellular fluid.

The total amount of calcium present in the adult human body is approximately 1100g (1.1 kg). Ninety-nine percent of it is deposited in the skeleton. Calcium in bone is found as hydroxyapatite crystals, forming a large stable pool. About 1 percent of the Ca^{++} in bone is available in the form of amorphous salts for rapid Ca^{++} ion exchange.

The adult human body contains between 500 g and 800 g of phosphorus, and 85 to 90 percent of that is stored in the skeleton, combined with calcium in a ratio of Ca/P 1.3:2.0 on a weight basis, forming crystalline salts of hydroxyapatites (Guyton, 1986).

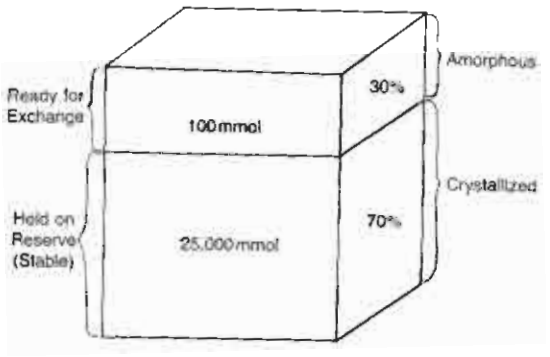

Fig. 2-1: Calcium in human bone. Seventy percent of the calcium salts containing about 25, 000 mmol are in crystallized stable state. Thirty percent of the calcium salts containing about 100 mmol are in amorphous exchangeable state. (Mettler, 1988)

2.1.4 Human Osteosarcoma

Bone sarcomas represent only 0.2% of all new cancers diagnosed, approximately 2,500 new cases are diagnosed in the United Sates annually (Fuchs & Pritchard, 2002). The incidence is approximately 3 cases per million people. Osteosarcoma is the most common primary bone tumour in humans and accounts for 20% of all bone malignancies (Fuchs & Pritchard, 2002). A biphasic incidence pattern is observed in human osteosarcoma, with the early peak occurring in adolescence as a primary cancer and then in the elderly as a secondary tumour associated with Paget's disease and irradiated bone (Fuchs & Pritchard, 2002). The human osteosarcoma stemming from abnormalities largely from chromosomal origin resembles canine osteosarcoma in histological appearance and biological behaviour (Slayter *et al.*, 1994; Fuchs & Pritchard, 2002; Ragland *et al.*, 2002). Osteosarcoma can arise in any bone but commonly occurs in the long bones of the lower extremity (Slayter *et al.*, 1994). Metastasis is to the lungs and occurs with a metastatic rate of 10-20% on presentation (Fuchs & Pritchard, 2002). Radiographic techniques used in the staging and diagnosis of human osteosarcoma include radiographs, CT, scintigraphy and MRI (Saifuddin, 2002).

The response to chemotherapy as measured by bone necrosis at the time of surgery is the single most important predictor of outcome in human osteosarcoma (Mercadante, 1997). Local control and control of metastasis are significantly achieved by chemotherapy. Surgery often includes limb-sparing techniques but may include amputation in more advanced cases (Mercadante, 1997). Conventional radiotherapy is typically not used in human osteosarcoma cases except peri-surgically for cytoreductive purposes (Mercadante, 1997). Few reports exist using targeted radiotherapy as a primary treatment, however where it has been reported a response to treatment has occurred (Bruland *et al.*, 1996; Franzius *et al.*, 1999; Sawyer *et al.*, 1999; Franzius *et al.*, 2001).

2.1.5 Human metastatic bone cancer

There are no reliable figures for the incidence of metastatic bone cancer, but from the one million people that die from cancer every year in the United States 70% are either from breast, lung or prostate cancer (Mundy, 2002). In the progressed state of the disease most of these patients have metastatic disease which would be estimated as 350,000 with metastatic bone cancer (Mundy, 2002).

The molecular pathways proposed for bone metastasis have been discussed and reviewed by Mundy, (2002). Osteolysis is not directly caused by the tumour cell but rather by activation of normal osteoclasts. While osteolytic or osteogenic bone lesions occur, generally both types of lesions exist in any one metastatic bone cancer (Mundy, 2002). In osteolytic lesions the primary target cell is thought to be the osteoclast. The metabolic pathways which lead to activation are mediated by the production of PTHrP/ PTH and Il-1, -6, -11 (Fig 2-2). These factors stimulate production via the osteoblast and stromal cells of the receptor activator of nuclear factor-κB (NF- κB) ligand (RANKL). PTHrP also has a negative effect on the production of osteoprotegerin (OPG). OPG functions as a decoy receptor that prevents binding of RANKL to RANK. Signaling through RANK in the osteoclast activates transcription factors AP1 and NF-κB, leading to osteoclast progenitors differentiating into mature osteoclasts (Mundy, 2002). Differentiation of osteoclast leads to an increase in bone resorption.

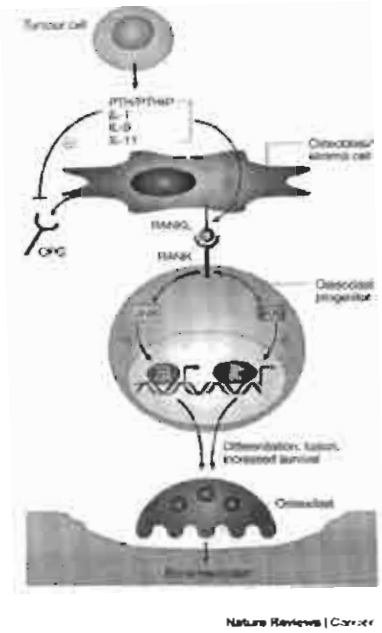

Fig 2-2: The RANK-RANKL system in osteolytic bone metastasis (Mundy, 2002)

In the case of osteoblastic lesions the model used is human prostate cancer which when undergoing metastasis produces a predominantly osteoblastic lesion. Production of factors such as fibroblast growth factors (FGFs), bone morphogenetic proteins (BMPs), platelet derived growth factor (PDGF), and transforming growth factor-β (TGF- β) by cancer cells stimulate osteoblast activity and bone formation (Mundy, 2002) (Fig 2-3). Proteases such as prostate specific antigen (PSA) are induced by urokinase (uPA). Proteases can activate latent TGF-β, release IGFs from inhibitory binding proteins (IGFBPs) and inhibit PTHrP, to promote bone formation (Mundy, 2002).

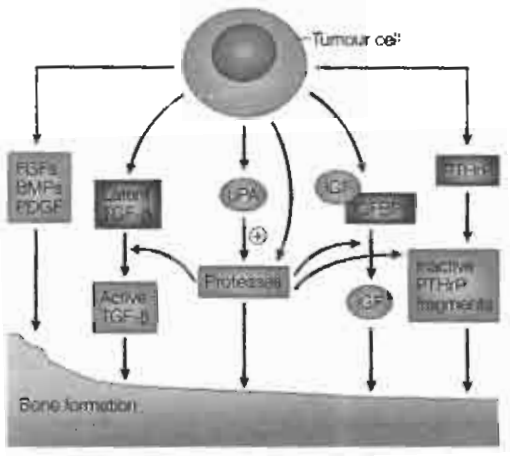

Fig 2-3: Model of osteoblastic bone metastasis caused by prostate cancer (Mundy, 2002)

Diagnosis of metastatic disease is similar as for osteosarcoma and includes radiographs, CT, scintigraphy and MRI (Forrest *et al.*, 1992; Leibman *et al.*, 2001; Davis *et al.*, 2002; Wallack *et al.*, 2002; Verma *et al.*, 2002). In most cases, this represents end stage disease and so commonly, the therapy is directed at palliation of bone pain (Mercadante, 1997). Therapy includes drug therapy, teleradiotherapy and radiopharmaceuticals. Commonly drugs used in the control of bone pain consist of non-steroidal antiinflammatory drugs (NSAIDS), narcotic analgesics and bisphosphonates which are the important aspect of this research. Teleradiotherapy plays an important role in the treatment of metastatic bone cancer, but is generally confined to single lesions or lesions confined to regional areas. Of primary interest eventually is the use of targeted radiotherapy for the treatment of metastatic bone pain (Bouchet *et al.*, 2000).

2.2 Bisphosphonates and Radionuclides

2.2.1 Bisphosphonates

The first indication that radioactive substances accumulate in bone came from the observations made in 1921 of luminous dial workers who had ingested radium (Bickel, 1921). In 1935 Chiewitz and Hevesey were the first to report the concentration of an artificially produced radionuclide, phosphorus-32, in bone. This deposition of phosphate in bone is the basis for what was to later become the most commonly used class of skeletal imaging agents, the technetium phosphates.

It was in 1958 that Bauer and Ray demonstrated that strontium-85 could be counted outside the body. Strontium-85, however, is not optimal for imaging or dosimetry, because it has a physical half-life of 65 days and releases a 510-keV gamma photon, but remained the radionuclide imaging agent of choice until the introduction of technetium-99m labelled phosphate (^{99m}Tc-P) by Subramanian and McAfee in 1971 (Subramanian & McAfee, 1971).

The ^{99m}Tc labelled radiopharmaceutical first described by Subramanian and McAfee (1971) was ^{99m}Tc-tripolyphosphate, which was one of a group of polyphosphate compounds having

in common a chain of phosphate groups bound by P-O-P bonds. Controversy soon followed regarding the optimal number of phosphate groups required for imaging (Dewanjee *et al.*, 1972; Subramanian *et al.*, 1972; Bok *et al.*, 1973; King *et al.*, 1973; Schumichen & Nakken, 1974; Rosenthall & Lisbona 1983). Pyrophosphate (PYP), (Fig 2-4) which contains the minimum number of phosphate groups possible (two), was found to have the best characteristics for imaging with ^{99m}Tc.

In 1972 hydroxyethylene diphosphonate (HEDP) (Fig 2-4) was introduced, (Subramanian *et al.*, 1972) which was the first of another class of ^{99m}Tc-P compounds, the bisphosphonates, which had in common multiple phosphate groups bound by P-C-P bonds. It had a faster clearance, greater deposition in bone, and better in vivo stability than pyrophosphate. In 1975 another bisphosphonate, methylene bisphosphonate (MDP), was introduced (Subramanian *et al.*, 1975), with 5 to 10 percent greater deposition in bone and a more rapid blood clearance than HEDP. It has since remained the most popular skeletal imaging agent, in spite of continous research (Fueger *et al.*, 2004).

Bisphosphonates form a family of drugs, which are characterized pharmacologically by their ability to inhibit bone resorption, and are pharmacokinetically similar in absorption, distribution and elimination (Lin, 1996). Development of bisphosphonates arose from the earlier studies which showed inorganic pyrophosphate P-O-P had the ability to bind strongly with calcium phosphate thereby inhibiting crystal formation, and to inhibit crystal dissolution in vitro (Lin, 1996). However, no effect in vivo was noted due to hydrolysis of pyrophosphate before it reached the bone (Lin, 1996). It was to resist hydrolysis that bisphosphonates were developed. They are characterized by P-C-P bonds.

Bisphosphonates are used as therapeutic agents for osteoporosis and bone pain associated with metastatic disease, Paget's disease, hypercalcemia of malignancy as well as in diagnostic nuclear medicine and targeted radiotherapy (Lin, 1996; Hahn *et al.*, 1990; Manolagas, 2000; Li *et al.*, 2001; Body & Mancini, 2002).

Since bisphosphonates are present at low levels in the plasma, their fate is best studied in the body once they have been labelled to ^{99m}Tc or ^{14}C. It needs to be noted that the radionuclide itself does effect organ distribution. ^{14}C radiolabelled palmidronate had a two fold greater uptake in bone than when labelled with ^{99m}Tc (Lin, 1996).

Most research into the antitumour effect of bisphosphonates has been in metastatic bone disease due to prostate and breast cancer (Body & Mancini, 2002). Some research has however been done into the effects of bisphosphonates in osteosarcoma (Pool *et al.*, 1988; Frith *et al.*, 1997; Body *et al.*, 1998; Giuliani *et al.*, 1998; Diel, 2000; Mackie *et al.*, 2001). Early results seem to show possible cytotoxic effects on osteosarcoma cell lines (Rogers *et al.*, 2000; Mackie *et al.*, 2001).

The basic philosophy around bisphosphonates in this field is that their principal target is bone (Subramanian *et al.*, 1973; Lin, 1996; Body & Mancini, 2002). Research has shown that the main effect of bisphosphonates is to inhibit bone resorption. It is thought that bisphosphonates are incorporated into the crystalline structure of exposed hydroxyapatite (lacunae). Bisphosphonates are released during resorption by the osteoclast and it thus results in inhibition of osteoclastic activity (Lin, 1996; Rogers *et al.*, 2000). Experimentally it has been shown that bisphosphonates disrupt intracellular metabolism that can lead to apoptosis (Ito *et al.*, 1999).

Most therapeutic bisphosphonates are given orally and are poorly absorbed. In the dog the bioavialability of etidronate and alendronate are 21 % (dosed at 50 mg/kg) and 1.76 % (dosed 10 mg/kg) respectively (Peter *et al.*, 1996; Mashiba *et al.*, 2001). Distribution is primarily to bone and with urinary excretion. Kinetically gastrointestinal tract (GIT) absorption of the drugs into the blood stream occurs via two pathways: transcellular (through cell) and intercellularly (between cells via tight junctions) (Lin, 1996). The size of bisphosphonates (> 0.150 kDa) plus their low lipophilicity and ionisation (negatively charged) prevent transcellular transport and significantly reduces intercellular transport (Lin, 1996). Absorption can further be reduced by complexing with calcium and other divalent cations. Oral absorption of bisphosphonates is dose-dependent, this is demonstrated by research which showed increase in bioavialability (0.5 % to 5 %) with inereasing dose (2 to 40 mg/kg) (Lin, 1996).

Although bisphosphonates have low lipophilicity at physiological pH (7.4) they are completely ionised and therefore expected to bind to plasma protein (Lin, 1996). They are indeed highly protein bound. However, this binding is concentration and calcium dependant. A concentration increase in the bisphosphonates in the blood leads to corresponding increase

in the unbound drug (Lin, 1996). There is also a species and drug variation in plasma protein binding, dogs and humans having a lower protein binding compared to rats, and clodronate is less bound than alendronate (Lin, 1996).

Bisphosphonates	Uses	MW (kDa)	Chemical structure
Alendronate	Medical therapy	0.221	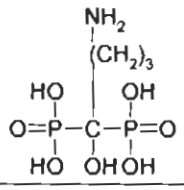
Clodronate	Medical therapy	0.240	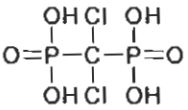
HEDP Etidronate	Medical therapy Radiotherapy	0.202	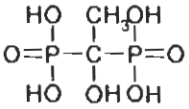
APD Palmidronate™ Aredia™	Medical therapy Radiotherapy	0.231	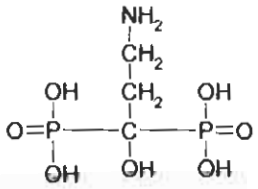
Tiludronate	Medical therapy		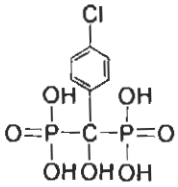
MDP Medronate	Diagnostic	0.172	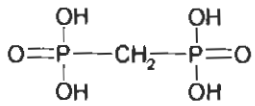
Ibandronate	Medical therapy	0.319	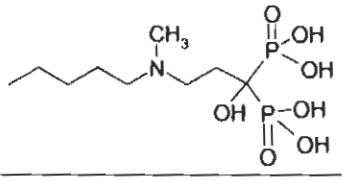

Fig 2-4: Phosphonates and phosphates: their uses, molecular weight and chemical structure.

Bisphosphonates	Uses	MW (kDa)	Chemical structure
EDTMP Lexidronate	Radiotherapy	0.428	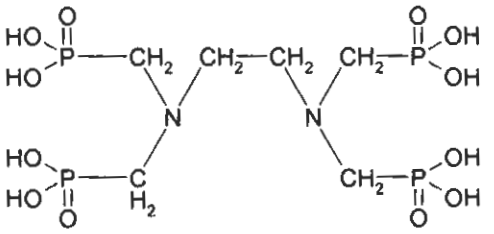
Risedronate	Medical therapy	0.283	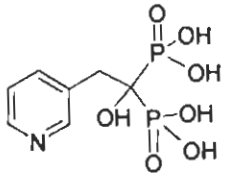
Zoledronate	Medical therapy	0.272	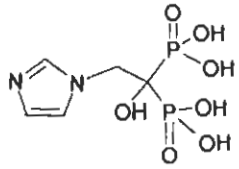
Pyrophosphate	Diagnostic	0.178	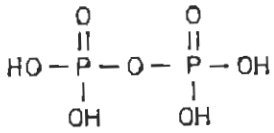

Fig 2-4: Phosphonates and phosphates: their uses, molecular weight and chemical structure.

To describe the kinetics of their tissue distribution a three-compartment model is the most appropriate. That is the blood pool, non-calcified tissue and bone or calcified tissue. There is a rapid distribution of bisphosphonates to non-calcified tissues. This is transient and is cleared rapidly from this tissue and transferred to bone or excreted by the kidneys. Bone shows an increase in uptake over time indicating movement of bisphosphonates from noncalcified tissue to bone. Non-calcified tissue can be made to retain bisphosphonates by high dosages given by rapid injection. The reason is thought to be due to binding of the bisphosphonates (due to high concentrations) with metals (calcium, iron, and magnesium) leading to large complexes which are phagocytosed by the liver and spleen (Lin, 1996). In mice, this has only been shown to occur, as with intravenous injection of clodronate, not with intraperitoneal or

subcutaneous injection. While this is experimentally important, it is unlikely that bisphosphonates will ever be given at high enough dosages clinically for this to occur.

Bone can of course not be regarded as a single compartment but rather to be consisting of trabecular bone and cortical or compact bone. It is known that the trabecular bone is metabolically the most active and therefore receives more blood, thus bisphosphonates show a higher accumulation in these areas. They would also display a proportionally larger amount of exposed hydroxyapatite crystals [$Ca_{10}(PO_4)_6(OH)_2$] due to bone resorption mediated by osteoclastic activity, as would areas showing increased metabolic activity such as injuries or cancerous bone. There is also a saturable uptake in bone for bisphosphonates with increasing dose as has been shown experimentally with alendronate and other bisphosphonates (Lin, 1996; Dormehl *et al.*, 1998) However if the dose is fractionated and given over time this effect seems to be ameliorated. There is also a gender and age difference in uptake; logically younger individuals have higher metabolic bone activity and therefore higher bisphosphonate uptake. Gender differences of lower uptake were only observed in juvenile females compared to juvenile male rats (Lin, 1996). No differences were found between adult rats. Where two bisphosphonates are administered together at high enough dosages competitive binding to exposed hydroxyapatite crystals occurs (Lin, 1996).

Little or no metabolism of bisphosphonates occurs within the body and they are consequently regarded as having low toxicity (Lin, 1996). Elimination from bone occurs over a prolonged period as the bisphosphonate is incorporated into bone and is only released when the bone undergoes resorption. Therefore, the half-life is dependent on the rate of bone turnover in the individual. The half-life for alendronate has been estimated to be 300 days and 10 years in dogs and humans respectively (Lin, 1996). In the rat this elimination from bone follows a biphasic manner and is thought to be due to different turnover in different parts of the bone. Elimination or excretion of bisphosphonates from the body is primarily through the kidneys. Research seems to indicate the process is a concentration-dependent saturable active transport mechanism (Lin, 1996). This process of excretion is not via the typical anion or cation renal transport systems since inhibitors of these systems probenecid and cimetidine respectively, when given at high doses in rats do not inhibit renal excretion of bisphosphonates (Lin, 1996).

2.2.2 Radionuclides

Radionuclides can decay by spontaneous fission, alpha decay, beta decay, electron capture, and isomeric transition (gamma emission).Only few of the more than 1000 existing radionuclides are clinically useful in diagnostic nuclear medicine, and for much the same reasons, suitable as tracers in drug development studies as applies in the present discussion. For these purposes suitable radionuclides have gamma energies between 20-600 kev and have physical properties such that a usable photon flux is available without excessive patient irradiation.The physical decay scheme largely determines the clinical detectability of the radiopharmaceutical, outside the patients body, whereas the chemical form determines the physical distribution and tissue localizing potential.

There are several ways in which suitable radionuclides are commonly produced,e.g. nuclear bombardment of stable elements in a nuclear reactor will produce unstable radionuclides with an excess of neutrons.These radionuclides usually undergo beta negative decay, followed by gamma emissions in order to reach stability. An example of an important (n,γ) reaction, as these are known, is in the production of ^{99}Mo, which is the parent nuclide of ^{99m}Tc through beta negative decay.

^{99m}Tc is currently the most widely used diagnostic clinical radionuclide. Its utility stems largely from its physical properties, which include the absence of particulate emissions, a half-life of 6 hrs, and a 140 kev photon which is ideally suited for use with conventional gamma cameras.The nuclide itself is prepared by separating it from the reactor-produced parent, ^{99}Mo. In generator systems (Fig 2-5) which are generally used in the clinic, molybdate is absorbed on an alumina column and ^{99m}Tc is eluted as pertechnetate ion using a 0.9% sodium chloride (saline) solution.^{99m}Tc has proved useful in imaging a wide variety of organ systems, and has been chemically attached to various carriers, including human serum albumin, macroaggregates of albumin, sulfur colloid, and polyphosphates, the latter of present interest.The technetium is primarily excreted via the gastrointestinal tract and kidney.The colon is the critical organ with respect to radiation exposure and receives 1-2 rads per 10 mCi of ^{99m}Tc-pertechnetate. For therapeutic radionuclides see Therapy paragraph 2.5 pg 48.

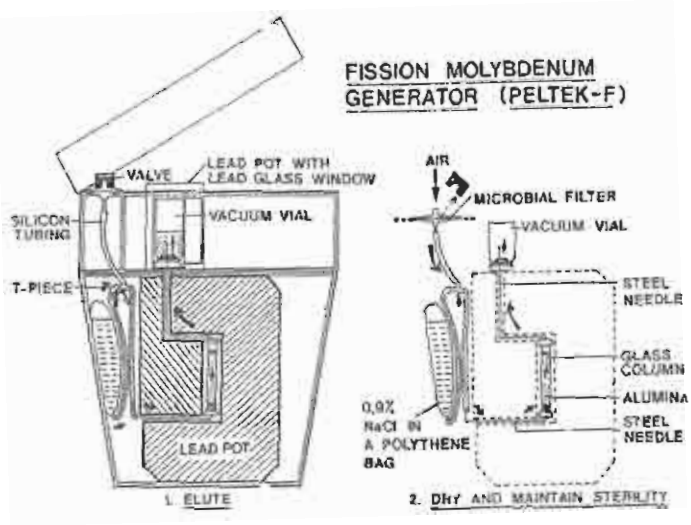

Fig 2-5: Fission molybdenum generator (Peltek F) interior view

2.3 Radiopharmacy and Scintigraphy

2.3.1 Radiopharmaceuticals

Labelling of phosphonate compounds with ^{99m}Tc to produce a radiopharmaceutical involves the use of the reducing agent stannous chloride dihydrate ($SnCl_2.2H_2O$), which when added to sodium pertechnetate (Na $^{99m}TcO_4$) and a phosphate/phosphonate compound in an acidic medium yields ^{99m}Tc-phosphate/phosphonate compounds. Other reducing agents such as ascorbic acid may also be used. If an oxidizing agent is present, stannic ions (Sn^{4+}) are generated, which can inhibit labelling. However, Coupal et al. (Coupall *et al.*, 1981) have shown that low concentrations of oxygen have little influence on either the radiochemical constituents or imaging quality.Commercial labelling kits are available from different manufacturers. Labelling yields are characteristically in excess of 95 percent, and the preparation remains usable for up to 8 hours after labelling. Inadequate labelling is manifested by visualization of technetium pertechnetate ($^{99m}TcO_4^-$) in the stomach, salivary glands and the thyroid. Najafi and Hutchison (1985) have examined the electrophoretic peaks of different MDP kits. Their results indicate that there are at least four different complexes that become labelled with ^{99m}Tc, depending on the age of the kit.

For most studies 10 to 30 mCi of the desired technetium phosphate/ phosphonate radiopharmacutical is administered intravenously,which yields a whole body and gonadal dose of 0.01 rad/mCi and 0.01 to 0.03 rad/mCi respectively. Blood clearance is relatively rapidly, with only 10 percent of the administered dose remaining in the bloodstream (mainly protein bound) at 2 to 3 hours. Approximately 50% is excreted in the urine by 4hrs through filtration and partial tubular resorption, which results in the bladder receiving the highest absorbed organ dose (0.1 to 0.2 rad /mCi). The majority of the remaining activity (~ 50%) localizes within the skeletal system within 1 hr and has an estimated biologic half-life of about 40 days (O'mara *et al.*, 1984). Scintigraphy is mostly done 3 hrs p.i.

The two principal factors that influence the accumulation of the technetium phosphate/ phosphonate compounds in bone are blood flow and extraction efficiency. A number of additional factors including capillary permeability, extracellular space hydrostatic pressure, electrical potential, and local changes in pH, probably exert their influence through changes in blood flow and extraction efficiency.

Skeletal uptake is not directly proportional to blood flow (Silberstein, 1984). It has been shown that an increase in blood flow of approximately 400% of normal results in about a 33% increase in ^{99m}Tc-MDP accumulation (Sagar *et al.*, 1979). An increased accumulation of radionuclide with the administration of sympathetic drugs, in the presence of tumour, infection, fracture, stroke, and neuropathy is most likely due to the inhibition of sympathetic control and the resultant recruitment of one third to one-half of the arterioles in bone that are normally closed (Shim, 1968; Thrall *et al.*, 1975; Charkes, 1980). It is believed that a much greater accumulation of radionuclide is observed in tumours, infections, fractures, because of marked enhancement of the extraction ratio in addition to an increase in blood flow. The 800% increase in accumulation of MDP in fracture sites, even though there is only a 100% increase in blood flow, has been attributed to an increased extraction ratio (Lavender *et al.*, 1979). The extraction ratio is in turn dependent on the amount of reactive new bone formation. The same effect of reactive new bone formation causing an increased extraction ratio occurs with osteoblastic tumours and osteomyelitis.

Which of the two major components of bone, the mineral or organic matrix, captures technetium phosphate compounds is not certain. A variety of investigations have suggested

that in normal bone, fractures, and neoplasms, the predominant deposition is in the mineral matrix. (Greiff, 1978; Christensen & Krogsaard, 1981). It is hypothesized that there is chemisorption at kink and dislocation sites on the hydroxyapatite crystals, with release of tin and which are hydrolysed and bound to bone either separately or together as hydrated tin oxide and technetium dioxide.

2.3.1.1 Quality control

Quality assurance is usually achieved through the combined efforts of reagent manufacturers, cyclotron and reactor operators, radiopharmaceutical manufacturers, and practitioners who prepare and ultimately administer the radiopharmaceutical to patients. To determine the suitability of particular samples of a radiopharmaceutical for human use, or in research and development quality control includes assessment or reassessment according to the following characteristics:

1. Biological criteria primarily refer to toxicity, sterility, apyrogenicity and therefore safety for application. Cell cultures and rodents are used according to prescribed protocols (United States Pharmacopoeia (USP), Nuclear Regulatory Commission (NRC)) for these checks.
2. Radionuclide purity describes the presence (undesirable) of other nuclides in a given radiopharmaceutical because of the increase in radiation exposure and false biokinetic information. A common example here is the presence of ^{99m}Mo breakthrough during the eluation of the ^{99m}Mo/^{99m}Tc generator with saline to obtain sodium pertechnetate for further use. This type of contamination is usually easily detected by using a scintillation counter and scaler, e.g. a dose calibrator or multichannel analyser which permits the detection and quantitation of any other gamma-emitting radionuclides that may be present.
3. Radiochemical purity describes the proportion of the total radioactivity in the desired chemical form. For example, if ^{99m}Tc-labelled diphosphonate contains 5 percent of the radioactivity of ^{99m}Tc-pertechnetate, the radiochemical purity is 95 percent. It is important that radiopharmaceuticals have an acceptable level of radiochemical purity. Not only do radiochemical impurities fail to generate useful information in nuclear medicine studies, but they can result in image degradation and unnecessary radiation

dose to the patient. ^{99m}Tc-pertechnetate increases background activity attributable to stomach, gut, and thyroid uptake (Vine & Wahl, 1982).

Chromatography has become the most widely used analytic tool for determining radiochemical purity. It separates a chemical mixture into its components by virtue of their differences in partition coefficients in certain solvents and support media, such as ethanol-acetone. The solvent moves along (up or down) the support medium by adsorption and capillary action, thus resolving the components of a radiopharmaceutical. These components are the pure radiopharmaceutical and its radiochemical impurities, under usual circumstances, free pertechmetate (TcO_4^-) and hydrolyzed reduced technetium (R-Tc) in the case of technetium. These different radiochemical species distribute themselves along the adsorbent (paper, silica gel, or silicic acid).

Paper chromatography can be either the ascending type, in which the mobile phase moves up, or the descending type, in which the mobile phase moves down the paper. Paper chromatograms (usually 20 to 30 cm in length) develop slowly and may take several hours.

Instant thin-layer chromatography (ITLC) is developed in the ascending manner and requires only 10 to 20 minutes for development. After the solvent front (S_f) moved the desired distance, the strip is removed from the chromatography chamber to dry. The strip is then cut into segments and the radioactivity of each segment is measured in an appropriate counter. The relative front (R_f) is a ratio determined by dividing the distance from the centre of its activity on the strip to the origin by the distance from the solvent front to the origin. The R_f values are determined with known radiochemical species. An R_f value of 1.0 means that the compound moves with the solvent front, whereas an R_f value of 0 means that the component remains at the origin.

a) ^{117m}Sn-PEI-MP
•ITLC-SG / Ethanol
–Rf = 1 : ^{117m}Sn
–Rf = 0 : ^{117m}Sn-PEI-MP
•Whatman 31ET/Citrate
–Rf = 1 : ^{117m}Sn-PEI-MP
–Rf = 0 : colloid
•Labelling efficiency
– » 99%
–Stable for 24h

b)

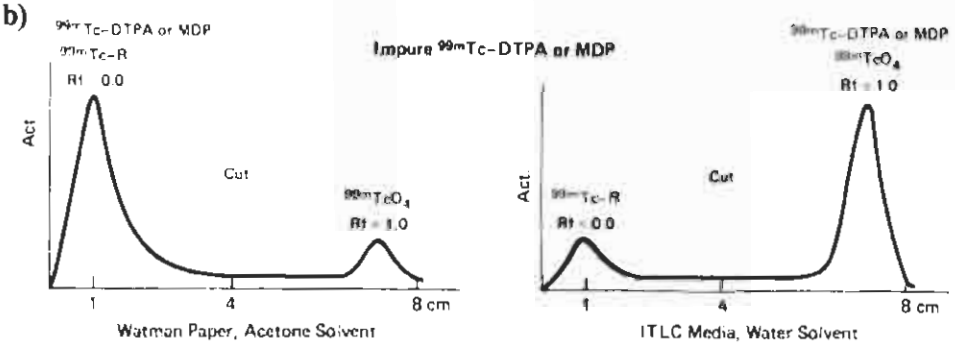

Fig 2-6: (a) ^{117m}Sn-PEI-MP quality control-example, (b) representative chromatograms of impure ^{99m}Tc-labelled products. (Kim, 1987)

2.3.2 Scintigraphy

2.3.2.1 The Gamma camera

The gamma camera records or images the distribution of radioactivity present in the patient (Fig 2-7a). The collimator is the initial image-defining component of the system and consists of energy-absorbing material e.g. lead between the patient and the gamma camera head in which one or more apetures admit radiation selectively from predefined sectors of space, thus mapping a projection of a selected volume of patient space onto the crystal plane of the camera head (Fig 2-7b). The parallel-hole collimator, generally in use in the clinic, has thousands of parallel channels uniformly distributed with their long axes perpendicular to the

crystal face (Fig 2-7 a, b, c). These channels are mostly hexagonal which improves sensitivity by an increased ratio of exposed-to-shielded crystal surface.

a) b)

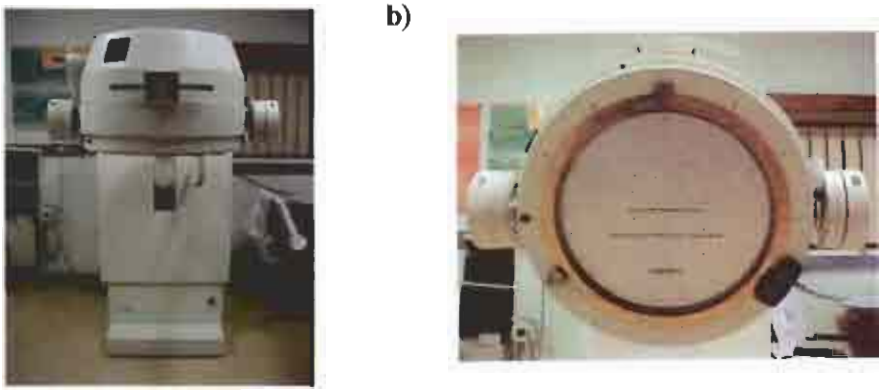

Fig 2-7: (a) Gamma camera as a unit and (b) the camera head

The walls of these channels, called septa, must be thick enough to prevent gamma rays from crossing channels on their way to the crystal. To maintain such septal penetration at an acceptable level (below 5%), a typical low-energy (<150-keV) collimator should have a septal thickness of ≥ 0.3 mm of lead whereas a typical medium-energy (< 400-keV) collimator requires a septal thickness of ≥ 4.65 mm of lead (both having hole diameters of 2.5 mm and channel lengths of 25 mm). Increased septal thickness diminishes sensitivity by reducing the ratio of exposed-to-shielded crystal surface.

a) b) c)

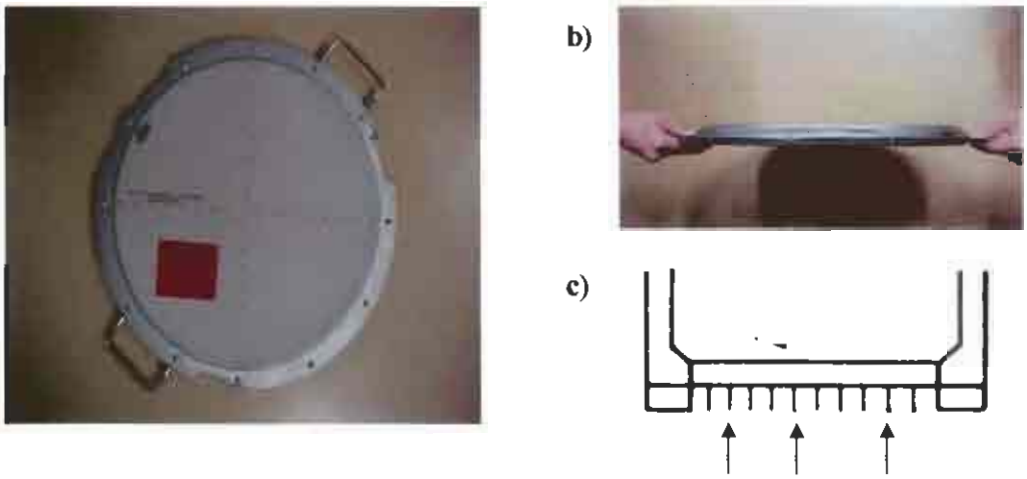

Fig 2-8: (a) Collimator view from the top and (b) from the side, (c) Schematic diagram (cross section) of a parallel hole collimator: only parallel entering rays will pass to the crystal (Kim, 1987)

In collimator design, resolution and efficiency are always in competition; the parallel-hole collimator provides the best trade off between these two performance characteristics for large-organ imaging procedures (Keller, 1968).

In the detection head of the conventional gamma camera, a suitably collimated gamma ray originating from within the patient hits the large (typically 54.6 cm in diameter and 1.27 cm thick) thallium activated sodium iodide crystal, producing a scintillation of light (Fig 2-9). The scintillation is detected by a bank of phototubes arranged in a closely packed hexagonal array, and optically coupled to the crystal. The light from the scintillation divides among the phototubes; those tubes close to the event will receive more light than those furthest away. Each tube converts the light it registered from a scintillation to a voltage pulse;each pulse is proportional in amplitude to the amount of light each tube received. The pattern of voltage pulses from all phototubes resembles the original scintillation distribution on the crystal and are "fixed" into graphical X- and Y-signals by positioning or localization matrix circuitry. The sum of the outputs from all of the PM tubes, the Z-signal, is proportional to the total amount of light produced by the scintillation event, i.e. the deposited energy of the incident gamma ray, and is input to the pulseheight analysers which determine whether the event is to be registered or discarded.

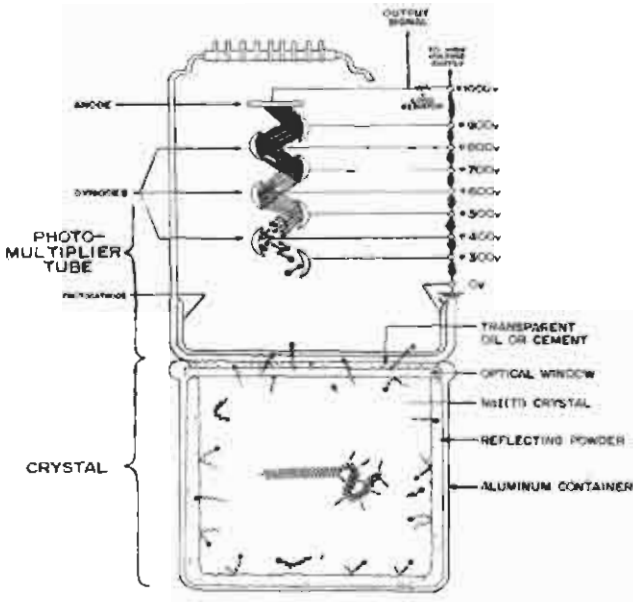

Fig. 2-9: Schematic representation of scintillation detection processes in the crystal and photomultiplier tube (Designed from Bernard *et al.*, 1976)

The pulse height analyzers (PHAs) or multichannel analyzers (MCAs) are voltage discriminators whose upper and lower limits are set to correspond to the photopeak(s), i.e. the energy peak characteristic of the isotope(s) being imaged. These limits define energy "windows" which may be either symmetric (i.e., centered upon a particular photopeak) or asymmetric (i.e., with a lower limit closer to and an upper limit further above the photopeak for a given window width), the latter mostly to reduce scatter (Gottschalk & Potchen, 1976).

The signalling processing circuitry in modern cameras is significantly more complex than the foregoing description suggests and varies considerably among manufacturers. Much of the circuitry, e.g., preamplifiers, pulse-height analyzers, etc., can be mounted directly onto the individual PM tube bases or adjacent circuit boards to minimize distortion associated with signal transmission to the console. Signal output to the console may be in digital format to further reduce distortion (Erickson & Rollo, 1983). The image storage and display system record the location of each scintillation event accepted by the pulse-height analyzers on both a permanent storage medium (ranging from film to digital memory) and a real-time display (CRT). Successive scintillations occurring in the same location in the crystal are mapped into the corresponding location in the storage medium and summed. In modern, computer based systems these events are mapped into a digital data matrix ranging in resolution from 32 x 32 to 512 x 512 picture elements or pixels. Such systems are not limited by the contrast and latitude limitations of film and therefore accurately record all of the dynamic range of the image.

2.3.2.2 The Computer

Camera/computer interface is accomplished by an acquisition processor, one or more analog to digital converters, and a buffer/image memory. New cameras digitize the X,Y,Z output at the detector. The acquisition processor controls certain camera functions, including zooming, improved spatial resolution, gated cardiac studies. The operator/computer interface is accomplished through terminal and display processors linked respectively to an operator console and one or more display devices, e.g. a video monitor. The typical console consists of an alpha numeric keyboard and cursor control, e.g. a tracker ball for graphic interaction with the processor (Fig 2-10). The user typically communicates with the operating system through a menu structure of commands encompassing the majority of commonly performed functions. Acquisition and analysis programs offer a number of common options (Sarper, 1984).

Fig 2-10: Operator/computer interface through terminal and display processors, a keyboard and cursor/tracker ball control.

Data acquisition is performed in one of two basic formats: matrix (frame) mode or list (serial) mode. In frame mode, scintillation events in the crystal are mapped into specific X, Y coordinates in memory (i.e. pixels) corresponding to their location in the crystal. Each new event occuring in any given pixel is summed to those previously recorded there. This mode may be used to acquire static, dynamic, or ECG gated studies.

Static frame mode acquisitions require predefinition of frame size and pixel depth (byte or word) appropriate, respectively, for the resolution and maximum count density of the study. Acquisition is terminated by specifying time, counts, or count density. This mode is commonly utilized to acquire multiple images from different projections as in regular bone scans and enables subsequent quantification of tracer distribution but provides no information regarding temporal changes.

Dynamic frame mode acquisition consists essentially of predefined series of frames acquired at predefined rates for a predefined number(s) of frames. This type of acquisition can often be subdivided into sequential phases of differing rates. Frame size and pixel depth must be specified. Although temporal information is thus preserved, there is little flexibility for reformatting of data, and image statistics degrade with increased temporal resolution.

Data analysis or processing encompasses all of the image enhancement, data restructuring, and data quantification functions available to the operator through the software. They are

typically accessed through the menu structure of the software and often may be linked into strings of commands, called macros.

Image enhancement includes those functions available to better define anatomic structures of interest on a visual display format. Included are basic functions such as background suppression and contrast modification as well as more sophisticated functions such as image smoothing, image filtering (both spatial and temporal), and various edge-enhancement techniques utilized to better define the margins of organs or other structures.

Image quantification software performs two generic functions: definition of that portion of the data to be quantified and the actual quantitative procedure(s). The most common method for defining regions of a study to be quantified, called regions of interest (ROI) definition, is to outline them or "paint" them with a light pen, cursor, or other means of graphic interaction (Fig 2-11). For special purposes, edge detection subroutines of varying sophistication are available to define manual estimations of an organ boundary. Extended over multiple frames of a temporal study involving a moving organ (e.g., the heart), these become edge-tracking subroutines.

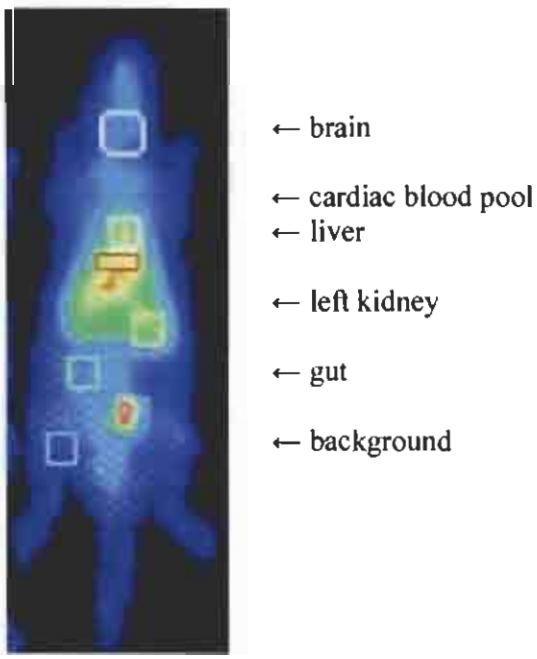

Fig 2-11: Example of a scintigraphic image of a rat with typical regions of interest (ROIs) defined.

Once one or more ROIs have been defined, the software can be instructed to quantitate the activity within these regions, determine their variation with time, fit these data to various

mathematical functions, or compare them or plot them in variety of formats for example the familiar time-activity curves (Fig 2-12). Mathematical operations such as integration, differentiation, smoothing, statistical fitting can be performed on this data to obtain biodistribution and/or biokinetics of the pharmaceutical under investigation.

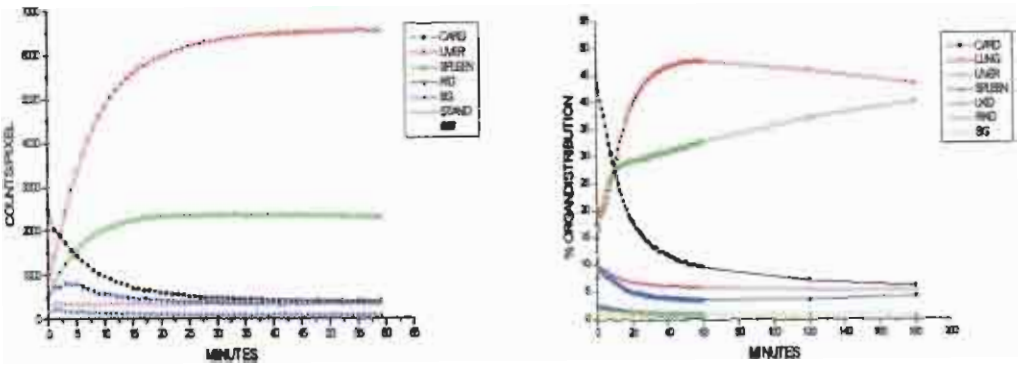

Fig 2-12: Examples of dynamic and % organdistribution graphs, as obtained from count rates temporally acquired.

2.3.2.3 Quality Control

The instrumentation employed in the modern nuclear medicine laboratory has evolved in a systematic fashion from a core of devices designed to detect the radiations emitted by radioactive materials through specific, well-known interactions with matter (ionization and scintillation). The basic detector technology is well established, and recent improvements in hardware performance have resulted largely from technical refinements. Despite technical sophistication the reliability of diagnostic information should remain a primary objective and it calls for regular quality assurance.

The interpretation of static images and dynamic function studies is critically dependent upon the quality of the images and the data generated by the scintillation camera. Changes in the camera performance can be detected by the evaluation of serial images of various test devices: uniform radioactive sources, bar phantoms, and special configurations of radioactivity and absorbers designed to simulate organs and lesions (Kim & Haynie, 1987).

The quality checks of collimator and detector head mounting, energy calibration of pulse-height analyzers, flood-field uniformity, sensitivity, and background-count rate, should be carried out each day the instrument is used (Kim & Haynie, 1987).

2.4 Bone Scintigraphs

2.4.1 Normal bone

Such scintigraphy using ^{99m}Tc-bisphosphonates is usually performed with a large field of view gamma camera and a low energy high resolution collimator. Static images are obtained about 3 hours after i.v. injection of the radioactive tracer. Although the maximum contrast (bone to background counts) is achieved at 4-6 hours this becomes an impractical point to scan post injection, and 3 hours is generally regarded as acceptable.

The quality of bone scans is dependent on several factors. Adequate hydration is required to maximise renal clearance, thus reducing tissue background and increasing the lesion to background ratio. Normal renal function is therefore also a requirement. Obesity which increases the target to detector distance increases scatter of the photons, as well as their absorption by overlying tissue, which all degrade the quality of bone scintigrams. High energy radionuclides, such as ^{188}Re and ^{166}Ho would require high or medium energy collimators for good scintigraphy whereby the images are not degraded from septal penetration. Radiopharmaceutical quality control is important to ensure adequate labelling efficiency, as well as to minimise the presence of particulate material, such as colloids, that will also degrade the images.The time between the injection and imaging will determine the amount of background activity that is present. Numerous drugs have been shown to affect the biologic distribution of bone-imaging agents (Alazraki, 1984).

Normal bone scans also demonstrate increased radiopharmaceutical uptake where the bone has maximum stress and modelling, particularly in areas of muscular attachment. The long bones are usually best defined at their ends, with the knees sometimes particularly prominent due to the relatively large mass of bone and less overlying tissue. In normal human adults (Fig 2-13) visualization of the distal long bones, particularly the radius, ulna, and fibula is often difficult on bone scans. In children and young adults bone scans are characterteristically of

better quality due to less overlying tissue, better renal clearance and increased osseous activity. The most prominent difference is significant activity in the growth plates near the epiphyses of long bones. At the other end of the spectrum a normal bone scan in elderly adults, particularly women, will show decreasing definition of ribs and fine details (Wilson 1981).

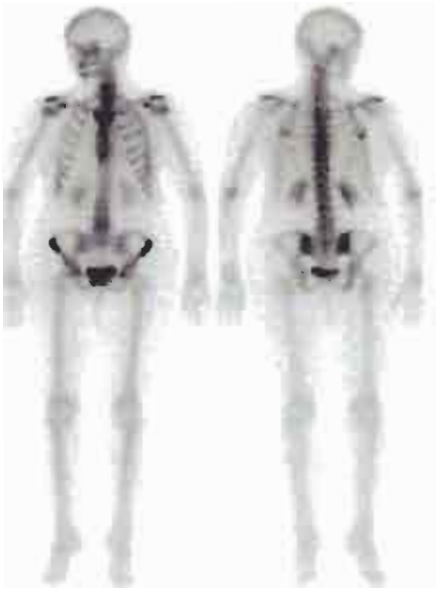

Fig 2-13: The normal human skeleton, anterior and posterior views

2.4.2 Traumatic Fracture in Humans

Nuclear medicine procedures allow for the detection of fractures in human patients by bone scintigraphy within hours of injury. Good quality images are, however, required for the detection of such fractures. Improved image quality can be obtained in most patients from delayed images, e.g. at 8 to 24 hours after injection. This allows the soft tissue clearance of the radiotracer to be maximal, and a focal abnormality is better detected because of the improved target to background ratio (Martin, 1983).

The scintigraphic pattern of fractures changes over a period of time, with three distinct stages apparent. The first phase (acute) persists for approximately 2 to 4 weeks after injury and is characterized by a diffuse region of increased tracer concentration around the fracture site. A distinct fracture line may be seen in this stage, especially in delayed images. The second

phase after 6 weeks (subacute) is characterised by a well-defined linear abnormality at the site of the fracture. This stage could last for 8-12 weeks and illustrates the most intense uptake at the fracture.The third and healing phase is characterized by a gradual reduction in the radioactive intensity of the abnormality, until the bone scan returns to normal. This time to reach a normal bone scan extends well beyond the time for clinical or even radiographic healing because of the increased metabolic activity and bone remodelling depicted here and that can take place for considerably longer than might be expected clinically. Compound fractures, or patients in whom orthopaedic devices, such as rods or screws are used require considerably more time for the bone scan to return to normal. Patients with delayed union or non-union may also show prolonged periods of radiotracer concentration at the fracture site (Fig 2-14). A distinction between delayed union and non-union may be difficult both clinically and scintigraphically, although follow-up scans may be of assistance in making the differentiation (Desai *et al.*, 1980).

Fig 2-14: Non union bone with radiotracer lingering around fracture site (Mettler, 1988)

2.4.3 Osteosarcoma

Radionuclide bone scanning is sensitive in the detection of most primary malignant bone tumours. Although there is some correlation of scan characteristics with the histologic type of tumours, (Mclean & Murray, 1984), the tissue specificity is much poorer. Additionally there are no scan characteristics to prove that a lesion is definitely malignant or benign. There are,

however, general characteristics of malignant tumours (e.g., very marked uptake) that are suggestive of malignancy. Scintigraphic characteristics potentially may be of value in lesions that are radiographically indeterminate; however the appearance of the lesion on routine radiography will, in general, be more diagnostic of tumour type. The main use of diagnostic radionuclide bone scanning in primary osseous tumours will be to confirm the presence of the lesion, or maybe multiple lesions, to assess the margins of the lesion, which is useful in therapy follow-up, and to detect metastatic disease (Fig 2-15).

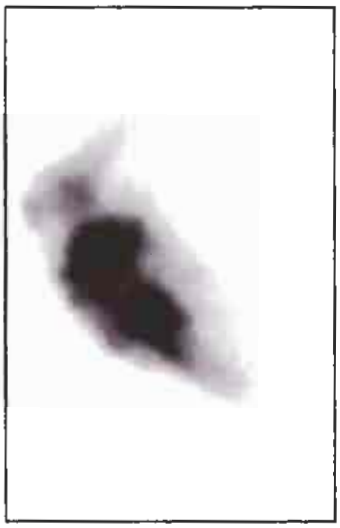

Fig 2-15: Osteosarcoma, very marked uptake with well visualised margins

Radionuclide bone scans have been very useful in the initial management of patients with osteosarcoma. Osteosarcoma appears to be very "hot" on the scintigram. Metastases within the same bone or distant to other bones can be detected by the bone scan. There is a significant tendency, however, for the margin of the actual tumour to be smaller than suggested on the radionuclide scans (Mckillop *et al.*, 1981; Chew & Hudson, 1982; Lamb *et al.*, 1990; Leibman *et al.*, 2001). This extended pattern is thought to be due to either hyperaemia associated with the tumour, marrow hyperaemia, medullary reactive bone or periosteal new bone adjacent to the tumour (Berg *et al.*, 1990).

In addition to distant skeletal metastases being identified, some nonosseous metastases may be detected with the technetium-phosphate scan, especially within the lungs (Goldstein *et al.*, 1980; Mcneil & Hanley 1980; Brown 1983; Gilberg *et al.*, 1983; Sandler *et al.*, 1984; Picci *et al.*, 2001).

2.4.4 Metastatic Disease

Accurate tumour staging is of prime importance in oncology (Saifuddin, 2002). There are marked differences in patient therapy and prognosis based upon the actual stage of disease. For example radical surgery is rarely indicated for tumours that have metastasised, but such surgery may be life saving in localised or regional disease.

Following the initial tumour staging, the patient's follow-up may rely on radionuclide bone scanning for evaluation of therapeutic response, bone pain, and screening of the symptomatic or asymptomic patient for metastatic disease. Although the early detection of metastatic disease may not affect outcome, it is useful both for prognosis and to prevent complications such as pathologic fractures of weight-bearing bones by early radiation therapy of metastasis.

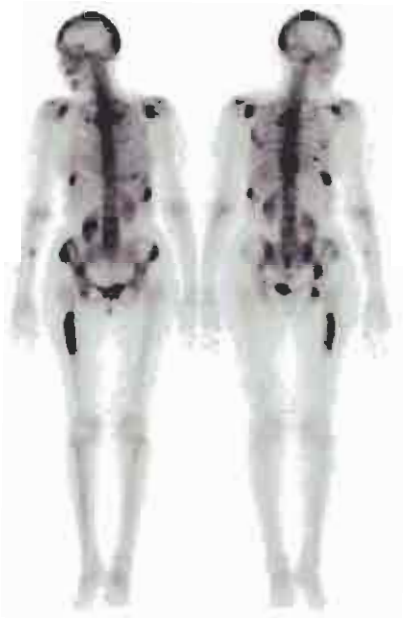

Fig 2-16: Metastatic bone tumours, anterior and posterior views

Some tumours, such as breast and prostate, have a propensity for early and asymptomatic metastases to bone. Conventional radionuclide bone scanning is very sensitive for detection of bone metastases in most neoplasms, with an overall false-negative rate approaching 2 % and a false-positive rate approaching 10 % (Muroff, 1980).

The typical appearance of osseous metastases is multiple noncontiguous asymmetric focal areas of increased activity (Fig 2-16). In metastatic disease, the distribution of lesion involvement is as follows: thorax and ribs, 37%; spine, 26%; pelvis, 16%; limbs, 15%; skull, 6% (Wilson & Calhoun, 1981).

2.5 Therapy

2.5.1 Radiation Effects from Radionuclides

Multi-site bone pain is a common symptom in advancing malignancies and may be difficult to manage effectively. Targeted radiotherapy using bone seeking radiopharmaceuticals offers the advantage of treating multiple pain sites simultaneously while minimizing toxicity to healthy tissues (Lewington, 1996). Sixty to eighty percent of patients with refractory symptoms benefit from this approach, up to 25 % reporting complete pain relief. Treatment is generally well tolerated, toxicity being limited to temporary myelosuppression.

Appropriate patient selection is critical to treatment success. Sites of pain should be correlated with focal abnormal uptake on conventional bone scintigraphy. Radiopharmaceutical uptake and retention are generally higher in osteoblastic metastases than in predominantly osteolytic disease, and has also been reported in osteosarcoma. Patients should be haematologically and biochemically stable before treatment. Contraindications to target therapy include limited bone marrow reserve and acute spinal cord compression, which should be managed by external beam radiotherapy (Serafini, 2001).

Any subatomic particle bearing an electric charge and having kinetic energy sufficient to produce ions will interact or *couple* strongly with the orbital electrons in any medium, such as tissue, through which it passes. Because of the strong coupling, energy losses to the orbitals will take place at closely spaced intervals even in the case of sparsely ionizing highly relativistic electrons. Charged particles having the requisite energy are said to be *directly ionizing*.

Directly ionizing particles lose energy to the orbitals in a number of relatively small increments. An occasional encounter may transfer enough energy to permit the ejected

electron to produce a recognizable ionization trail of its own. The average energy transfer, however, is less than 100 eV and the most probable transfer only 20 eV.

Spatial distribution patterns of ionizations and energy excitations will depend on the type of *quality* of the radiation producing them. Any relation between the biological and chemical effect and radiation quality must depend on the distribution patterns rather than inherent differences in the radiations themselves, for all are ultimately effective through ionizing electrons. The excitation and ionization pattern, and hence the biological effect, of an individual electron of given energy is independent of the nature of the radiation that produced it.

With these physical properties in mind, several radiopharmaceuticals have been developed for bone pain palliation. These include strontium-89 chloride , samarium-153-EDTMP and rhenium-186 HEDP (Atkins, 1998; Bouchet *et al.*, 2000). All of these are prepared by neutron irradiation of the respective suitable enriched isotopes in a nuclear reactor, followed by the relevant chemical processing. Factors influencing treatment selection include time to response, predicted response duration and myelotoxicity, all of which reflect the half-life of the radionuclide administered and dose rate achieved (Andrews, 1974). Treatment can be repeated to manage recurrent pain, although toxicity is cumulative in patients with advancing refractory malignancy.

^{153}Sm-EDTMP consists of ^{153}Sm complexed to the octa-anion ethylenediaminetetramethylphosphonate (EDTMP) and has extensively been studied (Goeckeler *et al.*, 1987; Holmes, 1992; Bruland *et al.*, 1996; Dormehl *et al.*, 1998). The high affinity of EDTMP for bone, coupled with the nuclear properties of ^{153}Sm (t½ = 46.75 h; maximum ß-particle energy = 0.8 MeV (1.3 x 10^{-13}J)), enables the radiopharmaceutical to alleviate the pain associated with metastatic bone cancer. This is a relatively mild treatment and after 7 weeks further treatment is necessary once radiation levels have declined and the pain palliation subsides (Alberts *et al.*, 1997). In order to improve the efficacy of the radiopharmaceutical, ^{153}Sm was replaced with ^{166}Ho, which has a higher-energy ß-particle (t½ = 26.9 h; maximum ß-particle energy = 1.86 MeV (3.0 x 10^{-13}J)). Although the chemistry of Ho and Sm is approximately similar (both are lanthanides), the skeletal localization of ^{166}Ho-EDTMP proved to be inferior to that of ^{153}Sm-EDTMP (Jarvis *et al.*, 1995) as the ^{166}Ho-EDTMP complex has a different biodistribution from that of ^{153}Sm-EDTMP (Dormehl *et al.*,

1993). No reliable response predictors have been identified although both reponse rate and quality of response are higher in patients treated early in the natural history of their disease than those with very extensive osseous metastases.

The radiobiology of targeted therapy for bone pain palliation is poorly understood. Issues requiring clarification include the existence of an absorbed dose threshold for pain relief, single administration versus fractionated treatment and the therapeutic potential of multi-modality therapy (Thrall, 1998).

One theory as to how radiopharmaceuticals work in pain palliation treatment is that the radionuclide is carried by the bone-seeking ability of its carrier (ligand) to areas of increased osteoblastic activity, where it then chemisorbs to the osseous tissue. Increased osteoblastic activity will be the result of the preceding increased osteoclastic activity, which, in turn, is a feature of metastatically affected areas of bone. Furthermore, prostate cancers initially metastasise almost uniformly as osteoblastic metastases. Radiation of the attached radionuclide will then cause death in a percentage of cells within the range of the ß-particle (3 mm soft-tissue penetration for ^{153}Sm and 8 mm for ^{166}Ho) or of the Auger electron (<1 mm for ^{117m}Sm). The resulting decrease in intra-osseous mass and pressure brings relief to the patient. However, it is found that the reduction in pain levels takes a few days, i.e. before the tumour cell mass shrinks. The mechanism is therefore more complex. One of the most radiation-sensitive cell types is the lymphocyte, which secretes a variety of cytokines that have been associated with pain modulation. Lymphocyte cell death at the tumour site is responsible for this rapid pain reduetion (Thrall, 1997).

Early reports indicate that superior response rates may be achieved by combining targeted treatment with conventional or low dose chemotherapy (Deregis *et al.*, 2003). The mechanism for this apparent synergy is unclear and merits further investigation. Other options for multi-modality pain control in combination with radionuclide treatment include bisphosphonate therapy, external beam radiation and radio frequency ablation.

Targeted therapy represents a logical, safe and effective approach for the management of multi-site metastatic bone pain and could be useful for osteosarcoma. The future lies in early intervention to achieve prolonged symptom control and in research to investigate novel radiopharmaceutieals for enhancing treatment efficacy.

New therapeutic radiopharmaceuticals could include different radionuclides with improved physical properties and/or modifications of ligands (Washiyama *et al.*, 2004). Such alternatives under investigation include, apart from ^{166}Ho, the two rhenium radionuclides, ^{186}Re and ^{188}Re, as well as ^{117m}Sn (Table 1.1).

^{188}Re-HEDP appears to fulfil the criteria of a good radiotherapeutic agent as it has stronger beta emision then ^{153}Sm and ^{186}Re (Knapp *et al.*, 1997; Lin *et al.*, 1997). An important consideration in ^{188}Re is that it is derived from a Tungsten-188/Rhenium-188 generator and therefore promotes ease of clinical application (Knapp *et al.*, 1997; Lin *et al.*, 1997). It has been reported on for palliation of bone pain in metastic bone cancer (Maxon *et al.*, 1992; Hsieh *et al.*, 1999; Li *et al.*, 2001). In a study by Palmedo *et al.*, (2000), the maximum tolerated dose of ^{188}Re-HEDP in prostate cancer patients with osseous metastases who were suffering from bone pain was investigated. Li *et al.*, (2001) also treated numerous patients to evaluate toxicity and control of bone pain in metastatic bone cancer. No reports were found in the literature on the use of ^{188}Re-HEDP in human or canine osteosarcoma.

^{186}Re-HEDP is well documented in the literature as an effective radiopharmaceutical for the palliation of metastatic bone pain (De Klerk *et al.*, 1997; Limouris *et al.*, 1997; Atkins, 1998; Palmedo *et al.*, 1999; Giakkakenas *et al.*, 2000; Liepe *et al.*, 2000; Brenner *et al.*, 2001). A single case report by Sawyer *et al.*, (1999) sought to demonstrate the usefulness of targeted radiotherapy using ^{186}Re-HEDP as a method for dose escalation in the treatment of osteosarcoma.

^{89}Sr and ^{32}P are commonly used in human medicine for bone palliation (Atkins, 1998; Liepe *et al.*, 2000; Kvinnsland *et al.*, 2002). A report comparing ^{153}Sm-EDTMP and ^{89}Sr distribution in canine osteosarcoma bone found a more uniform distribution for ^{89}Sr in the cancer and a lower radiation dose to bone marrow (Schoutens, 1988; Robinson *et al.*, 1995; Kvinnsland *et al.*, 2002).

A relatively new radiopharmaceutical ^{117m}Sn-DTPA has been reported to be effective in controlling metastatic bone pain (Atkins *et al.*, 1993; Srivastava *et al.*, 1998; Swailem *et al.*, 1998; Bishayee *et al.*, 2000). No reports were found in the literature on the use of ^{117m}Sn-DTPA for osteosarcoma.

^{117m}Sn is produced from enriched ^{117}Sn and activated by a (n,n') reaction for which the neutron capture cross-section is small, *viz.* 2.3 barn. It is therefore difficult to reach the high levels of specific activity that are needed for therapeutic purposes and this can only be done in high-flux research reactors like the Oak Ridge HFIR in the USA and the Petten HFR in The Netherlands. Although difficult to produce with the required specific activity, the interest in ^{117m}Sn arises from its favourable half-life (13.6 days) and discrete particle range (0.2-0.3 mm) in bone tissue, as compared with ^{153}Sm, ^{32}P and ^{166}Ho. Because it emits mono-energetic conversion electrons instead of a ß-particle the localized radiation permits large bone radiation doses without excessive radiation to the bone marrow. In addition, ^{117m}Sn as an Auger emitting radionuclide will introduce a highly localized distribution of electrons once inside the cell. Auger emission is a radioactive decay triggered by capture of an inner shell electron of the atom by the nucleus followed by emission of a cascade of electrons from the K and L electron shells. These electrons normally have a very low energy and therefore a very limited tissue range. Up to 25 electrons can be emitted, resulting in a local, high-density radiation. Together with the recoil of the daughter nuclide, which exists as a highly charged cation (up to +20), it has the potential to damage a cell severely at molecular level. A bone to marrow uptake ratio of 11 has been recorded for ^{117m}Sn-DTPA, which is far better than its closest rival, ^{153}Sm-EDTMP (Atkins *et al.*, 1993). As the energies of the ß-particles emitted by ^{166}Ho and ^{32}P are similar, a bone to marrow uptake ratio of about 1.3 is expected for a radiopharmaceutical containing ^{166}Ho. From this comparison it is understandable that marrow depression is recorded, especially for ^{89}Sr, and even for ^{153}Sm (Turner *et al.*, 1989; Bishayee *et al.*, 2000).

As is the case with all radiotherapeutic regimens (chemotherapeutic agents as well), the maximum dose of ^{117m}Sn-DTPA will be determined by the effects on normal tissue. Whether the range of the conversion electrons proves to be adequate to produce a therapeutic effect if the uptake is not in the tumour itself, as is the case with ^{117m}Sn-DTPA (Atkins *et al.*, 1993), remains to be proven. Selective uptake of ^{117m}Sn in the tumour by a designed ligand would certainly improve its therapeutic effect. Finally, the half-life of ^{117m}Sn proves to be suitable. It is known (Turner *et al.*, 1989) that the use of ^{89}Sr, with its long half-life of 50.5 days, requires radiation safety precautions for the collection of urine, for the discharge of patients and, in general for the responsible hospital staff. In this ^{117m}Sn has a long half-life (13.6 d) but not

excessive to complicate radiation safety precautions. Its short radiation range also contributes to minimize the dose received by hospital staff.

The oxidation state of the Sn is also important. Srivastava *et al.* (1998) showed that for ligands such as DTPA and MDP the bone uptake of Sn^{IV} was superior to that of Sn^{II}. For this reason ^{117m}Sn (IV)-DTPA was promoted in past investigations. Note that Sn^{II} is widely used as a reducing agent in ^{99m}Tc-labelled diphosphonates and it has been found to adsorb on to hydroxyapatite after dissociation from the diphosphonate carrier, which prevents its untimely hydrolysis (Claessens & Kolar, 2000; Yang *et al.*, 2004). Formation constants for Sn^{II} from which an encouraging blood plasma model could be drawn up, led to its investigation as a therapeutic nuclide in this study.

2.5.2 The Phosphonate Ligands

Modifications to the phosphonate ligands could further optimise the efficacy of the potential radiopharmaceutical for targeted, skeletal therapy. Sn^{II} is added during formulation of the above skeletal-imaging agents to reduce pertechnetate. HMDP (hydroxymethylene diphosphonate) is sometimes used to replace MDP in targeting bone. Studies showed that the cancerous/ compact bone uptake is greater for HMDP than for MDP. Another ligand used is HEDP (also known as Etidronate). HEDP has a hydroxy group which MDP lacks and seems suitable as a possible pain palliative radiopharmaceutical. Although the bone uptake of ^{99m}Tc-HEDP is lower and its blood clearance slower than of ^{99m}Tc-MDP (Bevan *et al.*, 1980), it gives a greater contrast between regions of higher and lower calcification rates. As the areas with higher rates of calcification appear to be the target of a possible palliative radiopharmaceutical, HEDP seems to be a promising candidate. Success with ^{186}Re-HEDP is well documented by De Klerk *et al.*, (1997) and clinical studies on an even more energetic ß-emitter (comparable with ^{166}Ho), ^{188}Re (half-life of 16.0 h and maximum ß energy of 2.1 MeV), complexed to MDP, HEDP and others as possible bone therapeuticals, are continously been performed (Maxon *et al.*, 1992; Palmedo *et al.*, 2000; Mitterhauser *et al.*, 2004).

APD (1-hydroxy-3-amine-propylidene diphophonate) functions by binding to the bone surface (to hydroxyapatite), thereby inhibiting resorption, the function of osteoclasts, and interfering with the maturation of osteoclast precursors (Schoutens, 1988). Furthermore APD

mobilizes Ca^{2+} and Mg^{2+} in blood plasma to such an extent that an increased amount of these two metal ions is available for deposition on to the bone, thus assisting in regenerating bone tissue (Thurlimann *et al.*, 1994). Thus APD repairs the damage by the osteoclasts and disrupts their action and is therefore effective as a pain palliation therapy for osteolytic bone cancer patients.

2.5.2.1 Polymeric Bisphosphonates

Another approach using water-soluble polymers as drug carriers was investigated. These polymers have been the subject of research for some time and have been studied as potential chemotherapy agents for cancer (Duncan *et al.*, 1996; Soyez & Schacht, 1997). The principle behind this approach is that water-soluble macro-molecules accumulate passively in solid tumours according to the "Enhanced Permeability and Retention Effect" (Maeda *et al.*, 2000). This is thought to be caused by the production in tumour cells of compounds such as vascular permeability factor (VPF) and bradikinine, which increase the vascular permeability of the tumour tissue (Fig 2-17). Retention is enhanced by the impairment of the lymphatic system in tumour tissue, retarding the removal of macromolecules from tumours. The polymer must therefore be large enough not to be taken up in healthy tissue, but not so large as to be trapped in organs such as the liver and kidneys (Fig 2-18). To extend this approach to therapeutic radiopharmaceuticals the water-soluble polymer polyethyleneimine was functionalised with methylenephosphonate groups to make the resulting water-soluble polymer, called PEI-MP, bone seeking. The extensive preclinical work using ^{99m}Tc labelled PEI-MP to ascertain the optimum fraction in terms of molecular mass (Dormehl *et al.*, 2001) is largely the topic of this thesis. Finding anionic species in a size fraction e.g. 10 to 30 kDa which presents good tumour uptake with the minimum uptake in healthy bones, kidneys or liver, would establish such a polymer as having the potential to deliver a therapeutic radionuclide selectively to tumours.

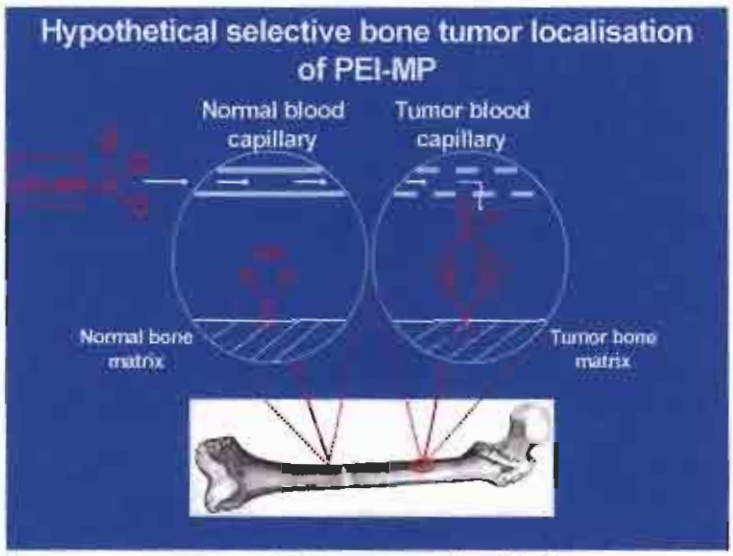

Fig 2-17: Schematic presentation of selective bone tumour localisation.

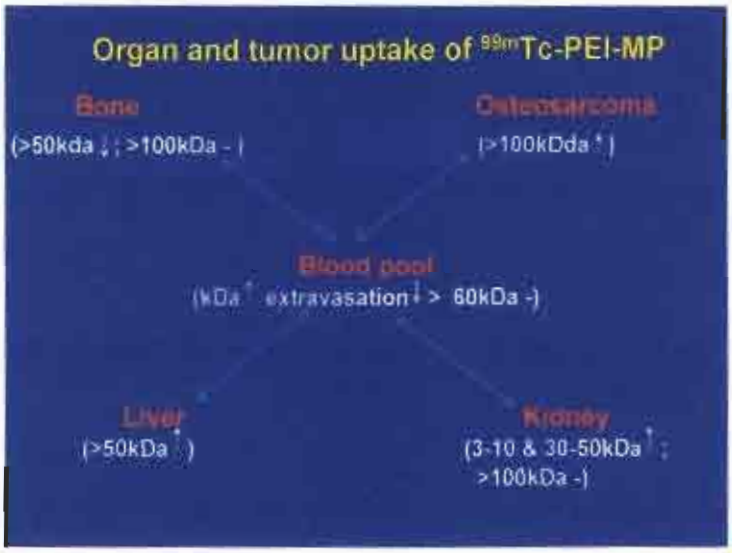

Fig 2-18: Organ and tumour uptake of ^{99m}Tc-PEI-MP, depending on its macromolecular size.

2.6 Modelling in Biomedical Research

2.6.1 Animal models

It is generally accepted that the use of animals in biomedical research has made a significant contribution to the welfare of both humans and animals in the past, and that future use of animals is necessary for further progress. It should be emphasised that a wide variety of

experimental animal species is necessary for the advancement of knowledge in biology, as well as for the development of methods for prevention, diagnosis and treatment of diseases of humans and animals (Brodey, 1979; Macewen, 1990).

As a general rule it is true to say that the main risk with radiopharmaceuticals is that of radiation induced damage. The labelled compounds are only present in miniscule concentrations so that the question of chemical toxicity seldom arises, although it is not always the case.

To minimalise the risk the minimum dose which produces clinical useful data has to be related to the radiation dose to the target organ, i.e., the organ receiving the largest radiation dose. In this respect the bladder and intestines should not be forgotten. In targeted radiotherapy (and palliation) the bone marrow is the dose-limiting organ. This is primarily trabecular bone. The radiosensitive cells in this area consists of the hemopoietic bone marrow cells, endosteal cells lying close to the bone surface, epithelial cells close to the surfaces in the air sinuses in the skull (Bouchet *et al.*, 1999). Because of the complex structure it has been difficult to calculate accurately the dose deposited to the sensitive tissues. A three-dimensional model has been reported to calculate the dose for trabecular bone by Bouchet *et al.*, (1999). Cortical bone is considered a separate region due to the cells at risk, these are: the osteoprogenitor cells which lie within a 10μm layer of the endostium (Bouchet & Bolch, 1999). Similarly a three dimensional model has been reported to calculate the dose for cortical bone (Bouchet & Bolch, 1999). Biodistribution studies in normal animals and in pathophysiological models can be helpful in predicting human radiation doses but the possibility of interspecies variation remains a constant and insoluble problem.

Biodistribution studies in the non-human primate will have to yield results similar to those in man. Confirming the validity of the chacma baboon (*Papio ursinus*) in the determination of useful biodistribution and subsequently dosimetry data from radiopharmaceuticals will allow extrapolation to man (Louw *et al.*, 1996) (Fig 2-19). Such data could subsequently be used to optimise various radiopharmaceuticals for targeted therapy.

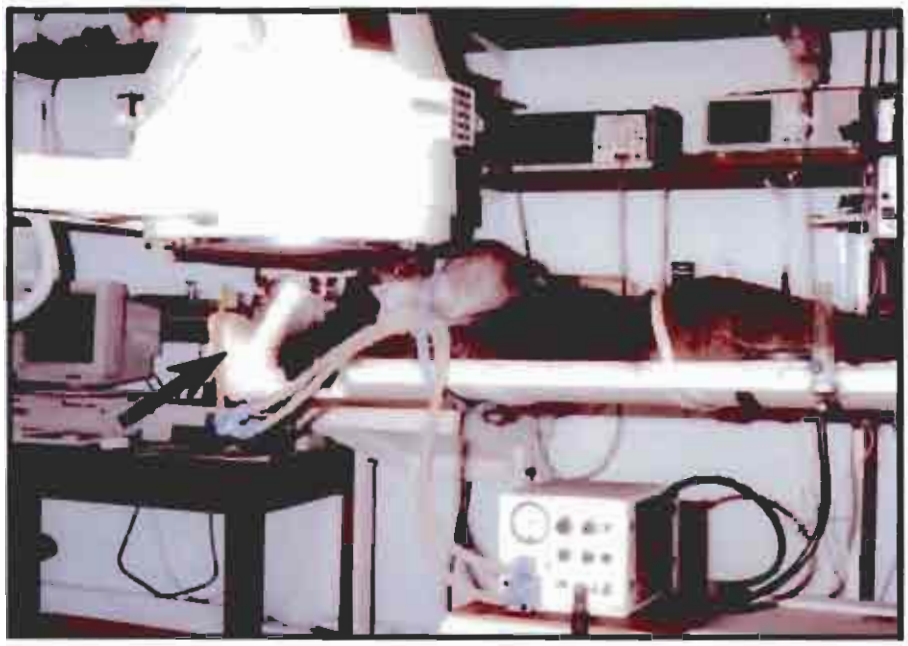

Fig 2-19: Prepared animal for scintigraphy. The size of the animal enables meaningful data extrapolation to man.

Canine osteosarcoma is a valid model for osteosarcoma in man and could also serve as a model for metastatic bone cancer in man (Knapp & Waters, 1997; Withrow *et al.*, 1991). However the owners of afflicted dogs have to agree to participate in such investigations. The murine model for research in oncology has for long been invaluable and logistically relatively easy to use. Numerous cell lines of various cancers have in the past been introduced into nude mice. Appropriately sized tumours of the particular cell lines thus induced have been researched and the information, whether of biological, histological or pharmacological nature usefully applied to human medicine.

The tumour uptake of the various therapeutic radiopharmaceuticals could be determined in vivo scintigraphically, thus yielding time-dependent wash-in, retention and wash-out information. Organ distribution data from rodents thus generated will allow some calculations on dosimetry and provided information amongst others as to the therapeutic potential and safety of the radiopharmaceutical.

However dosimetry calculations from a murine model do not truly extrapolate to man. The primate model would be more appropriate and would permit with confidence the use of MIRDOSE 3 software* modelled on a 32 kg human (Siegel *et al.*, 1999).

2.6.2 Dosimetry from MIRDOSE 3

There are inherent errors in extrapolating external beam dosimetry information to internally dosed emitters which have highly variable dose rates and are delivered over protracted periods of time (Siegel *et al.*, 1999). Therefore the experimental design for this study for dosimetry purposes used information derived from the recommendation made in MIRD Pamphlet 16 (Siegel *et al.*, 1999).

The MIRD Schema consists of a number of pamphlets that have been published over a number of years, details of which are reviewed by Stabin (1999). The MIRD Schema has as its goal an accurate determination of the time-dependent activity in the body tissues of a radiopharmaceutical (source e.g. trabecular bone) and its calculated absorbed dose to target regions (e.g. bone marrow) of the body. The term region designates sources of radiation in the body and designates targets for assessment of radiation-absorbed dose. The absorbed dose is defined as the energy absorbed per unit mass (Siegel *et al.*, 1999) .The mean dose in the MIRD Schema is given as

$$\overline{D} = \widetilde{A} \times S \qquad \text{Equation 1}$$

where $\overline{D}$ is the mean absorbed dose in Gy or rad, $\widetilde{A}$ is the accumulated activity in Bq/sec or μCi/hr and S is the mean absorbed dose per unit cumulated actively in Gy/Bq/sec or rad/μCi/hr.S is given in the MIRDOSE 3 software for the specific anthropomorphic model from the S -tables. The S -tables make the assumptions that the activity in the organs is homogenous and that the organ mass is standardized (Stabin *et al.*, 1999). These assumptions can be erroneous since organs are often not homogenous and for obvious reasons, there are variations in organ size amongst individuals (Stabin *et al.*, 1999). The absorbed dose to target can also be expressed as absorbed dose per unit administered activity, A_0 (Bq or μCi) and the

* MIRDOSE – Medical Internal Radiation Dosimetry

source region resident time τ, defined as $\tau = \tilde{A} / A_0$. Therefore, the mean dose to the target per unit administered activity is given as:

$$\overline{D}/A_0 = \tau \times S \qquad \text{Equation 2}$$

Thus the estimation of absorbed dose is dependent on two factors:

- Time-dependent (biokinetic) factors: those incorporated within τ or $\tilde{A}$ which incorporate characteristics of both uptake and retention of activity in the regions of interest (ROI) and includes the physical half-life of the radionuclide and the biologic half-life of the radiopharmaceutical.
- Time-independent (physical) factors: those represented by *S*. These are types and energies of the radiation emitted, geometrical aspects, distance between them and composition of absorbing and intervening media of the source and target regions.

The three phases involved in the determination of the absorbed dose are: (see scintigraphy):

- Data collection: Identification of source regions which would be the ROI containing activity, determination of temporal sampling and acquisition of counts or radioactivity, also tissue sampling (blood, urine). For the purposes of this study source regions are identified as areas in the animal showing significant uptake. In most cases these are: cardiac region, liver, left kidney, right kidney, trabecular bone (metaphyses of the long bones), cortical bone (diaphyses of the long bones) and background (an area over a muscle group).
- Data analysis: calculation of the activity in the ROI as a function of time. This would include calibration factors obtained from quantitative techniques.
- Data processing: integration of the time activity curves to obtain the sum of all nuclear transitions, the accumulated activity $\tilde{A}$ and residence time τ for each source region (ROI). These values are inserted in the eq. 1 and 2, and the S values obtained from the *S* tables, to yield the dose rates to the target organs.

2.6.3 Chemical Speciation and Blood Plasma Modelling

For a particular ligand (L) and metal ion (M) several complexes may form at different pH values, e.g. ML, MLH, M_2L, ML_2, MLOH (H = hydrogen ions). The distribution between

these different species is called the speciation of that ligand. Duffield and Williams defined speciation as follows: Speciation defines the oxidation state, concentration and composition of each of the species present in a chemical sample. Better computing and analytical methods have in recent years led to an increased understanding of the speciation underlying many chemical systems, with interesting conclusions to be drawn for medicine, industry and the environment.

To elucidate the performance of ligands chosen in treating metastatic bone cancer and osteosarcoma the reactions between metal ions and ligands need to be understood (Taylor & Williams, 1995). When looking at bonding between ligand and metal ion, one way to describe the phenomenon is to consider the thermodynamic equilibria that occur. The formation constant for the equilibruim of complex formation must be known.

Potentiometry is often used as a technique to calculate formation constants although the evaluation of the potentiometric data can be handled by different software packages. In this study the potentiometric data from potentiometric titration was analysed using the ESTA (Equilibrium Simulation by Titration Analysis) package of computer programs as deseribed by May *et al.*, (1985a & b).

The human body consists of cells that are surrounded by an aqueous medium. Since 70 % of the body is water, life is sustained in this medium by reaction between metal ions and ligands that occur in vivo. Studying the reactions between metal ions and ligands and using this to calculate the speciation of a particular metal ion, ligand or combination of the two is necessary if we are to understand more of the biochemistry and physiology in the human body (Taylor & Williams, 1995).

Calculating the speciation for a particular ligand and radionuclide combination in blood plasma will indicate whether a complex will survive the competition of metal ions and ligands occurring naturally in blood plasma. If so the ligand may be able to deliver the radionuclide to the bone and may be successful in the treatment of painful bone metastases or osteosarcoma, as has been the case with ^{153}Sm and ^{186}Re.

An essential process in the development of any speciation model is to define a series of chemical equilibria which represents the system under investigation. In defining the equilibria

all the chemical species involved and the equilibrium constants for the reactions have to be specified. The series of equilibria, together with the total or free component concentrations, constitute the computer model or database of the system. From these data, a series of simultaneous, mass-balance equations can be set up for the total component concentrations as a sum of all the individual species concentrations, and solved iteratively for the free component concentrations, and eventually the individual species concentrations.

The computer program ECCLES, Evaluation of Constituent Concentrations in Large Equilibrium Systems, (May *et al.*, 1977) predicts the speciation of metal ions or ligands in biological fluids such as blood plasma. May *et al.* (1977) wrote this program to simulate the nature of the metal ion binding to low-molecular-weight ligands (LWL) in human blood plasma because these play an important role in biological systems (Eichhorn, 1973).

The aqua-ion is a low-molecular-weight complex but because of its importance it is treated as a separate form of the metal ion. It must be present in all aqueous equilibrium systems and is often referred to as the free (uncomplexed) ion even though it is complexed to the solvent. In blood plasma, the total metal ion concentration is much less than the total protein concentration and the free metal ion is very much less than the concentration of metal-protein complex. This means that until a substantial portion of the metal ion is stripped off the protein, the free metal ion concentration remains constant, i.e. is effectively buffered by protein binding. For this reason May *et al.* (1977) assumed that the percentage distribution of transition metal ions among LWL was not controlled by protein binding.

The free metal ion as well as ligand concentrations used in the model are given in Table 2. The distribution of Ca^{II}, Mg^{II}, Mn^{II}, Fe^{III}, Cu^{I}, Cu^{II}, Ni^{II}, Zn^{II} and Pb^{II} among 5000 complexes formed with 40 or more ligands is computed. Because of the slow complexation kinetics of proteins, two extreme simulation conditions exist: one in which protein binding is neglected and one in which protein binding is explicitly included in the calculation. The simulation condition in which protein binding is neglected serves to illustrate the speciation immediately after injection.

Table 2-1: Ligand and free metal ion concentrations used in the blood plasma model (Zeevaart, 2001).

Component	Concentration (M)	Component	Concentration (M)
Alanate	3.7×10^{-4}	Tyrosinate	5.8×10^{-5}
Aminobutyrate	2.4×10^{-5}	Valinate	2.3×10^{-4}
Arginine	9.5×10^{-5}	Carbonate	2.5×10^{-2}
Asparaginate	5.5×10^{-5}	Phosphate	1.6×10^{-3}
Aspartate	5.0×10^{-6}	Thiocyanate	1.4×10^{-5}
Cysteinate	2.3×10^{-5}	Silicate	1.4×10^{-4}
Cystinate	4.0×10^{-5}	Sulphate	2.1×10^{-4}
Citrullinate	2.7×10^{-5}	Ammonia	2.4×10^{-5}
Glutamate	4.8×10^{-5}	Citrate	1.1×10^{-4}
Glutaminate	5.2×10^{-4}	Lactate	1.8×10^{-3}
Glycinate	2.4×10^{-4}	Malate	3.5×10^{-5}
Histidinate	8.5×10^{-5}	Oxalate	1.2×10^{-5}
Histamine	1.0×10^{-8}	Pyruvate	9.5×10^{-5}
Hydroxyprolinate	7.0×10^{-6}	Salicylate	5.0×10^{-6}
Isoleucinate	6.5×10^{-5}	Succinate	4.2×10^{-5}
Leucinate	1.2×10^{-4}	Ascorbate	4.3×10^{-5}
Lysinate	1.8×10^{-4}	OH^-	1.2×10^{-6}
Methionate	2.9×10^{-5}	Ca^{2+}	1.1×10^{-3}
Ornithinate	5.8×10^{-5}	Mg^{2+}	5.2×10^{-4}
Phenylalanate	6.4×10^{-5}	Cu^{+}	1.0×10^{-17}
Prolinate	2.1×10^{-4}	Cu^{2+}	1.0×10^{-20}
Serinate	1.2×10^{-4}	Fe^{2+}	1.0×10^{-21}
Threoninate	1.5×10^{-4}	Fe^{3+}	1.0×10^{-23}
Tryptophanate	1.0×10^{-5}	Pb^{2+}	1.0×10^{-14}
Serum Albumin*	7.2×10^{-4}	Mn^{2+}	1.0×10^{-12}
Transferrin*	2.5×10^{-5}	Zn^{2+}	1.0×10^{-9}
		Ni^{2+}	1.0×10^{-18}

*these proteins are only included in the model when calculating the equilibrium after some time

Introducing a new ligand in a pharmaceutical requires that the program's database of formation constants be expanded by constants describing the complexation of the ligand with various metal ions (including the metal ion used as a source of radiation) in order to elucidate the behaviour of the radiopharmaceuticals in the blood plasma. When a new metal ion is introduced the database has to be expanded to include formation constants describing the complexation of the metal ion with the ligands contained in the blood plasma. This is the area of greatest difficulty in speciation modelling as accurate equilibrium constants are not always readily available.

Generally it is assumed that a 5 to 10 percent error can be expected for biodistribution values predicted by ECCLES as it is an overall robust system and produces an indication rather than an exact percentage of each species. Furthermore, the output will only be as good as the input (formation constants) as is the case with all models.

However the choice of the radionuclide (half-life and radiation emissions, which dictate its radiobiological effects) and of the bone-localizing agent (the biochemical properties, which dictate its pharmacokinetics) will determine the therapeutic success of the modality (Volkert & Hoffman, 1999). Bone-seeking ligands that after intravenous administration survive in blood plasma and are not scavenged by the liver or kidneys, are taken up in the bone per definition. It can not however, be assumed that an intact radiopharmaceutical as such will be adsorbed on to bone. Affinity of the radionuclide AND ligand for hydroxyapatite is important, because of the bone seeking requirement (Claessens & Kolar, 2000).

The blood plasma speciation contributes not to the ability of a modality to be taken up in bone but to how it behaves in blood plasma: whether it forms neutral species (causing reticuloendothelial uptake) and whether it survives competition of blood low-molecular-weight ligands, after intravenous injection. However, with the blood plasma speciation, i.e. computer simulation, ECCLES it was possible to explain the results obtained with ^{153}Sm-EDTMP and ^{166}Ho-EDTMP in vivo in animals (Louw *et al.*, 1996). For this reason blood plasma speciation was employed in this thesis to serve as reference for an improved bone-seeking radiopharmaceutical before being tested in primates.

2.6.4 Compartmental Modelling

A considerable mathematical background has been developed for treating kinetic data from radionuclide tracers but the general formulation is quite formidable (Howard, 1974). It is assumed that a tagged/labelled compound is abruptly introduced into one body compartment, using compartment in a broad sense. It might refer to the bloodstream, to all body water, or to a single organ such as the lungs. The compound being traced is assumed to be uniformly distributed throughout each compartment that it enters but concentrations may vary widely from one compartment to another. The rate at which the tagged material leaves one

compartment for another is assumed to be proportional to the concentration of the material in the first compartment. The constants of proportionality are known as *transfer coefficients.*

Two-compartment systems represent the simplest cases in this approach (Fig 2-20 a, b). Mathematical complexities develop rapidly as more transfer coefficients are introduced into the system model. In general apart from intercompartmental transfer there will be some movement out of the second compartment, either as a irreversible excretion or as a transport to a third compartment. The introduction of transfer coefficients to account for such movement leads to equations with multiple exponential terms and with each coefficient a complicated function of the system parameters.

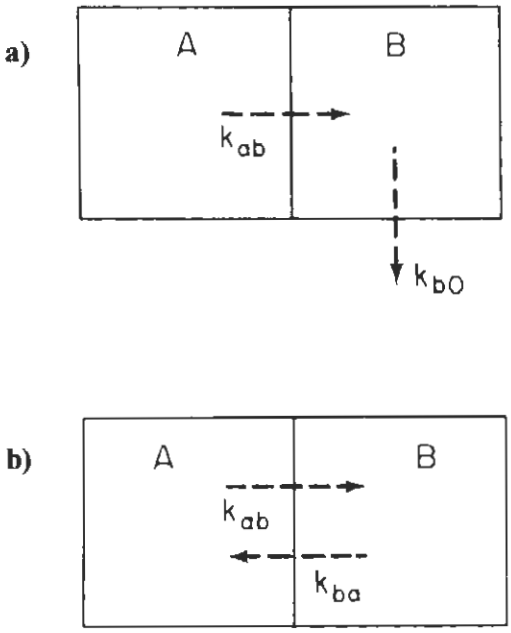

Fig 2-20: (a) A two-compartment system with only two transfer coefficients and (b) An isolated two-compartment system with no transfers to and from the outside (Andrews, 1974)

The mathematical treatment of a simple idealized model leads to a prediction of a series of parameters, the transfer coefficients *k* and volumes *v*. In practice, measurements give the time course of the concentrations in one or more compartments and these data are to be interpreted in terms of the parametric constants of the system. Empirical methods, aided by analog or digital computers, are usually invoked to analyze the system performance.

Exponential factors usually appear in equations when material transport is set proportional to the concentration in the driving compartment. A concentration-time curve might then be analyzed by assuming it to consist of a sum of a few exponentials and adjusting the constants in these components to obtain a best fit with the data. These best values are then interpreted in biological terms from the system-model.

In the simple case depicted in Fig 20 b, there is no excretion ($k_{b0} = 0$). At $t = 0$ the tagged quantities are Q_{0a} and zero, respectively. Then

$$\frac{dQ_b}{dt} = \lambda_{ab} Q_a - \lambda_{ba} Q_b$$

Which integrates to

$$Q_b = Q_{0a} \frac{\lambda_{ab}}{\lambda_{ab} + \lambda_{ba}} \left(1 - e^{-(\lambda_{ab} + \lambda_{ba})t}\right)$$

Q_b approaches an equilibrium value

$$Q_b = Q_{0a} \frac{\lambda_{ab}}{\lambda_{ab} + \lambda_{ba}}$$

λ_{ab} transfer coefficient per unit volumes, thus $\frac{k_{ab}}{v_a}$

Mathematical complexities develop rapidly as more transfer coefficients are introduced into the system model. In general there will be some movement out of the compartment, either as an irreversible excretion or as a transport to a third compartment. The introduction of the transfer coefficients to accounts for such movements lead to equations with multiple exponential terms and with each coefficient a complicated function of the system parameters.

Too much biological significance must not be attached to system parameters obtained from any of the analytical procedures. Although the methods may be mathematically elegant, a

considerable variation in the parameters is usually possible within the inevitable uncertainties in the observed data.

Although compartmental analysis was used on occasion in this research with six compartments considered, blood, bone, liver, kidney, bladder content and the rest, it is not necessary to subject the results of every tracer study to such an elaborate analysis. Routine diagnostic procedures and programmes exist in nuclear medicine instrumentation and investigations from which organ or system behaviour can be simply and adequately estimated. Those are the procedures extensively used in the present study to evaluate the pharmacokinetics of the various bone seeking radioligands.

2.7 References

ALAZRAKI, N. 1984. The musculoskeletal system. In Rocha AF, Harbert JC (eds): Textbook of nuclear medicine: Clinical application. p. 166. Vol 2. 2nd Ed. Philadelphia, Lea & Febiger.

ALBERTS, A.S., SMIT, B.J., LOUW, W.A.K., VAN RENSBURG, A.J., VAN BEEK, A., KRITZINGER, V., NEL, J.S. 1997. Dose response relationship and multiple dose efficacy and toxicity of Samarium-153-EDTMP in metastatic cancer to bone. *Radiother. Oncol.* 43:175-179.

ALLMAN, R., BROWER, B. Circulatory patterns of deossification. 1981. *Radiol Clin North Am* 19:553-569.

ANDREWS, H.L. 1974. Charged Particle Emission and Radioactive decay. In: Andrews HL, editor. Radiation Biophysics. New Jersey: Prentice-Hall, Inc., 83-99.

ATKINS, H.L. 1998. Overview of Nuclides for Bone Pain Palliation. *Appl Radiat Isot* 49(4):277-283.

ATKINS, H.L., MAUSNER, L.F., SRIVASTAVA, S.C., *et al.* 1993. Biodistribution of Sn-177m(4+) DTPA for palliative therapy of painful osseous metastases. *Radiobiology* 186 (1): 279-283.

BAUER, G.C.H., RAY, R.D. 1958. Kinetics of strontium metabolism in man. *J. Bone Joint Surg.* 40A: 171.

BERG, J., LAMB, C.R., O'CALLAGHAN, M.W. 1990. Bone scintigraphy in the initial evaluation of dogs with primary bone tumours. *J Am Vet Med Assoc* 196:917-920.

BEVAN, J.A., TOFE, A.J., BENEDICT, J.J., FRANCIS, M.D., BARNETT, B.L. 1980. 99m-Tc-HMDP: A radiopharmaceutical for skeletal and acute myocardial infarct imaging. (1) *J. Nucl. Med.* 21: 961-966.

BICKEL, A. 1921. Beitrag zur Thorium x-behandlung de periniciosen anemie. *Berl. Klin. Wochenscrift* 49: 1322.

BISHAYEE, A., RAO, D.V., SRIVASTAVA, S.C., BOUCHET, L.G., BOLCH, W.E., HOWELL, R.W. 2000. Marrow-sparing effects of 117mSn(4+)diethylenetriaminepentaacetic acid for radionuclide therapy of bone cancer. *J. Nucl. Med.* 41(12): 2043-2050.

BODY, J.J., BARTL, R., BURCKHARDT, P., DELMAS, P.D., DIEL, I.J., FLEISCH, H. *et al.* 1998. Current use of bisphosphonates in oncology. International Bone and Cancer Study Group. *J Clin Oncol* 16(12):3890-3899.

BODY, J.J., MANCINI, I. 2002. Bisphosphonates for cancer patients: why, how, and when? *Supp. Care Canc.* 10(5):399-407.

BOK, B., PEREZ, R., PANNECIERE, C., DI PAOLA, R. 1973. Bone scanning radiopharmaceutical: A comparison of three products. *J. Nucl. Med.* 14: 380.

BOUCHET, L.G., BOLCH, W.E. 1999. A three-dimensional transport model for determining absorbed fractions of energy for electrons within cortical bone. *J Nucl Med* 40(12):2115-2124.

BOUCHET, L.G., BOLCH, W.E., GODDU, S.M., HOWELL, R.W., RAO, D.V. 2000. Considerations in the selection of radiopharmaceuticals for palliation of bone pain from metastatic osseous lesions. *J. Nucl. Med.* 41(4):682-687.

BOUCHET, L.G., JOKISCH, D.W., BOLCH, W.E. 1999. A three-dimensional transport model for determining absorbed fractions of energy for electrons within trabecular bone. *J. Nucl. Med.* 40(11):1947-1966.

BRENNER, W., KAMPEN, W.U., KAMPEN, A.M., HENZE, E. 2001. Skeletal uptake and soft-tissue retention of 186Re-HEDP and 153Sm-EDTMP in patients with metastatic bone disease. *J. Nucl. Med.* 42(2):230-236.

BRODEY, R.S. 1979. The use of naturally occurring cancer in domestic animals for research into human cancer: general considerations and a review of canine skeletal osteosarcoma. *Yale J Biol Med* 52(4):345-361.

BROWN, M.L. 1983. Significance of the solitary lesion in pediatric bone scanning. Concise communication. *J. Nucl. Med.* 24: 114-115.

BRULAND, O.S., SKRETTING, A., AAS, M. 1996. Targeted radiotherapy of osteosarcoma using 153 Sm-EDTMP. A promising approach. *Acta Oncol* 35:381-384.

BURKHARDT, R., FRISCH, B., SCHALG, R., SOMMERFELD, W. 1982. Carcinomatous osteodysplasia. *Skeletal Radiol.* 8(3): 169-178.

CARTER, D.R., HAYES, W.C. 1977. The compressive behaviour of bone as a two-phase porous structure. *J. Bone Joint Surg.* 59A: 954.

CHARKES, N.D. 1980. Skeletal blood flow: Implications for bone-scan interpretation. *J. Nucl. Med.* 21:91-98.

CHEW, F.S., HUDSON, T.M. 1982. Radionuclide bone scanning of osteosarcoma: Falsely extended uptake patterns. *AJR* 139: 49-54.

CHIEWITZ, O., HEVESEY, G. 1935. Radioactive indicators in the study of phosphorus metabolism in rats. *Nature* (London) 136:754-755.

CHRISTENSEN, S.B., KROGSGAARD, O.W. 1981. Localization of Tc-99m MDP in epiphyseal growth plates of rats. *J. Nucl. Med.* 22:237-245.

CLAESSENS, R.A.M.J., KOLAR, Z.I. 2000.Affinity of tin(II) and tin(II) diphosphonates for hyrdoxyapatite: an experimental and model study. *Langmuir* 16: 1360-1367.

COUPALL, J.J., KIM, E.E., DELAND, F.H. 1981. Effects of dissolved oxygen on Tc-99m methylene diphosphonate. Concise communication. *J. Nucl. Med.* 22:153-156.

DAVIS, G.J., KAPATKIN, A.S., CRAIG, L.E., HEINS, G.S., WORTMAN, J.A. 2002. Comparison of radiography, computed tomography, and magnetic resonance imaging for evaluation of appendicular osteosarcoma in dogs. *J Am Vet Med Assoc* 220(8):1171-1176.

DE KLERK, J.M., ZONNENBERG, B.A., BLIJHAM, G.H., *et al.* 1997. Treatment of metastatic bone pain using the bone-seeking radiopharmaceutical Re-186-HEDP. *Anticancer Res.* 17 (3B): 1773-1777.

DEREGIS, C.J., MOORE, A.S., RAND, W.M., BERG, J. 2003. Cisplatin and doxorubicin toxicosis in dogs with osteosarcoma. *J Vet Intern Med* 17(5):668-673.

DESAI, A., ALAVI, A., DALINKA, M., *et al.*1980. Role of bone scintigraphy in the evaluation and treatment of non-united fractures. *J. Nucl. Med.* 21: 931-934.

DEWANJEE, M.K., FLETCHER, J.W., DAVIS, M.A. 1972. Chemical properties and biological distribution of technitium-tin-polyphosphates. *J. Nucl. Med.* 13:427.

DIEL, I.J. 2000. Antitumour effects of bisphosphonates: first evidence and possible mechanisms. *Drugs* 59(3):391-399.

DORMEHL, I. C., LOUW ,W. K. A., SCHNEEWEISS, F. H. A., MILNER, R., SCHMITT, G., CROFT, S. A. 1998. Uptake of ethylenediamine tetra-methylene phosphonic acid in normal bone after multiple applications - A primate study. *Arzneim. Forsch. / Drug Res.* 48(4):408-414.

DORMEHL, I.C., LOUW, W.K.A., HUGO, N., BEVERLEY, G.H., SWEETLOVE, A., KNOESEN, O. ^{153}Sm-EDTMP and ^{166}Ho-EDTMP as systemic radioisotopic bone therapeutic agents: Experimental pharmacokinetics and biodistribution studies in the baboon model', presented at the European Association of Nuclear Medicine Congress, Lausanne, Switzerland, October 1993.

DORMEHL, I.C., LOUW, W.K.A., MILNER, R.J., KILIAN, E., SCHNEEWEISS, F.H.A. 2001. Biodistribution and pharmacokinetics of variously sized molecular radiolabelled polyethyleneiminomethyl phosphonic acid as a selective bone seeker for therapy in the normal primate model. *Drug. Res.* 54: 258-263.

DORMEHL, I.C., REDELINGHUYS, F., HUGO, N., OLIVER, D., PILLOY, W. 1992. The baboon model under anaesthesia for in vivo cerebral blood flow studies using SPECT techniques. *J Med Prim* 21(5):270-274.

DORMEHL,I.C., LOUW, W.K., SCHNEEWEISS, F.H., MILNER, R., SCHMITT, G., CARL, U. *et al.* 1998. Uptake of ethylenediamine tetramethylene phosphonic acid in normal bone after multiple applications. A non-human primate study. *Arzneim. Forsch./Drug Res* 48(4):408-414.

DOMSTADT, P.A. 1980. 99m Tc-HMDP: A new bone imaging agent with a low tin content. *Radiology* 136: 209-211 .

DUFFIELD, J.R., WILLIAMS, D.R. 1989. Treatment using metal ions and complexes. *Chem. Br.*25: 375.

DUNCAN, R., DIMITRIJEVIC, S., EVAGORON, E.G. 1996. The role of polymer conjugates in the diagnosis and treatment of cancer. *S.T.P. Pharma. Sci.* 6: 237.

EICHHORN.1973. 'Inorganic Biochemistry', Elsevier, Amsterdam

ERICKSON, J.J., ROLLO, F.D. (eds). 1983. Digital nuclear medicine. J.B. Lippincott, Philadelphia.

FORREST, L.J., DODGE, R.K., PAGE, R.L., HEIDNER, G.L., MCENTEE, M.C., NOVOTNEY, C.A. *et al.* 1992. Relationship between quantitative tumor scintigraphy and time to metastasis in dogs with osteosarcoma. *J. Nucl. Med.* 33(8):1542-1547.

FRANZIUS, C., BIELACK, S., FLEGE, S., ECKARDT, J., SCIUK, J., JURGENS, H. *et al.* 2001. High-activity samarium-153-EDTMP therapy followed by autologous peripheral blood stem cell support in unresectable osteosarcoma. *Nucl. Med/Nukl. Med.* 40(6):215-220.

FRANZIUS, C., BIELACK, S., SCIUK, J., VOLLET, B., JURGENS, H., SCHOBER, O. 1999. High-activity samarium-153-EDTMP therapy in unresectable osteosarcoma. *Nucl. Med/ Nukl. Med.* 38(8):337-340.

FRITH, J.C., MONKKONEN, J., BLACKBURN, G.M., RUSSELL, R.G,, ROGERS, M.J. 1997. Clodronate and liposome-encapsulated clodronate are metabolized to a toxic ATP analog, adenosine 5'-(beta, gamma-dichloromethylene) triphosphate, by mammalian cells in vitro. *J Bone Miner Res* 12(9):1358-1367.

FUCHS, B., PRITCHARD, D.J. Etiology of osteosarcoma. 2002. *Clin Orthop* (397):40-52.

FUEGER, B.J., MITTERHAUSER, M., WADSAK, W., OFLUOGLU, S., TRAUB, T., KAEANIKAS, G., DUDCZAK, R., PIRICH, C. 2004. Bone lesion detection with carrier-added ^{99m}Tc-EDTMP in comparison with ^{99m}Tc-DPD. *Nucl. Med. Commun.* 25(4): 361-365.

GIAKKAKENAS, C., KALAFONOS, H.P., APOSTOLOPOULOS, D.J., ZARAKOVITIS, J., KOSMAS, C., VASSILAKOS, P.J. 2000. Preliminary results of the use of Re-186-HEDP for palliation of pain in patients with metastatic bone disease. *Am. J. Clin. Oncol.* 23 (1): 83-88.

GILBERG, L.A., WEISS, M.A., GELFAND, M.J., *et al.* 1983. Detection of renal metastasis of osteosarcoma by bone scan. *Clin. Nucl. Med.* 8: 325-326.

GIULIANI, N., PEDRAZZONI, M., PASSERI, G., GIRASOLE, G. 1998. Bisphosphonates inhibit IL-6 production by human osteoblast-like cells. *Scand J Rheumatol* 27(1):38-41.

GOECKELER, W.F., EDWARDS, B., VOLKERT, W.A., HOLMES, R.A., SIMON, J., WILSON, D. 1987. Skeletal localization of Samarium-153 chelates: Potential therapeutic bone agents. *J. Nucl. Med.* 28:495-504.

GOLDSTEIN, H., MCNEIL, B.J., ZURFALL, E. *et al.* 1980. Changing indications for bone scintigraphy in patients with oseosarcoma. *Radiology* 135:177-180.

GOTTSCHALK, A., POTCHEN, E.J. 1976. Diagnostic nuclear medicine. p. 63. The Williams and Wilkins Company Baltimore.

GREIFF, J. 1978. Autoradiographic studies of fracture healing using ^{99m}Tc-Sn-polyphosphate. *Injury* 9:271-277.

GRIGORIADIS, A.E., WANG, Z., WAGNER, E.F. 1996. Principles of bone biology, J.P. Bilezikian, L.G. Raisz, G.A. Rodan, Academic Press, 15-33.

GUYTON, A. 1986. Physiology of the human body. 7th Ed. WB Saunders, Philadelphia.

HAHN, K.A., HURD, C., CANTWELL, H.D. 1990. Single-phase methylene diphosphate bone scintigraphy in the diagnostic evaluation of dogs with osteosarcoma. *J Am Vet Med Assoc* 196(9):1483-1486.

HOLMES, R.A. 1992. [153Sm]EDTMP: a potential therapy for bone cancer pain. *Semin Nucl Med* 22(1):41-45.

HOWARD, L.A. 1974. Radiation Biophysics. pg 187-194. Prentice Hall, Inc. Englewood Cliff, Wes Jersey.

HSIEH, B.T., HSIEH, J.F., TSAI, S.C., LIN, W.Y., WANG, S.J., TING, G. 1999. Comparison of various rhenium-188-labeled diphosphonates for the treatment of bone metastases. *Nucl Med Biol* 26(8):973-976.

ITO, M., AMIZUKA, N., NAKAJIMA, T., OZAWA, H. 1999. Ultrastructural and cytochemical studies on cell death of osteoclasts indueed by bisphosphonate treatment. *Bone* 25(4):447-452.

JARVIS, N.V., WAGENER, J.M., JACKSON, G.E. 1995. Metal ion speciation in blood plasma as a tool for elucidating the in vivo behaviour of radiopharmaceuticals containing ^{153}Sm and ^{166}Ho. *J. Chem. Soc. Dalton Trans.* 1411-1415.

KELLER, E.L. 1968. Optimum dimensions of parallel-hole multi-apeture collimators for gamma ray cameras. *J. Nucl. Med.* 9(6):233-235.

KIM, E.E., HAYNIE, T.P. 1987. Nuclear diagnostic imaging: Practical applications. pg 93-94. Macmillan publishing co., Inc, New York.

KING, A.G., CHRISTY, B., HUPF, H.B., BLOCK, R.E. 1973. Polyphosphonates:A chemical analysis of average chain length and the relationship to bone deposition in rats. *J. Nucl. Med.* 14: 695-698.

KNAPP, D.W., WATERS, D.J. 1997. Naturally occurring cancer in pet dogs: important models for developing improved eancer therapy for humans. *Mol Med Today* 3(1):8-11.

KNAPP, F.F., JR., BEETS, A.L., GUHLKE, S., ZAMORA, P.O., BENDER, H., PALMEDO, H. *et al.* 1997. Availability of rhenium-188 from the alumina-based tungsten-188/rhenium-188 generator for preparation of rhenium-188-labeled radiopharmaceuticals for cancer treatment. *Anticancer Res* 17(3B):1783-1795.

KVINNSLAND, Y., BRULAND, O., MOE, L., SKRETTING, A. 2002. A method for measurement of the uptake patterns of two beta-emitting radionuclides in the same tissue section with a digital silicon detector: application to a study of $89SrCl_2$ and 153Sm-EDTMP in a dog with spontaneous osteosarcoma. *Eur J Nucl Med Mol Imaging* 29(2):191-197.

LAMB, C.R., BERG, J., BENGSTON, A.E. 1990. Preoperative measurement of canine primary bone tumors, using radiography and bone scintigraphy. *J Am Vet Med Assoc* 196:1474-1478.

LAVENDER. J.P., KHAN, R.A.A., HUGHES, S.P.F. 1979. Blood flow and tracer uptake in normal and abnormal canine bone: Comparisons with Sr-85 microspheres, Kr-81m and Tc-99m MDP. *J. Nucl. Med.* 20:413-418.

LEIBMAN, N.F., KUNTZ, C.A., STEYN, P.F., FETTMAN, M.J., POWERS, B.E., WITHROW, S.J. *et al.* 2001. Accuracy of radiography, nuclear scintigraphy, and histopathology for determining the proximal extent of distal radius osteosarcoma in dogs. *Vet Surg* 30(3):240-245.

LEWINGTON, V.J. 1996. Cancer therapy using bone-seeking isotopes. *Phys Med Biol* 41(10):2027-2042.

LI, S., LIU, J., ZHANG, H., TIAN, M., WANG, J., ZENG, X. 2001. Rhenium-188-HEDP to treat painful bone metastases. *Clin. Nucl. Med.* 26(11): 919-922.

LIEPE, K., FRANKE, W.G., KROPP, J., KOCH, R., RUNGE, R., HLISCS, R. 2000. [Comparison of rhenium-188, rhenium-186-HEDP and strontium-89 in palliation of painful bone metastases]. *Nukl. Med.* 39(6):146-151.

LIMOURIS, G.S., SHUKLA, S.K., CONDI-PAPHITI, A. *et al.*1997. Palliative therapy using rhenium-186-HEDP in painful breast osseous metastases. *Anticanser Res.* 17 (3B): 1767-1772.

LIN, J.H. 1996. Bisphosphonates: a review of their pharmacokinetic properties. *Bone* 18(2):75-85.

LIN, W.Y., LIN, C.P., YEH, S.J., HSIEH, B.T., TSAI, Z.T., TING, G. *et al.* 1997. Rhenium-188 hydroxyethylidene diphosphonate: a new generator-produced radiotherapeutic drug of potential value for the treatment of bone metastases. *Eur J Nucl Med* 24(6):590-595.

LOUW, W.K.A., DORMEHL, I.C., VAN RENSBURG, A.J., HUGO, N., ALBERTS, A.S., FORSYTH, O.E., BEVERLEY, G., SWEETLOVE, M.A., MARAIS, J., LOTTER, L.G., VAN ASWEGEN, A. 1996. Evaluation of Samarium-153-EDTMP and Ho-166-EDTMP in the normal baboon model. *Nucl. Med. Biol. 23:*935-940.

MACEWEN, E.G. 1990. Spontaneous tumors in dogs and cats: models for the study of cancer biology and treatment. *Cancer Metastasis Rev* 9(2):125-136.

MACKIE, P.S., FISHER, J.L., ZHOU, H., CHOONG, P.F. 2001. Bisphosphonates regulate cell growth and gene expression in the UMR 106-01 clonal rat osteosarcoma cell line. *Br J Cancer* 84(7):951-958.

MAEDA, H., WU, J., SAVA, T., MATSUMURA, Y., HON, K. 2000. Tumour vascular permeability and EPR effeccts in macromolecular therapeutics: a review. *J. Controlled Release* 65: 271-284.

MANOLAGAS, S.C. 2000. Birth and death of bone cells: basic regulatory mechanisms and implications for the pathogenesis and treatment of osteoporosis. *Endocr Rev* 21(2):115-137.

MARCUS, R. 1996. Principles of bone biology, J.P. Bilezikian, L.G. Raisz, G.A. Rodan, Academic Press, 1135.

MARTIN, P. 1983. Bone scan scintigraphy in the diagnosis and management of traumatic injury. *Semin Nucl. Med.* 13: 104-108.

MASHIBA, T., TURNER, C.H., HIRANO, T., FORWOOD, M.R., JACOB, D.S., JOHNSTON, C.C. *et al.* 2001. Effects of high-dose etidronate treatment on microdamage accumulation and biomechanical properties in beagle bone before occurrence of spontaneous fractures. *Bone* 29(3):271-278.

MATHEWS, M.B. 1975. Collagen in connective tissue macromolecular structure and evolution. Springer-Verlag, New York.

MAXON, H.R.3rd, SCHRODER, L.E., WASHBURN, L.C., THOMAS, S.R., SAMARATUNGA, R.C., BINIAKIEWICZ, D. *et al.* 1992. Rhenium-186(Sn)HEDP for treatment of osseous metastases. *Semin. Nucl. Med.* 22(1): 33-40.

MAY, P.M., MURRAY, K., WILLIAMS, D.R. 1985a. The use of glass electrodes for determination of formation constants-II, Simulation of titration data. *Talanta* 32: 483-489.

MAY, P.M., MURRAY, K., WILLIAMS, D.R. 1985b. The use of glass electrodes for determination of formation constants-III, Optimization of titration data: The ESTA library of computer programs. *Talanta* 35: 823-830, 927-932.

MAY, P.M., WILLIAMS, D.R., LINDER, P.W. 1977. Computer simulation of metal ion equilibria in biofluids; Models of low-molecular-weight complex distribution of calcium (II), magnesium (II), manganese (II), Iron (III), Copper (II), Zn(II), Pb (II) ions in human blood plasma. *J. Chem. Soc. Dalton Trans.* 588 - 595.

MCKILLOP, J.H., ETCUBANAS, E., GORIS, M.L. 1981. Indications for and limitations of bone scintigraphy in osteogenic sarcoma: A review of 55 patients. *Cancer* 48: 1133-1138.

MCLEAN, R.G., MURRAY, I.P. 1984. Scintigraphic patterns in certain primary malignant bone tumours. *Clin. Radiol.* 35: 379-383.

MCNEIL, B.J., HANLEY, J. 1980. Analysis of serial radionuclide bone images in osteosarcoma and breast carcinoma. *Radiology* 135: 171-176.

MERCADANTE, S. 1997. Malignant bone pain: pathophysiology and treatment. *Pain* 69(1-2):1-18.

METTLER, F.A. 1988. Radionuclide Bone Imaging and Dosimetry, Churchill Livingstone, New York, Edinburgh, London, Melbourne. pg 4-5.

MITTERHAUSER, M., TÖGEL, S., WADSAK, W., MIEN, L.K., EIDHERR, H., WIESNER, K., VIERNSTEIN, H., KLETTER, K., DUDCZAK, R. 2004. Binding studies

of [^{18}F]-fluoride and phosphonates labelled with [^{111}In], [^{99m}Tc], [^{153}Sm], and [^{188}Re] on bone compartments: a new model for the pre vivo evaluation of bone seekers? *Bone* 34: 835-844.

MUNDY, G.R. 2002. Metastasis to bone: causes, consequences and therapeutic opportunities. *Nat Rev Cancer* 2(8):584-593.

MUROFF, L.R. 1980 Syllabus for categorical course in nuclear medicine. Presented at the annual meeting of the American Roentgen Ray Society. Las Vegas, April 20-25.

NAJAFI, A., HUTCHISON, N. 1985. Electrophoretic analysis of different technetium-99m ($SnCl_2$) methylene diphosphonate complexes. *J. Nucl. Med.*26:524-530.

NIMNI, M.E. 1975. Molecular structure and function of collagen. P. 31. In Burleight, Poole AR (eds): Dynamics of connective tissue macromolecules. Elsevier Science Publishing, New York p 31.

O'MARA, R.E., WEBER, D.A. 1984. Osseous system. p. 1145. In Freeman L (ed): Freeman & Johnson's Clinic Radionuclide Imaging. 3rd Ed. Grune & Stratton, Orlando, FL.

OPPERHEIM, B.E., BECK, R.N. In: Diagnostic Nuclear Medicine, Ed. Alexander Gottschalk and James Potchen. The Williams and Wilkins Company Baltimore. 1932

PALMEDO, H., BENDER, H., DIERKE-DZIERZON, C., *et al.* 1999. Pain palliation with rhenium-186 HEDP in breast cancer patients with disseminated bone metastases. *Clin. Nucl. Med.* 24 (9): 643-648.

PALMEDO, H., GUHLKE, S., BENDER, H., SARTOR, J., SCHOENEICH, G., RISSE, J. *et al.* 2000. Dose escalation study with rhenium-188 hydroxyethylidene diphosphonate in prostate cancer patients with osseous metastases. *Eur J Nucl Med* 27(2):123-130.

PETER, C.P., GUY, J., SHEA, M., BAGDON, W., KLINE, W.F., HAYES, W.C. 1996. Long-term safety of the aminobisphosphonate alendronate in adult dogs. I. General safety and biomechanical properties of bone. *J Pharmacol Exp Ther* 276(1):271-276.

PICCI, P., VANEL, D., BRICCOLI, A., TALLE, K., HAAKENAASEN, U., MALAGUTI, C. *et al.* 2001. Computed tomography of pulmonary metastases from osteosarcoma: the less poor technique. A study of 51 patients with histological correlation. *Ann Oncol* 12(11):1601-1604.

POOL, B.L., BERGER, M., SCHLEHOFER, J.R., WINGEN, F. 1988. In vivo and in vitro investigations on biological effects of aromatic bis-(2-chloroethyl) amino-bisphosphonic acids, new agents proposed for chemotherapy of bone tumors: cytostatic activity in rat osteosarcoma; toxicity and genotoxicity in liver and bone marrow; mutagenicity in S. typhimurium. *Invest New Drugs* 6(2):67-78.

RAGLAND B.D., BELL W.C., LOPEZ R.R., SIEGAL G.P. 2002. Cytogenetics and molecular biology of osteosarcoma. *Lab Invest* 82(4):365-373.

ROBINSON, R.G., PRESTON, D.F., SCHIEFELBEIN, M., BAXTER, K.G. 1995. Strontium 89 therapy for the palliation of pain due to osseous metastases. *Jama.* Aug 2, 274 (5): 420-424.

RODAN. G.A., MARTIN, T.J. 2000. Therapeutic approaches to bone diseases. *Science* 289: 1508-1514.

ROGERS, M.J., GORDON, S., BENFORD, H.L., COXON, F.P., LUCKMAN, S.P., MONKKONEN, J. *et al.* 2000; Cellular and molecular mechanisms of action of bisphosphonates. *Cancer* 88(12 Suppl):2961-2978.

ROSENTHALL, L., LISBONA, R. 1983. Skeletal Imaging. Appleton & Lange, Norwalk, C.T.

SAGAR, V.V., PICCONE, J.M., CHARKES, N.D. 1979. Studies of skeletal tracer kinetics. III. Tc-99m (Sn) methylenediphosphonate uptake in the canine tibia as a function of blood flow. *J. Nucl. Med.* 20:1257-1261.

SAIFUDDIN, A. 2002. The accuracy of imaging in the local staging of appendicular osteosarcoma. *Skeletal Radiol* 31(4):191-201.

SANDLER, M.S., HEYMAN, S., WATTS, H. 1984. Localization of 99m Tc methylene diphosphonate within synovial fluid in osteosarcoma. AJR 143(2): 349-350.

SARPER, R.M. 1984. Nuclear medicine instrumentation. Charles C. Thomas, Springfield, III.

SAWYER, E.J., CASSONI, A.M., WADDINGTON, W., BOMANJI, J.B., BRIGGS, T.W. 1999. Rhenium-186 HEDP as a boost to external beam irradiation in osteosarcoma. *Br J Radiol* 72(864):1225-1229.

SCHOUTENS, A. 1988. Bone loss and bone blood flow in paraplegic rats treated with calcitonin, disphosphonate, and indomethacin. *Calsif. Tiss. Int.*, 42: 136-143.

SCHUMICHEN, C., NAKKEN, K.F. 1974. A comparison of the bone-seeking properties of short chained ^{99m}Tc-Sn-polyphosphates. *Nucl. Med./Nukl. Med.* 13: 139-143.

SERAFINI, A.N. 2001. Therapy of metastatic bone pain. Journal of Nuclear Medicine 42(6):895-906.

SHANE, E., BILEZIKIAN, J.P. 1995. Bisphosphonates on Bones, O.L.M. Bijvoet, H.A., Fleisch, R.E. Canfield and R.G.G. Russel, Elsevier, 8-14.

SHIM, S.S. 1968. Physiology of blood circulation of bone. *J. Bone Joint Surg.* 50A: 812.

SIEGEL, J.A., THOMAS, S.R., STUBBS, J.B., STABIN, M.G., HAYS, M.T., KORAL, K.F. *et al.* 1999. MIRD pamphlet no. 16: Techniques for quantitative radiopharmaceutical biodistribution data acquisition and analysis for use in human radiation dose estimates. *J. Nucl. Med.* 40(2):37S-61S.

SILBERSTEIN, E. 1984. Bone scintigraphy. Futura Publishing, Mount Kisco, NY.

SLAYTER, M.V., BOOSINGER, T.R., POOL, R.R., DÄMMRICH, K., MISDORP, W., LARSEN, S. 1994. Histopathological Classification of Bone and Joint Tumors of Domestic Animals. WHO Organization

SOYEZ, H., SCHACHT, E. 1997. Macromolecular derivatives of N, N-di-(2-chloroethyl)-4-phenylenediamine mustard: Synthesis and in vitro hydrolytic stability. *J. Control Release.* 45(3): 235-247.

SRIVASTAVA, S.C., ATKINS, H.L., KRISHNAMURTHY, G.T., *et al.* 1998. Treatment of metastatic pain with tin-117m Stannic diethylenetriaminepentaacetic acid: a phase I/II clinical study. *Clin. Cancer Res.* 4 (1): 61-68.

STABIN, M.G., TAGESSON, M., THOMAS, S.R., LJUNGBERG, M., STRAND, S.E. 1999. Radiation dosimetry in nuclear medicine. *Appl Radiat Isot* 50(1):73-87.

SUBRAMANIAN, G., BLAIR, R.J., KALLFELZ, E.A. 1975. ^{99m}Tc-MDP (methylene diphosphonate) a superior agent for skeletal imaging. *J. Nucl. Med.* 16: 744-755.

SUBRAMANIAN, G., MCAFEE, J.G. 1971. A new complex of ^{99m}Tc for skeletal imaging. *Radiology* 99:192-196.

SUBRAMANIAN, G., MCAFEE, J.G., BELL, E.G., *et al.* 1972. ^{99m}Tc labelled polyphosphate as a skeletal imaging agent. *Radiology* 102: 701-704.

SUBRAMANIAN, G., MCAFEE, J.G., BLAIR, R.J., *et al.* 1972. ^{99m}Tc-HEDP: A potential radiopharmaceutical for skeletal imaging. *J. Nucl. Med.* 13: 947-950.

SWAILEM, F.M., KRISHNAMURTHY, G.T., SRIVASTAVA, S.C., *et al.* 1998. In-vivo uptake and retention of Sn-117m (4+) DTPA in a human subject with metastatic bone pain and in normal mice. *Nucl. Med. Biol.* 25 (3): 279-287.

TAYLOR, D.M., WILLIAMS, D.R. 1995. Trace Element Medicine and Chelation Therapy. The Royal Society of Chemistry, Cambridge.

THRALL, D.E. 1997. Biologic basis of radiation therapy. *Vet Clin North Am [Small Anim Pract]* 27:21-36.

THRALL, D.E. 1998. Biologic Principles of Radiation Therapy. In: Morrison WB, editor. Cancer in Dogs and Cats. Medical and Surgical Management. Maryland: Williams & Wilkins, 399-413.

THRALL, J.H., GESLIEN, G.E., CORCORON, R.J., JOHNSON, M.C. 1975. Abnormal radionuclide deposition patterns adjacent to focal skeletal lesions. *Radiology* 115:659.

THURLIMANN, B., MORANT, R., JUNGI, W.F., RADZIWILL, A. 1994. Pamidronate for pain control in patients with malignant osteolytic bone disease: a prospective dose effect study. *Supp. Care Canc.* 2(1): 61-65.

TURNER, J.H., MARTINDALE, A.A., DE WITT, G.C., WEBB, J., SORBY, P., BOYD, R.E. 1989. Samarium-153-EDTMP therapy of disseminated skeletal metastasis. *Eur. J. Nucl. Med.* 15: 784-795.

VERMA, N., SINGH-WADHWA, S., CHAN, W.L. 2002. Bony metastases seen on scintigraphy with samarium-153. *Clin Nucl Med* 27(3):207.

VINE, E.N., WAHL, A.C. 1982. The chemical behaviour of tracer level technetium isotopes. *Int. J. Appl. Radiat. Isot.*, 33: 861-866.

VOLKERT, W.A., HOFFMAN, T.J. 1999. Therapeutic radiopharmaceuticals. *Chem. Rev.* 99: 2269-2292.

WALLACK, S.T., WISNER, E.R., WERNER, J.A., WALSH, P.J., KENT, M.S., FAIRLEY, R.A. *et al.* 2002. Accuracy of magnetic resonance imaging for estimating intramedullary osteosarcoma extent in pre-operative planning of canine limb-salvage procedures. *Vet Radiol Ultrasound* 43(5):432-441.

WASHIYAMA, K., AMANO, R., SASAKI, J., KINUYA, S., TONAMI, N., SHIOKAWA, Y., MITSUGASHIRA, T. 2004. ^{227}Th-EDTMP: A potential therapeutic agent for bone metastasis. *Nucl. Med. Biol.*31: 901-908.

WILSON, M.A. 1981. The effect of age on the quality of bone scans using technetium 99m pyrophoshate. *Radiology* 139:703-705.

WILSON, M.A., CALHOUN, F.W. 1981. The distribution of skeletal metastases in breast and pulmonary cancer. Concise communication. *J. Nucl. Med.* 22:594-596.

WITHROW, S.J., POWERS, B.E., STRAW, R.C., WILKINS, R.M. 1991. Comparative aspects of osteosarcoma. Dog versus man. *Clin Orthop* (270):159-68.

YANG, Y., LOU, S., PU, M., WANG, W., WANG, G., HE, J., LIU, G., BING, W., WEI, H. 2005. Labeling conditions, in vitro properties and biodistributions of various Sn-labeled complexes. *Appl. Radiat. Isot* 62: 597-603.

ZEEVAART, J.R. 2001. Metal ion speciation in blood plasma as a tool in predicting the in vivo behaviour of potential bone-seeking radiopharmaceuticals (PhD). Delft University of Technology, Netherlands:16.

Chapter 3 - Experimental Design

3.1 Aim

The aim of this research was to investigate novel bisphosphonate containing ligands for targeted radiotherapy of neoplastic bone disease using rodent and primate animal models and scintigraphy.

3.2 Materials – Experimental animals: primates, rodents

The success of the outcome requires that the normal primate (*Papio ursinus*) with its in vivo bisphosphonate behaviour for purposes of scintigraphic monitoring, using ^{99m}Tc-MDP, has to be validated as a useful model to interpret experimental results and extrapolate to man. This can be done in bone fracture healing experiments by observing the bone healing scintigraphically over time (see 2.4).

The rodent studies will be reserved for osteosarcoma bearing nude mice (Balb C) to assess tumour uptake of novel bisphosphonate containing ligands while Wistar rats will serve as rodent controls because their large body sizes allow better evaluation of scintigraphic images (see 2.4).

3.3 Methodology

3.3.1 Ligand biokinetics using scintigraphy and diagnostic radionuclides

The primate fracture healing experiment will involve controlled fractures of the forelimb bones of the primates, and fixation with different surgical implants. The fracture-healing process will be studied by radiography and ^{99m}Tc-MDP scintigraphy at regular intervals. Under ketamine barbiturate anaesthesia. The data from the scintigraphy will be analysed by the image profile feature available from most nuclear medical computer software, which facilitates consistent localization of the exact fracture area in each consecutive image as the study progresses.

The images will be studied for physiological bone activity and the time span of the healing process compared to known information from human patients (Greiff, 1978; Martin, 1983).

Likewise the normal primate will be evaluated as a model for the pharmacokinetics i.e. biodistribution, using scintigraphic monitoring, of a typical and well known therapeutic radiopharmaceutical generally used for palliation in painful human skeletal metastases viz ^{153}Sm-EDTMP (Serafini, 2001; Verma *et al.*, 2002). Comparing the results to available human data and establishing good agreement of the in vivo behaviour of the radiopharmaceutical will direct the meaningful continuation of these biodynamic investigations with novel bone seeking ligands (2.3.2).

A novel approach for ligand optimisation involving neoplastic tissues' abnormal blood supply (increased permeability) and lack of lymphatics will subsequently be investigated. Hereby radiolabelled macromolecules should accumulate selectively at the target site (Seymour, 1992). The synthesis of the macromolecule polyethyleneiminomethyl phosphonic acid (PEI-MP), and its labelling with ^{99m}Tc, as well as the required quality control will be the next steps. Macromolecular sizes ranging from 3 to 300 kDa will be considered and the label ^{99m}Tc will serve as tracer for the scintigraphic biodistribution studies to be performed in normal adult male primates. The results obtained from these studies should allow the identification of a suitable size-fraction, as a bone-seeking ligand. Molecular sizing of the polymeric PEI-MP can drastically alter its biodistribution and pharmacokinetic properties (Dormehl *et al.*, 2001), which can be exploited to suit different applications and targeting of specific organs, tissues and pathological affected areas, as well as allowing the sparing of vital organs and promoting speedy urinary excretion of the ligand (2.2.1 and 2.5.2).

3.3.2 Therapeutic radiopharmaceuticals: modelling and scintigraphy

In order to fulfil a therapeutic role the most suitable ligand would have to form a stable and appropriate complex with one or more of the therapeutic radionuclides e.g. ^{153}Sm, ^{186}Re and ^{117m}Sn(II) (Lewington, 1996). For informed selection of such a radionuclide which would be successfully complexed with the ligand PEI-MP for targeted delivery to osteosarcoma/metastatic bone tumours, metal ion speciation in blood plasma will be used to predict the in vivo behaviour of the potential bone-seeking therapeutic radiopharmaccuticals.

The blood plasma model ECCLES (Jarvis *et al.*, 1995) to be used here will include PEI-MP as ligand (2.5).

Favourable prediction of good in vivo behaviour of any of the complexes of PEI-MP labelled with therapeutic radionuclides will lead to the development of appropriate radiolabelling procedures. Such labelling procedures will have to yield radiochemical purities of the complexes of ≥ 95 %, little presence of colloids (< 1%), and in vivo and in vitro stability of the complex. The quality control on these requirements will be done by chromatography on ITLC-SG (ethanol) and cellulose ITLC (1.0 M Citrate, pH 7.0) (2.6.3).

It is known that changing the radionuclide label of a particular ligand might change the resultant pharmacokinetics (Lin, 1996; Mitterhauser *et al.*, 2004). It is therefore necessary that the biodistribution of variously molecular sized therapeutic complexes, e.g. ^{117m}Sn(II)-polyethyleneininomethyl phosphonate complexes all be investigated in the normal primate model to establish any possible differences from the Tc-counterparts and thus their potential as selective therapeutic bone agents according to the criteria mentioned before, including in vivo stability (Zeevaart *et al.*, 2004).

3.3.3 Radioligand uptake by osteosarcoma: scintigraphy and organ counting

From the normal bone studies the next step will be to investigate the potential exploitation of the EPR effect due to its macromolecular nature, where bone malignancies are present. Where available dogs with spontaneous occuring appendicular osteosarcomas, and intended for chemotherapy, will be administered with ^{99m}Tc-PEI-MP to assess bone tumour uptake of the labelled ligand. The ^{99m}Tc will purely serve as tracer. Tumour to background ratios will be determined scintigraphically. The tumour uptake of ^{117m}Sn-PEI-MP by different types of canine osteosarcoma induced into nude mice will subsequently be studied in a well counter. This study will continue also using ^{186}Re-PEI-MP as a potential radiopharmaceutical (2.5.2).

3.3.4 Computational procedures and statistical analysis

The reasoning behind the experimental and computational procedures applied in performing this research has been discussed, described and explained in chapter 2. Extensive experimental detail is provided as needed in the reports in chapters 4 to 12.

Statistical analysis will be performed to prove significance of the results. Comparisons between groups of animals e.g. control groups and/or groups with modified ligands require that mean percentage uptake and half-life of the radiopharmaceuticals ± SD in various organs be calculated for the various groups. From these values dosimetry i.e. radiation dose to target organs and tumours can be calculated using MIRDOSE. Comparisons will be assessed for significant differences between corresponding values using Student's two tailed t-test for paired variables on a 5% level of confidence.

3.3.5 Toxicity and pyrogenicity tests

All compounds will be tested beforehand for toxicity and pyrogenicity. The Standard SABS methods 6:12 (1992) will be used whereby five Balb C mice will be injected i.v. each with a dose of 0.165 mg/0.33 cc per mouse of the compound. They will be observed and monitored at 24 hrs and 48 hrs, and when found alive and well the injected compound to be used in these experiments will be regarded non toxic and fit for patient application.

Three rabbits will be observed and monitored over 2 hours for body temperature fluctuations, and an average obtained for each. Subsequently they will receive the compound (see above dose) injected i.v. and will be observed and monitored for 2.5 hours. Differences in patterns of temperature fluctuations will be recorded.The ligands for this investigation must comply with requirements for non-pyrogenicity of the tested compound for the investigations to continue.

3.4 Ethical Considerations

It must be emphasised that all animal experimentation will be carried out according to international ethics guidelines and after approval by the authorised Ethics Committees of the

Universities of Pretoria and Coimbra, under supervision (primate studies) of a qualified veterinarian.

3.5 Studies conducted and discussed in this thesis

These studies are listed under publications in § 1-5 pg 8.

3.6 References

DORMEHL, I.C., LOUW, W.K.A., MILNER, R.J., KILIAN, E., SCHNEEWEISS, F.H.A. 2001. Biodistribution and pharmacokinetics of variously sized molecular radiolabelled polyethyleneiminomethyl phosphonic acid as a selective bone seeker for therapy in the normal primate model. *Drug. Res.* 54: 258-263.

GREIFF, J. 1978. Autoradiographic studies of fracture healing using ^{99m}Tc-Sn-polyphosphate. *Injury* 9:271-277.

JARVIS, N.V., WAGENER, J.M., JACKSON, G.E. 1995. Metal ion speciation in blood plasma as a tool for elucidating the in vivo bchaviour of radiopharmaceuticals containing ^{153}Sm and ^{166}Ho.*J. Chem. Soc. Dalton Trans.* 1411-1415.

LEWINGTON, V.J. 1996. Cancer therapy using bone-seeking isotopes. *Phys Med Biol* 41(10):2027-2042.

LIN, J.H. 1996. Bisphosphonates: a review of their pharmacokinetic properties. *Bone* 18(2):75-85.

MARTIN, P. 1983. Bone scan scintigraphy in the diagnosis and management of traumatic injury. *Semin Nucl. Med.* 13: 104-108.

MITTERHAUSER, M., TÖGEL, S., WADSAK, W., MIEN, L.K., EIDHERR, H., WIESNER, K., VIERNSTEIN, H., KLETTER, K., DUDCZAK, R. 2004. Binding studies of [^{18}F]-fluoride and phosphonates labelled with [^{111}In], [^{99m}Tc], [^{153}Sm], and [^{188}Re] on bone compartments: a new model for the pre vivo evaluation of bone seekers? *Bone* 34: 835-844.

SERAFINI, A.N. 2001. Therapy of metastatic bone pain. *J. Nucl. Med.* 42(6):895-906.

SEYMOUR, L.W. 1992. Passive tumor targeting of soluble macromolecules and drug conjugates. *Crit Rev Ther Drug Carrier Syst* 9(2):135-187.

VERMA, N., SINGH-WADHWA, S., CHAN, W.L. 2002. Bony metastases seen on scintigraphy with samarium-153. *Clin Nucl Med* 27(3):207.

ZEEVAART, J.R., LOUW, W.K.A., KOLAR, Z.I., KILIAN, E., VAN RENSBURG, F.E., DORMEHL, I.C. 2004. Biodistribution and pharmacokinetics of variously molecular sized Sn-117m (II)-polyethylene-iminomethyl phosphonate (PEI-MP) complexes in the normal primate model as a potential selective therapeutic bone agent. *Arzneim. Forsch./Drug Res.* 54, No. 6, 340-347.

Chapter 4 – A Technique to Evaluate Bone Healing in Non-Human Primates Using Sequential ^{99m}Tc-Methylene Diphosphonate Scintigraphy

Abstract

The assesment of bone healing through sequential nuclear medical scintigraphy requires a method of consistent localization of the exact fracture area in each consecutive image as the study progresses. This is difficult when there is surrounding bone activity as in the early stages of trauma, and also if complications should set in. The image profile feature, available from most nuclear medical computer software, facilitates this procedure considerably, as is indicated in the present report on bone healing in baboons. Together with roentgenology and histology a ^{99m}Tc-MDP study was in this way successfully done on the healing of long bone fractures experimentally induced in non-human primates. Different surgical implants were used. The result indicated that ^{99m}Tc-MDP accurately reflects the physiological activity in bone. The time-activity curves obtained are presently being studied together with extensive histology, bearing possible clinical application in mind.

Eine Methode zur Bewertung Der Knochenheilung mittels der sequentiellen ^{99m}Tc-MDP Szintigraphie

Die Bewertung der Knochenheilung durch sequentielle nuklearmedisinische Szintigraphie erfordert eine Methode der konsequenten Lokalisierung des genauen Knochenbruchgebietes in jedem aufeinanderfolgenden Bild im Verlaufe der Untersuchung: dies ist bei benachbarter Knochenaktivität, wie im frühen Stadium der Verletzung oder bei Komplikationen schwierig. Das meist in nuklearmedizinischer „software" vorhandene Bildprofilprogramm erleichert dieses Verfahren beträchtlich. Wie dieser Bericht über die Knochenheilung bei Pavian en zeigt. Zusammen mit Röntgenologie und Histologie konnte eine ^{99m}Tc-MDP Untersuchung dieser Art erfolgreich zum Studium der Heilung von experimentellen Knochenbrüchen bei nicht-menschlichen Primaten angewendet werden. Verschiedene chirurgische Implantationen wurden vorgenommen. Die Ergebnisse zeigten, daß ^{99m}Tc-MDP die physiologische Aktivität in Knochen genau reflektiert.

Derzeit werden die Zeit-Aktivität-Kurven zusammen mit umfassender Histologie im Hinblick auf eine klinische Verwendung untersucht.

4.1 Introduction

This study was performed to devise and assess a sensitive non-invasive method for investigating the healing process of long bones in non-human primates. A specific clinical application in mind is the early detection of non-healing or delayed healing of fractures in the aged.

Important for accurate evaluation is the consistency of the localisation of the fracture site and the region of healthy bone from each scintiscan for the entire study. The present report concerns a technique which seems to be successful for this purpose and is found useful towards the clinical application.

4.2 Materials and Methods

Four adult chacma baboons (*Papio Ursinus)* were used in this experiment. All four animals were clinically and radiographically normal. They were housed indoors in environmentally controlled rooms for the duration of the experiment and they were fed a balanced commercial diet with water freely available. Eight forearms, i.e. a total of 16 radius and ulna bones were osteotomized with a Gigli saw to create simple standard and controlled fractures. The following internal fixation plates were used:

1. Standard Müller compression plate (Vitalium) with 6 holes, on 1 radius and 1 ulna.
2. Standard Müller compression plate (Vitalium) with 4 holes, on 1 radius and 1 ulna.
3. Sherman plate (stainless steel) 6 holes, on 2 radii and 1 ulna.
4. Sherman plate (stainless steel) 4 holes, on 1 ulna.
5. [1]Mennen clamp-on plate (stainless steel) on 3 radii and 3 ulnae[2], (Fig 4-1)

[1] Reference: In press – Journ. Of Bone and Joint Surgery
[2] Two bones had to be withdrawn from the experiment due to the onset of infection and required additional surgery.

Fig 4-1: The Mennen clamp-on plate in position on a cadaver forearm

The Sherman and Mennen plates were protected by the above elbow casts of fibre glass material (e.g. "Scotchcast and Lightcast").

Post-operatively two weekly X-rays of the forearms, lateral and anterior-posterior, were taken. X-rays were done on the same day, but preceding the isotope study. Sections of the osteotomized areas of the radii and ulnae were taken for histology at different times post-operatively from a similar concomitant group. This was accompanied by extensive radionuclide evaluation of the fractures.

The baboons were each intravenously injected with approximately 7 mCi of ^{99m}Tc-MDP (3, 4, 5). In each case scanning of the relevant bones commenced 3 hrs post injection using an Ohio Nuclear (ON 410 Sigma) large field gamma camera. Data were stored on disc for evaluation through an A^2 MDS data processor. The complete study consisted of a pre-operative scan to obtain a baseline image for each bone (Fig 4-2) followed by scans at 3 days and again 1 week post-operatively and thereafter at weekly and fortnightly intervals, as the lesions stabilized. To evaluate the degree of bone activity at the site of fracture, use was made of the image profile facility of the computer software. A profile was chosen along the length of the fractured bone, with a width corresponding to the maximum width of the bone. Such a profile curve represents the distribution of radioactivity along the bone as countrate per channel. A peak is found which represents increased activity across the fracture. This fracture peak can be consistently localized with respect to elbow and wrist activity.

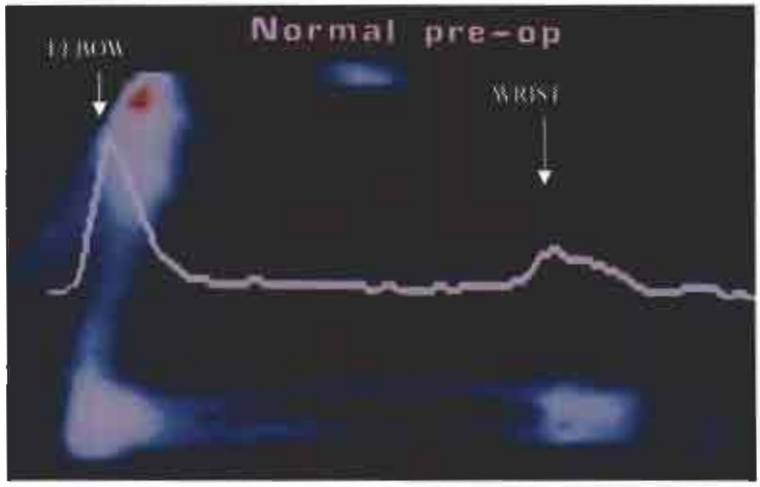

Fig 4-2: Normal forearm and profile; elbow and wrist areas clearly indicated

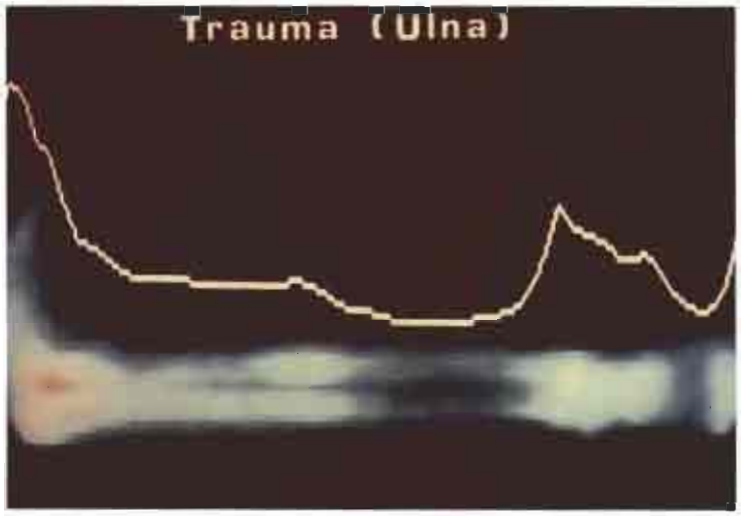

Fig 4-3: Three days post-operative trauma visible on the profile of the right ulna

The area under this peak is an indication of the total uptake of radioactivity by active bone in the immediate vicinity of the fracture. To obtain the total count across the fracture an integration was performed across the peak and an average countrate/channel (L) was calculated. The same procedure followed across a region of normal bone and an average normal countrate per channel (N) was obtained. The ratio L/N is the factor used to follow bone activity with time in the region of the fracture. An average curve for each of 3 surgical procedures (Mennen, Sherman, Müller) was obtained (Fig 4-7) and could be compared to the available histology and X-rays.

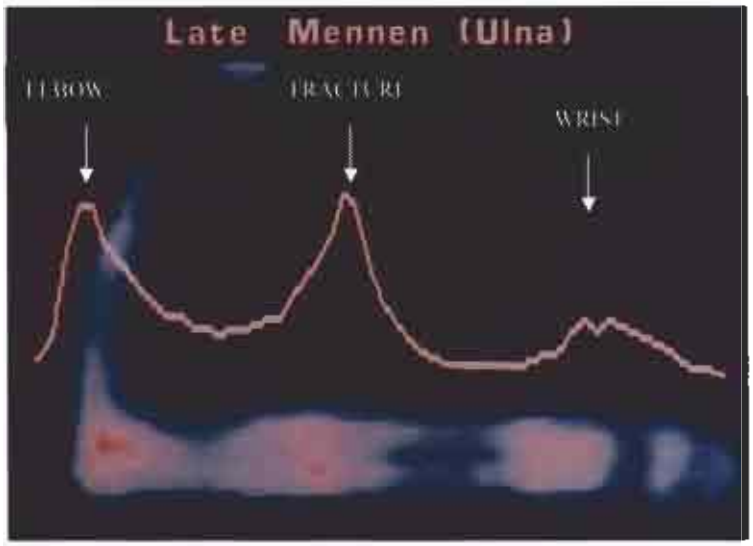

Fig 4-4a: Early healing (inflammatory) stage – 3 weeks post-operative. The profile is of the right ulna. The implant is a Mennen plate.

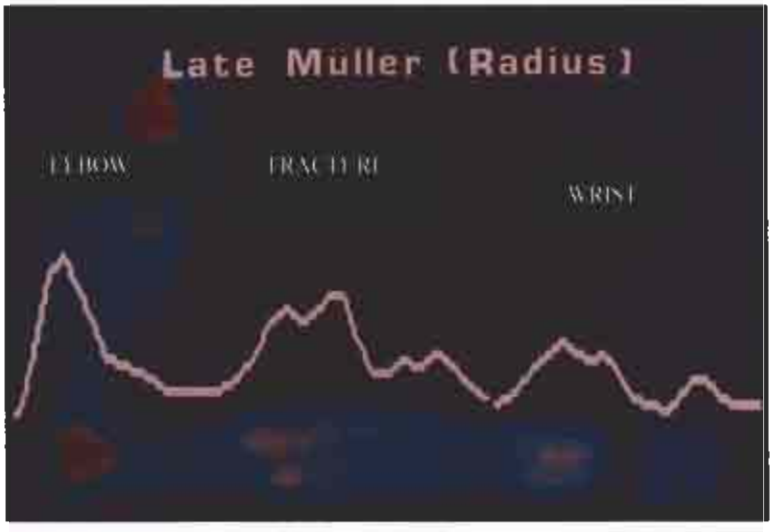

Fig 4-4b: A three week post-operative study with a standard 4 hole Müller plate. The profile is of the right radius.

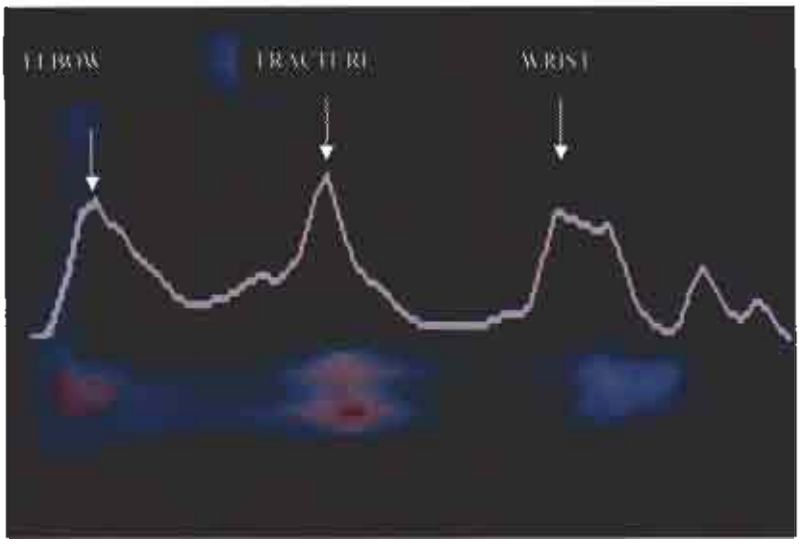

Fig 4-5a: A six week post-operative study with a Mennen plate. Profile of left ulna.

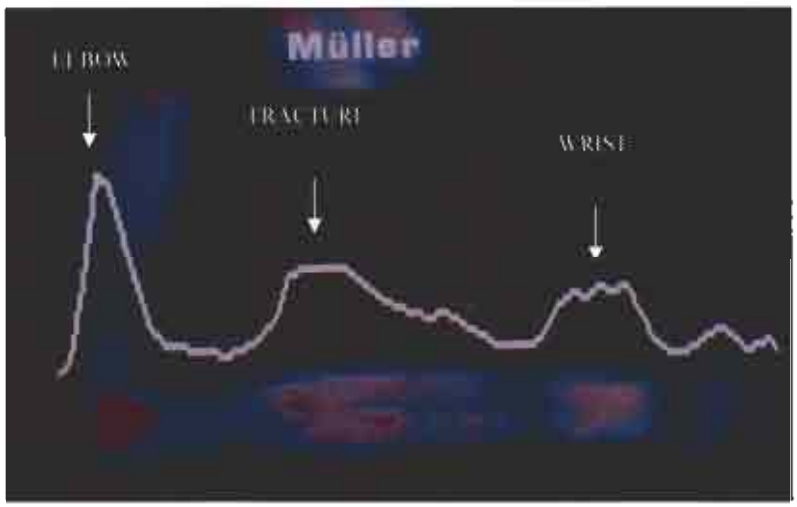

Fig 4-5b: Study of a 4-hole Müller plate – 6 weeks post operative. Profile of the right radius

4.3 Results

A typical pre-operative scan (Fig 4-2) and the subsequent post-operative stages of trauma (at approximately 3 days post operation), early healing (within 3 weeks of the operation) and late healing (after about 6 weeks) are presented in Figs. 4-3, 4-4, 4-5, together with their corresponding profiles. The elbow, wrist and fracture areas are marked by arrows. From Figs. 4-4 and 4-5 a comparison can be drawn between the effects of Mennen and standard Müller plates on the development of the fracture with time and on the surrounding bone. It is

interesting to note the initial spread in the "hot spot" as obtained by Müller implant in the early stages, with respect to the well defined area of increased radioactivity with a Mennen plate. In late stages the bone activity induced by the screws (Müller plate) can clearly be distinguished from the fracture.

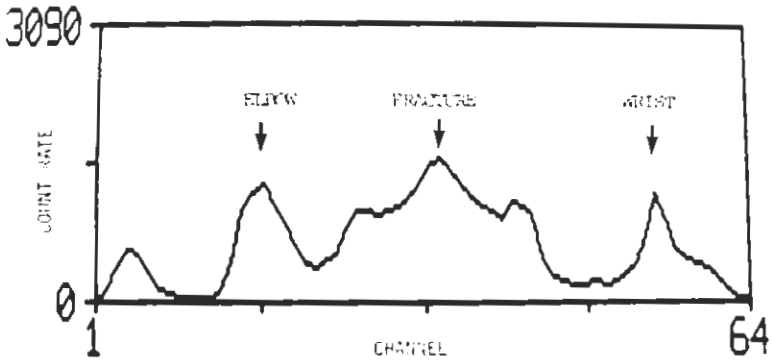

Fig 4-6: A typical late study with a Müller plate distinguishing between " fracture" and "screw" activity, peaking left and right from fracture.

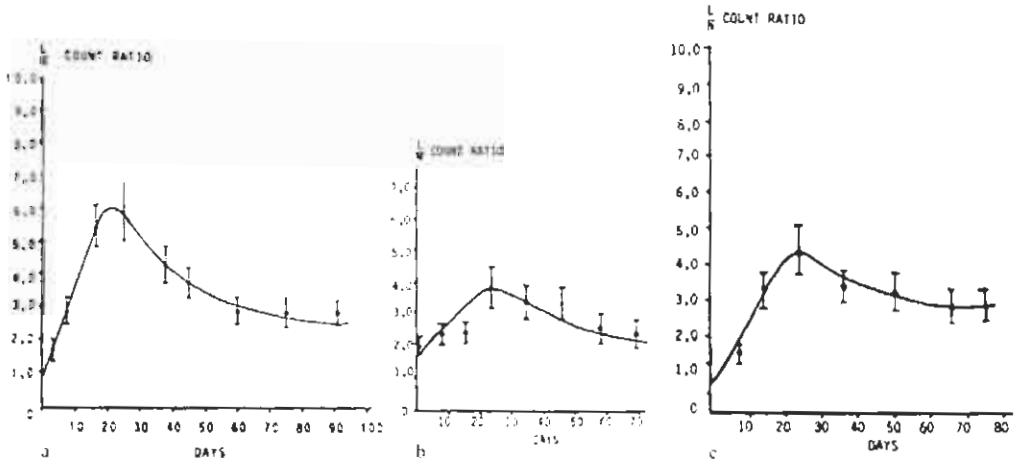

Fig 4-7: L/N vs time curves. (a) Mennen implant. (b) Sherman implant. (c) Müller implant

The time-activity curves (L/N vs time) summarize the results (Fig 4-7). These represent the 3 different implants and show very little difference in the time to peak, which turns out to be 3 weeks at the eventual stabilizing time of the lesion, round about 55-60 days. The experimental errors indicated in the time-activity curves were obtained from the statistics of the radioactive countrate and the degradation of the results on applying mathematical procedures.

Roentgenological plates indicate normal bone healing i.e. callus formation in all the studies, but do not reflect any quantifiable indication of the healing process.

Histology on 8 specimens of fracture areas corresponding to different stages of healing demonstrates vascularization of the fracture area and ossification.

4.4 Discussion

The profile evaluation method used in the radionuclide study allows accurate lesion localization with respect to elbow and wrist. The exact position of the lesion becomes clear in the late studies when trauma in the immediate environment had sufficiently cleared. It is then also possible to distinguish the fracture activity from "screw activity" (Fig 4-6). This exact fracture position is then used for the evaluation, also in the early studies. In this way an accuracy, otherwise attained with difficulty, is introduced into the nuclear medical study.

The radionuclide study gives an indication of the degree and extent of operative trauma as well as of the early bone healing periods in the pre-callus stage (i.e. inflammatory stage) and of bone healing activity in the bone forming stage (2). It also gives an indication of the duration of the healing process. The radioisotope study shows only vascularized bone. Bone chips which were inserted in a control study were not demonstrated until after 3-4 weeks when vascularization takes place. Contrary to the roentgenological procedure where a shadow of the accumulated healing stages is visualized, the radionuclide study demonstrates very sensitively the bone healing stage as such. Scintigraphically, however, it is not possible to distinguish between the effects of the different implants inserted on the bone fractures. Differences in metal type (e.g. stainless steel, vitalium), thickness and shape as well as biological differences as age (6) of the animal and variation in bone type cannot be corrected for.

Histology on 8 specimens of fracture areas corresponding to different stages of healing demonstrates an encouraging relationship with the (L/N) curve.

It therefore seems possible to use nuclear scintigraphy in this manner, as based on the profile technique to demonstrate quantitatively (L/N) and qualitatively bone healing at any given stage. A further study is in progress to extensively correlate the L/N curve with histological change in the long bone of the primate, with eventual clinical application in mind.

4.5 References

1. **GREIFF, J.** 1979. Bone healing in rabbits after compression osteosynthesis: a comparative study between the radiological and histological findings. *Injury* 10: 257-267.

2. **GREIFF, J.** 1981. Bone healing in rabbits after compression osteosynthesis, studies by Tc-99m (Sn) Polyphosphate Scintimetry and Autoradiology. *J. Nucl. Med.* 22: 693-698.

3. **RUDD, T.G., ALLEN, D.R., HARTNETT, D.E.** 1977. Tc-99m methylene disphosphonate versus Tc-99m pyrophosphate: biologic and elinical comparison. *J. Nucl. Med.* 18: 872-876.

4. **RUDD, T.G., ALLEN, D.R., SMITH, F.D.** 1979. Tc-99m labelled methylene disphosphonate and hydroxyethylidine disphosphonate – biologic and clinical comparison. *J. Nucl. Med.* 20: 821-826.

5. **SUBRAMANIAN, G. MCAFEE, J.G., BLAIR, R.J., et al.** 1975. Technetium-99m methylene diphosphonate – a superior agent for skeletal imaging: comparison with other technetium complexes. *J. Nucl. Med.* 16: 744-755.

6. **WILSON, M.A.** 1981. The effect of age on the quality of bone scans, using Tc-99m pyrophosphonate. *Radiology* 139: 703-705.

Chapter 5 - Evaluation of Samarium-153 and Holmium-166-EDTMP in the Normal Baboon Model

Abstract

Bone-seeking radiopharmaceuticals such as ethylenediaminetetramethylene phosphonate (EDTMP) complexes of samarium-153 and holmium-166 are receiving considerable attention for therapeutic treatment of bone metastases. In this study, using the baboon experimental model, multicompartmental analysis revealed that with regard to pharmacokinetics, biodistribution, and skeletal localisation, ^{166}Ho-EDTMP was significantly inferior to ^{153}Sm-EDTMP and ^{99m}Tc-MDP. A more suitable ^{166}Ho-bone-seeking agent should thus be sought for close similarity to ^{153}Sm-EDTMP to exploit fully the therapeutic potential of its shorter half-life and more energetic beta radiation.

Key Words: Samarium-153, Holmium-166, EDTMP, Pharmacokinetics, Baboon model

5.1 Introduction

Radiation teletherapy is effective to control or palliate isolated skeletal metastases. Difficulties associated with its application in multifocal disease together with recent availability of various new bone-seeking radiopharmaceuticals led to renewed interest in treatment with internal radionuclide therapy (9, 10). Although the current treatment objective is primarily for palliative purposes, a potential use in curative therapy should also be investigated (10, 22). Therapeutic success will hinge on many interrelated factors, such as the careful choice of a radionuclide (of which the biochemical properties dictate its pharmacokinetics and biodistribution) (12, 26, 28).

Radionuclides suitable for therapeutic purposes, but with diverse nuclear properties such as samarium-153 ($t_{½}$ 46.7 h; β^- 805 [21%]; 702 [44%] and 632 [34%] keV), max. soft tissue penetration ~0.3 cm; γ (103 [28%]keV) and holmium-166 ($t^{½}$ 26.9 h; β^- 1776 [48%]; and 1840 [51%] keV max. soft tissue penetration 0.84 cm; γ (81 keV [62%] and 1380 [1%] keV) can be

considered. These nuclear properties and resultant radiobiological effects may render useful ^{153}Sm- and ^{166}Ho-based radiopharmaceuticals with complementary therapeutic applications (21, 29).

Samarium (Sm) and holmium (Ho) are lanthanides with similar chemical properties. They form stable complexes with bone-seeking phosphonates such as ethylenediamine tetramethylene phosphonic acid (EDTMP). ^{153}Sm-EDTMP has been experimentally investigated in animals and tested in humans for pain palliation of bone metastases (4, 5, 8, 14, 15, 25), while ^{166}Ho-EDTMP and ^{166}Ho-DOTMP (tetrazazcyclododecane tetramethylene phosphonic acid) have been evaluated in experimental animals for bone marrow ablation (1, 20). However, more information regarding the pharmacokinetics, biodistribution, and bone localisation of ^{153}Sm-EDTMP and ^{166}Ho-EDTMP is needed before treatment protocols in humans can be concluded. For this purpose extensive in vivo experimentation in animal models cannot be avoided. The use of non-human primates such as baboons (*Papio* ssp.) is justified in these investigations. The baboon model conforms to many of the required criteria of parallelism (e.g. anatomical, physiological, immunological, and radiobiological) of the human (6, 7, 18).

This investigation concerned the pharmacokinetics, biodistribution, and bone localisation of ^{153}Sm-EDTMP and ^{166}Ho-EDTMP in the normal baboon experimental model, before a clinical trial in humans with metastatic bone cancer was considered. The pharmacokinetics, biodistribution, and bone localisation of ^{153}Sm-EDTMP and, subsequently, also ^{166}Ho-EDTMP were scintigraphically compared with those of ^{99m}Tc-MDP by dynamic and static studies. From these results, together with urine excretion data, compartmental modelling could be done and the in vivo behaviour of ^{153}Sm-EDTMP and ^{166}Ho-EDTMP could be described. These results were also applied to calculate ^{153}Sm- and ^{166}Ho-cumulated activities and absorbed doses in various organs.

5.2 Materials and Methods

5.2.1 Radionuclides

Both ^{153}Sm and ^{166}Ho were prepared by neutron irradiation of 99% enriched $^{152}Sm_2O_3$ (1.0-2.0 mg, 48 h) and $^{165}Ho_2O_3$ (1.0-2.0 mg, 48 h) in the Safari-1 Research Reactor using a thermal flux of 2.78 x 10^{13} n $cm^{-2}s^{-1}$. Typical specific activities of 272.3 x 10^4 MBq/ mmole for $^{152}Sm_2O_3$ and 65.53 x 10^4 MBq/mmole for $^{166}Ho_2O_3$ were obtained. Following irradiation, the oxide targets were dissolved in 0.2 mL HCl (1.0 M for $^{153}Sm_2O_3$ and 2.0 M for $^{166}Ho_2O_3$), diluted to 0.1 M HCl with sterile deionised water and filtered (Millex-GV, 0.22 µm, Millipore Bedford, MA). When necessary a carrier solution $SmCl_3$ was added to obtain a samarium concentration of 2.8 mM and an activity of 1554 MBq/mL 2 days after irradiation. Gamma-ray spectra obtained by counting aliquots of the $^{153}SmCl_3$ and $^{166}HoCl_3$ stock solutions with a Ge(Li)-gamma detector revealed within the $^{153}SmCl_3$ the presence of only ^{152}Eu, ^{154}Eu, and ^{155}Eu. The ^{152}Eu activity at the end of irradiation was less than 6.8 x 10^{-4} % of ^{153}Sm, while those of ^{154}Eu and ^{155}Eu were < 4.3 x 10^{-5} % and 2.6 x 10^{-5} % respectively. The only radionuclide present with ^{166}Ho was ^{153}Sm at an activity of ~0.6 % of ^{166}Ho.

5.2.2 The Ligand and Complexing with ^{153}Sm and ^{166}Ho

EDTMP was prepared by the condensation of ethylenediamine, phosphorous acid and formaldehyde by a modified Mannich reaction in the presence of hydrochloric acid (19). Recrystallisation from water/ methanol and water yielded white crystals, m.p. 214°C (lit. m.p. 214°C). Analysis: Found; C, 16.83 %; H, 4.62 %; N, 6.52 %; Calculated for $C_6H_{20}N_2O_{12}P_4$; C, 16.52 %; H, 4.62 %; N, 6.42 %.

The EDTMP reagent was prepared in 10-mL vials by lyophilising 1-mL aliquots of 50 mg/mL EDTMP solution of pH 8.5. The dry product was sealed under nitrogen. Sterility, apyrogenicity, and toxicity were ascertained by standard methods.

For complexing 1-mL aliquots of $^{153}SmCl_3$, alternatively $^{166}HoCl_3$ (containing the prescribed amount of activity and Sm^{3+} and Ho^{3+}) were added to lyophilised EDTMP reagent kits. The solutions were left for 30 min, diluted to 5 mL, and counted, whereafter 3 µL samples were

chromatographically analysed. After sealing, the vials containing the final products (pH 7.0-8.0) were sterilised by autoclaving. Radiochemical purity was determined by thin layer chromatography on cellulose thin-layers (TLC aluminium sheets, cellulose, 0.1 mm, E. Merck, Darmstadt, Germany) using pyridine: ethanol: water (1:2:4) as solvent (25). ^{153}Sm-EDTMP as well as ^{166}Ho-EDTMP was found at R_f 0.75-0.85, and uncomplexed Sm^{3+} and Ho^{3+} remained at the origin. Labelling efficiencies were greater than 97 % for both ^{153}Sm-EDTMP and ^{166}Ho-EDTMP.

5.2.3 Blood and Urine Collection after Administration of ^{153}Sm-EDTMP and ^{166}Ho-EDTMP

The animal experimentation was done according to the National Code for Handling and Use of Animals in Research, Education, Diagnosis and Testing of Drugs and Related Substances in South Africa and approved by the Ethics Committee of the University of Pretoria.

Anaesthesia was induced in healthy, male baboons (*Papio ursinus*) of average weight 27.5 (+-2.0) kg with ketamine hydrochloride (Ketalar, Parke Davis, SA, 10 mg/kg) and maintained with pentobarbitone sodium as a solution of 9 mg/mL in Ringer's lactate (Sagatal, Maybaker, SA) at a rate of 30 mL/h in the vena cephalica. A 7F urinary catheter was placed in the urinary bladder to facilitate the collection of urinary samples.

Doses of 370 MBq ^{153}Sm-EDTMP (n = 6) and ^{166}Ho-EDTMP (n = 6) were administered. One lyophilised kit containing 50 mg EDTMP was used for each animal. Blood and urine samples were collected at fixed intervals for 4 h. The activity and volume of each sample were measured immediately and registered.

5.2.4 Biodistribution of ^{153}Sm-EDTMP and ^{166}Ho-EDTMP

Twelve healthy male baboons (six each for ^{153}Sm-EDTMP and ^{166}Ho-EDTMP) (average weight 27.5 kg) were used in this study. Anaesthesia in each case was induced with ketamine hydrochloride (10 mL/kg) and maintained as above by an IV administration of pentobarbitone sodium solution.

Scintigraphy was performed (Siemens Orbiter) with the animal positioned in the supine position for planar images. The data acquisition initially involved a view of the thorax, liver and kidneys and was performed as a dynamic study of 30 x 1 min frames on a countdown bolus injection of 111 MBq ^{153}Sm-EDTMP or 185 MBq ^{166}Ho-EDMP. Static images of 4-min duration each followed at 2, 3, 4, 5 and 7 h after the injection of the tracer. These images presented the skeletal structure of the skull to the pelvis as two matched images.

From the dynamic study, time-activity curves were obtained for the cardiac, kidney, and liver regions. Regions of interest (ROI) placed on areas of the bony structures of the skull, shoulder, sternum, ribs, and pelvis, as well as appropriate muscular background areas (no other organs were at this stage visible) from the static images, rendered relative region-to-muscular background ratios after natural background subtraction and consequently percentage uptake of ^{153}Sm and ^{166}Ho by the bone. This uptake of ^{153}Sm and ^{166}Ho by the bone was compared to ^{99m}Tc-MDP (185 MBq) uptake previously measured similarly in the same animals at the same time intervals but starting 3 h after ^{99m}Tc-MDP administration. Kinetic data from the dynamic studies and data from the static studies were normalised in agreement, with urine activity values expressed as a percentage of the injected activity. Blood sample activity was corrected with estimated blood volume and compared to injected activity to determine percentage blood activity at a specific time. These percentages were used to normalise ROI counts over the left ventricle in the dynamic study. These calibrated data were fitted to a multicompartment model using the Simulation Analysis and Modelling (SAAM-30) software and performed once for each of ^{153}Sm and ^{166}Ho on average raw data.

Six compartments were considered – *viz.* blood, bone, kidney, liver, urinary bladder, and the remainder of the body. Transfer rates, half-lives, and ^{153}Sm and ^{166}Ho-distributions for the different compartments were simulated using the compartmental model.

5.2.5 Dosimetry

The Medical International Radiation Dosimetry (MIRD) dose calculation system was used (16). The blood, bone, liver, kidney, urinary bladder content, and rest of the body were selected as source organs for absorbed dose calculations. Target organs were the ovaries, bone marrow, colon, lung, stomach, urinary bladder wall, breast, liver, oesophagus, thyroid, skin,

bone surface, and remainder of the body. The absorbed dose D (r_k) to each target organ k as the sum of the contributions of n source organs h for the radionuclide r was calculated using the following equation:

$$D(r_k) = A_h(0, \infty)\, S(r_k \leftarrow r_h)\, F$$

Where $A_h(0, \infty)$ is the cumulated activity in source organ h, $S(r_k \leftarrow r_h)$ the mean dose per unit accumulated activity (rad/μCi h), received by target organ k from source organ h and F the conversion factor from rad/μCi to mSv/MBq.

The cumulated activity ($A_h(0, \infty)$ for each source organ and the blood was calculated as the integral of the time-activity curve up to 4 h, plus the integral of the physical decay of the activity at 4 h. Cumulated bladder activity was calculated using only the 0-to-4 h period assuming voiding at 4h. The total absorbed dose of each target organ k is the sum of the contributions from the n source organs to that specific target organ. The effective dose was calculated according to the latest recommendations of the International Commission on Radiological Protection (13). The effective dose E can be considered as a rough estimate of the comparable whole body irradiation and was calculated from the formula

$$E = \sum_T W_T . H_T$$

Where W_T is the weighting factor for tissue or organ T and H_T is the equivalent dose in tissue T, given in Sv. The equivalent dose H_T was calculated using the formula

$$E = \sum_T W_R . D(r_k)_R$$

With W_R the radiation weighting factor (equal to 1 for the radionuclides under discussion) and $D(r_k)_R$ the absorbed dose for the different organs and tissue.

5.3 Results

Scintigraphy images of individual representative animals 4 h after injection of 111 MBq ^{153}Sm-EDTMP or 185 MBq ^{166}Ho-EDTMP are shown, respectively, in Fig 5-1b, c. These images reveal selective skeletal and little nonosseous tissue accumulation. For qualitative comparison, a typical skeletal image of 185 MBq ^{99m}Tc-MDP uptake previously measured in the same group of animals is presented (Fig 5-1a)

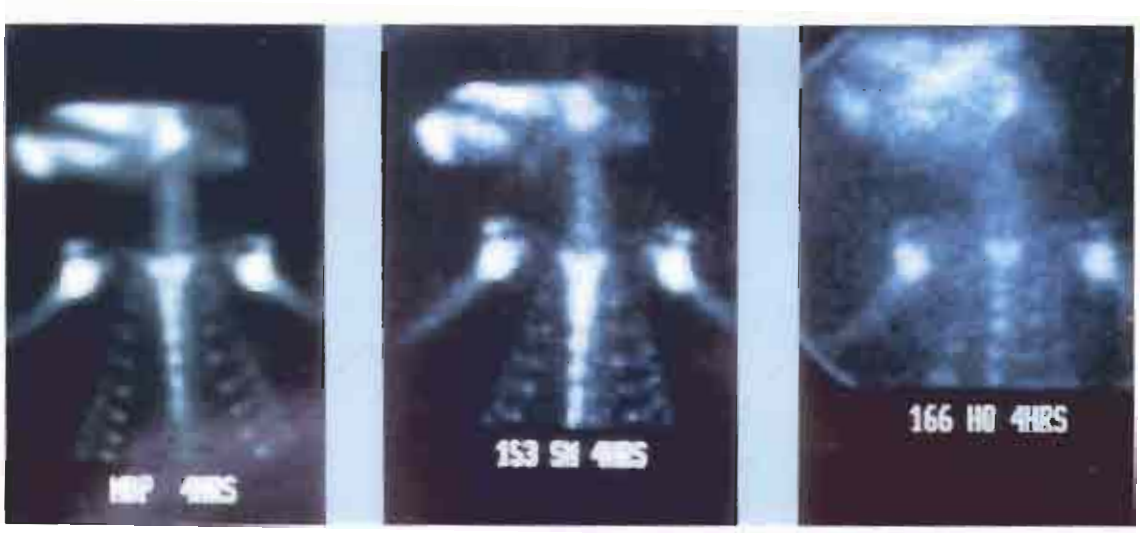

Fig 5-1: From left to right typical scintigrams of baboons indicating skeletal localisation of (a) ^{99m}Tc-MDP, (b) ^{153}Sm-EDTMP (111 MBq), and (c) ^{166}Ho-EDTMP (185 MBq) 4 h postinjection.

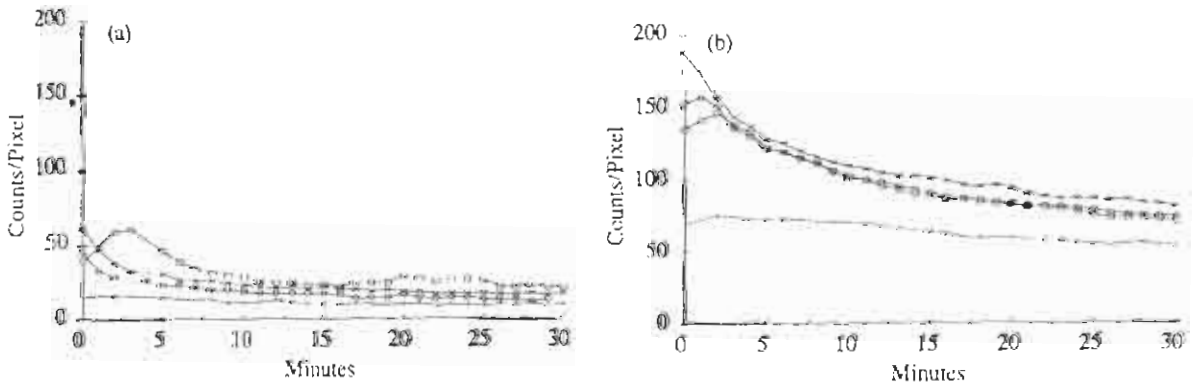

Fig 5-2: Time activity curves (counts/pixel) for the bloodpool (x), liver (○), kidney (□), and background (+) obtained from dynamic studies (0 to 30 min postinjection) with 111MBq ^{153}Sm-EDTMP (a) and 185 MBq ^{166}Ho-EDTMP (b), respectively.

The time-activity curves for the bloodpool, liver, kidney, and background obtained from dynamic studies (0 to 30 min) with ^{153}Sm- and ^{166}Ho-EDTMP are presented in Fig 5-2a, b. The resulting tracer uptake in the bone structure, which was measured at 4, 5, 6, and 7 h by static acquisition, produced additional count rate data that are shown as target-to-background ratios in Fig 5-3. The uptake ratio of ^{99m}Tc-MDP in the bone is included for comparison.

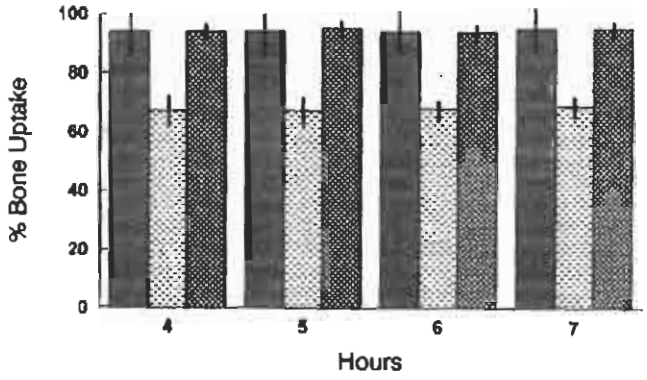

Fig 5-3: Percent bone uptake (region of interest-hip) of 185 MBq ^{99m}Tc-MDP, 185 MBq ^{166}Ho-EDTMP, and 111 MBq ^{153}Sm-EDTMP 4 to 7 hours post injection. SD ranges are indicated

The above data were used for compartmental analysis, and the fitted curves from these calculations are shown in Fig 5-4 a, b for ^{153}Sm-EDTMP and ^{166}Ho-EDTMP, respectively.

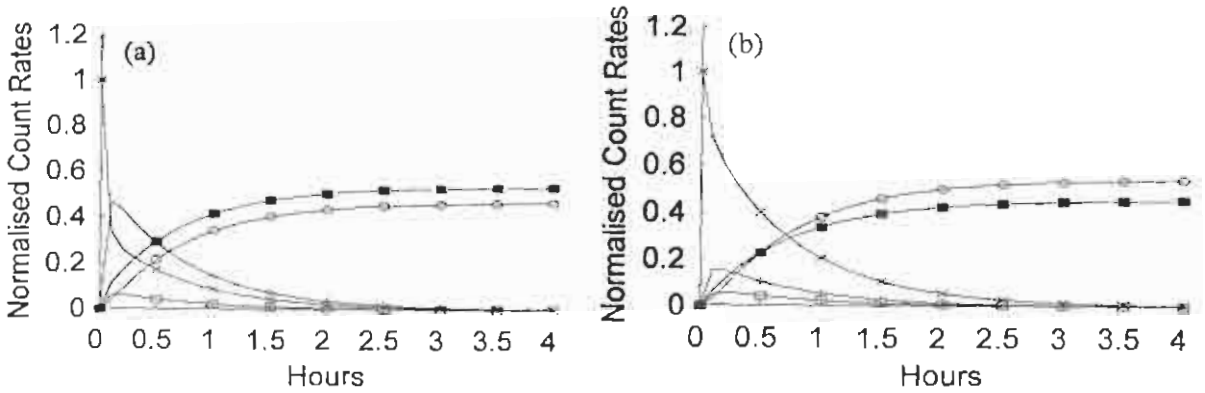

Fig 5-4: Compartmental analysis showing fitted curves for the bloodpool (x), urine (○), bone (■), kidney (□), and remainder of the body (+) of ^{153}Sm-EDTMP (a) and ^{166}Ho-EDTMP (b)

Transfer rates and half-lives for the various organs appear in Table 5-1 and tracer distribution in Table 5-2.

The total absorbed dose and effective dose to each target organ appear in Table 5-3. The effective dose was 0.208 mSv/ MBq for ^{153}Sm and 0.293 mSv/MBq for ^{166}Ho.

Table 5-1: Transfer Rates and Half-Lives of Clearance from Various Organs of ^{153}Sm and ^{166}Ho

	Sm-153		Ho-166	
Compartment	**Transfer Rate (Min^{-1})**	**Half-Life (Min^{-1})**	**Transfer Rate (Min^{-1})**	**Half-Life (Min^{-1})**
Blood-bone	0.033		0.013	
Bone-Blood		43 000		∞
Blood-Liver	0.000016		0.0000002	
Blood-Kidney	0.029		0.015	
Kidney-Urine	0.141		0.167	
Blood-Remainder	0.252		0.067	
Remainder-Blood		4.0		2.5

Table 5-2: Tracer Distribution of ^{153}Sm and ^{166}Ho

	Maximum %		Time of Max (h)		% at 4 h	
Organ	**Sm-153**	**Ho-166**	**Sm-153**	**Ho-166**	**Sm-153**	**Ho-166**
Bone	53	45	4	4	53	45
Urine	46	54	4	4	46	54
Kidneys	5.8	5.0	0.2	0.2	0	0
Remainder	46	15	0.1	0.1	1	0
Blood	100	100	0	0	0	0.4
Liver	0.03	0		0		0

5.4 Discussion

Intravenous administered bone-seeking internal radioisotopic agents distribute via the circulatory system throughout the body while simultaneously accumulating in the bone (2). The transfer rates of 3.3%/min of the ^{153}Sm-EDTMP from the blood to the bone (Table 5-1) and 2.9%/min from blood to kidney resulted in a maximum bone accumulation of 53% reached after 4 h (Table 5-2). This corresponded with previous results obtained in experimental animals and human (3-5, 8, 25).

There is a slight washout of ^{153}Sm from the bone with a long half-live of 43, 000 min (Table 5-1). The blood-to-bone transfer rate of ^{166}Ho-EDTMP of 1.3%/min and blood-to-kidney transfer rate of 1.5% is lower than that of ^{153}Sm-EDTMP (Table 5-1), resulting in a maximum accumulation of 45% after 4 h (Table 5-2). There was no washout of ^{166}Ho from bone, resulting in a half-life of infinity (∞) (Table 5-1). Forty-six percent of ^{153}Sm-EDTMP and 54% of ^{166}Ho-EDTMP were excreted in the urine (Table 5-2). The bone-to-background (cardiac bloodpool) uptake for ^{166}Ho-EDTMP was 69% in comparison to 91% for ^{153}Sm-EDTMP and 95% for ^{99m}Tc-MDP (Fig 5-3).

These results indicate that ^{166}Ho-EDTMP, in comparison to ^{153}Sm-EDTMP, exhibits poorer in vivo biodistribution and pharmacokinetic properties in the baboon model, which contrasts with previous findings in dogs (1). A possible reason for the discrepancy between these data and that of Appelbaum *et al.* (1) may be related to high plasma citrate levels in the baboon experimental animals. The fact that the ^{166}Ho-EDTMP is a weaker complex than ^{153}Sm-EDTMP (27) may account for more transchelation of ^{166}Ho-to-plasma citrate.

The highest absorbed doses were received by the bone marrow and the bone surface for both ^{153}Sm-EDTMP and ^{166}Ho-EDTMP (Table 5-3). The higher urinary accumulation and higher energy of ^{166}Ho leads to high radiation dose to the urinary bladder wall.

The count rate/unit activity was higher for ^{166}Ho than for ^{153}Sm (Fig 5-2 a, b). This is due to the scatter contribution from the high-energy γ-photon emitted by ^{166}Ho (1.38 MeV), as is also visible on the ^{166}Ho scintigram (Fig 5-1c). The effect of the scatter on the percentage distribution was never more than 2 %, tending to reduce the skeletal uptake of ^{166}Ho.

Table 5-3: Total Absorbed Dose in mSv/ MBq Injected Dose for Various Target Organs

		Sm-153		Ho-166	
Organ	**W_t**	**Dose (mGy/ MBq)**	**Eff. Dose (mSv/ MBq)**	**Dose (mGy/ MBq)**	**Eff. Dose (mSv/ MBq)**
Ovaries	0.20	0.007	0.00144	0.003	0.00061
Bone Marrow	0.12	1.240	0.14879	1.565	0.18778
Colon	0.12	0.007	0.00090	0.003	0.00031
Lung	0.12	0.009	0.00110	0.031	0.00368
Stomach	0.12	0.003	0.00041	0.001	0.00018
Urinary Bladder Wall	0.05	0.551	0.02757	1.566	0.07831
Breast	0.05	0.003	0.00016	0.001	0.00007
Liver	0.05	0.007	0.00033	0.010	0.00049
Oesophagus	0.05	0.010	0.00050	0.016	0.00080
Thyroid	0.05	0.006	0.00029	0.012	0.00060
Skin	0.01	0.004	0.00004	0.002	0.00002
Bone Surface	0.01	2.6441	0.02641	1.920	0.01920
Remainder	0.05	0.010	0.00050	0.016	0.00080
Total	1		0.20844		0.29289

W_t is the tissue weighting factor used in the calculation of effective dose

The total absorbed dose of ^{153}Sm for various target organs as presented in Table 5-3 corresponds to the calculated values of Logan *et al.* (17). In contrast, the calculated ^{166}Ho bone marrow dose (even if corrections are made for the lower bone uptake in the baboon model) differs considerable from the values for ^{166}Ho-EDTMP obtained by Appelbaum *et al.* (1) in a beagle (dog) model. This discrepancy model might be *inter alia* due to their use for S-values for human children, whereas adult human S-values were used for calculating the results in Table 5-3.

Considering the above biodistribution and pharmacokinetic imperfections of ^{166}Ho-EDTMP compared to ^{153}Sm-EDTMP, the development of a different palliative ^{166}Ho-based bone therapeutic agent with similar biodistribution and pharmacokinetic properties as ^{153}Sm-EDTMP might be a worthwhile approach.

The more energetic ß-emissions of ^{166}Ho (with its ~ 8.0 mm max. soft-tissue penetration) may be more efficient for the treatment of large nonossified tumours. These tumours respond poorly to ^{153}Sm-EDTMP owing to the matrix localisation properties of the phosphonates and limited (~3 mm) soft-tissue penetration of the ^{153}Sm ß-emissions (15). Its half-life of 26.9 h is

long enough to eliminate logistic problems, but is sufficient to provide a higher radiation dose rate than ^{153}Sm, which is advantageous for radiotherapeutic treatments (23, 24, 26).

5.5 Conclusion

Bone-seeking phosphonate complexes of ^{153}Sm and ^{166}Ho can form complementary therapeutic radiopharmaceutical agents owing to their different physical properties with regard to half-life and beta energies. Both ^{153}Sm and ^{166}Ho are lanthanides that easily form EDTMP complexes with a high radiochemical purity. The role of ^{153}Sm-EDTMP is defined and confirmed as a therapeutic agent for treatment of painful skeletal metastases. This comparative study of ^{153}Sm-EDTMP and ^{166}Ho-EDTMP in the baboon model reveals, despite their similar chemical characteristics, a significantly inferior performance of ^{166}Ho-EDTMP with regard to bone localisation, biodistribution and pharmacokinetics. Pursuing clinical trials on humans with ^{166}Ho-EDTMP is perhaps not justified. However, the development of more suitable bone-localising ligand(s) for ^{166}Ho should be seriously considered.

5.6 References

1. **APPELBAUM, F.R., BROWN, P.A., SANDMAIER, B.M., STORB, R., FISHER, D.R., SHULMAN, H.M., GRAHAM, T.C., SCHUENING, F.G., DEEG, H.J., BIANCO, J.A., KETRING, A.R., KAPLAN, D.** 1992. Specific marrow abliation before marrow transplantation using an aminophosphonic acid conjugate ^{166}Ho-EDTMP. *Blood* 80: 1608-1613.

2. **ARNOLD, J.S.** 1979. Kinetic analysis of bone imaging agents. In: *Principles of Radiopharmacology.* Vol. III (Edited by Colombetti L.G.), PP. 205-223. CRC Press, Boca Raton, FL.

3. **BAYOUTH, J.E., MACEY, D.J., KASI, L.P., FOSELLA, F.V.** 1994. Dosimetry and toxicity of samarium-153-EDTMP administered for bone pain due to skeletal metastases. *J. Nucl. Med* 35: 63-69.

4. **EARY, J.F., COLLINS, C., STABIN, M., VERNON, C., PETERSDORF, S., BAKER, M., HARTNETT, S., FERENCY, S., ADDISON, S.J., APPELBAUM, F., GORDON, E.E.** 1993. Samarium-153-EDTMP biodistribution and dosimetry estimation. *J. Nucl. Med* 34: 1031-1036.

5. **FARHANGHI, M., HOLMES, R.A., VOLKERT, W.A., LOGAN, K.W., SINGH, A.** 1992. Samarium-153-EDTMP: Pharmacokinetic, toxicity and pain response using escalating dose schedule in treatment of metastatic bone cancer. *J. Nucl. Med* 33: 1451-1458.

6. **FRIDMAN, E.P., POPOVA, V.N.** 1988. Species of the genus *Papio (Cercopithecidae*, Primates*)* as subjects of biomedical research: I. Biological basis of experiments on baboons. *J. Med. Primatol.* 17: 291-307.

7. **FRIDMAN, E.P., POPOVA, V.N.** 1988. Species of the genus *Papio (Cercopithecidae*, Primates*)* as subjects of biomedical research: II. Quantitative characteristics of contemporary use of baboon species in medical and biological investigations. *J. Med. Primatol.* 17: 309-318.

8. **GOECKLER, W.F., EDWARDS, B., VOLKERT, W.A., HOLMES, R.A., SIMON, J., WILSON, D.** 1987. Skeletal localization of samarium-153-chelates: Potential therapeutic bone agents. *J. Nucl. Med.* 28: 495-504.

9. **HOEFNAGEL, C.A.** 1991. Radionuclide therapy revisited. *Eur. J. Nucl. Med.* 18: 408 – 431.

10. **HOLMES, R.A.** 1992. [^{153}Sm]EDTMP: A potential therapy for bone cancer pain. *Semin. Nucl. Med.* 22: 41-45.

11. **HOSAIN, F., SPENCER, R.P.** 1992. Radiopharmaceuticals for palliation of metastatic osseous lesions: Biologic and physical background. *Semin. Nucl. Med.* 22: 11-16.

12. **HUMM, J.L.** 1986. Dosimetric aspects of radiolabeled antibodies for tumour therapy. *J. Nucl. Med* 27: 1490-1497.

13. International Commision on Radiological Protection. (1990) 1990 recommendations of the ICRP. *Ann.* ICRP 21: 1-201.

14. **LATTIMER, J.C., CORWIN, L.A., STAPLETON, J., VOLKERT, W.A., EHRHARDT, G.J., KETRING A.R., HEWETT, J.E., SIMON, J., GOECKELER, W.F.** 1990. Clinical and clinopathological effects of samarium-153-EDTMP administered intravenously to normal beagle dogs. *J. Nucl. Med* 31: 586-593.

15. **LATTIMER, J.C., CORWN, L.A., STAPLETON, J., VOLKERT, W.A., EHRHARDT, G.J., KETRING, A.R., ANDERSON, S.K., SIMON, J., GOECKLER, W.F.** 1990. Clinical and clinicopathological response to canine bone tumor patients to treatment with samarium-153-EDTMP. *J. Nucl. Med* 31: 1316-1325.

16. **LOEVINGER, R., BUDLINGER, T.F., WATSON, E.E.** 1991. MIRD *Primer for Absorbed Dose Calculations,* pp. 1-21. Society of Nuclear Medicine, New York.

17. **LOGAN, K.W., VOLKERT, W.A., HOLMES, R.A.** 1987. Radiation dose calculations in persons receiving injection of samarium-153 EDTMP. *J. Nucl. Med* 28: 505-509.

18. **LOUW, W.K.A., VAN RENSBURG, E.J., IZATT, H., ENGELBRECHT, R.I.** 1991. Nucleoid sedimentation analysis of DNA supersructure, γ-radiation-induced damage and repair in human and chacma baboon (*Papio ursinus)* peripheral lymphocytes. *Int. J. Radiat. Biol.* 59: 951-962.

19. **MOEDRITZER, K., IRANI, R.R.** 1966. The direct synthesis of α-amino-methyl-phosphonic acids: Mannich-type reactions with orthophosphorous acid. *J. Org. Chem.* 31: 1603-1607.

20. **PARKS, N.J., KAWAKAMI, T.G., AVILA, M.J., WHITE, R., CAIN, G.R., RAAKA, S.D., HORNOFF, W., FISHER, P., MOORE, P, SEIBERT, J.A., GARLICH, J., SIMON, J., CHAMPLIN, R.** 1993. Bone marrow transplantation in dogs after radio-ablation with a new Ho-166 amino phosphonic acid bone-seeking agent (DOTMP). *Blood* 82: 318-325.

21. **RAO, D.V., HOWELL, R.W.** 1993. Time-dose-fractionation in radioimmunotherapy: Implications for selecting radionuclides. *J. Nucl. Med* 34: 1801-1810.

22. **ROBINSON, R.G.** 1990. Systemic radioisotopic therapy of primary and metastatic bone cancer. *J. Nucl. Med* 31: 1326-1327.

23. **SPENCER, R.P.** 1986. Applied principles of radiopharmaceutical use in therapy. *Nucl. Med. Biol.* 13: 461- 463.

24. **SPENCER. R.P.** 1987. Short-lived radionuclides in therapy. *Nucl. Med. Biol.* 14: 537-538.

25. **TURNER, J.H., MARTINDALE, A.A., SORBY, P., HETHERINGTON, E.L., FLEAY, R.F., HOFFMAN, R.F., CLARINGBOLD, P.G.** 1989. Samarium-153-EDTMP therapy of disseminated skeletal metastasis. *Eur. J. Nucl. Med.* 15: 784-795.

26. **VOLKERT, W.A., GOECKELER, W.F., EHRHARDT, G.J., KETRING, A.R.** 1991. Therapeutic radionuclides: Production and decay property considerations. *J. Nucl. Med* 32: 174-185.

27. **WAGENER, J.M., JARVIS, N.V.** 1995. Complexation of trivalent lanthanides by ethylenediaminetetramethylphosphonate (EDTMP). *S. Afr. J. Chem.* 48: 85-89.

28. **WESSELS, B.W., ROGUS, R.D.** 1983. Radionuclide selection and model absorbed dose calculations for radiolabeled tumor associated antibodies. *Med. Phys.* 11: 638-645.

29. **WHELDON, T.E.** 1993. Radionuclide therapy of cancer: Particle range and therapeutic effectiveness. *Nucl. Med. Commun.* 14: 408-410.

Chapter 6 - Uptake of Ethylenediamine Tetramethylene Phosphonic Acid in Normal Bone after Multiple Applications: A non-human primate study

Summary

Palliation of bone pain in patients with bone metastases has previously been evaluated using ^{153}Sm (samarium) complexed to bone seeking ethylenediamine tetramethylene phosphonic acid (CAS 1429-50-1, EDTMP). Repeated application of the radioligand as needed was found progressively less effective. This study questions whether EDTMP exerts a blocking function, limiting access to bone or osseous tumours with successive administration.

The pharmacokinetics and biodistribution of ^{153}Sm-EDTMP in the normal experimental baboon (n = 6) during three successive applications (6 weekly) each with two different concentrations of EDTMP (0.7 and 1.4 mg/kg b.wt.) were investigated using bone scintigraphy. ^{153}Sm-EDTMP (111 MBq) was injected in each case and monitored for 5h. Curves of tracer kinetics and bone to background uptake were obtained, also blood and cumulative urine curves. Comparisons were statistically assessed in each group between successive applications and between EDTMP concentrations.

Partial blocking with the low EDTMP concentration reached statistical significance after the third application. The first application of the high EDTMP concentration yielded lower uptake in the bone than did low EDTMP pointing to blocking by the high concentration, but not seen with repeated applications.

Continual application of high concentration EDTMP could lead to reduced level of calcium in serum and increased parathyroid hormone levels which might trigger osteoblastic activity and bone remodelling. This would partially affect the blocking which was more obvious at low EDTMP concentration.

Zusammenfassung

Aufnahme von Ethylendiamin-tetramethylen-phosphonsäure in gesunde Knochen nach Mehrfachapplikation/ Eine Primatenstudie

Bei Patienten mit Knochenmetastasen wurde mit Hilfe von ^{153}Sm (Samarium), komplexiert mit Ethylendiamin-tetramethylen-phosphonsäure (CAS 1429-50-1, EDTMP), die Affinität zu Knochengewebe besitzt, eine palliative Schmerzbehandlung bewirkt. Wiederholte Applikationen des Radioliganden erwiesen sich zunehmend als weniger efffektiv. Die vorliegende Studie beschäftigt sich mit den Fragen, ob EDTMP die ^{153}Sm-EDTMP-Inkorporation blockiert oder begrenzt, wenn der Ligand sukzessiv appliziert wird.

Die Pharmakokinetik und die Blutverteilung von ^{153}Sm-EDTMP im gesunden Versuchstier (Pavian) während drei aufeinanderfolgender Applikationen (0.7 und 1.4 mg/kg Körpergewicht) wurden mittels Knochenszintigraphie untersucht. 111 MBq ^{153}Sm-EDTMP wurden jeweils injiziert und 5 h lang gemessen. Die Kurven für die Tracerkinetik, für die Aufnahme in die Knochen relativ zum Hintergrund, für Blut und den angesammelten Urin wurden ermittelt. Vergleiche zwischen den aufeinanderfolgenden Applikationen und zwischen den beiden EDTMP-konzentrationen wurden in jeder Gruppe statistisch ausgewertet.

Teilweise Blockierung der ^{153}Sm-EDTMP-Aufnahme durch die niedrigere EDTMP-Konzentration erreichte erst nach der dritten Applikation statistische Signifikanz. Die erste Applikation mit der höheren EDTMP-Konzentration ergab eine geringere Knochenaufnahme als die mit der niedrigeren EDTMP-Konzentration, was auf eine Blockierungseffekt bei der höheren Konzentration hinweist. Bei wiederholten Applikationen wurde das nicht beobachtet. Kontinuierliche Applikation der höheren EDTMP-Konzentration könnte zu einem verminderten Kalzium-Spiegel im Serum und demzufolge zu einem erhöhten Parathormon-Spiegel führen, wodurch osteoblastische Aktivitäten und Knochenwierderaufbau ausgelöst würden.

Key Words: Bisphosphonate, multiple applications; Bone metastases; Samarium-153, complexed to ethylenediamine tetramethylene phosphonic acid; ^{153}Sm-EDTMP.

6.1 Introduction

Radiation teletherapy has been found effective to control or palliate isolated skeletal metastases. The therapeutic success in multifocal disease with bone seeking radiopharmaceuticals will hinge on many interrelated factors, such as the careful choice of the radionuclide (of which the half-life and radiation emissions dictate its radiobiological effect) and on the bone localizing agent (of which the biochemical properties dictate its pharmacokinetics and biodistribution [1, 2, 3]. ^{153}Sm ($t_{½}$ = 46.7 h; ß = 805 keV [21%]; 702 keV [44%] and 632 keV [34%]; max. soft-tissue penetration ≈ 0.3 cm; γ = 103 keV [28%]) is a radionuclide with nuclear properties suitable for therapeutic purposes. It is furthermore a lanthanide which forms a stable complex with bone seeking phosphonates such as ethylenediamine tertramethylene phosphonic acid (EDTMP). ^{153}Sm-EDTMP has been experimentally investigated in animals and successfully tested in humans for pain palliation of bone metastases [4-9].

Information regarding the pharmacokinetics, biodistribution and bone localization of ^{153}Sm-EDTMP is needed to direct treatment protocols in humans. Such information has been obtained during extensive in vivo experimentation in non-human primates [9]. Preliminary patient studies, however, have shown that ^{153}Sm-EDTMP progressively loses its palliative effect with repeated administration as it becomes necessary. Dogs with osteosarcoma and treated with ^{153}Sm-EDTMP also showed no improved efficacy after a second administration (own experience). The question arises whether EDTMP exerts a blocking function, limiting access to the bone or osseous tumour with successive administration, or whether radiation damage to the vasculature system disturbs proper access of the radioligand into the tumour.

Bisphosphonates and multidentate phosphonates such as EDTMP are chemically stable and are not significantly metabolized. They are tightly bound to bone matrix and are powerful inbibitors of osteoclast mediated bone resorption [10]. Once taken up by the bone, bisphosphonates are liberated again only when the bone in which it was deposited is resorbed [11]. For example. The half-life of the bisphosphonate alendronate ([4-amino-1-hydroxy-butylidene]bisphosphonate) in bone was estimated to be about three years for dogs and ten years for humans [11, 12]. There are also data, although conflicting, that the affinity of

radiolabelled bisphosphonates for diagnostic bone imaging is altered in the presence of therapeutic administered bisphosphonates [13].

This investigation concerns the pharmacokinetics, biodistribution and bone localization of ^{153}Sm-EDTMP in the normal baboon experimental model during three successive applications (6-week intervals which resemble the patient protocol) with two different concentrations of EDTMP to possibly confirm its blocking effect.

Such information could assist in optamizing the ligand as well as possibly lead to improved patient treatment protocols for palliation of painful bone metastases.

6.2 Materials and Methods

6.2.1 Radiopharmaceuticals

Isotopically enriched $^{152}Sm_2O_3$ (> 98%) targets were irradiated for maximum time of 50 h and a neutron flux of 1.0 x 10^{19} cm^{-2} s^{-1} in the Safari-1 Research Reactor. Following irradiation the targets were dissolved in 0.25 ml 0.2 mol/l HCl/mg Sm_20_3 and diluted to result in a solution, which is 0.04 mol/l in HCl, and filtered (0.22 μm).

EDTMP was synthesized in house by W.K.A Louw. The ^{153}Sm-Ca/Na-EDTMP is prepared by adding one part of the $^{153}SmCl_3$ solution to three parts of 0.22 μm filtered Ca/Na-EDTMP solution (46.6 mg EDTMP X H_2O/ml and 7.05 mg/ml Ca as Ca $(OH)_2$ adjusted to pH 7.9-8.0 with NaOH) to form a solution containing samarium (< 200μg/ml), EDTMP X H_2O (35 mg/ml), and 53 mg/ml Ca (as Ca $(OH)_2$). pH 7.5-8.0. This solution is then diluted with an appropriate volume of Ca/Na-EDTMP/0.4 mol/l HCl (3:1), to yield the individual animal doses containing ≈ 185 MBq ^{153}Sm and 0.7 mg EDTMP/kg b.wt. (low administered EDTMP level), and ≈ 185 MBq ^{153}Sm and 1.4 mg EDTMP/kg b.tw. for the high EDTMP level. Terminal sterilization of the product is achieved by steam autoclaving whereafter it is stored frozen to minimize hydrolysis. The maximum lapse of time between production and administration was not more than three days.

Complex identity and radiochemical purity was determined by thin-layer chromatography on cellulose thinlayers (TLC aliminium sheets, cellulose (0.1 mm), E. Merck, Damstadt, Germany), using ammonia (≈ 25 %): methanol: water (0.1:1:2) as solvent. ^{153}Sm-EDTMP was found at $^{188}R_f = 0.75$-0.85 and uncomplexed Sm^{+3} remained at the origin. The yield of the complex (always ≥ 99%) was determined by ion exchange on CM-Sephadex C-25 (Sigma Chemical Co.).

6.2.2 Biodistribution of ^{153}Sm-EDTMP in the primate model

The animal experimentation was done according to the National Code for the Handling and Use of Animals in Research, Education, Diagnosis and Testing of Drugs and Related Substances in South Africa, and the protocol approved by the authorised Ethics Committee of the University of Pretoria. The animals were obtained from a registered breeder, kept under environmentally controlled conditions and fed fresh fruit and special primate pellets.

Twelve healthy male baboons (Papio ursinus), six each for the low and high EDTMP concentration (average weight 27.5 kg) were used. Anaesthesia in each case was induced with ketamine hydrochloride (10ml/kg i.m. Ketalar, Parke Davis, S.A.), and maintained by an i.v. administration of pentabarbital sodium solution (9mg/ml in saline; Sagatal, Maybaker, S.A.) at a rate of 30 ml/h in the vena cephalica from which, contralaterally, blood samples could be drawn. A urinary catheter (foley) was placed in the bladder to facilitate the collection of urine samples. Blood pressure and heart rate were continually monitored as well as blood gases.

Scintigraphy was performed (Siemens Orbiter gamma camera) with the animal in the supine position for planar images. The data acquisition initially involved a view of the thorax, liver and kidneys, and was performed as a dynamic study of 120 x 1 min frames on a count down bolus injection of 111 MBq ^{153}Sm-EDTMP. Static images of the 4 min duration each followed at 2, 3, 4 and 5h after the tracer injection. These images were chosen to present the skeletal structure from the skull to the pelvis as two matched images.

Blood urine samples were collected at fixed intervals for 5 h, i.e. every 3 min for the first hour and then hourly. The activity and volume of each sample were measured and registered.

From the dynamic study time-activity curves were obtained for the cardiac, kidney and liver regions. ROI (region of interest) placed on areas of the bony structures of the skull, shoulder, sternum, ribs and pelvis as well as muscular background areas (no organs were visible at this stage) from the static images rendered relative region to background ratios after background subtraction. Consequently relative uptake of ^{153}Sm by the bone was calculated with bone and background taken as 100 %. Blood clearance and cumulative urine curves were also obtained. After 6 and later 12 weeks the same procedure was repeated for the six baboons in the low EDTMP concentration group.

A similar procedure followed also with three applications for the six baboons in the group receiving high EDTMP concentrations. Comparisons were drawn in each group between the successive applications and also between low and high concentrations. The statistical analysis was performed by Student's t-test for paired variables on a 5 % level of confidence.

6.3 Results

Time-activity curves for cardiac blood pool, kidney and liver obtained from the dynamic studies (0-120 min) with 0.7 mg ^{153}Sm-EDTMP/kg b.wt. after each of the consecutive tracer applications (time intervals of 0, 6 and 12 weeks) are presented in Fig 6-1a, b, and c. No significant differenees in the early biokinetics appear from these curves. Consequently the early phase (up to the first 120 min.) average washout rates from the cardiac bloodpool, kidneys, liver and whole blood sampling (Fig 6-1d) expressed in terms of $t_{½}$ of clearance and presented in Table 6-1 are not statistically significantly different, but show a tendency of slower clearance especially for the kidney, liver and blood with repeated applications. The urine excretion of the tracer after the first application furthermore reached a higher (by 21 %) cumulative value after 5 h than for the second and third applications which in turn did not differ from each other, (Fig 6-1e). Large standard deviations of the order of 40 % jeopardised statistical validation in this case. Partial renal clearances estimated from the blood curves also did not differ significantly.

Table 6-1: Mean half-times of tracer clearance obtained from the dynamic organ distribution studies, for low and high concentrations of EDTMP after repeated administrations at 0, 6 and 12 weeks.

Low [EDTMP]	$t_{½}$ (min)		
	0 week	**6 week**	**12 week**
Cardiac blood pool	3.0 ± 0.5	4.0 ± 0.6	4.0 ± 0.4
Kidney	13.1 ± 4.1	16.3 ± 5.1	18.4 ± 4.2
Liver	12.4 ± 4.1	14.2 ± 5.3	18.6 ± 4.3
Blood samples	6.9 ± 1.4	9.1 ± 2.0	8.3 ± 2.1
High [EDTMP]	$t_{½}$ (min)		
	0 week	**6 week**	**12 week**
Cardiac blood pool	4.0 ± 0.3	4.0 ± 0.5	4.0 ± 0.3
Kidney	14.4 ± 4.1	14.6 ± 5.5	25.8 ± 7.1*
Liver	15.5 ± 5.3	15.4 ± 5.5	18.1 ± 4.3
Blood samples	8.1 ± 4.5	8.5 ± 3.0	8.1 ± 3.1
*$p < 0.05$			

Table 6-2: Percentage skeletal uptake of tracer with low and high EDTMP concentration at 2, 3, 4 and 5 h after administration during 0, 6 and 12 weeks repeated studies.

Low [EDTMP]	Percentage uptake in bone (%)		
	0 week	**6 week**	**12 week**
2 h	84.1 ± 4.3	75.8 ± 3.0	78.0 ± 4.6
3 h	82.4 ± 5.1	79.4 ± 5.2	79.5 ± 4.5
4 h	86.7 ± 4.7	81.2 ± 2.51	74.1 ± 5.0*
5 h	88.1 ± 4.4	81.8 ± 3.9	76.2 ± 3.6*
High [EDTMP]	**0 week**	**6 week**	**12 week**
2 h	75.5 ± 2.6	77.2 ± 4.1	77.2 ± 4.1
3 h	81.4 ± 3.3	79.2 ± 6.2	78.0 ± 5.2
4 h	82.4 ± 2.1	81.0 ± 7.9	80.4 ± 6.4
5 h	84.4 ± 5.3	86.7 ± 5.1	81.9 ±3.3
*$p < 0.02$			

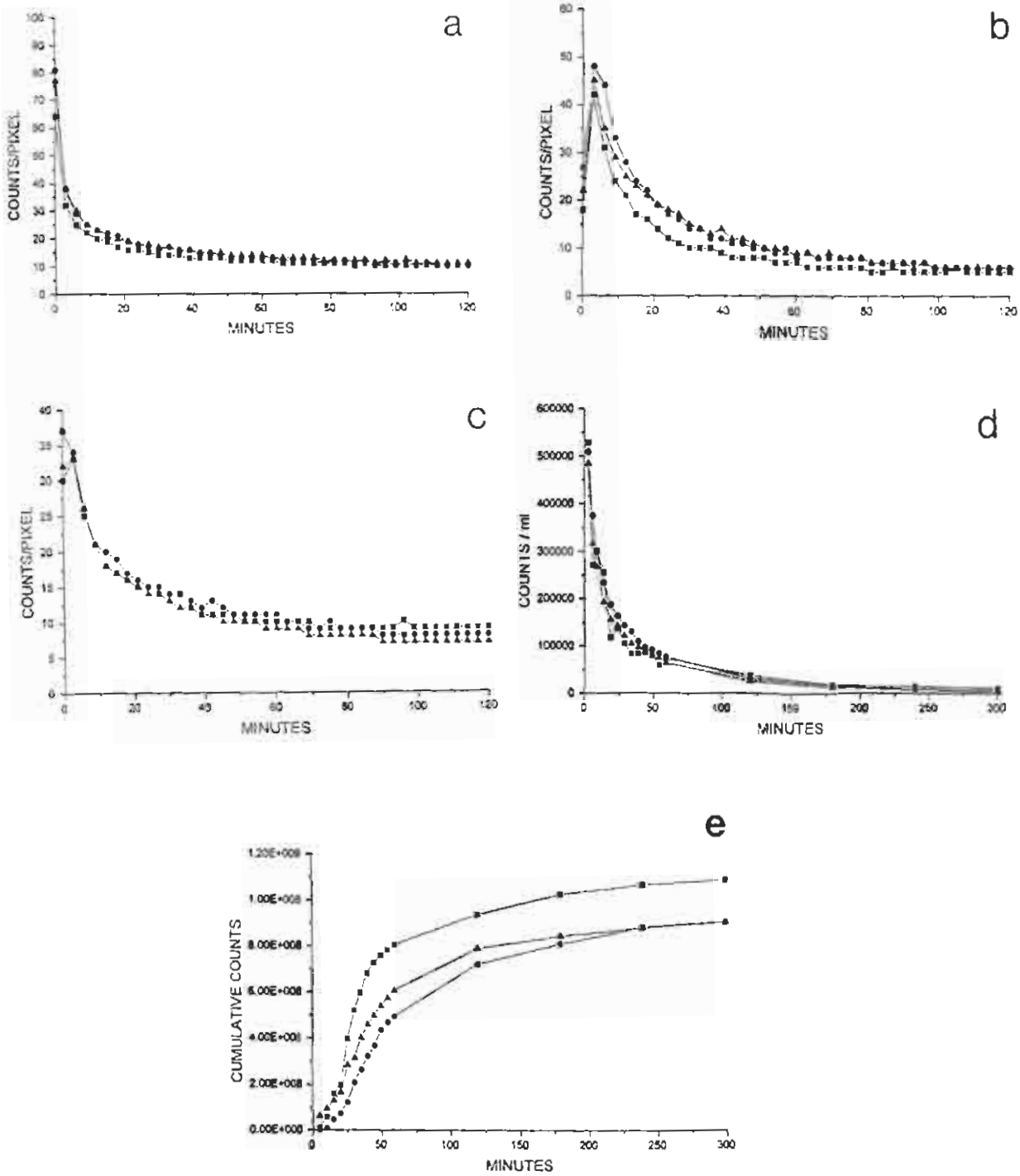

Fig 6-1: Mean (n = 6) time activity curves from the 2-h dynamic study of the cardiac blood pool (a), kidney (b) and liver (c) after 0-week (■), 6 week (●), and 12-week (▲) applications of ^{153}Sm-EDTMP with low concentration of EDTMP. Mean (n = 6) blood clearance (d), and cumulative urine values (e) of ^{153}Sm-EDTMP (low concentration) taken over 5 h after 0-week (■), 6 week (●), and 12-week (▲) application.

The tracer uptake and retention in the bone structure which was measured at 2, 3, 4 and 5 h by static acquisition produced additional count rate data which are shown as percentage bone uptake of the tracer (considering only the skeletal and soft tissue compartments; only these were still visible) at 2, 3, 4 and 5 h (Fig 6-2. Table 6-2). Decreased uptake is seen at the 4 and 5 h with consecutive applications – on the average 6 % less between the first two applications and likewise (6.3 %) between the second and third injections. Statistical significant differences are reached between the 0 and 6 week injections at 2 h ($p < 0.05$), but not at 5 h ($0.05 < p < 0.01$) between the 0 and 12 week administrations at 4 and 5 h ($p < 0.02$), but not at 3 h ($0.05 < p < 0.01$). It is at 4 and 5 h that maximum uptake of ^{153}Sm-EDTMP has been proven to occur [9].

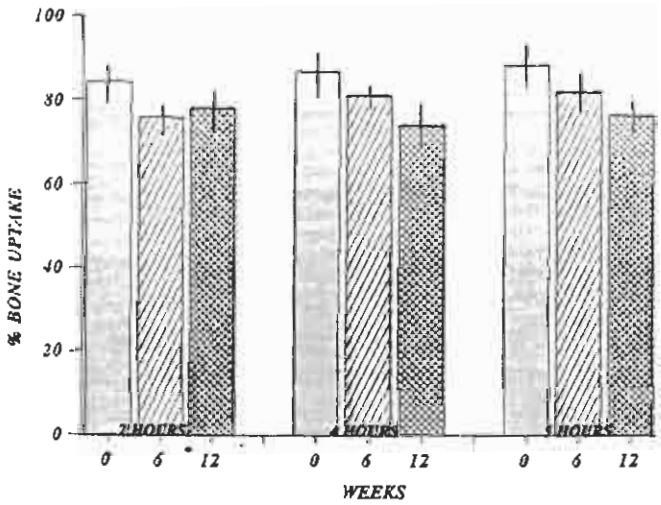

Fig 6-2: Histogram of mean percentage bone uptake of ^{153}Sm-EDTMP (low concentration) obtained from 2 h, 4 h and 5 h static scintigraphy after 0-week, 6 week and 12 week applications

In the high group EDTMP of animals which received the 1.4 mg EDTMP/kg b.wt. the time-activity curves of cardiac bloodpool and liver indicated no biokinetic and biodistribution differences between the tracer applications (0, 6 and 12 weeks; Fig 6-3a and c). The kidneys, however, (Fig 6-3b), presented markedly delayed excretion of the tracer at the third application. This is confirmed by the $t_{½}$-values for the kidney clearance in Table 6-1 ($t_{½}$ = 25.8 ± 7.1) at the third application ($p < 0.05$). Delayed kidney clearance is also illustrated (Fig 6-3e) in the cumulative urine values after 12 weeks, where a clear blocking effect of ^{153}Sm-EDTMP excretion is seen in the first 30 min after the application of the high EDTMP concentration followed by the subsequent sudden increase of tracer clearance.

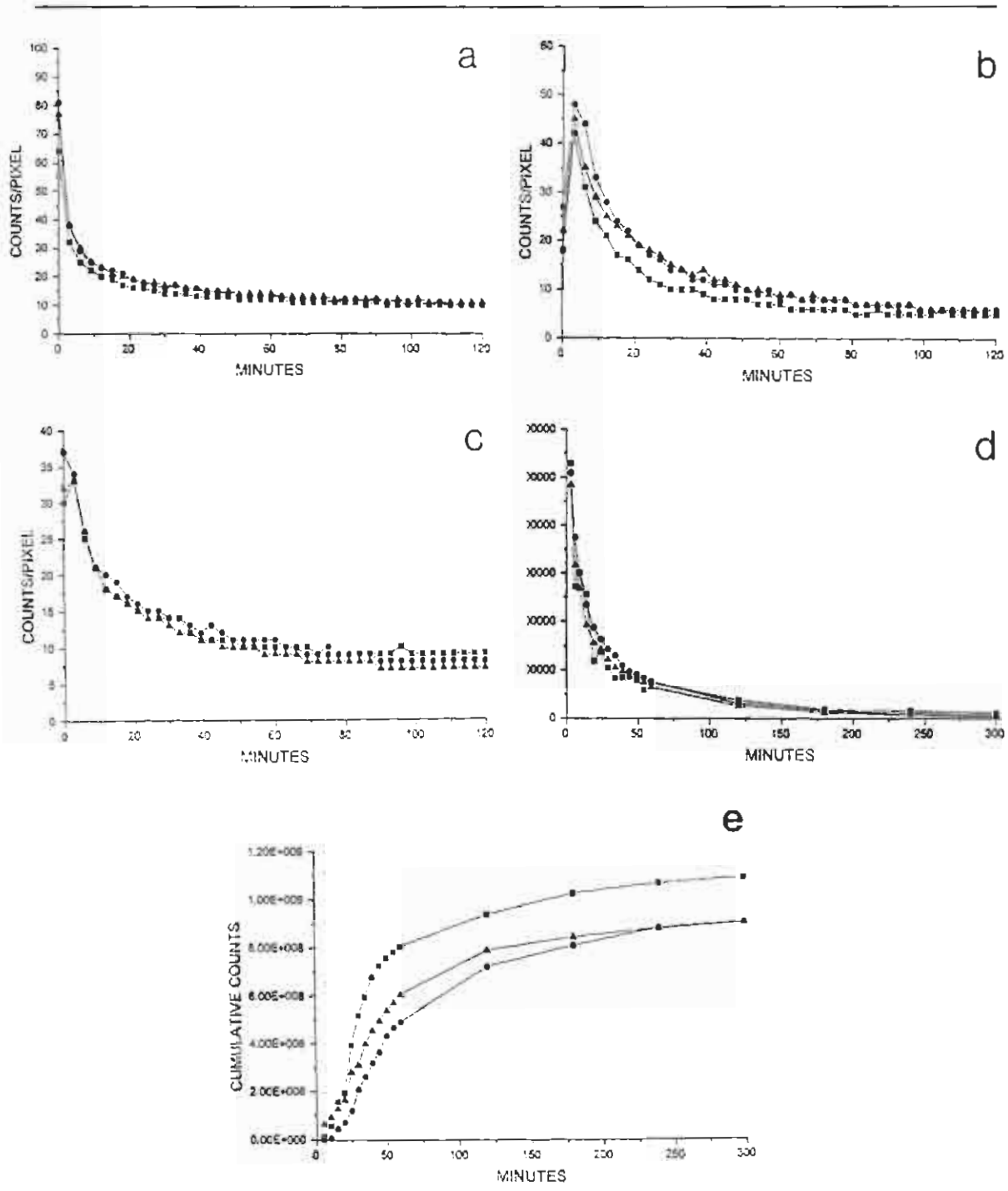

Fig 6-3: Mean (n = 6) time activity curves from the 2 h dynamic study of cardiac blood pool (a), kidney (b), and liver (c) after the 0-week (■), 6 week (●), and 12-week (▲) applications of ^{153}Sm-EDTMP with high concentration EDTMP. Mean blood clearance (d) and cumulative urine values (e) of ^{153}Sm-EDTMP (high concentration taken over 5 h after 0-week (■), 6 week (●), and 12-week (▲) applications.

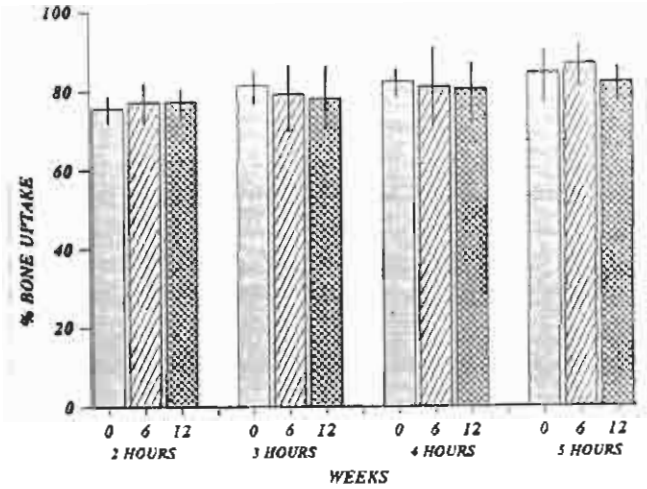

Fig 6-4: Histogram of mean percentage bone uptake of ^{153}Sm-EDTMP (high concentration) obtained from 2 h, 3 h, 4 h and 5 h static scintigraphy after 0-week, 6 week, and 12-week applications.

The blood clearance curves show no differences between the three applications (Fig 6-3d and Table 6-1), and from these the calculated renal clearance values were also not different.

The tracer uptake and retention of the high EDTMP concentration in the bone structure as measured during the static studies at 2, 3, 4 and 5 h show no statistical significant changes between the 0, 6 and 12 weeks administrations (Fig 6-4, Table 6-2). At 0 weeks, however, the tracer with the high concentration of EDTMP indicates reduced uptake with respect to the low concentration ($p < 0.05$). This pattern was not repeated at 6 and 12 week (Fig 6-2 and 6-4). The scintigrams (which are not shown here) clearly illustrate reduced skeletal uptake with repeated administration.

6.4 Discussion

Two principle factors lead to the accumulation of radiopharmaceuticals in bone. These are blood flow and extraction efficiency [14]. An additional factor to consider is capillary permeability [14]. In a recent review [10] of bisphosphonates used for senile osteoporosis it was reported that the incubation of the bisphosphonate alendronate with human bone particles result in rapid, reversible and saturable bonding. Alendronate is an aminobisphosphonate which has higher antiresorbing activity than the bisphosphonate etidronate which has no

amino group [10]. EDTMP is a multidentate aminophosphate ligand [10] which localizes in bone by bridging hydroxyapatite [15] and can therefore be presumed to similarly participate in saturable bonding which could influence the extraction efficiency of the ligand during multiple applications.

A phenomenon of partial blocking indeed appears present in this primate study with the low EDTMP concentration, as can be seen from the reduced ^{153}Sm-EDTMP uptake in the bone with repeated applications. The effect reached statistical significance only after the third application ($p < 0.02$). Furthermore already at the first application (0 weeks) of the high concentration of EDTMP a lower bone uptake was observed when compared to the lower concentration probably pointing to a blocking phenomenon by the high concentration of the EDTMP. The 0-week values of the high concentration do not show much change with repeated applications. It can be speculated that continual application of EDTMP, especially at high concentration, will lead to reduced calcium serum levels increasing parathyroid hormone concentrations [10, 13] which in turn might trigger osteoblastic activity and some bone remodelling, thus partially offsetting the blocking which was consequently more clearly illustrated at the low EDTMP concentration [16, 17].

In this study, haemodynamically monitored under controlled anaesthesia and each animal being its own reference, no blood flow changes need to be considered. Early changes in capillary permeability could maybe follow from localized radiation damage to the skeletal microvasculature and could also cause reduction in bone metabolism visible in the subsequent administrations [18]. However the 0-week difference between the low and high EDTMP concentrations ^{153}Sm-EDTMP cannot be attributed to the radiation damage effects and bone metabolism, and would seem to negate radiation effects at this stage. So also does the fact that no reduction in uptake is seen for the high EDTMP concentration with multiple applications and the same radioactive dose as with the low EDTMP concentration. In considering the early biokinetic data it should noted that renal excretion is the only route of elimination of bisphosphonates. Animal and human studies indicate that systemically administered bisphosphonates are partially taken up by bone and the remainder excreted by the kidneys [10].

The effect of delayed kidney clearance ($t_{½}$) seen in this study progressively with multiple administrations of ^{153}Sm-EDTMP and especially pronounced after the third application of the

high EDTMP concentration could possibly be explained by a saturable transport mechanism in the kidneys by bisphosphonates, also seen in rat studies [10, 19]. Compromising the renal excretion as seems the case in this study with multiple ^{153}Sm-EDTMP applications could also explain the general delayed clearance pattern seen in the dynamic studies [15]. However no significant differences could be found in partial renal clearances calculated from the blood clearance curves.

Bisphosphonates bind preferentially to bones with high turnover rates and their distribution is not homogeneous. The preferential localization of bisphosphonates could be due to larger exposure of hydroxyapatite at sites prepared for undergoing bone resorption which makes them accessible to the drugs in circulation [20]. Trabecular bone account for 80 % of the bone turnover although it represents only 20 % of the skeleton [21]. The near absence of long bones in the ^{153}Sm-EDTMP scintigrams and the high activity in the trabecular bone (ribcage, vertebrae, sternum, shoulder and wrist joints) have been found typical of ^{153}Sm-EDTMP [9], ^{186}Re-HEDP (hydroxyethylidenediphosphonate) [22] but to some extent different from the routinely used diagnostic ligand ^{99m}Tc-MDP (methylenediphosphonate). Although all bisphosphonates have similar physicochemical properties, their anti-resorbing activities differ substantially [14]. This could be the reason for the conflicting data on possible impaired sensitivity of the radiopharmaceutical bone imaging after previous bisphosphonate therapy [12, 23, 24, 25].

6.5 Conclusion

The results of the present primate study clearly indicate a blocking effect to the entry of ^{153}Sm-EDTMP into normal bone with repeated applications of the low EDTMP concentration. To avoid this effect during palliative treatment of patients with skeletal metastases the use of the higher concentration EDTMP ligand could be recommended but only on condition that no renal damage takes place. Due to the bone remoddelling effect seen here at high EDTMP concentration, its combination with a stronger ß-emitter (^{166}Ho) could maybe enhance the palliative effect.

6.6 Literature

1. **WESSELS, B.W., ROGUS, R.D.** 1984. *Med. Phys.* 11: 638

2. **HUMM, J.L.** 1986. *J. Nucl. Med.* 27: 1490

3. **VOLKERT, W.A., GOECKLER, W.F., EHRHARDT, G.J.J.** 1991. *J. Nucl. Med.*32: 174

4. **GOECKLER, W.F., EDWARDS, B., VOLKERT, W.A.** 1987. *J. Nucl. Med.* 28: 494

5. **TURNER, J.H., MARTINDALE, A.A., SORBY, P.** 1989. *Eur. J. Nucl. Med.* 15: 784

6. **LATTIMER, J.C., CORWIN, L.A., STAPLETON, J.** 1990. *J. Nucl. Med.* 31: 586

7. **FARBANGHI, M., HOLMES, R.A., VOLKERT, W.A.** 1992. *J. Nucl. Med.*33: 1451

8. **EARY, J.F., COLLINS, C., STABIN, M.** 1993. *J. Nucl. Med.* 31: 1031

9. **LOUW, W.K.A., DORMEHL, I.C., VAN RENSBURG, A.J.** 1996. *J. Nucl. Med. Biol.* 23: 935

10. **LIN, J.H.** 1996. *Bone* 18: 22

11. **LIN, S.H., DUGGAN, D.E., CHEN, I.W.** 1991. *Drug Metab. Dispos.* 19: 926

12. **GERTZ, R.I., HOLLAND, S.D., KLINE, W.B.** 1993. *Osteopor. Int.* 19

13. **PERCHERSTORFER, M., SCHILLING, T., JANISCH, S.** 1993. *J. Nucl. Med.* 34: 1039

14. **GARCIA, J.F., METTLER, F.A.** 1988. Radionuclide and bone imaging densitometry, Churchill Livingston, New York

15. **HOLMES, R.A.** 1993. *Semin. Oncol.* 20: 22

16. **HORTOBAGYI, G.N., LIBSHITZ, H.I., DEABOLD, J.E.** 1984. *Cancer* 53: 577

17. **CLOLEMAN, R.E., MASHITER, G., WHITACKER, K.B.** 1988. *J. Nucl. Med.* 29: 1354

18. **CHARKES, N.D., SILVERMAN, C.** 1992. *J. Nucl. Med.* 33: 1780

19. **LIN, J.H., CHEN, I.W., DE LUNA, F.A.** 1992. *Drug Metab. Dispos.* 20: 608

20. **SAHNI, M., GUENTHER, H.L., FLEISCH, H.** 1993. *J. Clin. Invest.* 91: 2004

21. **FLEISCH, H.** 1993. *Stampth* 8: 24

22. **PALMEDO, H., BENDER, H., SCHOMBURG, A.** 1996. *Nucl. Med.* 35: 63

23. **KRASNOW, A.Z., COLLIER, B.D., ISITMAN, A.T.** 1988. *Clin. Nucl. Med.* 13: 264

24. **WESTMARK, K.D., NAGEL, J.S., FRANCESHI, D.** 1990. *N. Engl. J. Med.* 232: 1633

25. **SERAFINI, A.N.** 1994. *Int. J. Rad. Oncol. Biol. Phys.* 30: 1187

Chapter 7 - Biodistribution and Pharmacokinetics of Variously Sized Molecular Radiolabelled Polyethyleneiminomethyl Phosphonic Acid as a Selective Bone Seeker for Therapy in the Normal Primate Model

Summary

An ideal radiopharmaceutical for the treatment of neoplastic and inflammatory (benign) bone disease would be a radiolabelled compound that predominantly accumulates in bone lesions with limited access to normal bone and other organs. Neoplastic tissue's abnormal blood supply (increased permeability) and lack of lymphatics will selectively accumulate radiolabelled macromolecules. This enhanced permeability and retention effect forms the basis of this study, using various molecular sizes of the radiolabelled macromolecule polyethyleneiminomethyl phosphonic acid (PEI-MP) for increased selectively of the bone seeking radiopharmaceuticals. PEI-MP was synthesized by condensation of polythyleneimine, phosphonic acid and formaldehyde, followed by fractionation into different molecular sizes by membrane ultrafiltration. Labelling efficiency to ^{99m}Tc (as radiotracer) was ≈ 99 % with complexes stable for 24 h. The pharmacokinetics and biodistribution of various ^{99m}Tc-PEI-MP fractions were investigated using 4 experimental baboons (*Papio ursinus)* per fraction. Scintigraphy was performed on the baboons under general aesthesia of pentobarbital i.v. After an i.v. bolus of ^{99m}Tc-PEI-MP (≈ 185 MBq) both dynamic studies (30 x 1 min frames), and static studies (2 min acquisition every 4 h) were done, as well as blood samples and urine collected. From the results macromolecules with sizes ranging between 30-300 kDa were characterized by excessive liver (21 % - 57% retained activity) and kidney (40 % retained activity) uptake and accompanying long residing times ($t_{½}$ up to 24 h). The percentage bone uptake averaged at 8 % for these particles excluding sizes 100-300 kDa where very little bone uptake was seen (< 1 %). In this case the blood clearance was also slow ($t_{½}$ ≈ 2 h). The fraction size 10-30 kDa had comparatively low accumulation and short residence times in the liver and kidneys (resp. 20 %, $t_{½}$ = 22 ± 4 min; 17.5 %, $t_{½}$ = 20 ± 3 min) and although the bone uptake of 18 % in this case was high, it is still low for a bone seeking agent. These

particles cleared the blood with $t_{½}$ = 25 ± 2 min and seemed suitable for labelling with a therapeutic radioisotopic agent.

Zusammenfassung

Verteilung und Pharmakokinetik von radioaktiv markierter Polyethyleniminomethylphosphonsäure unterschiedlicher Molekülgröße als selektiver Knochensucher im normalen Primatenmodell.

Ein ideales Radiopharmazeutikum für die Behandlung von neoplastischen und entzündlichen (benignen) Knochenkrankheiten stellt eine radioaktiv markierte Verbindung dar, die sich vorwiegend an Knochenläsionen anreichert und zu normalen Knochen und anderen Organen einen möglichst begrenzten Zugang hat. Die anomale Blutversorgung infolge steigender Gefäßpermeabilität sowie das Fehlen lymphatischer Gefäße in neoplastischem Gewebe können eine selektive Akkumulation radioaktiv markierter Makromoleküle bewirken. Diese erhöhte Permeabilität und der Retentionseffekt bilden die Basis für die vorliegende Arbeit, die verschiedene Molekülgrößen des radioaktiv markierten Makromoleküls Polyethyleneiminomethylphosphonsäure (PEI-MP) für zunehmende Selektivität des knochensuchenden Radiopharmazeutikums benutzt. PEI-MP wurde durch Kondensation von Polyethyleneiminophosphonsäure mit Formaldehyd synthetisiert. Die Fraktionierung in verschiedene Molekülgrößen erfolgte mittels Membranultrafiltration. Die Markierungseffizienz des Komplexes mit ^{99m}Tc als Radiotracer betrug ca. 99 % bei 24 stündiger Stabilität. Die Pharmakokinetik und die Bioverteilung von verschiedenen ^{99m}Tc – PEI-MP-Fraktionen wurde an 4 Pavianen (*Papio ursinus)* pro Fraktion untersucht. Szintigraphische Messungen wurden an den Versuchstieren unter allgemeiner Anästhesie mit Pentobarbital durchgeführt. Nach einem i.v. Bolus von ca. 185 MBq ^{99m}Tc-PEI-MP erfolgten dynamische (30 x 1 min Bilder) und statische Untersuchungen (Akquisition: 2 min Dauer für 4 h). Zusätzlich wurden Blutproben genommen und Urin gesammelt. Die Resultate zeigten, daß Makromoleküle, deren Größe zwischen 30 und 300 kDa lag, durch exzessive Aufnahme in Leber und Nieren (verbleibende Radioaktivität: 21-57 % bzw. 40 %) sowie bei gleichzeitig langer Verweildauer ($t_{½}$ bis zu 24 h) charakterisiert waren. Die durchschnittliche prozentuale Aufnahme in die Knochen betrug 8 % für diese Makromoleküle, ausschließlich solcher, deren Größe 100-300 kDa betrug und die eine sehr kleine (< 1 %) Knochenaufnahme zeigten. In

diesem Falle war die Blut-Clearance auch langsam ($t_{½}$ = 2 h). Die 10-30 kDa-Fraktion zeigte eine relativ niedrige Akkumulation und Verweildauer sowohl in Leber (20 %, $t_{½}$ = 22 ± 4 min) als auch in den Nieren (17.5 %, $t_{½}$ = 20 ± 3 min). Obwohl die Knochenaufnahme dieser Fraktion mit 18 % hoch erschien, war sie für einen Knochensucher relativ niedrig. Ihre Blut-Clearance betrug 25 ± 2 min und schien daher für eine Markierung mit einem therapeutischen Radioisotop geeignet zu sein.

Key Words: Bone disease, inflammatory, neoplastic; Polyethyleneiminomethyl phosphonic acid, biodistribution, macromolecules, pharmacokinetics; Radionuclide therapy; Technetium ligands

7.1 Introduction

A variety of skeletal diseases e.g. osseous metastases, various bone tumours and inflammatory skeletal disease such as ankylosing spondylitis, Paget's disease and rheumatoid arthritis result in severe skeletal pain, immobility, anxiety, and severely diminish a patient's quality of life.

Radiation teletherapy is to some extent effective to control or palliate isolated skeletal pain foci from these diseases. Difficulties associated with its application in multifocal disease together with recent commercial availability of various bone seeking radiopharmaceuticals e.g. strontium-89 (^{89}Sr), samarium-153 (^{153}Sm)-ethylenediaminetertramethylene phosphonate and rhenium-186 (^{186}Re)-hydroxyethylidene diphosphonate [1, 2], led to renewed interest in systemic treatment with internal radionuclide therapy. Intravenously administered bone-seeking radioisotopic agents distribute via the circulatory system throughout the body while simultaneously accumulating in bone. The material not taken up by the bone is efficiently cleared through the kidneys into the bladder [1,2]. Using this modality all involved osseous sites can be treated simultaneously with limited associated toxicity. Selective absorption into bone and especially into diseased bony areas limits irradiation to the normal tissues and increases the therapeutic ratio.

Therapeutic (and also diagnostic) success of a radiopharmaceutical will hinge on many interrelated factors, such as the careful choice of a radionuclide (of which its half-life and

radiation emissions dictate its radiobiological effects and its diagnostic image quality), linked to a bone localising agent of which the biochemical properties dictate its pharmacokinetics and biodistribution.

The basic principle for the design of diagnostic and therapeutic radiopharmaceuticals is the incorporation of a suitable radionuclide in an appropriate chemical compound to attain the highest target-to-background concentration ratio. The important concern, especially with therapeutic radiopharmaceuticals, is to maximise the radiation dose to the lesion while minimising that to the remainder of the body, most specifically to the critical organ in this case, the radiosensitive bone marrow.

Bisphosphonate and aminophosphonic acids (e.g. ethylenediaminetetramethylene phosphonic acid [EDTMP] are chemically stable and are not significantly metabolised. They bound tightly to the bone matrix, and once taken up by bone are liberated only when the bone in which it was deposited is resorbed [3].

Particle-emitting radionuclides, e.g. ß-emitting ^{153}Sm, have been complexed with bisphosphonates and substituted organic amine phosphonic acid derivatives, e.g. EDTMP, wherein the nitrogen and phosphorus are interconnected by an alkylene or substituted alkylene group. Certain of these complexes have been shown to be very selective for the skeletal system with very low soft tissue uptake [4]. The complexes also tend to concentrate in areas of fast growing bone much more readily than in normal bone. The radionuclides used are mostly ß-particle emitting , and a high radiation dose is delivered in the area where they are deposited. Thus therapeutic radiation doses can be delivered specifically to calcific tumours. These complexes (e.g. ^{153}Sm-ethylenediaminetetramethylene phosphonate) have been found useful in the treatment of such tumours in humans and animals [5-8]. Unfortunately the selectivity towards fast growing bone (tumour areas) is not adequate so as to avoid bone marrow suppression, which limits the radioactivity dose that can be given to a patient, and thus also therapeutic efficacy of the agent. Any radionuclide that ends up on trabecular bone, or in the inner surface of cortical bone, will deposit energy in the radiosensitive bone marrow [9].

The principle factors that lead to the accumulation of radiopharmaceuticals in bone are blood flow, extraction efficacy and capillary permeability. The discovery that macromolecules and

small particles accumulate passively in solid tumour tissue has had enormous implications for improved design of targeted chemotherapy [10, 11]. This phenomenon has been called the "enhanced permeability and retention effect" (EPR-effect) and has been attributed to two main factors: tumour vasculature often displays a disrupted endothelium (i.e. becomes leaky), which allows macromolecular extravasation to a greater extent than seen via most other endothelial barriers, and also a lack of effective lymphatic drainage, leading to macromolecular accumulation. General tumour tissues and inflammatory areas are characterized by an increased permeability of capillary endothelial layers to blood-borne macromolecules. Administration of radiolabelled macromolecules thus leads to a selective accumulation of radioactivity in these areas. Furthermore, if these tumours or inflammatory areas are calcified or associated with the bone matrix, the selective retention of the phosphonate containing macromolecule will also be enhanced by its binding to hydroxyapatite bone matrix. At the same time the normal bone (and especially the radiosensitive red marrow) is protected by the normal impermeability of their capillary endothelial layers to blood-borne macromolecules ($\geq$ 60 kDa) [12]. Higher and more effective therapeutic doses are thus attainable.

With small molecules (e.g. ^{153}Sm-EDTMP) a significant part of the administered radioactivity is eliminated in the kidneys by glomerular filtration. By increasing the molecular weight, glomerular elimination, and thus also administered dose can be reduced [13].

The biodistribution and pharmacokinetics of various radionuclide complexes were studied in this investigation in the normal chacma baboon (*Papio ursinus)*. These studies were conducted by injecting the ^{99m}Tc complexes of polyethyleneiminomethyl phosphonic acid (PEI-MP) fractions of various molecular sizes into the experimental animals to obtain the gamma ray images of the entire animal at various times up to 4 h after injection. In this manner an optimal molecular size of polymeric macromolecular radioactive compounds can be determined with optimal protection of normal bone, liver and kidney. ^{99m}Tc is in this study used as a tracer isotope to follow the pharmacokinetics, with no therapeutic properties.

7.2 Materials and Methods

7.2.1 Synthesis of polyethyleneiminomethyl phosphonic acid (PEI-MP)

PEI-MP was prepared by the condensation of polyethylenimine (PEI), phosphorous acid and formaldehyde by a modified Mannich reaction in the presence of hydrochloric acid [14, 15].

Phosphorous acid (18.36 g) (Riedel-de Haën, Seelze, Germany), was dissolved in 51.3 ml concentrated hydrochloric acid (32 %, pro analysi, E, Merck, Darmstadt, Germany), while stirring and heating to 80 °C. After dropwise addition of 32 % formaldehyde solution (pro analysi, E. Merck), the temperature was raised to 90 °C (refluxing temperature) and a solution of 8.33 g polyethyleneimine (Polymin, water-free, BASF, Ludwigshafen, Germany) in 40 ml water, was slowly added to the reaction mixture at a rate of 0.3 ml/min. The reaction mixture was continuously purged with argon. When addition of the polyethyleneimine solution was completed, the reaction mixture was stirred under reflux for another hour, then allowed to cool slowly over night during which the product separated as a viscous oil. After decanting the mother liquid, 50 ml water was added to the oily precipitate which formed a doughy mass upon stirring.

The liquid phase was decanted and the process repeated twice whereafter the doughy material was dissolved in 37 ml of molar sodium carbonate solution to form the water soluble sodium salt of PEI-MP (pH 7.0). After lyophilization 12 g of PEI-MP was obtained.

7.2.2 Purification and fractionation of PEI-MP

The macromolecule PEI-MP as prepared above, was further purified and fractionated into different macromolecular sized fractions by membrane ultrafiltration using commercially available polyethersulfone membranes. An aqueous solution of sodium PEI-MP was subjected to a sequential ultrafiltration process through a sequence of 300, 100, 50, 30, 10 and 3 kDa ultrafiltration membranes (Filtron Technology Corp., Northborough, MA, USA). The membrane retentates were washed with distilled water to theoretically calculated purity of 99 %, to yield 3-10, 10-30, 30-50, 50-100, and 100-300 kDa macromolecular sized fractions (see Table 7-1).

Table 7-1: Percentage yield of PEI-MP fractions obtained by membrane ultrafiltration.

Fraction (kDa)	Percentage yield
< 3	28.1
3-10	7.8
10-30	0.2
30-50	6.4
50-100	32.4
100-300	17.7
> 300	7.8

Typical elemental analysis gave a C: N molar ratio of 2.97: 1, which on the basis of a empirical formula of a PEI-MP monomer of $C_9H_{18}N_3O_9P_3$, indicates a high level of methylphosphonation, in contrast to PEI with a monomer empirical formula of $C_6H_5N_3$ and a ratio C: N of 2:1.

7.2.3 Labelling of PEI-MP with ^{99m}Tc

The ligand PEI-MP was labelled with ^{99m}Tc (as tracer) by adding sodium pertechnetate (up to 50 mCi) to lyophilized kits of the ligand (10 mg) and a reducing agent (stannous chloride dihydrate 0.5 mg) to produce the labelled complex (pH 5.0-5.5). The radiolabelled complexes were analysed for radiochemical purity using instant thin-layer chromatography on silica gel impregnated glass-fibre sheets as stationary phase and acetone and 0.9 % sodium chloride solutions as mobile phase. The radiochemical purity of the complexes was > 95 %.

7.2.4. Biodistribution of ^{99m}Tc-PEI-MP

Twenty healthy adult baboons, average weight 27.5 kg, were used in this study and received i.v. ^{99m}Tc-PEI-MP of various molecular sizes. All studies were performed after approval by the Ethics Committee of the University of Pretoria, according to the guidelines of the National Code for Animal Use in Research, Education, Diagnosis and Testing of Drugs and Related Substances in South Africa.

The baboons (n = 4 in each group) were subjected to identical experimental procedures except for the mentioned differences in molecular size of the injected ^{99m}Tc-PEI-MP molecules. Five different fractions (groups) of the PEI-MP macromolecule were studied, viz in the following ranges: (1) 3-10, (2) 10-30, (3) 30-50, (4) 50-100 and (5) 100-300 kDa. Induction of anaesthesia was performed with ketamine hydrochloride (10 mg/kg i.m.), (Ketalar Parke Davis, Cape Town, S.A.), and immediately followed by a maintained controlled infusion of 6 % sodium pentobarbitone solution (Sagatal Kyron Laboratories Pty. Ltd., Benrose, S.A.) at 30 ml/h. The animal in the supine position under the gamma camera was injected i.v. with a bolus of 185-259 MBq of ^{99m}Tc-PEI-MP and data acquisition started on a count down with a Siemens Orbiter gamma camera (Siemens, Erlangen, Germany) in 64 x 64 word mode performing a 30 min dynamic study (30 x 1 min frames). At 1, 2, 3 and 4h, and also at 24 h static images of 120 s were acquired.

Blood and urine samples were collected at fixed intervals for 4 h, viz every 3 min for the first hour, then hourly for blood samples, and urine every five min for the first hour, subsequently hourly.

Regions of interest (ROIs) were placed on the images of cardiac blood pool, liver, lung, spleen, kidneys, and spine (the vertibrae) to obtain time-activity curves of the dynamic study. Similarly, data of countrate per pixel for the ROIs, which were decay corrected, were obtained from the static images. These were normalised to extend the time-activity curves of the dynamic study to 4 h.

Blood clearance and cumulative urine curves were also obtained in all cases so that average relative organ distributions of the retained activity and eventually of the injected dose (i.d.) could be obtained for all ^{99m}Tc-labelled molecular size fractions. These could be compared for optimal distribution characteristics for therapy according to the mentioned criteria. The statistical analysis was performed by student's t-test for paired variables on a 5 % level of confidence.

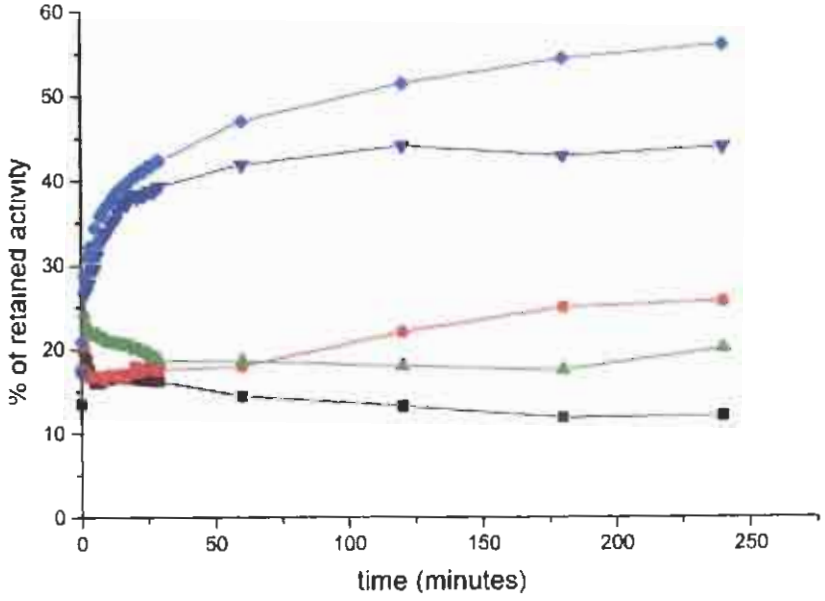

Fig 7-1: Percentage of retained body activity for different ^{99m}Tc-PEI-MP fractions in the primate liver. ■ = Fraction 3-10, ● = Fraction 10-30, ▲= Fraction 30-50, ▼= Fraction 50-100, ♦ = Fraction 100-300 kDa.

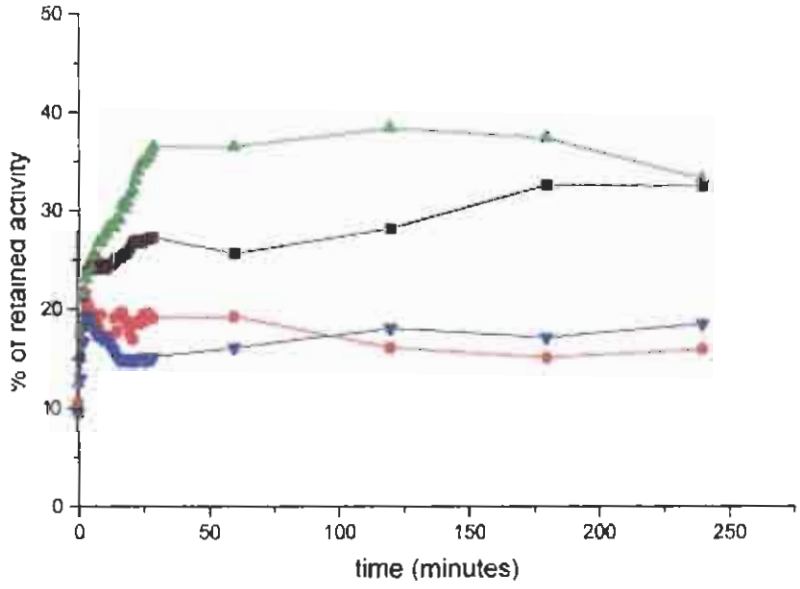

Fig 7-2: Mean percentage of retained body activity for different ^{99m}Tc-PEI-MP fractions in the primate kidney. ■ = Fraction 3-10, ● = Fraction 10-30, ▲= Fraction 30-50, ▼= Fraction 50-100 kDa.

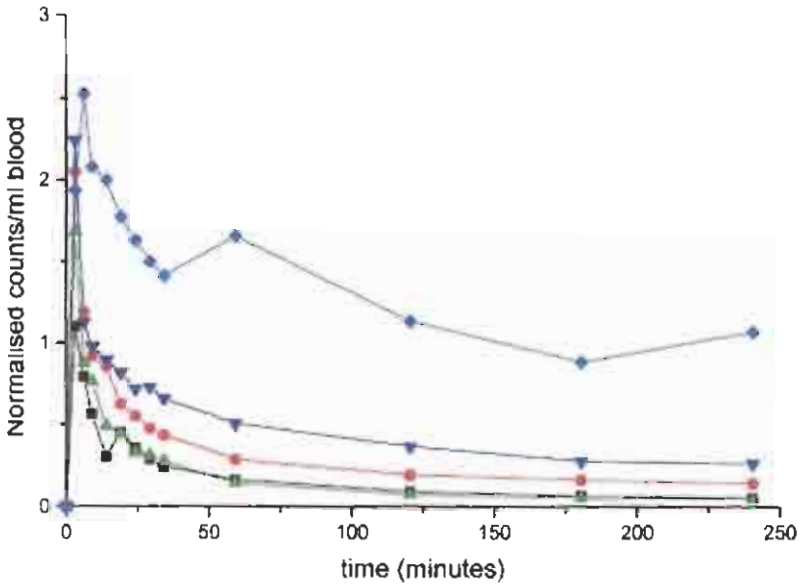

Fig 7-3: Normalized blood clearance for different ^{99m}Tc-PEI-MP fractions. ■ = Fraction 3-10, ● = Fraction 10-30, ▲= Fraction 30-50, ▼= Fraction 50-100, ♦ = Fraction 100-300 kDa.

7.3 Results

The mean (n = 4) half-life of retention of the different ^{99m}Tc-PEI-MP fractions are given in Table 7-2 for various body compartments including the cardiac blood pool. Also in Table 7-2 is the highest mean percentage uptake (n = 4) of the different fractions during the first 4 h in the various compartments. The mean (n = 4) percentage of injected dose of the different ^{99m}Tc-PEI-MP excreted by the kidney after 4 h post injection are presented in Table 7-3. Mean time activity curves as a percentage of retained body activity for the different ^{99m}Tc-PEI-MP fractions for the liver and kidney are presented in Fig 7-1 and 7-2, as well as normalised blood clearance curves in Fig 7-3.

Table 7-2: Mean $t_{½}$ in min (n = 4) and mean maximum percentage uptake (in the first 4 h) of the various ^{99m}Tc-PEI-MP fractions in the various body compartments of the primate model.

Fraction (kDa)	$t_{½}$ (min) and percentage of uptake					
	Cardiac blood pool	Liver	Kidney	Lung	Spleen	Bone
3-10	10 ± 1	90 ± 22	> 4 h	10 ± 1.5	75 ± 2	> 2 h
	15 ± 4 %	16 ± 1 %	36 ± 4 %	8 ± 2 %	10 ±1 %	8 ± 1 %
10-30	10 ± 1.5	22 ± 3	20 ± 3	15 ± 3	60 ± 9	> 4 h
	15 ± 3 %	20 ± 2 %	18 ± 4 %	12.5 ± 4 %	12.5 ± 1 %	18 ± 1 %
30-50	6 ± 2	60 ± 15	> 4 h	8 ± 2	45 ± 8 %	> 4 h
	10 ± 4 %	20 ± 2 %	40 ± 5 %	7.5 ± 2 %	8 ± 3 %	9 ± 0.5 %
50-100	12 ± 1.5	> 4 h	>4 h	22 ± 2	>4 h	> 24h ± 2h
	15 ± 4 %	43 ± 3 %	15 ± 2 %	9 ± 3 %	8 ± 0.5 %	7 ± 0.5 %
100-300	2h ± 0.1 h	24h ± 1.5h	-	2.5h ± 0.5h	> 24h ± 2h	-
	30 ± 7 %	57 ± 9 %	-	7.5 ± 2 %	5.5 ± 2	-

Table 7-3: Mean percentage (n= 4) of injected dose of different ^{99m}Tc-PEI-MP fractions excreted through kidneys after 4 h.

Fraction (kDa)	% of injected dose excreted through the kidneys after 4 h
3-10	40.6
10-30	52.8
30-50	62.0
50-100	28.2
100-300	12.2

7.4 Discussion

Increasing the size of macromolecules of ^{99m}Tc-labelled PEI-MP results in marked changes in their pharmacokinetics and biodistribution (Table 7-2). In normal bone of the primate model there was almost complete exclusion (< 1 %) of the particles larger than 100 kDa. The highest

relative skeletal uptake of 18 % was demonstrated by the 10-30 kDa fraction (Table 7-2), but this is still considerably lower than that known for ^{153}Sm-EDTMP (> 50 %) [16].

All macromolecules of sizes > 50 kDa experienced an excessively high uptake and prolonged retention by the liver, which would led to unacceptable high radiation doses eventually form the corresponding therapeutic agents (Fig 7-1). A measurable liver accumulation is present for all particle ranges (Table 7-2), contrary to ^{153}Sm-EDTMP which demonstrates minimal liver uptake (<0.03 %) [16]. However, the retention time ($t_{½}$) of the smaller particles in the liver is short (maximum 90 min for fraction 3-10 kDa (Table 7-2) and lowest ($p < 0.05$) for 10-30 kDa.

No uptake by the kidney is observed for the PEI-MP fraction 100-300 kDa. For the fraction 50-100 kDa there is kidney uptake which is largely retained at about 15 % of body activity. The fraction 3-10 kDa demonstrates initial high kidney uptake and an increasing percentage of retained activity with time (t > 4h). This is also the case with fraction 30-50 kDa. The high (> 20 %) initial kidney uptake of fraction 10-30 kDa experiences fast washout within the first 30 min, and is soon reduced to around 50 % of the initial uptake (Fig 7-2) which is significantly lower than for the other fractions with molecular size < 50 kDa. Blood clearance ($t_{½}$) from the cardiac blood pools was < 15 min, except for fraction 100-300 kDa where there was a prolonged retention of particles in the circulation ($t_{½} \approx 2$ h). The lung clearance rate followed a similar pattern with prolonged retention for fraction 100-300 kDa ($t_{½} \approx 2.5$ h). In all other cases $t_{½}$ for the lung was < 30 min (Table 7-2). The percentage uptake and retention for the spleen lies around 10 % for all particle sizes, but $t_{½}$ is prolonged for sizes > 50 kDa. Clearance curves obtained from the blood samples (Fig 7-3) are found to be multiphasic because of the particle size ranges of each fraction.

The highest percentage of injected dose excreted in the urine at 4 h was found for the fraction 30-50 kDa, followed by 10-30 kDa (62 % vs 52.8 %, respectively) (Table 7-3). Because urinary excretion of 30-50 kDa PEI-MP is 50 % higher than for 3-10 kDa, and ≈ 7 % higher than for 10-30 kDa, the radiation dose from the retained activity to all organs except the kidney, can be expected to be lowest for 30-50 kDa PEI-MP. High radiation dose to the kidneys will follow in this case because most of the ^{99m}Tc-PEI-MP (30-50 kDa) will be handled by the kidney over a prolonged time interval ($t_{½} > 4$ h).

7.5 Conclusion

This study demonstrated the required reduced normal bone uptake of ^{99m}Tc-PEI-MP, especially noted for fraction 100-300 kDa. Although the value for 10-30 kDa is by comparison more than double that for the other fractions, some retention in bone is necessary such as in an osseous tumour where it would be beneficial to maximize duration of radiation.

To further optimise the molecular size of the macromolecule for its selectivity towards neoplastic and inflammatory diseased areas, potentially harmful kidney and liver uptake should be minimized. This would immediately exclude the fractions with sizes larger than 50 kDa because of liver exposure. Of the smaller fractions, 30-50 kDa and 3-10 kDa seems to leave especially the kidneys vulnerable to radiation exposure (Table 7-2).

In conclusion it would seem that the fraction 10-30 kDa could optimally fit required criteria with relatively low accumulation in normal bone, but with some bone retention indicated. Access into a lesion which depends on the degree of vascular disruption could be fairly early for this fraction because of its relatively small molecular size. The liver and kidney also seem to enjoy most protection with this fraction.

The next step would be to label PEI-MP (10-30 kDa) with ^{153}Sm or $^{186/188}$Re, and to investigate biodistribution, pharmacokinetics and therapeutic efficacy in osseous tumour bearing animal models.

7.6 Literature

1. **LEWINGTON, V.J.** 1996. Cancer therapy using bone-seeking isotopes. *Phys. Med. Biol.* 41: 2027.

2. **ATKINS, H.L.** 1998. Overview of nuclides for bone pain palliation. *Appl. Radiat. Isot.* 49: 277.

3. **LIN, J.H.** 1996. Bisphosphonates: A review of their pharmacokinetic properties. *Bone* 18: 75.

4. **GOECKELER, W.F., EDWARDS, B., VOLKERT W.A.** et al. 1987. Skeletal localisation of Samarium-153 chelates: Potential therapeutic bone agents. *J. Nucl. Med.* 28: 495.

5. **TURNER, J.H., MARTINDALE, A.A., SORBY, P.** et al. 1989. Samarium-153 EDTMP therapy of disseminated skeletal metastasis. *Eur. J. Nucl. Med.* 15: 784.

6. **ALBERTS, A.S., SMIT, B.J., LOUW, W.K.A.** et al. 1997. Dose response relationship and multiple dose efficacy and toxicity of Samarium-153-EDTMP in metastatic cancer to bone. *Radiother.Oncol.* 43: 175.

7. **LATTIMER, J.L., CORWIN, L.D., STAPLETON, J.** et al. 1990. Clinical and clinopathologic effects of Samarium-153-EDTMP administered intravenously to normal Beagle dogs. *J. Nucl. Med.* 31: 586.

8. **MILNER, R.J., DORMEHL, I.C., LOUW, W.K.A.,** et al. 1998. Targeted radiotherapy with Sm-153-EDTMP in nine cases of canine primary bone tumours. *J. S. Afr. Vet. Ass.* 69: 12.

9. **VAN RENSBURG, A.J., ALBERTS, A.S., LOUW, W.K.A.** 1998. Quantifying the radiation dosage to individual skeletal lesions treated with Samarium-153-EDTMP. *J. Nucl. Med.* 39: 2110.

10. **SEYMOUR, L.W.** 1992. Passive tumor targeting of soluble macromolecules and drug conjugates. *Critical Reviews in Therapeutic Drug Carrier Systems* 9.

11. **DUNCAN, R., DIMITRIJEVIC, S., EVAGOROU, E.G.** 1996. The role of polymer conjugato in the diagnosis and treatment of cancer. *S. T. P. Pharma Sci.* 6: 237.

12. **LOUW, W., DORMEHL, I., MILNER, R.J.,** et al. 1998. Biodistribution of radiolabelled polymin-mp of different molecular sizes as a selective bone seeker for therapy in animal models. *Eur. J. Nucl. Med.* 25: 1167.

13. **LáZNICEK, M., LáZNIKOVá, A., BUDSKY, F.,** et al. 1994. Comparison of biological characteristics of EDTMP complexes with ^{99m}Tc, ^{111}In, ^{153}Sm in rats. *Appl. Radiat. Isot.* 45: 949.

14. **MOEDERITZER, K., IRANI, R.R.** 1966. The direct synthesis of α-amine-methyl-phosphonic acids: Mannich-type reactions with orthophosphorous acid. *J. Org. Chem.* 31: 1603.

15. **MANECKE, V.G., STOCKHAUSEN, K., GERGS, P.** 1969. Amphotere Ionenaustauscher (Teil IV). *Macromolek. Chemie* 128: 229.

16. **LOUW, A., DORMEHL, I.C., VAN RENSBURG, A.** et al. 1996. Evaluation of Samarium-153 and holmium-166-EDTMP in the normal baboon model. *Nuc. Med. Biol.* 23: 935.

Chapter 8 - Optimalisation of Radiolabelled Polymin-MP of Different Molecular Sizes as a Selective Bone Seeker for Therapy in Animal Models

Abstract

Abnormal blood supply and lack of lymphatics of neoplastic tissue lead to enhanced permeability and retention effects which form the basis of this study using various sizes of the radiolabelled macromolecule polyethyleneimonomethyl phosphonic acid (polymin-mp) to increase the selectivity of bone seeking pharmaceuticals. Polymin-mp was synthesised and fractionated by membrane ultrafiltration into different molecular sizes, viz. 3-10, 10-30, 30-50 and 100-300 kDa. Labelling efficiency to ^{99m}Tc as radiotracer was 99 % with complexes stable for 24 hours. The pharmacokinetics and biodistribution of all ^{99m}Tc-polymin fractions were investigated in five experimental baboons per fraction and dogs (n = 5) with naturally occurring appendicular osteosarcomas. Scintigraphy followed a bolus injection of ^{99m}Tc-polymin (185 MBq) to the baboons and data were acquired as 30 x 1 min frames dynamic, and hourly static studies for four hours. Regular blood and urine samples were taken. The dogs underwent static studies of the tumours at four hours p.i. For baboons, the macromolecular size fraction 10-30 kDa had comparatively low accumulation and short residence times in the liver and kidney (resp. 20 %, $T_{½}$ = 22 ± 4 min; 18 %, $T_{½}$ = 20 ± 3) and although the bone uptake in this case was comparatively high , it is still low for a bone seeking agent, e.g. 40 % for ^{153}Sm- EDTMP. Results from the dogs showed good uptake in the tumour (e.g. 1: 4, 1: 8 and 1: 9) with 3-10 kDa but reduced uptake with larger molecular sizes.

Keywords: Radiopharmaceutical, neoplastic bone diseases, targeted therapy, polyethyleneiminomethyl phosphonic acid

8.1 Introduction

An ideal radiopharmaceutical for treatment of neoplastic and inflammatory bone disease should predominantly accumulate in the bone lesions with limited access to normal bone and other organs. Neoplastic tissue tends to display abnormal blood supply (increased permeability) and lack of lymphatics leading to selective accumulation of macromolecules [1]. These effects of enhanced permeability and retention form the basis of this study: to use various molecular sizes of radiolabelled macromolecule polyethyleneiminomethyl phosphonic acid (polymin-mp) for increased selectivity of the bone seeking radiopharmaceutical, and to investigate the pharmacokinetics and biodistribution in the normal primate model and in dogs with spontaneously occurring appendicular osteosarcomas.

8.2 Materials and Methods

Polymin-mp was synthesised by the condensation of polyethyleneimine, phosphorous acid and formaldehyde in the presence of hydrochloric acid (modified Mannich reaction) [2]. Then followed fractionation into different molecular sizes by membrane ultrafiltration, viz. 3-10, 10-30, 30-50, 50-100, and 100-300 kDa. Subsequently labelling was performed with ^{99m}Tc as radiotracer. A labelling efficiency of ~ 99 % was reached.

For the animal experimentation five experimental baboons (Papio ursinus, ~ 28 kg) per size fraction of macromolecules were used and dogs (n = 5) with spontaneous appendicular osteosarcomas. All animals received general anaesthesia for the duration of the scintigraphic investigation, i.e., pentobarbitone infusion (Sagatal: 6 %, 30 mL/hr). The scintigraphy (Siemens Orbiter tomographic camera) of the baboons were performed after an i.v. bolus injection of ^{99m}Tc-polymin-mp (185 MBq) on a count down for dynamic data acquisition (30 x 1 min frames) followed by static images of 5 minutes every hour for 4 hours. Blood and urine samples were collected every 10 minutes for the first hour and then hourly until the fourth hour. Scintigraphy for the dogs consisted of static images of the tumour and contralateral sites at four hours p.i.

From the time activity curves percentage organ distribution and retention times could be evaluated (Table 8-1) which would allow the calculation of percentage injected dose and dosimetry, when urinary excretion is taken into consideration.

Table 8-I: Half-life and *highest percentage* of the different ^{99m}Tc-polymin-mp fractions in various organs of the primate model.

Fraction (kDa)	$T_{½}$ (min) and percentage of uptake					
	Cardiac	**Liver**	**Kidney**	**Lung**	**Spleen**	**Bone**
3-10	10 ± 1 min	90±22 min	> 4 h	10±1.5min	75 ± 2 min	> 2 h
	15 ± 4 %	16 ± 1 %	36 ± 4 %	8 ± 2 %	10 ±1 %	8 ± 1 %
10-30	10±1.5 min	22 ± 4 min	20 ± 3 min	15 ± 3 min	60 ± 9 min	> 4 h
	15 ± 3 %	20 ± 2 %	18 ± 4 %	12.5 ± 4 %	12.5 ± 1 %	18 ± 1 %
30-50	6 ± 2 min	60 ±15min	> 4 h	8 ± 2 min	45 ± 8 %	> 4 h
	10 ± 4 %	20 ± 2 %	40 ± 5 %	7.5 ± 2 %	8 ± 3 %	9 ± 0.5 %
50-100	12±1.5min	> 4 h	>4 h	22 ± 2 min	>4 h	> 4h
	15 ± 4 %	43 ± 3 %	15 ± 2 %	9 ± 3 %	8 ± 0.5 %	7 ± 0.5 %
100-300	2h ± 0.05 h	24h ± 1.5h	-	2.5h ± 0.5h	> 24h ± 2h	-
	30 ± 7 %	52 ± 9 %	-	7.5 ± 2 %	-	-

8.3 Results

The biodistribution in normal primates is described in Table 8-I where half life times ($T_{½}$) of clearance of various fractions of ^{99m}Tc-polymin-mp and maximum percentage of tracer accumulation in 4 hours are presented.

For dogs with appendicular osteosarcoma the smaller size fractions of polymin-mp showed higher uptake into the lesions; see Figure 8-1 where the uptake of ^{99m}Tc-polymin-mp (10-30 kDa) into the lesion reached 4: 1 at three hours. This uptake was lower in the two cases (not depicted here) with macromolecular size range of 100-300 kDa, and reached up to 11: 1 for the size range of 3-10 kDa.

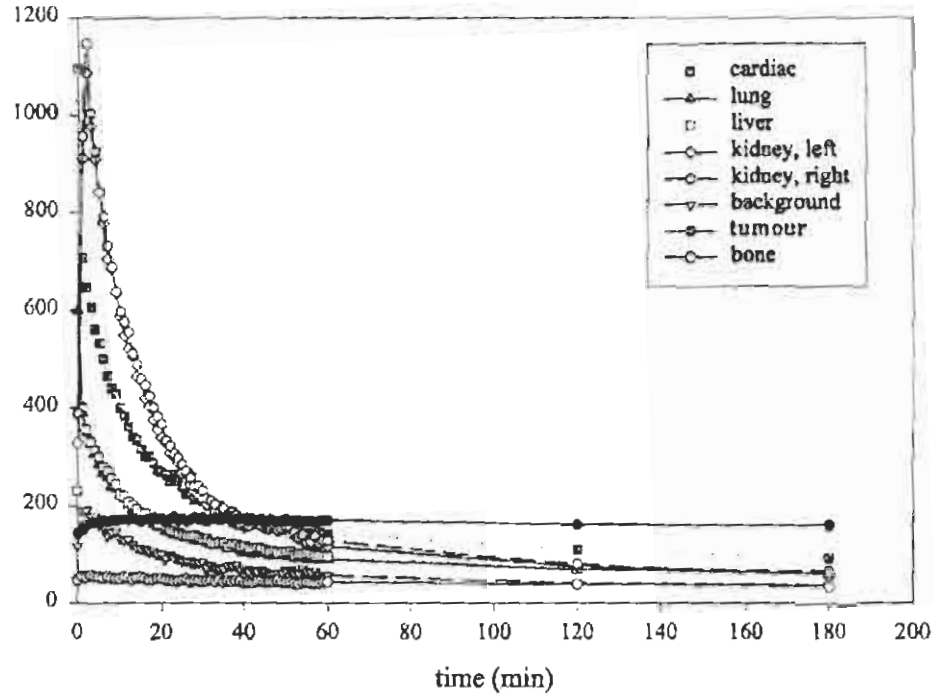

Figure 8-1: Uptake of ^{99m}Tc-polymin (10-30 kDa) into various organs of the Dalamation as a function of time (1 hr dynamic study and up to 3 hr static study).

8.4 Discussion

^{99m}Tc-polymin-mp of various molecular sizes have distinct differences in biokinetics which predominantly pertain to the rate of removal from the cardiac blood pool, i.e., clearance either by involvement of the liver or the kidney or both. Substantial liver and kidney participation (20 % and 40 % resp. max. uptake) for the fraction 30-50 kDa leads to fast clearance for blood pool ($T_{½}$ = 6 min), and fast blood clearance as measured from blood samples ($T_{½}$ = 20 min). Reduced liver and kidney involvement, as with 3-10 kDa and 10-30 kDa leads to delayed cardiac blood clearance (10 min and 25 min resp. for both fractions). The slow although substantial liver participation for 50-100 kDa, and 100-300 kDa lead to long retention in the cardiac blood pool (12 min and 2 hrs resp.), as well as to slow clearance from the blood (45 min and 75 min resp.). The highest normal bone participation, viz. 18 %, occurs for the fraction 10-30 kDa, but this is still much lower than the 40 % or higher of EDTMP and other characteristic biphosphonate accumulation in normal bone. This fraction seems to be the best compromise for low tracer uptake in both liver and kidney. The uptake in bony lesions e.g., the osteosarcoma in the Dalmation of 100-300 kDa was clear from the images with very

little normal bone participation. Even better tumour uptake is obtained with the 3-10 kDa fraction ranging from 9: 1 to 11: 1 with respect to normal bone than was obtained with 10-30 kDa (4: 1).

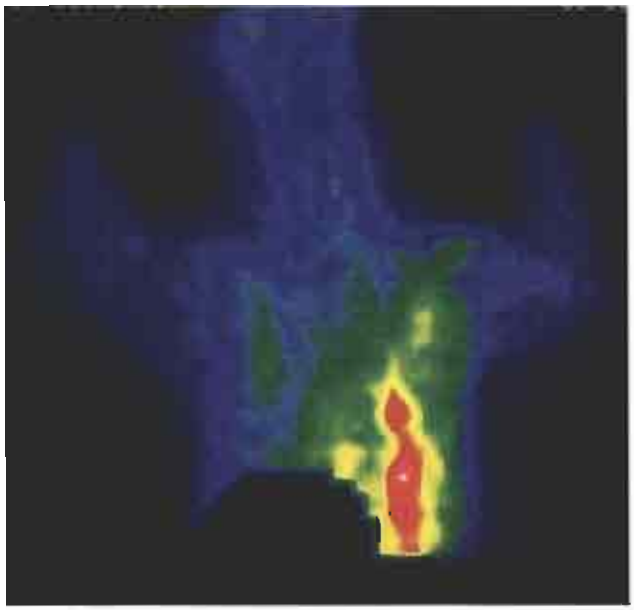

Fig 8-2: Dorsoventral ^{99m}Tc-PEI-MP (100-300 kDa; 185 MBq) bone scan of a dog (Dalmation) with osteosarcoma of the right scapula (95% scapula involvement)

8.5 Conclusion

From the biokinetics and organ distribution of the various polymin-mp fractions the next step would be to label the polymin-mp with either ^{153}Sm or $^{186/188}$Re and to apply the agent for therapeutic purposes in cases of osteosarcoma or bone metastases [3]. It is expected that the organ distribution especially for the $^{186/188}$Re polymin-mp will be similar to that obtained from ^{99m}Tc polymin-mp so that enough data already exist for dosimetric calculation.

8.6 References

1. **MAEDA, H., WU, J, SAWA, T., MATSUMURA, Y., HORI, K.** 2000. Tumour vascular permeability and EPR effects in macromolecular therapeutics: a review. *J. Controlled Release* 65: 271-284.

2. **MOEDRITZER, K., IRANI, R.R.** 1966. The direct synthesis of α-amino-methyl phosphonic acids: Mannich-type reaction with orthophosphorous acid. *J. Org. Chem.* 31: 1603-1607.

3. **PARK, C.H.** 1997. The role of radioisotopes in radiation oncology. 24: 639-654.

Chapter 9 - Metal ion Speciation in Blood Plasma Incorporating the Water-soluble Polymer, Polyethyleneimine Functionalised with Methylenephosphonate Groups, in Therapeutic Radiopharmaceuticals

Summary

A water-soluble polymer, polyethyleneimine functionalised with methylenephosphonate groups (PEI-MP) and labelled with ^{99m}Tc, has shown selective uptake into bone tumours. Apparent formation constants for the complexation of important blood plasma metal ions and metal ions of radionuclides used in therapeutic radiopharmaceuticals (excluding Tc) with PEI-MP were measured potentiometrically. These were added to the ECCLES data base in order to construct a blood plasma model for PEI-MP. From this model it could be predicted that the polymer would not deliver the therapeutic radionuclides ^{153}Sm, ^{166}Ho, ^{212}Pb, ^{213}Pb and ^{89}Sr to bone. This was clinically verified for ^{153}Sm. However good uptake of ^{99m}Tc-PEI-MP could be demonstrated in dogs. Due to the similar chemistry of Re as compared to Tc, it can be expected that PEI-MP labelled with ^{186}Re or ^{188}Re could result in effective therapeutic radiopharmaceuticals for bone cancer.

9.1 Introduction

The use of ^{153}Sm complexed to the octaanion ethylenediaminetetramethylene-phosphonate (EDTMP), in pain palliation therapy for metastatic bone cancer is well established (1) and has been extensively studied in clinical trials in a number of countries. Studies were undertaken to elucidate the in vivo behaviour of ^{153}Sm-EDTMP (2, 3). The use of the blood plasma model, ECCLES (4), has proved particularly useful and it was found that predictions made by the model were closely comparable to clinical observations.

Improvement of the therapeutic efficacy of bone-seeking radiopharmaceuticals could possibly be achieved by using ^{166}Ho ($t_{½}$ = 26.9 hr; maximum ß-particle energy = 1.86 MeV (3.0×10^{-13} J)) instead of ^{153}Sm ($t_{½}$ = 46.75 hr; maximum ß-particle energy = 0.81 MeV (1.3×10^{-13} J)). However, experiments using both baboon (2) and rat (3) models showed poor uptake of ^{166}Ho from ^{166}Ho-EDTMP. Blood plasma modelling (2) was able to explain the deficiency of EDTMP in this regard. Thus, a more suitable ligand than EDTMP is needed to deliver a high percentage of injected ^{166}Ho to bone tumours. Attempts with other bisphosphonate ligands have proven to be ineffective (5-8). The behaviour of these bisphosphonates (used in treatment of bone diseases (9)) in conjuction with ^{153}Sm and ^{166}Ho could be prognosticated, using ECCLES (4).

Water-soluble polymers as drug carriers have been the subject of research activity for some time (10) and have been studied as potential chemotherapy agents for cancer (11). The principle behind this approach is that water soluble macromolecules accumulate passively in solid tumours according to the "Enhanced Permeability and Retention Effect" (12). This phenomenon is thought to be caused by the production in tumour cells of compounds such as Vascular Permeability Factor (VPF) and Bradykinine that increase vascular permeability of the tumour tissue. Retention is enhanced by impairment of the lymphatic system in tumour tissue, retarding the removal of macromolecules from tumours. The polymer must therefore be large enough not to be taken up in healthy tissue but not so large as to be trapped in organs such as liver or kidneys. In this paper it is assumed that this phenomenon also applies to secondary metastasis – although the latter has a different physiology.

To extend this approach to therapeutic radiopharmaceuticals, the water-soluble polymer, polyethyleneimine (see Fig 9-1) was functionalised with methylenephosphonate groups to make the resulting water soluble polymer bone-seeking – PEI-MP. Extensive pre-clinical work using ^{99m}Tc-labelled PEI-MP has been done to ascertain the optimum fraction in terms of mass (13). It has been found that anionic species in the fraction 10 to 30 kDa achieve good tumour uptake with minimal uptake in healthy bone, kidneys or liver. The polymer thus have the potential to selectively deliver a therapeutic radionuclide to tumours.

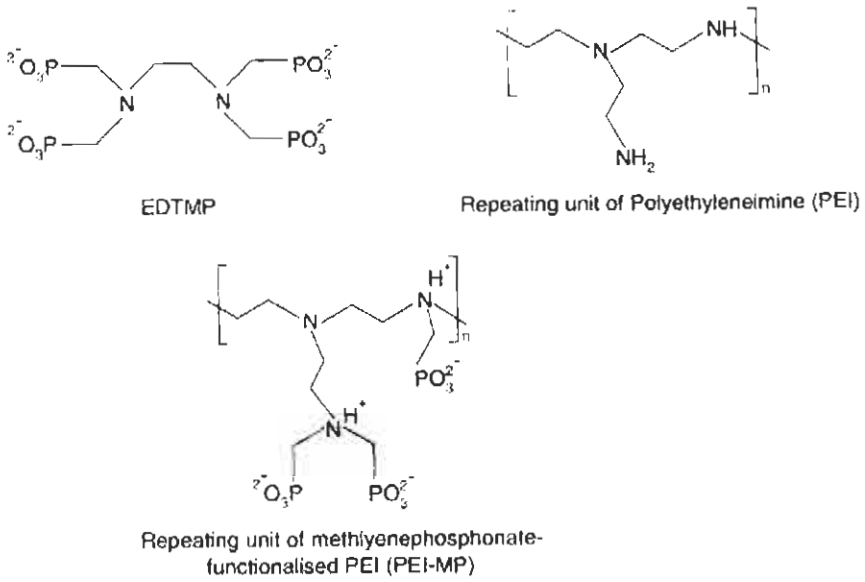

Fig 9-1: The ligand EDTMP and polymer repeating units discussed in this paper

The object of the research reported in this paper, was to construct a blood plasma model including PEI-MP. This should enable an informed selection of a therapeutic radionuclide for delivery to metastatic bone tumours by PEI-MP. In order to achieve this, apparent formation constants of blood plasma metal ions as well as radionuclides of interest had to be measured. This may be achieved, as was previously done with polyethyleneimine (PEI) (14), by treating the water soluble polymer as a collection of separate repeating units. Potentiometric titrations, in which the repeating unit is considered to be the ligand, yield data that may be analysed by computer codes such as ESTA (15). Apparent formation constants are then added to the blood plasma model, ECCLES (4), which predicts the speciation of metal ions in the plasma. This gives an indication of the ability of the radiopharmaceutical to survive competition for the radionuclide by other blood plasma ligands. This approach is novel in so far as polymers were considered not yet previously included in work performed using the ECCLES code. Therapeutic ß-particle emitting radionuclides under consideration were ^{153}Sm, ^{166}Ho, ^{89}Sr, ^{186}Re and ^{188}Re. In addition to blood plasma metal ions, potentiometric titrations involving Sm(III), Ho(III) and Sr(II) were performed. Unfortunately the complex redox chemistry of Re makes potentiometry with this metal unreliable. Recently, α-emitting radionuclide couples, ^{212}Pb/^{212}Bi and ^{213}Pb/^{213}Bi together with EDTMP have been studied (16) as potential therapeutic radiopharmaceuticals for metastatic bone cancer. In order to predict the in vivo behaviour of these radionuclides with PEI-MP, potentiometric titrations were also performed with Pb(II).

9.2 Experimental

9.2.1 Synthesis of PEI-MP

Synthesis of the polymer was achieved using Mannich type reaction as described by Moedritzer and Irani (17). Phosphorous acid (18.4 g) and concentrated hydrochloric acid (51.3 ml) were added to a reaction vessel equipped with a thermometer, magnetic strirrer bar, dropping funnel and condenser. The reaction was performed under an inert atmosphere of argon. Dissolution of the phosphorous acid was achieved by stirring and heating to 80°C. The dropping funnel was charged with formaldehyde solution (23.3 ml) which was added dropwise to the reaction mixture. On completion, the temperature was raised to 90°C (refluxing temperature) and a solution of polyethyleneimine (8.33 g in 40 ml water; Polymin^{TM} Water-Free, a BASF product in which the ratio of primary, secondary and tertiary amine groups is 1: 1: 1; see Fig 9-1) was slowly added to the reaction mixture at a rate of 0.3 ml/min with the aid of a peristaltic pump. The reaction mixture was continuously purged with argon. On completion of the addition of polyethyleneimine, the mixture was stirred under reflux for an additional hour, then allowed to cool slowly during which the product separated as a viscous oil. After decanting the mother liquor, 50 ml water were added to the oil which formed a doughy mass upon stirring.

The liquid phase was decanted and the process repeated twice. The doughy material was dissolved in 37 ml molar sodium carbonate solution to form the water-soluble sodium salt of the PEI-MP. After lyophilisation, 12 g of product were obtained. Microanalysis: Found: C, 23.11; H, 5.98; N, 8.91; Na, 9.86 % Calculated for $C_9H_{22}P_3N_3O_9Na_2.H_2O$: C, 22.84; H, 5.11; N, 8.87; Na, 9.72 %. Potentiometric titrations to determine protonation constants were used to double-check the purity of the ligand.

To obtain the 10 to 30 kDa fraction, an aqueous solution of sodium PEI-MP was subjected to ultrafiltration through the appropriate membranes (Filtron Technology Corporation). The membrane retentates were washed with distilled water to a theoretically calculated purity of 99 % and lypholised.

Due to the scarcity of the 10-30 kDa fraction, PEI-MP used in potentiometric titrations was not fractionated. However, apparent protonation formation constants were calculated for the 10-30 kDa fraction and found to be practically identical to the unfractionated polymer (see Table 9-1). This is because the polymer was treated in calculations as a collection of monomeric units. It is thus assumed that the calculation of apparent formation constants by potentiometry is not affected by the molecular size fraction of the polymer.

Table 9-1: Comparative apparent protonation constants for PEI-MP and Polymin Water-free determined in this study at 25.0 ± 0.1°C and I = 150 mmol dm^{-3} NaCl. Charges on the repeating units have been omitted for simplicity. L represents the repeating unit as Fig 9-1. The protonation formation constants in italics are those calculated for the 10 to 30 kDa fraction of the polymer.

Equilibrium	**log *K* PEI-MP**	**log *K* Polymin Water-free**	**log *K*[#] Polymin Water-free [14]**
$H + L \leftrightarrow HL$	9.34 (1) (9.47 (1))	9.24 (< 1)	9.71
$H + HL \leftrightarrow H_2L$	7.54 (1) (7.48 (1))	6.60 (1)	7.70
$H + H_2L \leftrightarrow H_3L$	5.95 (1) (5.86 (1)	*Not found	2.64
$H + H_3L \leftrightarrow H_4L$	3.26 (2) (3.42 (2))	-	-
$3H + 2L \leftrightarrow H_3L_2$	-	28.93 (1)	30.87
$5H + 2L \leftrightarrow H_5L_2$	-	37.10 (2)	41.58
Number of data points	436 382	582	-
Hamilton R-factor	0.0120 (0.0114)	0.00687	-

*The protonation constant is probably < 2 and could thus not be detected within the pH range used in this work;

#Measured at 25.0± 0.1°C and I = 0.1 mol dm^{-3} $NaNO_3$

9.2.2 Metal ion solutions

Fresh metal ion solutions were employed in the titrations. These were made by dissolving reagent grade chloride salts of the metal ions in distilled water and standardised by complexometric titration using EDTA and a Metrohm Titrino equipped with a copper selective electrode. Where necessary, solutions were acidified to prevent hydrolysis.

9.2.3 Potentiometry

Potentiometric titrations were performed using a Metrohm Titroprocessor 670 with a Metrohm 665 dosimat and a combination glass electrode (Ag/AgCl reference). The electrode was calibrated regularly using strong acid-base titration data. All titrations were performed under an inert atmosphere of nitrogen and solutions were held at a constant ionic strength of 0.15 mol/l NaCl and a temperature of 25.0 ± 0.1°C. The titrations were performed beginning at low and ending at high pH, adding 0.10 ml aliquots of 0.050 mol/l NaOH (carbonate-free) in 0.10 mol/l NaCl. Protonation constants were calculated from the data obtained from titrations of the ligand in the presence of various hydrochloric acid concentrations. Metal-PEI-MP apparent formation constants were calculated from titration data at five different metal: ligand ratios varying from 2: 1 to 1: 3. For titrations involving lanthanides, precipitates formed at low pH, as was found for EDTMP (3). By pH 5, the solutions had cleared and data points from here onwards were used in calculations. Data were analysed by the ESTA (15) library of programmes. During the analysis the previously determined protonation constants were held constant. Hydrolysis constants and pK_W were taken from the literature (18) and held constant during optimisation procedures. The models were tested for plausibility by comparing experimental and calculated formation and deprotonation curves. Formation constants for PEI-MP with Re and Tc were not measured as both can exist in different oxidation states and change between these states easily making it virtually impossible to accurately study the complexes involved by potentiometry.

9.2.4 Blood plasma modelling

All constants measured in this study were added to the ECCLES database (4). The concentration of the repeating unit of PEI-MP used in modelling was 8.5×10^{-5}mol/l. This

value is representative of actual clinical amounts, and is similar to that previously employed during EDTMP work (2). The metal ion concentrations employed ranged from 1.0×10^{-6} to 1.8×10^{-6} mol/l which also resembles clinical amounts.

The plasma mobilisation index (p.m.i.) is defined as:

$$\text{p.m.i} = \frac{\text{Total concentration of low - molecular - weight complex species in the presence of drugs}}{\text{Total concentration of low - molecular - weight complexes in normal plasma}}$$

The p.m.i. values give an indication of which metal ions are mobilised by the added drug. This may be used as a screening method to predict the loss of biologically important metal ions from blood plasma. Remedial actions such as taking supplementary metal ions may then be followed, if necessary. In this study, p.m.i. values were computed by ECCLES for the blood plasma metal ions Ca(II), Mg(II). Ni(II) and Zn(II).

9.2.5 Preparation of ^{153}Sm-PEI-MP

^{153}Sm was prepared by neutron irradiation of 1.0-2.0 mg $^{152}Sm_2O_3$ (99 % enriched) for 24 h in the SAFARI-1 reactor at a neutron flux of 1×10^{14} neutron $cm^{-2}s^{-1}$. Typical specific activities of ~ 4000 MBq/mg of $^{152}Sm_2O3$ were obtained. Using the necessary shielding, the irradiated oxide was dissolved in 250 µl of 0.2 M HCl solution, diluted to 0.04 M HCl with sterile deionised water and filtered. (Millex-Gv, 0.22 µm, Milipore Bedford, M.A.)

Complexation was achieved by adding 0.3 ml of the ^{153}Sm solution above to 0.9 ml PEI-MP solution (48 mg Na-PEI-MP/ml, pH = 8.0). This was diluted up to 5 ml and sterilized by ultrafiltration (0.22 µm).

Complexation yields were determined by separating the complexed and uncomplexed ^{153}Sm species on a carboxymethyl sephadex cation exchange column (19). Complexation yields of > 99 % were obtained.

9.2.6 Preparation of ^{99m}Tc-PEI-MP

As is the procedure for ^{99m}Tc-radiopharmaceuticals, lyophilised, labelling kits of the ligand were prepared in advance and stored in a freezer until the day of use. The kits were prepared by mixing 5 µl of a solution containing 250 mg of $SnCl_2.2H_2O$ crystals in 0.5 ml HCl (c) with an aqueous PEI-MP solution (48 mg Na-PEI-MP/ml, pH = 8.0) where after the pH was adjusted to 6. This mixture was dispensed into 5 vials and freeze dried. The evacuated vials were stored below 0°C until used.

The final solutions for injection were prepared by adding 0.3 ml ^{99m}Tc (111 to 185 MBq), obtained from a ^{99}Mo/^{99m}Tc generator, to the above vials. Radiochemical purity was checked using instant thin-layer chromatography on silica gel impregnated glass-fibre sheets as stationary phase and acetone and 0.9 % sodium chloride solutions as mobile phase. Complexation yields of > 99 % were recorded.

9.2.7 Determination of biodistributions in the canine model

Animal experimentation was done according to the National Code for the Handling and Use of Animals in Research, Education, Diagnosis and Testing of Drugs and Related Substances in South Africa, and the protocols approved by the authorised Ethics Committee of the University of Pretoria.

Healthy adult German Shepherd dogs were studied. Anaesthesia in each case was induced via an indwelling catheter (Jelco) with a mixture of ketamine hydrochloride (3 mg/kg, i.v., Ketalar, Parke Davis, S.A.) and medetomine hydrochloride (0.1 mg/10 kg, i.v. Domitor, Novartis, SA) and maintained by an i.v. administration of pentobarbitone sodium solution (20 mg/ml, 10ml diluted in 200 ml saline, Kyron Laboratories, SA) at a constant rate of 20-30 ml per hour for the first 2 hours and then the infusion was stopped for the last hour. Blood samples were collected via an indwelling catheter placed in the opposite forelimb. A urinary catheter (Foley's) was placed in the bladder to facilitate the collection of urine samples. Arterial blood pressure (Hewlett Packard Life Scope 12) and heart rate were continually monitored by indwelling femoral arterial catheter (Jelco 18 G). Oxygen saturation, expired

carbon dioxide and respiratory rate were also monitored (Hewlett Packard Life Scope 12) for the duration of the anaesthesia.

Scintigraphy was performed (Siemens Orbiter γ-camera, low energy collimator, energy peak 140 keV, window 15 %) for ^{99m}Tc –PEI-MP and ^{153}Sm-PEI-MP (energy peak 103 keV, window 15 %). The animals were positioned in the supine position for planar images. Static images of 2 min duration were recorded in 64 x 64 word mode at 1, 2 and 3 hours after a bolus injection of between 111 and 185 MBq of the ^{99m}Tc and ^{153}Sm labelled PEI-MP.

Using these static images the relative region to background ratios were calculated by placing ROI (region of interest) on areas of the cortical bone, liver, kidneys, cardiac blood pool, lungs and muscular background. These values were used to obtain the relative biodistributions.

9.3 Results and Discussion

9.3.1 Potentiometry

The results of modelling for PEI-MP using the computer programme ESTA (15) are given in Table 9-1 and 9-2. Good fits, indicated by low Hamilton R-factors and standard deviations in log ß values, were obtained for all the systems studied. For the parent polymer, PEI, the same model as previously applicable at a different anionic strength, was found to be plausible (14).

For the repeating unit-proton system, pK_a's corresponding to protonation of nitrogen centres functionalised with methylenephophonate groups could not be calculated as they are probably too high for the potentiometric method used here. Comparisons of pK_a's of nitrogens in ligands to which methylenephosphonate groups are successfully added are given in Tables 9-3 and 9-4. It can be seen that these increase with increasing number of methylenephosphonates presumably due to attractive electrostatic effects. Hence pK_{a1} for ammonia rises from 9.43 to 12.4 and for ethylenediamine from 9.61 to 13.0. For ethylenediamine it can be further seen that pK_{a2} rises from 6.83 to 9.78 as more methylenephosphonate groups are added. The pK_a's of the nitrogens become very large and some doubt as to their accuracy is therefore suggested (18).

Table 9-2: Apparent formation constants for PEI-MP determined in this study at 25.0 ± 0.1°C and I = 150 mmol dm^{-3} NaCl. Charges on metal-ions, hydroxide, the polymer repeating unit and complexes have been omitted for simplicity. L represents the repeating unit as Fig 9-1.

Equilibrium	log *K* Ca(II)	log *K* Mg(II)	log *K* Sr(II)	log *K* Ni(II)	log *K* Zn(II)	log *K* Pb(II)	log *K* Sm(III)	log *K* Ho(III)
Binuclear species								
$2M + L \leftrightarrow M_2L$	8.81(1)	8.81(2)	7.34(1)	13.61(4)	15.50(5)		16.08(9)	14.73(13)
$M_2L + H \leftrightarrow M_2(HL)$	8.16(2)	8.01(3)	8.05(2)	6.01(5)	5.59(5)		6.79(13)	5.94(20)
$M_2(HL)+H \leftrightarrow M_2(H_2L)$		5.76(7)			4.42(3)			
$M_2L + OH \leftrightarrow M(H_{-1}L)$	3.86(2)	3.94(3)	3.84(2)					
$M_2(H_{-1}L)+OH \leftrightarrow$ $M_2(H_2L)$		2.87(4)						
Mononuclear species								
$M + L \leftrightarrow ML$				8.83(2)	10.34(2)	7.51(2)		
$ML + H \leftrightarrow M(HL)$				7.09(3)	6.45(3)	7.48(2)		
$M(HL) + H \leftrightarrow M(H_2L)$				5.57(3)	5.33(3)	6.20(2)		
$M(H_2L) + H \leftrightarrow M(H_3L)$						4.42(3)		
$M + L + OH \leftrightarrow M(H_{-1}L)$				14.72(3)	16.10(3)	11.70(2)	14.32(5)	12.85(7)
Number of data points	304	314	327	253	383	300	106	102
Hamilton R-factor (R-limit)	0.0170 (0.00192)	0.0258 (0.00195)	0.0155 (0.00179)	0.0160 (0.00807)	0.0201 (0.00689)	0.0115 (0.00806)	0.0174 (0.0124)	0.0240 (0.0111)

When modelling the protonation titrations for PEI-MP, it became apparent that two fewer protons then expected were dissociating in the pH band 2-11. It is therefore assumed that these protonation constants must exceed 11 and correspond to the protonation of the two nitrogen centres functionalised with methylenephosphonate groups. The first pK_a that could be calculated must correspond to the unfunctionalised tertiary nitrogen. This is supported by the results obtained for the parent polymer, where pK_{a1}, corresponding to the protonation of this nitrogen, was found to be almost identical (see Table 9-1). The rest of the pK_a's are for the protonation of methylenephosphonate groups and are in good agreement with results obtained for similar ligands (see Table 9-4).

Table 9-3: Comparison of protonation constants for methylenephosphonate functionalised ammonia ligands (17). All data were measured at 25°C and 0.1 M ionic strength.

Ligand	pK_{a5}	pK_{a4}	pK_{a3}	pK_{a2}	pK_{a1}
NH_3					9.43
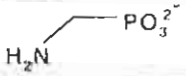				5.40	10.06
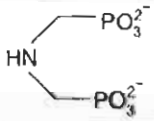		0.9	5.04	6.08	10.79
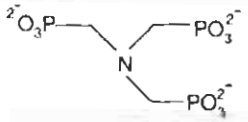	1.08	4.62	5.90	7.30	(12.4)

For metal-ligand systems, a typical example of the approach used in model selection and validation is shown in Fig 9-2. In this diagram, the curves for the calculated and experimental deprotonation function, $\bar{Q}$ (the average number of protons released on complexation per metal ion), for the Ca(II)-PEI-MP system are shown. The dashed curve is $\bar{n}$, the protonation state of the repeating unit in the absence of the metal ion. Interpretation of these curves assists greatly in model selection. In the example shown, $\bar{Q}$ rises to 0.5 for all titrations meaning that one proton is being released on complexation for every two metal ions. At pH between 6 and 7, $\bar{n}$ is approximately 2. Hence, in the absence of the metal ion the repeating unit would be of the form H_2L. In the presence of metal ions, one proton is lost per two metal ions. Therefore the predominant species present in this pH range would be $M_2(HL)$ as found in the

model and illustrated in the species distribution curve (Fig 9-3). Similar reasoning can be used to arrive at the M_2L species in the region of pH 9. Above pH 10, $\bar{Q}$ rises above $\bar{n}$. This indicates that the glass electrode detects more free protons in the system than would be expected from the repeating unit. These come from either deprotonation of coordinated water or a nitrogen centre. Comparing the constant obtained for the formation of the $M_2(H_1L)$ species with the first hydrolysis constant for Ca(II) would indicate that the latter is more likely. A similar deprotonation reaction is observed for Mg(II) and Sr(II) with constants remarkably close to that of Ca(II).

Table 9-4: Comparison of protonation constants for methylenephosphonate functionalised ethylenediamine ligands (17). All data were measured at 25°C and 0.1 M ionic strength except for PEI-MP at 25°C and 0.15 M ionic strength.

Ligand	pK_{a4}	pK_{a3}	pK_{a2}	pK_{a1}	pK_{a0}	pK_{a-1}
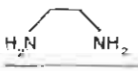					6.83	9.61
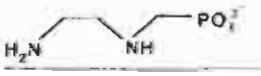				4.85	7.35	10.3
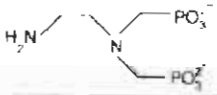			4.10	6.34	8.41	10.85
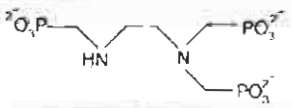		3.03	5.48	6.70	8.76	10.9
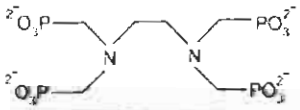	3.02	5.17	6.42	7.94	9.78	13.0
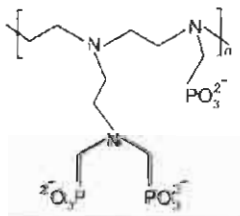	3.26	5.95	7.54	9.34	Not found[a]	Not found[a]

a: The value is probably too high to be determined by the experimental setup used in this work.

The presence of dinuclear species is similar to that found for other phosphonate ligands previously studied (5-8). In this case it is expected that one repeating unit could accommodate two metal ions at the two methylenephosphonate functionalised nitrogen centres.

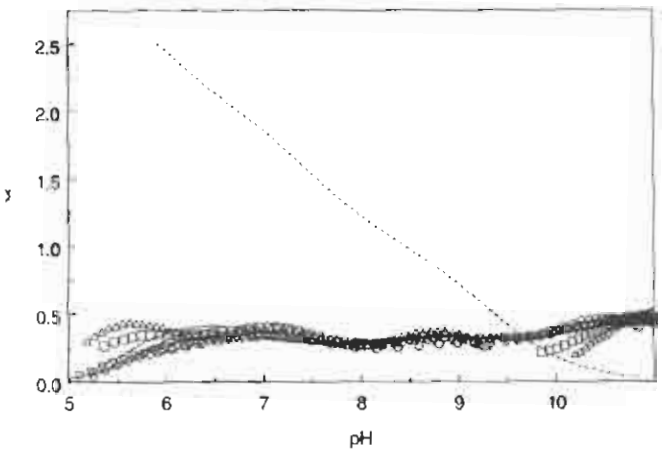

Fig 9-2: Experimental (points) and modelled (lines) deprotonation ($\overline{Q}$) curves for Ca(II) complexation by the repeating unit of PEI-MP. The dashed line is the $\overline{n}$ curve and represents the protonation state of the ligand in the absence of the metal ion. The five separate titrations are represented by (○) 0.000852 mol dm^{-3} Ca(II), 0.00869 mol dm^{-3} repeating unit of PEI-MP and 0.00997 mol dm^{-3} HCl; (□) 0.000852 mol dm^{-3} Ca(II), 0.00174 mol dm^{-3} repeating unit of PEI-MP and 0.00997 mol dm^{-3} HCl and (Δ) 0.000852 mol dm^{-3} Ca(II), 0.00261 mol dm^{-3} repeating unit of PEI-MP and 0.00989 mol dm^{-3}HCl; (◊) 0.00128 mol dm^{-3} Ca(II), 0.00100 mol dm^{-3} repeating unit of PEI-MP and 0.0102 mol dm^{-3} HCl and (▽) 0.00170 mol dm^{-3} Ca(II), 0.00100 mol dm^{-3} repeating unit of PEI-MP and 0.00101 mol dm^{-3} HCl; versus 0.0500 mol dm^{-3} NaOH in 0.010 mol dm^{-3} NaCl. All solutions were at 25°C and 0.15 mol dm^{-3} NaCl or 0.15 mol dm^{-3} total ionic strength.

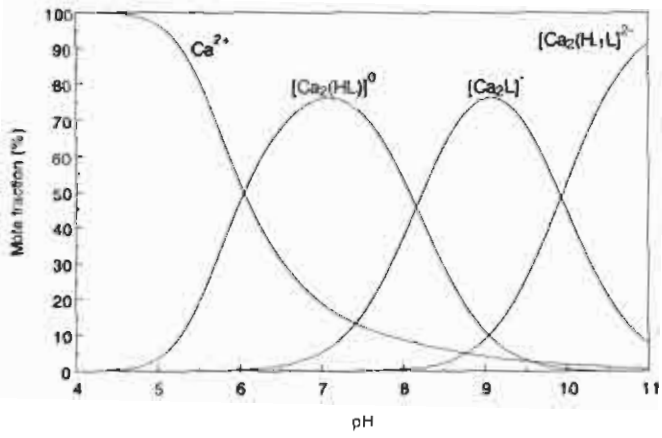

Fig 9-3: Species distribution curves for Ca(II) complexation by PEI-MP at 25°C and 0.15 mol dm^{-3} as calculated from the formation constants in Table 9-2. Concentrations used were 0.000852 mol dm^{-3} Ca(II) and 0.00174 mol dm^{-3} repeating unit of PEI-MP

The formation function (not shown here), $\bar{Z}$ (the average number of repeating units per metal ion), rises to 0.5 which corroborates the model of one repeating unit per two metal ions. At low free repeating unit concentrations, "backfanning" occurs indicating that hydrolysis or deprotonation of the repeating unit to a greater extent than expected, is occurring. This is in agreement with the deprotonation function information.

The protonation constant for the M_2L species lies between pK_{a1} and pK_{a2}. It is therefore likely that the nitrogen centre –not functionalised with methylenephosphonate groups- is being protonated. Similarly, for Mg(II), the complex is protonated at the same nitrogen after which successive protonation of methylenephosphonate groups occurs.

The formation constant for the M_2L species for the alkaline earth metals are in the expected order Sr(II) < Ca(II). However, the constant for Mg(II) is equal to that of Ca(II). This is unexpected as Mg(II) is a harder metal ion. An explanation could be that, as found with EDTMP, stability is less than expected due to steric hindrance derived from a number of negatively charged oxygen donor groups having to "fit" around small Mg(II) ion.

For the transition metal ions, Ni(II) and Zn(II), it was found that the composition of the complexes was strongly dependent on the ratio of repeating unit to metal used and is reflected in the deprotonation curves for Zn(II) complexation in Fig 9-4. At the highest metal: ligand ratio (2: 1), the curve flattens off at just above 0.5 at low pH indicating that complexes are formed predominantly in the ratio 2: 1. For this titration, sensible data points end at about pH = 7 as the free ligand concentration becomes zero under these conditions. At pH = 4, $\bar{Q}$ has risen to about 0.5 for this titration whereas $\bar{n}$ is at 3. Therefore, in the absence of the metal ion, the ligand would be in the form H_3L. In the presence of the metal ion, one proton is lost per two metal ions. Hence the species predominating at this pH value should be $Zn_2(H_2L)$. As pH increases to 7, $\bar{Q}$= 1 and $\bar{n}$ = 2. Hence the predominating species should be Zn_2L. As the concentration of repeating unit in relation to the metal ion increases so the curves show inflections at 1.0 and 1.5. Therefore both mononuclear and dinuclear complexes are formed. At higher ligand: metal ratios, mononuclear species predominate.

For Ni(II) and Zn(II) it is presumed that the ML species is formed by complexation of the metal ions by the nitrogen centre functionalised with two methylenephosphonate groups. The

M_2L species must therefore be formed by complexation by the nitrogen centre functionalised with one methylenephosphonate group of the second metal ion. It is difficult to speculate regarding the role of the unfunctionalised nitrogen centre in complexation.

Protonation of the Ni(II) and Zn(II) complexes takes place at phosphonate centres and not at the unfunctionalised nitrogen centre. This may be seen by comparison of the protonation constants for the complexes with those of the repeating unit.

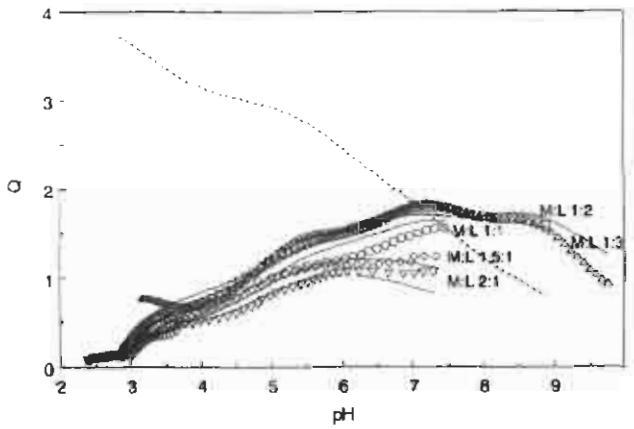

Fig 9-4: Experimental (points) and modelled (lines) deprotonation ($\bar{Q}$) curves for Zn(II) complexation by the repeating unit of PEI-MP. The dashed line is the $\bar{n}$ curve and represents the protonation state of the ligand in the absence of the metal ion. The five separate titrations are represented by (○) 0.000100 mol dm^{-3} Zn(II), 0.00100 mol dm^{-3} repeating unit of PEI-MP and 0.00990 mol dm^{-3} HCl; (□) 0.00100 mol dm^{-3} Zn(II), 0.00201 mol dm^{-3} repeating unit of PEI-MP and 0.00997 mol dm^{-3} HCl and (Δ) 0.000100 mol dm^{-3} Zn(II), 0.00301 mol dm^{-3} repeating unit of PEI-MP and 0.00971 mol dm^{-3}HCl; (◊) 0.00201 mol dm^{-3} Zn(II), 0.00100 mol dm^{-3} repeating unit of PEI-MP and 0.0102 mol dm^{-3} HCl and (▽) 0.00150 mol dm^{-3} Zn(II), 0.00100 mol dm^{-3} repeating unit of PEI-MP and 0.00101 mol dm^{-3} HCl; versus 0.0500 mol dm^{-3} NaOH in 0.010 mol dm^{-3} NaCl. All solutions were at 25°C and 0.15 mol dm^{-3} NaCl or 0.15 mol dm^{-3} total ionic strength.

For Pb(II), deprotonation curves rise to 1.0 for all titrations (Fig 9-5). This is an indication that only mononuclear complexes are formed with the repeating unit which is perhaps due to the large ionic radius of the Pb(II) ion (1.2 Å) making it sterically difficult for the repeating unit to accommodate two metal ions.

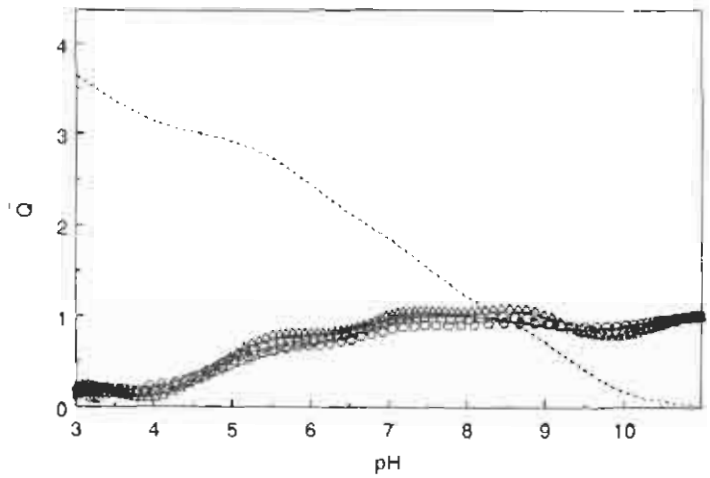

Fig 9-5: Experimental (points) and modelled (lines) deprotonation ($\bar{Q}$) curves for Pb(II) complexation by the repeating unit of PEI-MP. The dashed line is the $\bar{n}$ curve and represents the protonation state of the ligand in the absence of the metal ion. The three separate titrations are represented by (○) 0.000871 mol dm^{-3} Ca(II), 0.00100 mol dm^{-3} repeating unit of PEI-MP and 0.0101 mol dm^{-3} HCl; (□) 0.000871 mol dm^{-3} Pb(II), 0.00140 mol dm^{-3} repeating unit of PEI-MP and 0.0100 mol dm^{-3} HCl and (Δ) 0.000871 mol dm^{-3} Pb(II), 0.00200 mol dm^{-3} repeating unit of PEI-MP and 0.00996 mol dm^{-3}HCl; *versus* 0.0500 mol dm^{-3} NaOH in 0.010 mol dm^{-3} NaCl. All solutions were at 25°C and 0.15 mol dm^{-3} NaCl or 0.15 mol dm^{-3} total ionic strength.

The Pb(II), Zn(II) and Ni(II) models contain "hydrolysis" species. Here, the extra proton detected by the electrode could originate from coordinated water or the ligand. Inspection of the hydrolysis constants for these three metal ions indicates that the latter is more likely. Therefore deprotonation of one of the functionalised nitrogens takes place.

For the lanthanides, Sm(III) and Ho(III), models containing mononuclear and dinuclear species were found – as was found for Ni(II) and Zn(II). The Ho(III) complexes are generally less stable than those of Sm(III) – as was found for EDTMP (3). The expected order due to the lanthanide contraction is reversed, presumbaly due to steric effects caused by the large number of negatively charged oxygen donors having to "fit" around the smaller Ho(III) ion.

9.3.2 In vivo speciation calculated by ECCLES

The speciation of the repeating unit of PEI-MP in normal blood plasma is given in Table 9-5. As has previously been found with bisphosphonates and aminomethylenephosphonates (2, 5,

6, 8), the repeating unit has a strong affinity for Ca(II) and Mg(II). The p.m.i. curves, however, indicate that little mobilisation of the blood plasma metal ions, Ca(II), Mg(II), Zn(II) and Ni(II) occurs at the likely clinical concentration of PEI-MP in the blood plasma (Fig 9-6). This is an encouraging result as the side-effects due to mobilisation of blood plasma metal ions can be predicted to be negligible.

Table 9-5: Speciation of PEI-MP in normal blood plasma as calculated by ECCLES. L = repeating unit of PEI-MP as illustrated in Fig 9-1.

Species	Mol %
$[Ca_2(HL)]^+$	70.6
$[Ca_2L]^0$	12.2
$[Mg_2(HL)]^+$	10.6
$[Mg_2L]^0$	2.7
H_2L^{2-}	1.8
HL^{3-}	1.3
$[Mg_2(H_2L)]^{2+}$	0.2
$[Ca(H_1L]^-$	0.1

For Pb(II) and Sr(II), no difference in speciation for these two metal ions in the absence or the presence of PEI-MP could be discerned by ECCLES. Therefore, PEI-MP will be unable to compete in vivo for these metal ions above the ligands cysteinate and phosphate which respectively strongly complex these metal ions in blood-plasma. Hence it is unlikely that the polymer will be able to deliver therapeutic radioisotopes of these metal ions to bone tumours.

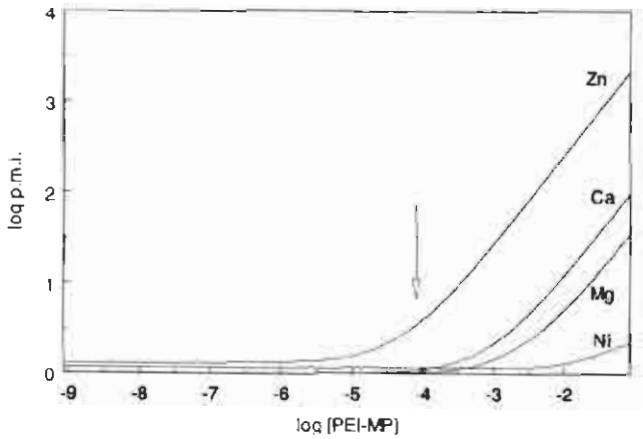

Fig 9-6: Plasma mobilisation index (p.m.i.) curves for blood plasma metal ion versus PEI-MP concentration. The arrow indicates a typical PEI-MP concentration used clinically

The speciation of Sm(III) and Ho(III) in the presence of PEI-MP in blood plasma is presented in Table 9-6. Transferrin was not included as kinetics of complexation for lanthanides is slow and would probably not occur before bone localization. From this result it is clear that no Sm(III) or Ho(III) remains bound to PEI-MP in blood plasma. Citrate competes favourably for the lanthanides and thus the distribution of the lanthanides in blood plasma is almost exclusively determined by their affinity for and complexation to citrate.

The main reason for poor retention of Sm(III) or Ho(III) by PEI-MP in blood plasma lies in its affinity for Ca(II). 82.8 % of the ligand is bound to Ca(II) rather than Ln(III). This means that almost all of the lanthanide ion is available to complex to citrate. Therefore results from the animal test with ^{153}Sm-PEI-MP should be comparable with results for ^{153}Sm-Citrate. The only species to be considered for liver uptake is $[SmCit]^0$ (neutral species at low concentrations form fine precipitates or colloids) which is only present in a small percentage at physiological pH.

Table 9-6: Speciation of Sm(III) and Ho(III) in the presence of PEI-MP in blood plasma

Species	Mol % Sm(III)	Mol % Ho(III)
$[LnCit(OH)]^-$	66.4	69.9
$[LnCit(OH)_2]^{2-}$	26.1	19.8
$[LnCit]^0$	3.0	4.2
$[LnSla]^{2+}$	1.8	3.3
$[Ln(CO_3)]^+$	0.8	0.6

Where Cit = citrate and Sla = salicylate

9.3.3 Animal studies

Tables 9-7 and 9-8 present the calculated biodistribution achieved for ^{99m}Tc-PEI-MP and ^{153}Sm-PEI-MP as studied in canine subjects. In interpreting the in vivo results it is important to note that the values presented here are comparisons of the activity measured (counted pixels) in a defined area in the different organs. These values were then normalized between the organs and expressed as percentage biodistribution, which has no correlation with the percentage of injected dose but rather to percentage of retained activity in the body. Organs

with no or low uptake were ignored. Furthermore it must be kept in mind that only the distribution of the radionuclide entity of the complex is observed which is not necessarily the same as the radionuclide-ligand complex that has been administered, due to possibilities of in vivo transchelators.

Table 9-7: Biodistribution of intravenously administered ^{99m}Tc-PEI-MP (10-30 kDa) in dogs (three dogs studied), as % retained activity.

	Cortical Bone	Liver	Kidneys	Cardiac blood pool	Lung	Background
1 h	10 ± 1	21 ± 2	22 ± 1	20 ± 2	17 ± 1	10 ± 1
2 h	11 ± 1	21 ± 2	21 ± 1	20 ± 2	17 ± 1	10 ± 1
3 h	12 ± 1	21 ± 2	19 ± 1	20 ± 2	18 ± 0.5	10 ± 1

Table 9-8: Biodistribution of intravenously administered ^{153}Sm-PEI-MP (10-30 kDa) in dogs (four dogs studied), as % retained activity.

	Cortical bone	Liver	Kidneys	Cardiac bloodpool	Lung	Background
1h	7 ± 1	24 ± 3	19 ± 2	23 ± 2	16 ± 1	11 ± 1
2h	7 ± 1	28 ± 6	18 ± 3	22 ± 1	14 ± 2	10 ± 1
3h	7 ± 1	30 ± 6	18 ± 3	21 ± 1	14 ± 2	10 ± 1

If the results of the two radionuclides are compared for the 10-30 kDa section of the polymer, it follows that, at three hours after injection, the relative bone uptake for ^{153}Sm is 7 % while for ^{99m}Tc it is 12 %. For ^{153}Sm the uptake is especially low (this is as predicted that no Sm(III) remains complexed to PEI-MP – the bone seeker) especially after three hours. ^{99m}Tc in the pertechnetate form stays bound to PEI-MP during the tests as free pertechnetate would have been demonstrated in thyroid uptake. No difference in the background and excretion rate (presented by the kidney uptake) for ^{99m}Tc-PEI-MP and ^{153}Sm-EDTMP were recorded. However the blood pool and liver uptake are both higher for ^{153}Sm than for ^{99m}Tc indicating that ^{153}Sm is distributed throughout the body – an indication that it is no longer complexed by the polymer.

These results agree with those predicted by the blood plasma model. Although the latter predicted that no Sm(III) would stay complexed to PEI-MP, a low bone uptake could still be foreseen as citrate is metabolized by all parts of the body including the bone. The distribution of ^{153}Sm throughout the body of the canine subjects corresponds with this prediction. This reasoning is further justified by the recording of higher bone uptake of ^{153}Sm-PEI-MP in 'trabecular' (growing) bone where there is higher metabolic activity (13).

As the biodistribution fro ^{153}Sm-PEI-MP can therefore be estimated with that of ^{153}Sm-citrate the liver uptake (expressed as a liver to bone ratio) is lower than expected, if compared with animal studies using ^{153}Sm-citrate [20-22]. A possible explanation for this apparent discrepancy can be found in the pH sensitive speciation of Sm(III)-Citrate. The pH of the injected formulation (bolus) contributes to the liver uptake as set out in Appendix A.

For ^{153}Sm-PEI-MP which was prepared at pH = 7.8, the neutral M_2L species forms to a small extent (9 %) while M_2LOH (63 %) and MLOH (28 %) account for the complexation of most of the ^{153}Sm in the bolus. At first, Sm(III) is complexed to PEI-MP in the injected bolus. As it passes the bone the complex is absorbed due to PEI-MP's phosphonate moiety, at first resulting in a higher than expected bone uptake. As time passes the complex reaches equilibrium with the blood plasma and citrate competes for the Sm(III) and once equilibrium is achieved, complexes all the injected Sm(III). As only a small amount of $[SmCit]^0$ colloid is present, a low liver uptake is recorded. As other Sm(III)-citrate species distribute through the body, they are absorbed on the basis of metabolic activity of citrate in all organs including the liver, bone, muscle and blood. The decline in bone uptake with time as well as the higher uptake in trabecular bone (13), can both be explained by this mechanism. Although Sm(III)-phosphate-albumin ternary complexes will also contribute towards liver uptake (23) evidence for the formation of this species only exists after longer periods (22 h) and is presumed to have little effect in the 3 h study for ^{153}Sm-PEI-MP.

9.4 Conclusion

A water-soluble polymer was successfully included in the ECCLES model for blood plasma. Prognostications made by the programme could be verified by clinical observations. The anionic fraction of the 10-30 kDa range of the polymer can be prognosticated to poorly

deliver the therapeutic radionuclides ^{153}Sm, ^{166}Ho, ^{212}Pb, ^{213}Pb and ^{89}Sr to bone. This was clinically verified for ^{153}Sm. Better although not good, uptake of ^{99m}Tc-PEI-MP could be demonstrated in dogs. This confirms that the ligand tends to have less leakage from healthy vascular tissue into healthy bone than other bisphosphonate ligands. This could result in increased leakage from disrupted vascular tissue into lesions, with a resulting increased lesion to normal ratio if it is complexed by a radionuclide that is able to remain coordinated to PEI-MP in blood plasma. Due to similar chemistry of Re as compared to Tc, it can be expected that PEI-MP labelled with ^{186}Re or ^{188}Re could result in effective therapeutic radiopharmaceuticals for bone cancer. In addition, speciation calculations illustrated the importance of pH in an intravenously administered preparation.

9.5 Appendix

Speciation calculations involving Sm(III)-citrate. If the results achieved with ^{153}Sm-citrate in the literature are analysed we find the following. Durbin *et al.* (24) showed that citrate complexed with transition lanthanides (for example Sm(III)) localises mainly in the liver and to a lesser extent in the bone tissue. O'Mara *et al.* (25) confirmed this and proposed that the found reticuloendothelial (liver, spleen and lungs) accumulation could by ascribed to colloid formation. No proposal was made as to the identity of the colloid. Later work by Woolfenden *et al.* (20), Turner *et al.* (21) and Tse *et al.* (22) all register high liver uptake (although not identical) in different animal types. Turner and co-workers (21) identified a Sm-Na-CO_3 species as being responsible for the colloid formation.

From these animal studies (20-22) the following can be noted on the biodistribution of ^{153}Sm-citrate. The pH of the injected radiopharmaceutical is of great importance. With the help of speciation calculations (Table 9-9) it can be shown that at pH values lower than employed in this study, the speciation of Sm(III)-citrate changes dramatically. It is important to compare the neutral $[SmCit]^0$ species (which would be likely to form precipitates or colloids) and the total of other species (which are all soluble) at different pH values. The neutral $[SmCit]^0$ species is more prevalent at lower pH values. At pH = 5, 82.1 % is in the form of $[SmCit]^0$ and at this pH the colloids from used for radiation synovectomy (26, 27), which will be irreversible filtered by the liver if injected intravenously (28). Although one can argue that blood plasma will buffer and adjust an injected bolus of pH = 6, to pH = 7.4, this will require

some time. The liver and reticuloendothelial cells should irreversibly filter all colloids present in the injected bolus. If the above literature results are compared according to the pH of the injected dose there appears to be a correlation (Table 9-10). The trend of lower pH, higher liver uptake is followed for all three sets of results.

Other aspects to note are the concentration of injected therapeutic preparations (higher than the concentrations used in the blood plasma model although instant mixing is assumed) and the formation of ternary complexes [23]. Both these aspects are kinetically controlled. In reality the injected bolus is pumped speedily through the body and is exchanged with organs while being diluted to the equilibrium conditions. On the other hand, evidence for the formation of the Sm(III)-phosphate-albumin ternary complexes (which will also contribute towards liver uptake [23[) only exist after longer periods (22h). Although the values reported in Table 9-10 are for results gathered after 24 h, the corresponding 6 h liver to bone ratio values are even higher; 20.9 and 27.7 for Turner [21] *et al.* and Tse *et al.* [22] respectively. It is therefore assumed that the existence of ternary complexes does not explain high liver uptake shortly after administration.

Liver uptake (Table 9-10) was expressed as a ratio of the liver to bone uptake using as input the percentage of injected dose per gram of organ for both the liver and bone. As only relative organ uptake values are available for PEI-MP a direct comparison with these results is impossible but from Table 9-8 it is clear that the liver: bone ratio will be significantly lower for PEI-MP.

Table 9-9: Species distribution of Sm(III) citrate at various pH values

pH	% [SmCit] (neutral)	% $[SmCitOH]^-$	% $[SmCit(OH)_2]^{2-}$	% $[SmCit_2]^{3-}$
5	82.1	7.1	–	8.5
5.5	66.5	17.5	–	15.3
6	42.6	40.6	0.7	15.9
6.5	22.3	64.4	3.4	9.8
7	8.7	75.3	11.9	4.0
7.4	3.1	68.2	27.6	1.5

Table 9-10: The ratio of liver to bone uptake 24 hrs after injection in various animals

	Woofenden *et al.* [20]	**Turner *et al.* [21]**	**Tse *et al.* [22]**
pH	5-6	6-7	6.5
Liver: Bone	19.5	16.3[a]	10.3[a, b]
Type of Tumor	V-2 Carcinoma	B16 Melanoma	Dunning R3327-H
Animal	Rabbits	C-57 black mice	Copenhagen-Fisher rats

9.6 References

1. USA Food and Drug Administration approval for ^{153}Sm-EDTMP (^{TM}Quadramet) granted during March (1997).

2. **JARVIS, N.V., WAGENER, J.M., JACKSON, G.E.** 1995. *J. Chem. Soc., Dalton Trans.* 1411

3. **WAGENER, J.M., JARVIS, N.V.** 1995. *S. Afr. J. Chem.* 48: 85

4. **MAY, P.M., WILLIAMS, D.R., LINDER, P.W.** 1977. *J. Chem. Soc., Dalton Trans* 588

5. **ZEEVAART, J.R., JARVIS, N.V., LOUW, W.K.A., JACKSON, G.E., CUKROWSKY, I., MOUTON, C.J.** 1999. *J. Inorg. Biochem.* 73: 265

6. **ZEEVAART, J.R., JARVIS, N.V., CUKROWSKI, I., JACKSON, G.E.** 1997. *S. Afr. J. Chem* 50: 189

7. **CUKROWSKI, I., ZEEVAART, J.R., JARVIS, N.V.** 1999. *Anal. Chim. Acta* 379: 217

8. **ZEEVAART, J.R., JARVIS, N.V., LOUW, W.K.A., JACKSON, G.E.** 2001. *J. Inorg. Biochem.* 83: 57

9. **BIJVOET, O.L.M, FLEISCH, H.A., CANFIELD, R.E., RUSSELL, R.G.G.**(Eds). 1995. Bisphosphonate on bones, Elsevier, Amsterdam

10. **DUNCAN, R., KOPEČEK, J.** 1984. *Adv. Polym. Sci.* 57: 51

11. **SOYEZ, H., SCHACHT, E.** 1999. Pharmaceutical Technology Europe, November p. 50

12. **SEYMOUR, L.W.** 1992. *CRC Crit. Rev. Ther. Drug Carrier Syst.* 9: 249

13. **DORMEHL, I.C., LOUW, W.K.A, MILNER, R.J., KILIAN, E., SCHNEEWIESS, F.H.A.** 2001. *Drug Res.* 51: 258

14. **JARVIS, N.V., WAGENER, J.M.** 1995. *Talanta* 42: 219

15. **MAY, P.M., MURRAY, K.** 1988. *Talanta* 35: 927 and refernces therein

16. **HASSFJELL, S.P., HOFF, P., BRULAND, Ø.S., ALSTAD, J.** 1994. *J. Labelled Comp. Radiopharm.* 34: 717

17. **MOEDRITZER, K., IRANI, R.R.** 1966. *J. Org. Chem.* 31: 1603

18. **MARTELL, A.E., SMITH, R.M.** 1977 and 1989. Critical Stability Constants. Vols. 3 and 6, Plenum, New York and references therein.

19. **GOECKLER, W.F., EDWARDS, B., VOLKERT, W.A., HOLMES, R.A., SIMON, J., WILSON, D.** 1987. *J. Nucl. Med.* 28: 176

20. **WOOLFENDEN, J.M., HALL, J.N., BARBER, H.B., WACKS, M.E.** 1983. *Int. J. Nucl. Med. Biol.* 10: 251

21. **TURNER, J.H., MARTINDALE, A.A., DE WITT, G.C., WEBB, J., SORBY, P., BOYD, R.E.** 1987. *Eur. J. Nucl. Med.* 13: 432

22. **TSE, J.W., WIEBE, L.I., NOUJAIM, A.A.** 1989. *Nucl. Med. Biol.* 16: 17

23. **NEUMAIER, B., RÖSCH, F.** 1999. *Radiochim Acta* 84: 201

24. **DURBIN, P.W., ASING, C.W., JOHNSTON, M.E., HAMILTON, J.G., WILLIAMS, M.H.** 1956. USAEC Report. ORINS-1 p. 171

25. **O'MARA, R.E., MCAFEE, J.G., SUBRAMANIAN, G.** 1968. *J. Nucl. Med.* 10: 49

26. **FERRO-FLORES, G., GARCIA-SALINAS, L., PEDRAZA-LOPEZ, M., GONZALEZ-ZAVALA, M.A., TENDILLA, J.I., LOPEZ-GÓMEZ, M.A.** 1997. *J. Radioanal. Nucl. Chem.* 222: 93

27. **PRABHKAR, G., JOSHI, S.H., RANGANTHA, D.K., UMAMAHESWARI, S., ANANTHAKRISHNAN, M., RAMAMOORTHY, N.** 2000. *Nucl. Med. Biol.* 27: 353

28. **NEVES, M.** Personal communication

Chapter 10 - ^{117m}Sn and ^{186}Re radiolabelling of polyethyleneiminomethyl phosphonic acid (PEI-MP), a potential selective therapeutic bone tumour seeker

10.1 Introduction

An ideal radiopharmaceutical for the diagnosis and/ or treatment of neoplastic and inflammatory (benign) bone disease would be a radiolabelled compound that predominantly accumulates in bone lesions with limited access to normal bone and other organs. Water soluble polymers are under development as vehicles for systemic drug delivery due to enhanced permeability and retention effect whereby neoplastic tissue selectively accumulates macromolecules. In previous studies the ^{99m}Tc-PEI-MP 10-30 kDa fraction showed promising biodistribution and pharmacokinetic properties in primates and dogs, as well as good tumour localization in dogs with natural osteosarcomas. Metal ion speciation studies, however predicted that the polymer would not deliver therapeutic radionuclides such as ^{153}Sm to bone, but that $^{117m}Sn^{II}$ will remain bound to PEI-MP in the blood plasma. The purpose of this study was therefore to evaluate the labelling of 10-30 kDa PEI-MP with ^{117m}Sn and ^{186}Re, both radionuclides with proven therapeutic properties.

10.2 Materials and Methods

PEI-MP was synthesized by condensation of polyethylenimine, phosphonic acid and formaldehyde (Fig 10-1). The 10-30 kDa fraction was prepared using membrane ultrafiltration techniques. ^{117m}Sn was prepared by the ^{117}Sn (n, n')^{117m}Sn reaction in the HFR-Petten reactor, the Netherlands. The irradiated metal was dissolved in 10 M HCl at 60°C under Ar and diluted to 3.3 M with water. PEI-MP (10-30 kDa, 100mg) was dissolved in 1.2 ml water and 0.2 ml 10M NaOH. To this an aliquot containing 2.6 mg Sn was added and the pH adjusted to 6.0. Radiochemical purity was determined by chromatography on ITLC-SG (ethanol) and cellulose thin layers (1 M citrate, pH 7.0) (Fig 10-1). ^{186}Re was prepared by the ^{185}Re (n,γ) ^{186}Re reaction in the SAFARI-1 reactor, Pelindaba, Pretoria, South Africa. The irradiated metal was dissolved in 10 % H_2O_2, evaporated to dryness (80°C), whereafter an

aliquot containing 25 µg Re was added to a PEI-MP freeze dried labelling kit (10 mg Na-PEI-MP; 0.5 mg $SnCl_2.2H_2O$) at a pH of 1.0. After incubation at ± 90°C (30 min) the pH was adjusted to 6.0. Radiochemical purity was determined by chromatography on ITLC-SG (ethanol) and cellulose ITLC (1.0 M citrate, pH 7.0) (Fig 10-2).

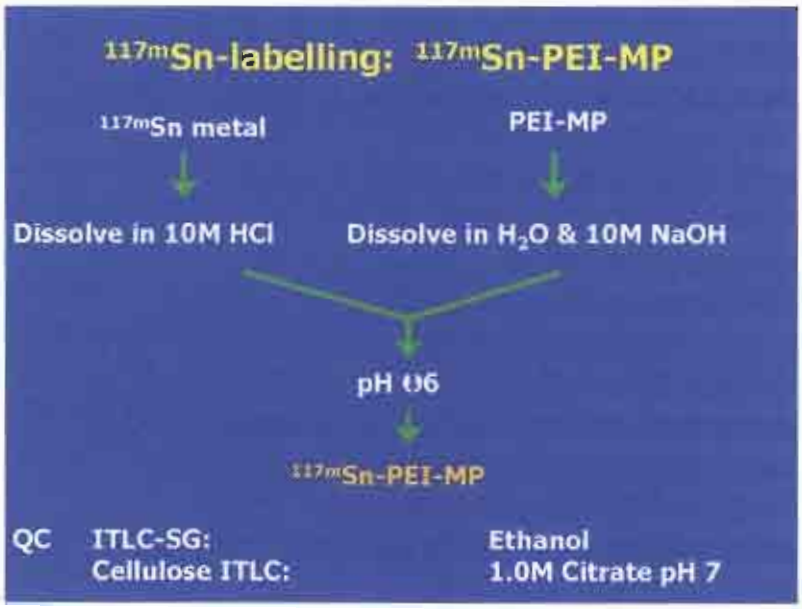

Fig 10-1: ^{117m}Sn-labelling: ^{117m}Sn-PEI-MP

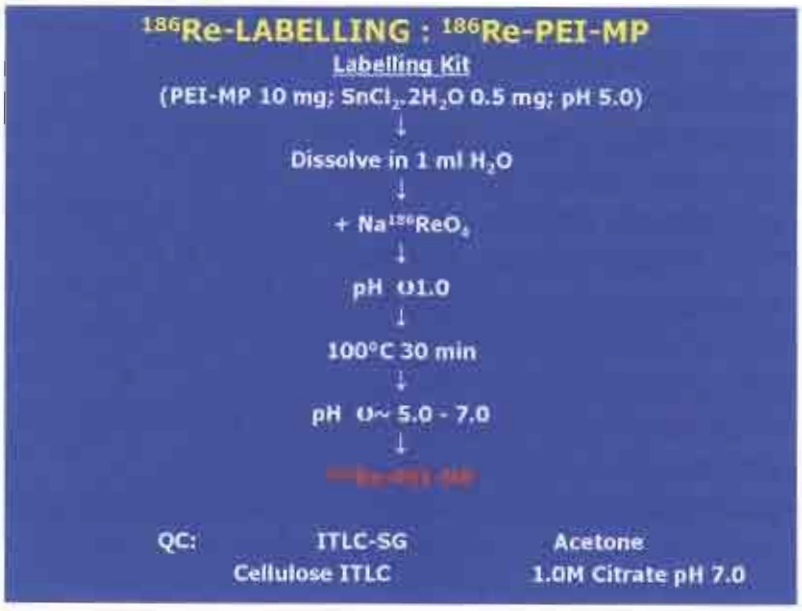

Fig 10-2: ^{186}Re-labelling: ^{186}Re-PEI-MP

10.3 Results

Both ^{117m}Sn-PEI-MP and ^{186}Re-PEI-MP gave radiochemical purities ≥ 98 % with < 1.0 % colloids. For ^{117m}Sn-PEI-MP the respective percentages were the same for 1 week while those for ^{186}Re-PEI-MP stayed the same for 48h.

10.4 Conclusion

These results indicate that PEI-MP can be labelled successfully with radioisotopes that have proven therapeutic properties. The next step would be to investigate their biodistribution, pharmacokinetics and therapeutic efficacy in animals bearing osseous tumours.

Chapter 11 - Biodistribution And Pharmacokinetics of Variously Molecular Sized ^{117m}Sn(II)-Polyethyleneiminomethyl Phosphonate (PEI-MP) Complexes in the Normal Primate Model as a Potential Selective Therapeutic Bone Agent.

Summary

In the search for a cure for metastatic bone cancer, ^{117m}Sn with its conversion electrons and low energy photons both of discrete energies, shows little bone marrow toxicity, providing the opportunity to increase the administered dose. Selective accumulation in lesions would capitalise on this advantage. The 10-30 kDa fraction of the water-soluble polymer polyethyleneimine, functionalised with methyl phosphonate groups (PEI-MP) and labelled with Tc, has shown selective uptake into bone tumours. Furthermore using speciation calculations it was predicted that the Sn(II)-PEI-MP complex would remain intact in the blood plasma. Because of this positive indication animal experiments were carried out to test this prediction. This paper relates the labelling, biodistribution and pharmacokinetics of various fractions of ^{117m}Sn (II) PEI-MP in the normal primate model, and points to promising therapeutic possibilities.

Zusammenfassung

Verteilung und Pharmakokinetik von ^{117m}Sn(II)-Polyethyleneiminomethyl-Phosphonat-Komplexen unterschiedlicher Molekulargröße im normalen Primatenmodell als potentielle selektive Knochentherapeutika. Bei der Suche nach eine kurativen Behandlung gegen metastierenden Knochenkrebs zeigte Sn-117m mit seinen Konversioselektronen geringe Knochenmarktoxizität. Dies ermöglicht eine Erhöhung der verabreichten Dosis, was zu einer gewünschten Kumulierung am Ort der Läsionen führt. Die 10-30 kDa-Fraktion des wasserlößlichen Polymers Polyethylenimin, das Methylphosphonat-Gruppen enthält (PEI-MP)

und mit Tc-99m markiert wurde, zeigte selektive Aufnahme in die Knochentumoren. Anhand spezieller Berechnungen wurde die Voraussage getroffen, daß der Sn(II)-PEI-MP-Komplex im Blutplasma intakt bleibt. Zur überprüfung dieser Vorausage wurden entsprechende Tierversuche durchgeführt.

In der vorliegenden Arbeit wird über die Markierung, Verteilung und Pharmakokinetik verschiedener Fraktionen der Sn-117m-PEI-MPs im normalen Primaten modell berichtet, wobei vielversprechende Ergebnisse im Hinblick auf eine therapeutische Verwendung erzielt werden konnten

Key words: Bone therapeutics; Polyethyleneiminomethyl phosphonate, ^{117m}Sn(II) labelled; polymer, enhanced permeability and retention effect

11.1 Introduction

In principle, internal radionuclide therapy (IRT) works by the delivery of large radiation doses to the targeted diseased tissues while sparing normal tissues. Ideally 100% target localization of the radiopharmaceutical is the aim, but in practice this has hardly been attained, and is a major disadvantage of clinically established IRT agents. This lack of selectivity causes systemic radiotoxicity to radiosensitive tissues/organs, which limits the applied doses with resulting low palliative or curative rates [1,2].

In recent years there has been an increasing awareness that the lack of selectivity of low molecular weight antitumour drugs could be related to their pharmacokinetic properties, i.e. their short half-life in the bloodstream and their rapid diffusion throughout the body resulting in an essentially even tissue accessibility [3].

Therefore, one approach to alter the pharmacokinetic behaviour and to overcome the radiotoxicity of IRT agents to normal tissues is to attach the appropriate therapeutic radionuclide to a water-soluble macromolecule, such as the polymers presently under investigation. These

form chemically stable in vivo vehicles for systemic drug delivery due to the enhanced permeability and retention (ERP) effect whereby neoplastic tissue selectively accumulates macromolecules [3,4,5].

This strategy can also be applied by labelling the macromolecular bone tumour seeker PEI-MP = $\{\text{-}CH_2CH_2\text{-}N\ [CH_2CH_2\text{-}NH^+\{CH_2PO_3^{2-}\}_2]\text{-}CH_2CH_2\text{-}NH^+\ [\{CH_2PO_3^{2-}\}]\ \text{-}\}_n$ with an appropriate therapeutic radionuclide. The chemical properties of this labelled compound should be such that an in vivo stability can be assured while the species that predominantly forms in vivo is charged, as neutral species could form colloids with subsequent liver uptake [6,7].

In previous studies, the macromolecular 10-30 kDa PEI-MP (polyethyleneimine functionalised with methyl phosphonate groups) labelled with ^{99m}Tc (a diagnostic radionuclide) showed promising biodistribution and pharmacokinetic properties (viz. localisation in bony tissue, and fast renal clearance) for normal primates and dogs [8], as well as good tumour localization in dogs with natural occurring osteosarcoma [9]. Metal ion speciation studies, however predicted that the polymer would not deliver the therapeutic radionuclides ^{153}Sm, ^{166}Ho, ^{212}Pb, ^{213}Pb and ^{89}Sr to bone. These studies were also clinically verified for ^{153}Sm [7]. Additional speciation studies with Sn(II) predicted that it will remain bound to PEI-MP in blood plasma and therefore will exhibit only slight reticuloendothelial uptake [10]. Blood plasma modelling can also be used to predict the speciation of complexes at elevated levels of Ca(II) which characterises sites of metastasis where high bone turnover occurs [11]. PEI-MP is furthermore easy to complex with Sn(II) that contains ^{117m}Sn (half-life = 13.60 days), a low energy electrons and photons emitting radionuclide with proven therapeutic properties [12, 13].

The biodistribution and pharmacokinetics of variously molecular sized [^{117m}Sn(II)] Sn(II)-PEI-MP (to be abbreviated as ^{117m}Sn-PEI-MP) complexes (up to 30 kDa) were studied in this exploratory investigation using scintigraphy as well as blood and urine sampling for radioactivity determination in the normal chacma baboon (*Papio ursimus*) in order to assess their possible usefulness as optimal therapeutic agents. The choice of Sn(II) instead of Sn(IV) is debated elsewhere [10] and therefore great care was taken with these experiments to insure that a Sn(II) complex is injected.

11.2 Materials and methods

11.2.1 Polyethyleneiminomethyl phosphonic acid (PEI-MP)

PEI-MP was prepared, fractionated (based on molecular size and not molar mass) and characterised as described previously [8].

11.2.2 Preparation of ^{117m}Sn (II) PEI-MP and the determination of its radiochemical purity

^{117m}Sn(II)-PEI-MP was prepared according to a similar procedure as described previously [10].

The radionuclide ^{117m}Sn was produced by fast neutron irradiation of tin metal – enriched in ^{117}Sn to 92% - according to the nuclear reaction ^{117}Sn (n,n') ^{117m}Sn. The irradiation of 8.6 mg targets were performed in the High Flux research nuclear reactor at Petten, the Netherlands, at a neutron flux of about 10^{14} $cm^{-2}s^{-1}$ and took 21 days followed by a decay period of 4 days and subsequent shipping to South Africa. The specific activity achieved on the day of preparation (7 days after end of irradiation) was 2 mCi ^{117m}Sn / mg Sn. Using the necessary shielding, the irradiated metal was dissolved in 1 ml of concentrated HCl solution at 60 °C under Ar over a period of 1 h and was diluted with 2 ml water. In a separate vial 100 mg (211 µmol, as expressed for the monomer which has a molar mass of 473.2 g / mol) of PEI-MP (typically the 10-30 kDa fraction) was dissolved in 1.2 ml water and 0.2 ml 10 mol dm^{-3} NaOH using a small magnetic stirrer bar. To this an aliquot of the ^{117m}Sn-labelled $SnCl_2$ solution (strongly acidic) containing 2.6 mg (22 µmol) Sn was added. After addition the pH is gradually adjusted to pH = 6 with a 1 mol dm^{-3} NaOH solution while being heated and stirred [10].

The radiochemical purity was checked chromatographically. Five µl of this solution was spotted on ITLC-SG (silica gel impregnated glass fibre sheets, Gelman Sciences Inc. Ann Arbor, MI, USA) and cellulose (TLC aluminium sheets, cellulose 0.1 mm, E. Merck AG. Darmstadt,

Germany) chromatograms and developed in ethanol and 1 mol dm^{-3} citrate (pH = 7.0) respectively. After scanning the chromatograms with a radiation sensitive scanner, the first showed that ≥ 98 % of the activity remained at the origin, indicating that less than 2 % unbound Sn(II) was present. The chromatograms developed in 1mol dm^{-3} citrate showed ≥ 99 % of the activity on the solvent front, indicating less than 1 % colloidal species remaining at the origin. The chromatograms were repeated daily and after one week the respective percentages were the same. This indicated that the complex is stable and almost no colloids are formed.

For verification purposes the radiochemical purity was also checked at pH = 7.4 and pH = 6 found to be 99.2% and 97% respectively but the formulation at pH = 6 was preferred as it would help to prevent oxidation of Sn(II). All the above solutions were prepared with de-aerated water and kept under Ar. For the ITLC-SG chromatograms ethanol proved to be a more effective developer than acetone because $SnCl_2$ is more soluble in ethanol and moves to the front.

In both cases a negative control was also performed. Free Sn(II) (in the form of $SnCl_2$ in HCl) was spotted on ITLC-SG and developed with ethanol. The result was that > 95% of the activity moved with the solvent front. Sn(II)-colloids were made by adjusting the solution above to pH = 9. After spotting on cellulose and development in citrate > 98% of activity was found in the lower part of the chromatogram (R_f 0 - 0.5). These negative controls confirmed that the selected chromatographic material and mobile phase are able to determine colloids as well as free Sn(II).

11.2.3 Biodistribution and Pharmacokinetics of ^{117m}Sn-PEI-MP

Six normal male baboons, average weight 27.5 kg, were used in the study and received i.v. ^{117m}Sn-PEI-MP of various molecular sizes. All studies were performed after approval by the Ethics Committee of the University of Pretoria, according to the guidelines of the National Code for Animal Use in Research, Education, Diagnosis and Testing of Drugs and Related Substances in South Africa.

The baboons were subjected to identical experimental procedures except for the mentioned differences in molecular sizes of the injected ^{117m}Sn-PEI-MP. Three different size fractions were

studied, viz. in the following ranges (1) 3-8 kDa (number of experiments n =1), (2) 8-10 kDa (n=1), (3) 10-30 kDa (n=3). This last fraction was of special interest, since it ideally suited the characteristics sought for an optimal therapeutic agent as gathered from data on ^{99m}Tc-PEI-MP in primate models (8).

Induction of anaesthesia was performed with ketamine hydrochloride (10 mg/kg i.m., Ketalar Parke Davis, Cape Town, S.A.), and immediately followed by a maintained controlled infusion of a 6 % sodium pentobarbitone solution (Sagatal, Kyron Laboratories Pty. Ltd., Benrose, S.A.) at 30 ml/h. The animal in the supine position under the gamma camera was injected i.v. with a ± 4 ml bolus containing 111-148 MBq of ^{117m}Sn-PEI-MP (± 2.3 mg Sn and ± 90 mg PEI-MP formulated at pH 6 to prevent premature oxidation of Sn(II)) and data acquisition started on a count down with a Siemens Orbiter, large view gamma camera (Siemens, Erlangen, Germany) in 64 x 64 word mode performing a 60 min dynamic study (60 x 1 min frames). At 1, 2 and 3 h, and in some cases at 24 h static images of 120 s were acquired.

Blood and urine samples were collected at fixed intervals for 3h, viz. every 3 min for the first h, then hourly for blood samples, and for the urine every 5 min for the first h, subsequently hourly. The activity and volume of each sample, and cumulative urine volumes were recorded. Regions of interest (ROIs) were placed on the images of cardiac blood pool, liver, lung, spleen, kidneys, and bone (cortical and trabecular) to obtain time-activity curves for these compartments from the dynamic study. Similarly, data of count-rate per pixel for the ROIs, which were decay-corrected, were obtained from the static images. These were normalised, according to acquisition protocol, to extend the time-activity curves of the dynamic study to 3 h from which t½, the halftime of clearance, could be calculated.

Blood clearance and cumulative urine curves were also obtained in all cases so that relative organ distributions of the retained activity and eventually of the injected dose (i.d.) could be obtained for all ^{117m}Sn labelled molecular size fractions. These could be compared for optimal distribution characteristics for therapy according to the mentioned criteria.

11.2.4 Blood plasma modelling

The ECCLES (Evaluation of Constituent Concentrations for Large Equilibrium studies) program was used for speciation calculations in this paper. The ECCLES database was previously updated to include all formation constants for Sn(II) [10]. To simulate areas of higher or lower calcification the free Ca(II) concentration in blood plasma model was manipulated as to achieve 0.1, 10 and 100 fold Ca(II) levels.

11.3 Results

None of the animals showed any adverse effects from the labelled fractions at any time during the study and thereafter.

Scintigraphic images of individual representative animals after injection of the various ^{117m}Sn-PEI-MP fractions are shown. Fig 11-1 presents the thorax images at 1, 2, 3 and 24 h after injection of the 10-30 kDa fraction. Liver uptake is visible as well as high blood pool activity while only low bone uptake is present even at 24 h. This is confirmed from the mean time activity curves (T-A-C) (Fig 11-2) up to 3 h after injection. Fig 11-3 presents the mean (n=3) blood clearance curve for the same set of animals and confirms continuing high blood pool activity even from 1 h onwards. However, after 24 h most of the activity is cleared as can be seen in the scintigraphic image, extreme right in Fig 11-1. Accumulative urinary excretion of activity is shown as percentage of injected dose (i.d.) in Fig 11-4.

Fig 11-5 presents scintigraphic images (head, thorax and abdominal/pelvic area) of the baboon injected with the 3-8 kDa fraction of ^{117m}Sn-PEI-MP, 3 h after administration. Note the reduced liver uptake while the blood clearance of ^{117m}Sn-PEI-MP for this fraction is much faster (Fig 11-7). However most significant is the high cortical bone uptake (Fig 11-6). The accumulative urine curve indicates continuing excretion of the activity (Fig 11-8). Little retention of activity in the bladder is visible after 3 h (Fig 11-5). The results are summarized in Table 11-1 which represents the mean t½ of clearance and mean maximum percentage retained body activity between 2 and 3

h p.i. of the 10-30 kDa fractions of ^{117m}Sn-PEI-MP as well as individual corresponding values for the other fractions. For comparison, 99mTc-PEI-MP fractions taken from a previous study [8] are included together with cumulative urinary excretion as percentage i.d. and t½ of blood clearance from blood sampling. Results from blood plasma modelling are presented in Table 11-2 and 11-3.

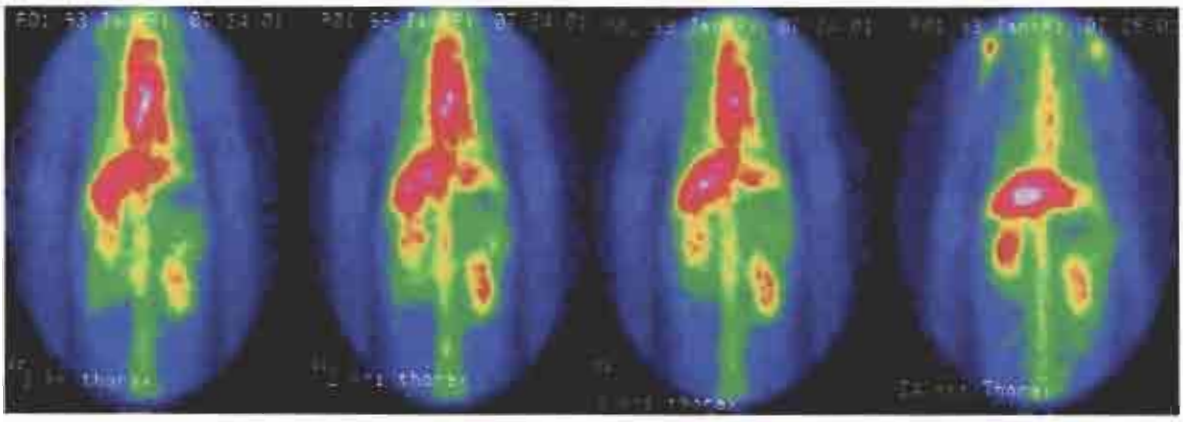

Figure 11-1: Scintigraphic images of the thorax at 1, 2, 3 and 24 h (from left to right) p.i. of ^{117m}Sn-PEI-MP, fraction 10-30 kDa.

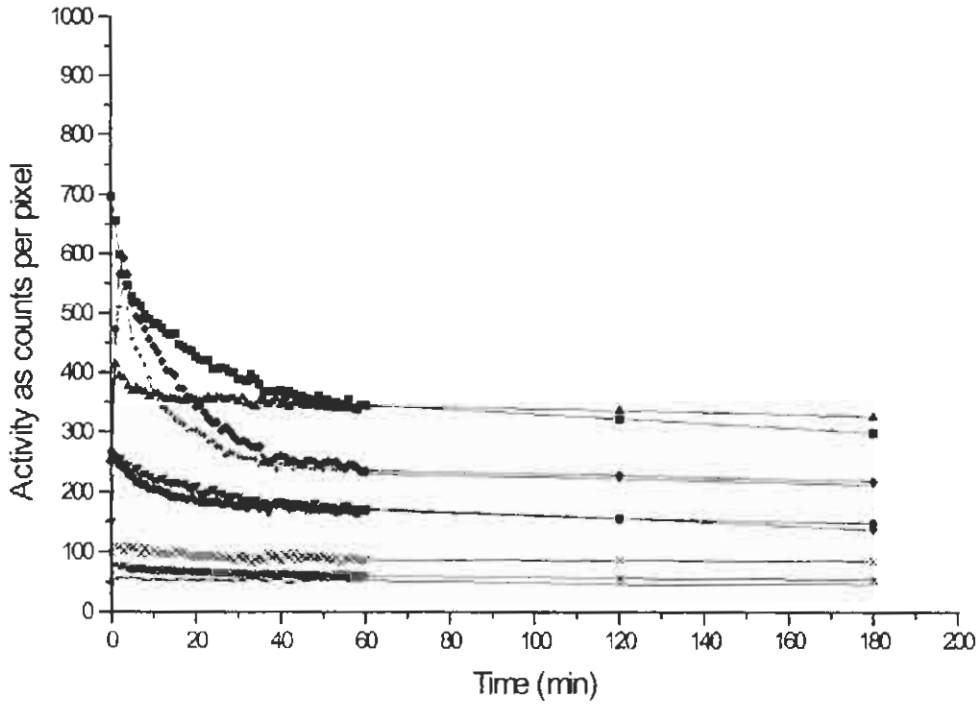

Fig 11-2: Mean time activity curves (n= 3), fraction 10-30 kDa, for cardiac blood pool (■), lung (●), liver (▲), spleen (▼), left kidney (♦), right kidney (+), shoulder (x), arm (☼) and background (bottom curve) vs time in min.

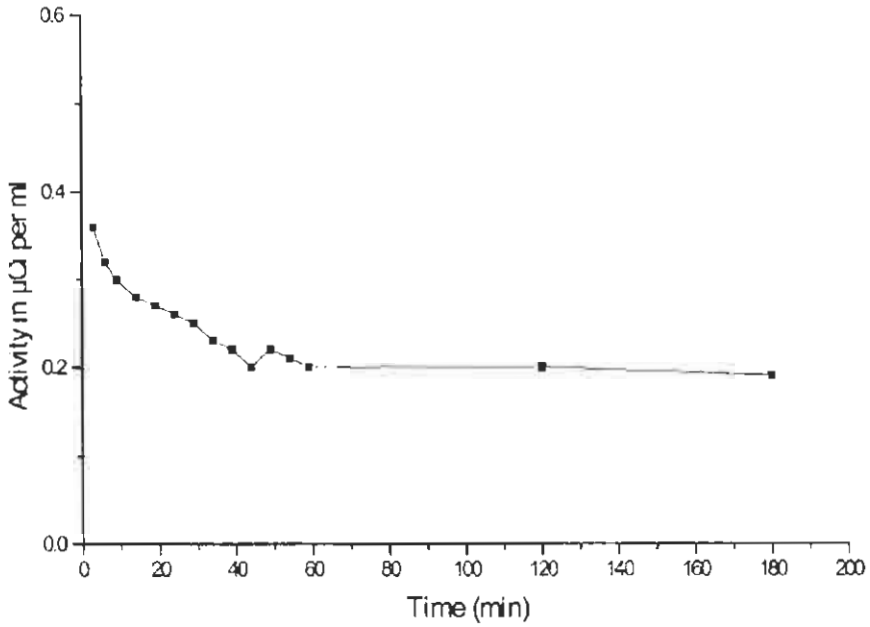

Figure 11-3: Mean blood clearance curve (n = 3), normalised to injected dose, for the 10-30 kDa fraction vs time in min.

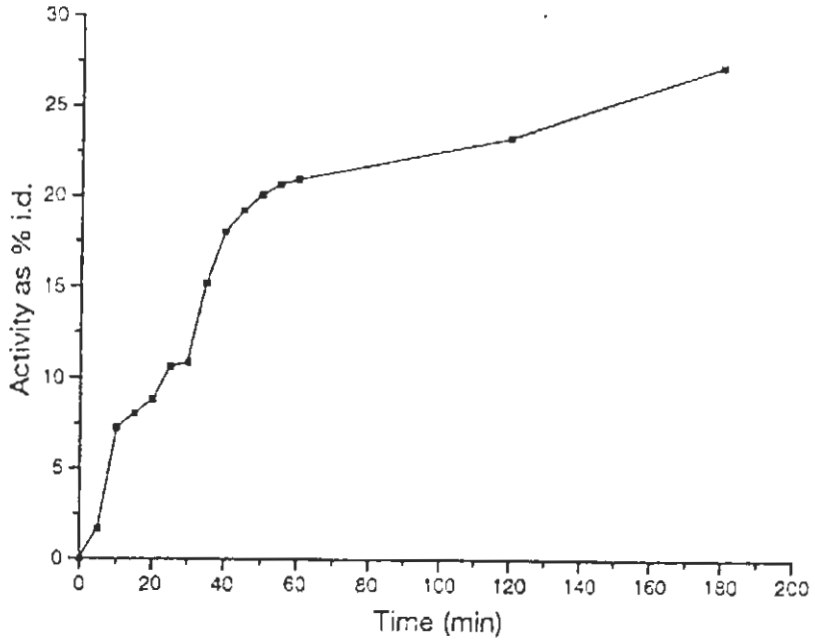

Figure 11-4: Mean cumulative urinary excretion curve (n=3) for fraction 10-30 kDa as percentage of i.d. (injected dose)

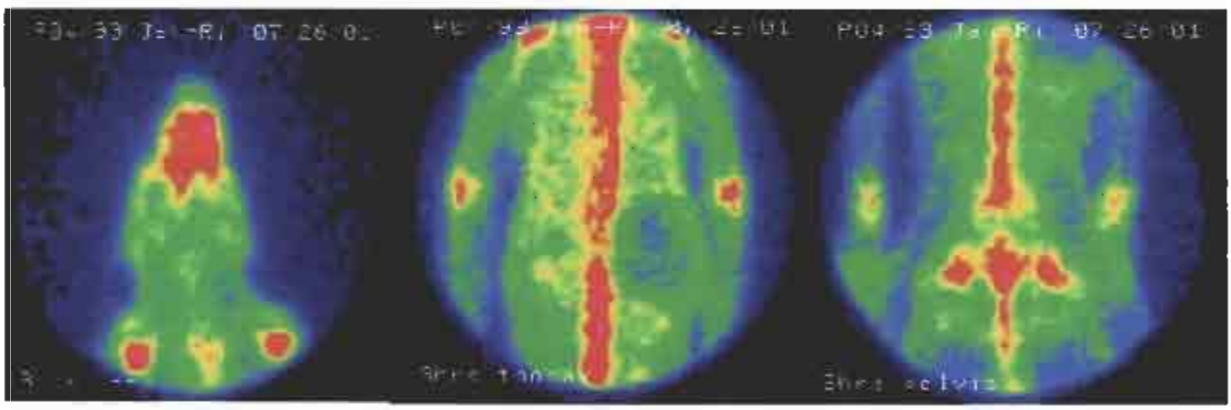

Figure 11-5: Scintigraphic images of the head, thorax and pelvic area (from left to right), 3 h p.i. ^{117m}Sn-PEI-MP, fraction 3-8 kDa.

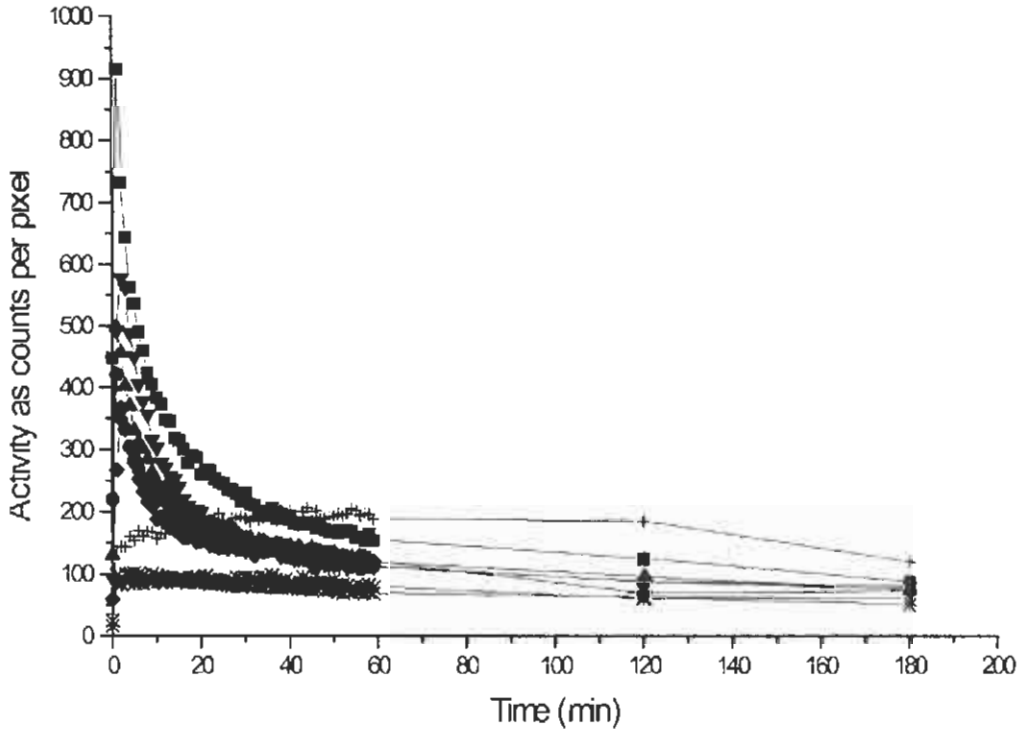

Figure 11-6: Individual time activity curves, fraction 3-8 kDa, for cardiac blood pool (■), lung (●), liver (▲), left kidney (▼), right kidney (♦), shoulder (+), arm (x), background (☼) vs time in min.

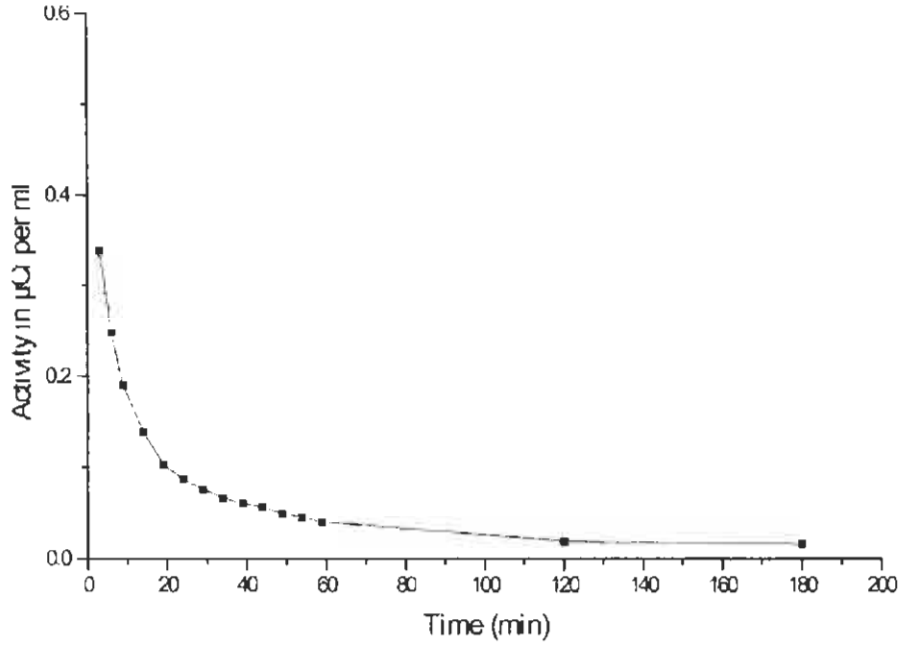

Figure 11-7: Individual blood clearance curve for the 3-8 kDa fraction.

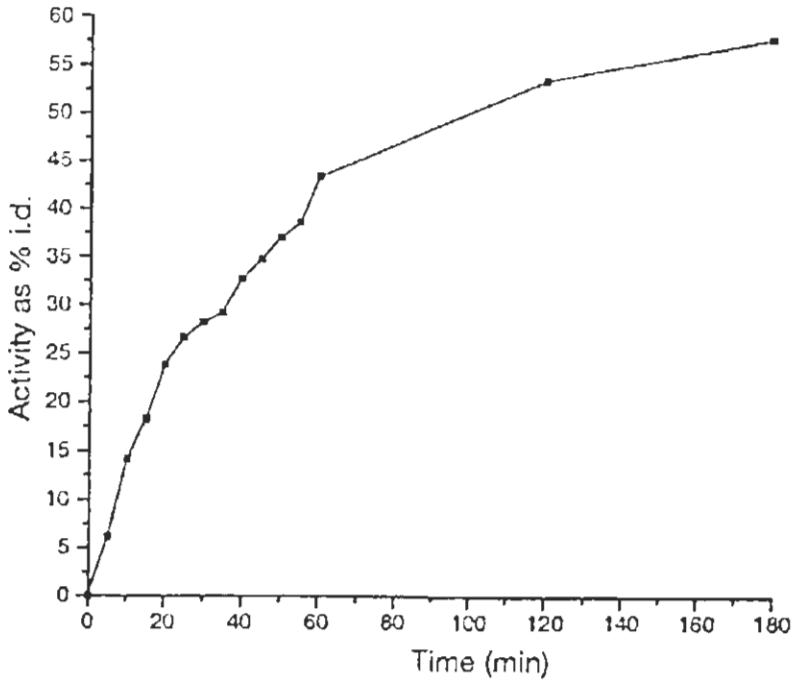

Figure 11-8: Individual cumulative urinary excretion curve for fraction 3-8 kDa as a percentage of i.d. (injected dose).

11.4 Discussion

Due to limited and costly availability of ^{117m}Sn and because the blood plasma model indicated that positive results were to be expected with ^{117m}Sn-PEI-MP [10], only a small number of animal tests were needed to confirm the predictions. As a follow up on previous ^{99m}Tc-PEI-MP studies [8] it was decided to carry out a limited number of tests on non-human primates, like baboons, that are best suited for this explorative study as they answer many of the criteria of parallelism to the human. Because the ^{99m}Tc-PEI-MP, 10-30 kDa fraction gave the best biodistribution and kinetics with small inter-animal variations per fraction [8], three animals were chosen for investigation with the ^{117m}Sn-PEI-MP 10-30 kDa fraction, while only one animal/fraction was investigated with the 3-8 and 8-10 kDa fractions. These single-animal experiments gave some useful information, but naturally presented statistics shortcomings. The lack of a visible spleen compartment in the 3-8 kDa fraction animal was due to gastric bloat. This fraction yielded a fast clearance from all compartments (t½), except from bone, where it accumulates, as is known of a phosphonate [14]. (Table 11-1)

In comparison with the ^{99m}Tc-PEI-MP (3-10 kDa fraction), the significant differences for the 3-8 kDa fraction reside in the kidney (t½ and max % uptake) and bone (max % uptake). The contribution of some larger molecules in the 3-10 kDa vs. the 3-8 kDa fraction could be a reason for lower accessibility to normal bone in the former case. An estimation of 11 % uptake for the non-visualised spleen in the animal injected with the 3-8 kDa fraction of ^{117m}Sn-PEI-MP was made after comparing the 3-10 kDa ^{99m}Tc-PEI-MP complex. The ^{117m}Sn-PEI-MP complex with smallest molar size behaves as if the ligand is a monomer phosphonate ligand, e.g. as ^{153}Sm-EDTMP [14] however with considerably lower bone uptake for ^{117m}Sn-PEI-MP. The complex remains intact in the blood plasma long enough for the ^{117m}Sn to reach the target, the bone (in Table 11-1 the cortical bone), because it is small enough to escape from the circulation and small enough to avoid trapping by the liver.

Table 11-1: Mean t½ in minutes and mean maximum % uptake between 2 and 3 h p.i. of ^{117m}Sn-PEI-MP, fraction 10-30 kDa, and ^{99m}Tc-PEI-MP fractions in various body compartments of the primate with corresponding individual values for fractions 3-8 and 8-10. Cumulative urinary excretion is presented as % i.d. (percentage of injected dose) and t½ of blood clearance in min.

Fraction kDa and ^{117m}Sn	Maximum % uptake and $t_{½}$ (min)						Urine (%)	Blood $t_{½}$ (min)
	Cardiac blood pool	Liver	Kidney	Lung	Spleen	Cortical bone		
3-8	17 (8min)	13 (10min)	13 (12min)	13 (12min)	11	22 (>4h)	55	12
(n = 1)					(estimation)			
8-10	22 (22 min)	24 (> 4 h)	13 (10 min)	16 (> 4 h)	10 (> 4 h)	5 (> 4 h)	25	20
(n= 1)								
10-30	24 ± 2.7	23 ± 1	15 ± 1.1	11 ± 1.4	10 ± 1.3	5 ± 1.3	40	5
(n = 3)	(44 ± 12 min)	(> 4 h)	(30 ± 6 min)	(> 120 min)	(> 4 h)	(> 4 h)		
^{99m}Tc								
3-10	15 ± 4	16 ± 1	36 ± 4	8 ± 2	10 ± 1	8 ± 1	40.6	5
(n = 4)	(10 ± 1 min)	(90 ±22 min)	(> 4 h)	(10 ±1.5 min)	(75 ± 2 min)	(> 4 h)		
10-30	15 ± 3	20 ± 2	18 ± 4	13 ± 4	13 ± 1	18 ± 1	52.5	6
(n = 4)	(10 ±1.5 min)	(22 ± 3 min)	(20 ± 3 min)	(15 ± 3 min)	(60 ± 9 min)	(> 4 h)		
Background compartment not included in table								

The baboon which received the 8-10 kDa ^{117m}Sn-PEI-MP fraction had only one functioning kidney, which could have influenced clearance rates from most compartments and explain the low (25%) excretion in the urine. The drastic reduction in bone uptake from the 8-10 kDa fraction and upwards may be because the critical molecular weight above which diffusion becomes restricted in continuous endothelium is about 5 kDa [15].

Statistically, the results of the 10-30 kDa ^{117m}Sn-PEI-MP fraction (n=3) can be regarded as the most useful. The small inter-animal deviations throughout, which were also observed previously with 10-30 kDa ^{99m}Tc-PEI-MP [8], point to the consistency of the in vivo behaviour of this fraction. In comparison to the ^{117m}Sn-PEI-MP 3-8 and 8-10 kDa fractions, the larger 10-30 kDa ^{117m}Sn-PEI-MP exhibits a prolonged retention in all compartments, together with low bone uptake and a reduction in urine excretion, as can be expected from its larger hydrodynamic volume and its resultant slower diffusion through the endothelium as well as a decrease in renal excretion rate.

The fact that the ^{117m}Sn bound to the 10-30 kDa fraction remains in the blood plasma in healthy animals (see Table 11-1 and Fig 11-4) can be explained by two possibilities, one that the ^{117m}Sn-PEI-MP, as complex remains bound in blood plasma but this particular size of the polymer complex is too big to escape from intact vasculature while a significant portion is trapped by the liver. In this case the complex between the polymer, a phosphonate and therefore a bone-seeker, and the ^{117m}Sn(II) remains in the blood pool and can only escape from circulation to accumulate in the bone, if the vasculature is damaged. A low bone-uptake follows as well as completed renal excretion after 24 h. This is confirmed in (Fig 11-1 and 11-2).

The alternative is that the ^{117m}Sn dissociates from the complex and attaches to other blood plasma ligands like histidinate or remains as $^{117m}Sn(OH)_2$. Therefore the biodistribution observed could not be that of the ^{117m}Sn-PEI-MP complex but of some other species also taken up by the liver and excreted slowly. In such a process some of the ^{117m}Sn would inevitably have been trapped in the red blood cells as it is known that $Sn_3(PO_4)_2$ (which is always part of the commercial redblood-cell kit administered before ^{99m}Tc [16] itself) is trapped inside the red blood cells where

it reduces the Tc(VII). It was, however found in this study that, even after 3 h p.i. >99% of the activity was in the serum. It therefore seemed unlikely that the ^{117m}Sn-PEI-MP complex had dissociated.

The first possibility is conclusively confirmed in the animal tested with the smaller 3-8 kDa fraction of ^{117m}Sn-PEI-MP where the complex is small enough to escape even from intact vasculature resulting in substantial higher bone uptake being recorded (Fig 11-5 and 11-6). Furthermore from Fig 11-2 and 11-5 the shoulder (trabecular bone) to cortical bone ratio can be calculated for the 10-30 kDa as well as the 3-8 kDa fraction. The ratios for the different fractions of ^{117m}Sn-PEI-MP differ, 1.7 for the bigger and 2.6 for the smaller fraction. In the shoulder, high bone turnover takes place and therefore this is a site for preferential localisation of bisphosphonates [17], labelled either with ^{99m}Tc or other radionuclides. The 3-8 kDa section of ^{117m}Sn-PEI-MP is small and therefore this fraction will act as a monomer (phosphonate) and increased uptake in the shoulder is thus expected, while the 10-30 kDa fraction is too large to escape from the intact vasculature at normal bone as well as in the shoulder. The substantial higher shoulder to normal bone ratio for the 3-8 kDa fraction of ^{117m}Sn-PEI-MP resembles the known preferential uptake in joints for ^{99m}Tc- MDP [17]. These observations therefore prove that the blood plasma modelling, suggesting that the Sn(II)-PEI-MP complex remains intact in blood plasma, is indeed correct.

Compared to its ^{99m}Tc-labelled counterpart, the 10-30 kDa ^{117m}Sn-PEI-MP exhibits systemic anomalies regarding its pharmacokinetics and biodistribution, e.g. in the cardiac blood pool and in bone. These anomalies are difficult to explain.

It is known that there is an increased Ca(II) ion concentration at the site of bone remodelling [18]. This will include all growing bone and sites of metastasis. To some extent the blood plasma modelling could be used to gain information in this regard [11]. By varying the Ca(II) concentration artificially, a site of metastasis can be simulated with a Ca(II) concentration 10 or even 100 times of the normal value. From Table 11-2 it is clear that increased Ca(II) concentrations as known to exist at sites of high bone turnover cause the ligand to exclusively be complexed to Ca(II) while a decrease in Ca(II) concentration causes a shift of ligand

complexation towards Mg(II). The Ca(II) concentration also has an impact on the distribution of Sn(II) (Table 11-3). Higher Ca(II) concentration alters the speciation of Sn(II) so that more Sn(II)-histidinate and Sn(II)-cysteinate complexes are formed while the Sn(II)-PEI-MP complexes are reduced. $Sn(OH)_2$ (insoluble) also forms at elevated levels of Ca(II) while lower Ca(II) levels strengthen the Sn(II)-PEI-MP complexes. If the Sn(II)-PEI-MP complex were to pass through a particular microenvironment with higher or lower Ca(II) concentration (e.g. calcified tissue) it might considerably change the species distribution of the complex and therefore alter the biodistribution of these compounds.

Table 11-2: Species distribution (in percentage) of PEI-MP in normal blood plasma at normal, elevated and reduced Ca(II) levels

	Normal Ca(II) levels	**Ca(II) x 10**	**Ca(II) x 100**	**Ca(II) x 0.1**
Ca_2LH	68	84	85	3
Ca_2L	12	15	15	0.5
Mg_2LH	10			57
Sn_2LOH	3	1		3
Mg_2L	2.5			14
LH_2	2			10
LH	1			7
$Sn_2L(OH)_2$	1	0.3		1
L = PEI-MP				

Table 11-3: Species distribution (in percentage) of Sn(II) in normal blood plasma incorporating the ligand PEI-MP at normal, elevated and reduced Ca(II) levels, respectively

	Normal Ca(II) levels	**Ca(II) x 10**	**Ca(II) x 100**	**Ca(II) x 0.1**
M_2(PEI-MP)(OH)	57	15	0.4	63
M_2(PEI-MP)$(OH)_2$	26	7	0.2	29
M(His)OH	7	31	29	3
$M(OH)_2$	5	23	43	2
M(Cys)	3	15	21	1.5
M(His)	0.5	2	2	0.3
M(PEI-MP)	0.5			0.5
M = Sn (II), His = histidine and Cys = cysteinate				

In addition it could be suggested that the longer retention in all compartments and lower bone uptake, of the ^{117m}Sn-PEI-MP 10-30 kDa fraction, in comparison to its ^{99m}Tc-counterpart,

originates from it being a larger molecule. The Sn-presence in both the ^{117m}Sn-PEI-MP and ^{99m}Tc-PEI-MP complexes are comparable, as the Sn/PEI-MP of the ^{99m}Tc-PEI-MP labelling kits [8] and the Sn/PEI-MP ratio of the present preparations are of the same order of magnitude. However, during the ^{117m}Sn-PEI-MP complex preparations, care was taken to keep the tin in the reduced Sn(II) oxidation state, while during the preparation of ^{99m}Tc-labelling kits, and during the labelling process, where the Sn(II) is used as a reductant for Tc, it is unavoidable that some of the Sn(II) will become oxidised to Sn(IV). This, as well as the additional Tc in the complex, may have an effect on the overall charge and molecular conformation of the polymer complex, leading to altered biological behaviour [5].

Bisphosphonates are excellent bone seeking carriers for both tin and technetium and also prevent them from untimely hydrolysis in the blood. It is however likely that following delivery of these complexes to the hydroxyapatite bone matrix, the metals will dissociate from their respective ligands from where they will follow different routes, e.g. with ^{99m}Tc-methyldiphosphonate it is known that the complex dissociates, followed by chemisorption of the phosphonate at the bone mineral and adsorption of technetium at the organic phase of the bone [19]. Tin bisphosphonate species also dissociate near the hydroxyapatite surface, but the tin is transferred from the bisphosphonate environment in solution to the phosphate environment at the hydroxyapatite surface nearby [17]. These arguments as well as the predicted in vivo stability of the Sn-PEI-MP complex [10], suggest that the behaviour of the Sn-complex should be regarded as a more accurate criterium for the in vivo behaviour of the PEI-MP polymer. The previous argument of dissociation with accompanying attachment to blood plasma seems to speak against this although most probably both conditions/reactions occur, resulting in the possibility for different uptake of PEI-MP labelled by Tc or Sn(II).

The blood plasma model predicted [10] that the ^{117m}Sn-PEI-MP complex would not dissociate although the model does not consider the polymer size. Although there is chemically no difference between complexes of smaller and bigger sizes, a difference in biodistribution was recorded for the 3-8 and 10-30 kDa fractions of ^{117m}Sn-PEI-MP. This difference largely proves that the ^{117m}Sn-PEI-MP complex does not dissociate and it is therefore expected that ^{117m}Sn-PEI-MP (10-30 kDa section) remains complexed in blood plasma, circulates in the vasculature from

which it cannot escape due its size until it finds ruptured vasculature. At the location of an osteosarcoma one would expect passive accumulation of the complex through the hyper permeable blood vessels into the tumour, where the complex will dissociate and the Sn(II) be adsorbed onto hydroxyapatite [17] in bone resorption areas within the cancerous area. Ultimate prove of the preferential location of the complex in the tumour should follow from studies on osteosarcoma bearing animal models.

11.5 Conclusion

It is easy to synthesize PEI-MP, purify and fractionate it into variously sized fractions which can readily be labelled with ^{117m}Sn to obtain a labelled product of high radiochemical purity and *in vitro* stability. This in vivo study confirmed the demand for reduced uptake of ^{117m}Sn-PEI-MP by normal bone and kidneys, especially noted for fractions >8kDa. Furthermore the theoretical and now proven indications of in vivo stability of Sn(II)-PEI-MP as well as the potential to exploit the EPR effect due to its macromolecular nature, suggest that ^{117m}Sn-PEI-MP can fundamentally be a promising therapeutic radiopharmaceutical for the treatment of malignant bone diseases, pending proper dosimetry. The anomalies between the pharmacokinetis and biodistribution of 10-30 kDa ^{117m}Sn-PEI-MP and ^{99m}Tc-PEI-MP indicate that it cannot simply be assumed that the in vivo behaviour a polymeric ligand complexed with different metal ions will be identical and therefore cautions that appropriate pre-clinical in vivo experimental work is a prerequisite while *in vitro* studies (such as blood plasma modelling) can assist in reducing the number of animal tests needed.

11.6 Literature

1. **VOLKERT, W.A., HOFFMAN, T.J.** 1999. Therapeutic radiopharmaceuticals. *Chem. Rev.* 99: 2269-2292

2. **ERCAN, M.T., CAGLAR, M.** 2000. Therapeutic radiopharmaceuticals. *Curr. Pharm. Design* 6: 1085-1121

3. **KRATZ, F., SCHÜTTE, M.T.** 1998. Anticancer metal complexes and tumour targeting strategies. *Cancer J.* 11: 60-67

4. **MAEDA, H., WU, J., SAWA, T., et al.** 2000. Tumor vascular permeability and the EPR effect in macromolecular therapeutics: a review. *J. Controlled Release* 65: 271-284

5. **SEYMOUR, L.W.** 1992. Passive tumor targeting of soluble macromolecules and drug conjugates. *Crit. Rev. Ther. Drug Carrier Systems*, 9:135-187

6. **ZEEVAART, J.R., JARVIS, N.V., LOUW, W.K.A., JACKSON, G.E.** 2001. Metal ion speciation in blood plasma incorporating the tetraphosphonate, N,N-dimethylenephosphonate-1-hydroxy-4- aminopropilydenediphosphonate (APDDMP), in therapeutic radiopharmaceuticals. *J. Inorg. Biochem.* 83: 57-65

7. **JARVIS, N.V., ZEEVAART, J.R., WAGENER, J.M., LOUW, W.K.A., DORMEHL, I.C., MILNER, R.J., KILIAN, E.** 2002. Metal ion speciation in blood plasma incorporating the water-soluble polymer, polyethyleneimine functionalised with methylenephosphonate groups, in therapeutic radiopharmaceuticals. *Radiochim. Acta* 90: 237-246

8. **DORMEHL, I.C., LOUW, W.K.A., MILNER, R.J., KILIAN, E., SCHNEEWEISS, F.H.A.** 2001. Biodistribution and Pharmacokinetics of variously sized molecular radiolabelled polyethyleneiminomethyl phosphonic acid as a selective bone seeker for therapy in the normal primate model. *Arzneim.-Forsch./Drug Res.* 51: 258-263

9. **DORMEHL, I.C., SCHNEEWEISS, F.H.A., LOUW, W.K.A., MILNER, R.J., KILIAN, E.** Nov. 2000. Optimalisation of radiolabelled polymin-MP of different molecular sizes as a selective bone seeker for therapy in animal models. Proceedings of the Medical Radiation Physics and Engineering Conference (MeRPE 2000), Lisbon, Portugal.

10. **ZEEVAART, J.R., LOUW, W.K.A., KOLAR, Z.I., WAGENER, J.M., JARVIS, N.V., CLAESSENS, R.A.M.J.** 2003. A thermodynamic approach (using speciation studies) towards the evaluation and design of bone-seeking radiopharmaceuticals as illustrated for ^{117m}Sn(II)-PEI-MP. *J.Radioanal. Nucl. Chem.* 257: 83.

11. **JARVIS, N.V., WAGENER, J.M., JACKSON, G.E.** 1995. Metal ion speciation in blood plasma as a tool for elucidating the in vivo behaviour of radiopharmaceuticals containing ^{153}Sm and ^{166}Ho. *J. Chem. Soc. Dalton Trans.* 1411-1415

12. **ATKINS, H.L., MAUSNER, L.F., SRIVASTAVA, S.C., MEINKEN, G.E., CABAHUG, C.J., D'ALESSANDRO, T.** 1995. Tin-117m(4+)-DTPA for palliation of pain from osseous metastases: a pilot study. *J. Nucl. Med.* 36: 725-729

13. **BOUCHET, L.G., BOLCH, W.E., GODDU, S.M., HOWELL, R.W., RAO, D.V.** 2000. Considerations in the selection of radiopharmaceuticals for palliation of bone pain from metastatic osseous lesions. *J. Nucl. Med.* 41: 682-687

14. **LOUW, W.K.A., DORMEHL, I.C., VAN RENSBURG, A.J., HUGO, N., ALBERTS, A.S., FORSYTH, O.E., BEVERLEY, G., SWEETLOVE, M.A., MARAIS, J., LOTTER, L.G. AND VAN ASWEGEN, A.** 1996. Evaluation of Sm-153 and Ho-166-EDTMP in the normal baboon model. *Nucl. Med. Biol.* 23: 935-940

15. **PETERS, A.M., JAMAR, F.** 1998 The importance of endothelium and interstitial fluid in nuclear medicine. *Eur. J. Nucl. Med.* 25: 801-815

16. **SAHA G.B.** 1997. Fundamentals of nuclear pharmacy, p.p.118-119, Springer Verlag, New York.

17. **CLAESSENS, R.A.M.J., KOLAR, Z.I.** 2000. Affinity of tin(II) and tin(II) diphosphonates for hydroxyapatite: an experimental and model study. *Langmuir* 16: 1360-1367

18. **ZEEVAART, J.R.** 2001. Metal ion speciation in blood plasma as a tool in predicting the in vivo behaviour of potential bone-seeking radiopharmaceuticals. PhD thesis, p.p. 153-156, Delft University Press, Delft

19. **SCHWARTZ, Z., SHANI, J., SOSKOLNE, W.A., TOUMA, H., AMIR, D., SELA, J.** 1993.Uptake and biodistribution of technetium-99m-MD ^{32}P during rat tibial bone repair. *J. Nucl. Med.* 34: 104-108

Chapter 12 - ^{117m}Sn and ^{186}Re Radiolabelling of Polyethyleneiminomethyl Phosphonic Acid (PEI-MP), followed by In Vivo Targeting of Induced Osteosarcoma in Nude Mice

12.1 Aim

Water-soluble polymers are under development as vehicles for systemic drug delivery due to the effect of enhanced permeability and retention whereby neoplastic tissue selectively accumulates macromolecules. The 10-30 kDa fraction of the polymer ^{99m}Tc-PEI-MP previously presented promising biodistribution and pharmacokinetics in primates and dogs and good tumour location in natural canine osteosarcoma. The purpose of this study was therefore to evaluate the labelling of 10-30 kDa PEI-MP with ^{117m}Sn and ^{186}Re, both nuclides with proven therapeutic properties and subsequently to confirm scintigraphically the potential of ^{117m}Sn-PEI-MP as a selective therapeutic bone tumour seeker in Balb C nude mice with induced canine osteosarcoma.

12.2 Methods

^{117m}Sn metal was dissolved in 10M HCl at 60°C under Ar and diluted to 3.3 M with water. PEI-MP (10-30 kDa; 100 mg) was dissolved in 1.2 ml water and 0.2 ml 10 M NaOH. An aliquot containing 2.6 mg Sn was added and the pH adjusted to 6.0. ^{186}Re metal was dissolved in 10 % H_2O_2, evaporated to dryness (80°C), whereafter an aliquot containing 25 µg Re was added to a PEI-MP freeze dried labelling kit (10 mg Na-PEI-MP; 0.5 mg $SnCl_2.2H_2O$) at a pH of 1.0. After incubation at ± 90°C (30 min) the pH was adjusted to 6.0. BALB C nude mice were subcutaneously injected with 5 M cells, cultured from spontaneous canine osteosarcoma, and with high lung metastatic capacity (HPOS). At 4 weeks the tumour bearing mice were injected 75 µCi ^{117m}Sn-PEI-MP and scintigraphy was performed. Organ and tumour counting in a well counter followed.

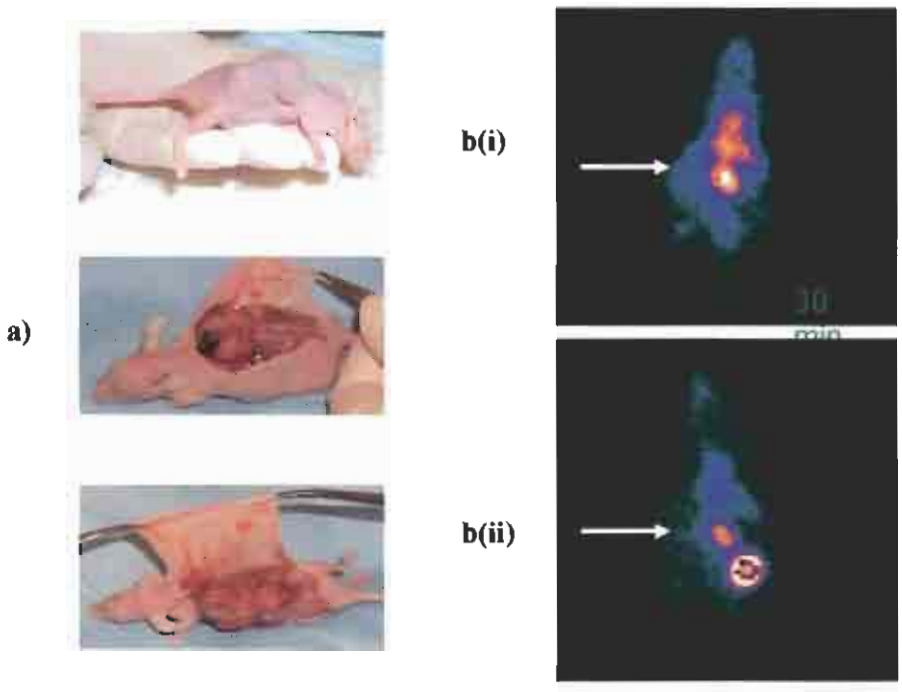

Fig 12-1: (a) A Balb C nude mouse with induced cancer osteosarcoma from the HPOS cell line (b) Scintigraphic images of above osteosarcoma bearing nude mouse at (i) 30 min and (ii) 210 min p.i.

12.3 Results

Both ^{117m}Sn-PEI-MP and ^{186}Re-PEI-MP gave radiochemical purities > 98 % with 1.0 % colloids. For ^{117m}Sn-PEI-MP the respective percentages were constant for one week, while those for ^{186}Re-PEI-MP stayed the same for 48h. Tumour to background uptake within the period of 30-210 min post injection was around 8.0-6.0. Normal bone could not be visualized, but cartilage had similar uptake as the tumour.

12.4 Conclusion

These results indicate that PEI-MP can be labelled successfully with radioisotopes that have proven therapeutic properties. The bone tumour targeting properties of ^{117m}Sn-PEI-MP were also confirmed.

12.5 References

1. **MAEDA, H., WU, J., SAWA, T., MATSUMURA, Y., HORI, K.** 2000. Tumour vascular permeability and EPR effect in macromolecula therapeutics: A review. *J. Controlled Release* 65: 271-284

2. **LOUW, W., DORMEHL, I., MILNER, R.J., SCHNEEWIESS, F., CHARPARRO, F., KILIAN, E., WAGENER, J.** 1998. Biodistribution of radiolabelled polymin-MP of different molecular sizes as a selective bone seeker for therapy in animal models. *Eur. J. Nucl. Med.* 25: 1167

3. **DORMEHL, I.C., LOUW, W.K.A, MILNER, R.J., KILIAN, E., SCHNEEWEISS, F.H.A.** 2001. Biodistribution and pharmacokinetics of variously sized molecular radiolabelled polyethyleneiminomethyl phosphonic acid as a selective bone seeker for therapy in the normal primate model. *Arzneim-Forsch/Drug Res.* 51: 258-263.

4. **LOUW, W.K.A, DORMEHL, I.C., VAN RENSBURG, A.J., HUGO, N., ALBERTS, A.S., FORSYTH, O.E., BEVERLEY, G., SWEETLOVE, M.A., MARAIS, J., LOTTER, M.G., VAN ASWEGEN, A.** 1996. Evaluation of Samarium-153 and Holmium-166-EDTMP in the normal baboon model. *Nucl. Med. Biol.* 23: 935-940.

Chapter 13 - Comparison of Tumour Uptake in Different Types of Osteosarcoma Mice as Studied with the Potential Bone-seeking Radiopharmaceutical, ^{117m}Sn(II)-PEI-MP

13.1 Aim

In the search for a cure for metastatic bone cancer, Sn-117m with its conversion electrons with discrete energies shows little bone marrow toxicity, providing the opportunity to increase the administration dose. Selective accumulation in lesions would capitalise on this advantage. The 10-30 kDa fraction of the water-soluble polymer polyethyleneimine, functionalised with methylene phosphonate groups (PEI-MP) and labelled with Tc-99m, has proved a promising agent for selective uptake into bone tumours (1). From speciation calculations using the ECCLES database it was predicted (2) that Sn(II) will stay bound to the polymer in the blood plasma and therefore should deliver the therapeutic radionuclide Sn(II)-117m to bone with only a slight reticuloendothelial uptake (Fig 13-1). As this was the first blood plasma model that has been compiled for Sn(II), predictions about the behaviour of Sn(II)-117m-PEI-MP in blood plasma were verified with primate tests (3). The biodistribution studies on these healthy animals confirmed these predictions.

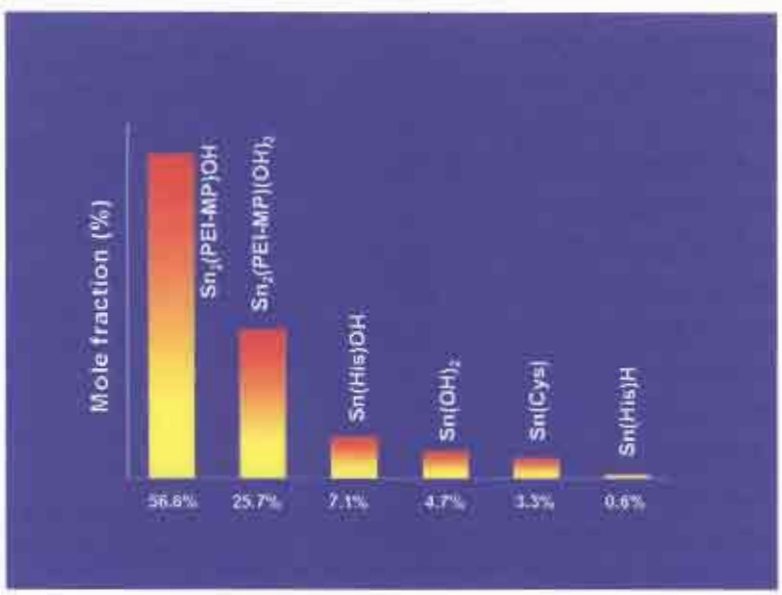

Fig 13-1: Sn(II): Bloodplasma modelling

13.2 Method

To test the tumour selectiveness, tests in nude Balb C mice containing canine osteosarcomas were carried out. HMPOS (fast growing and metastasizing) and POS (slower growing but not per se metastisizing) cells were implanted and the results compared with each other (Fig 12-1 , 13-2).

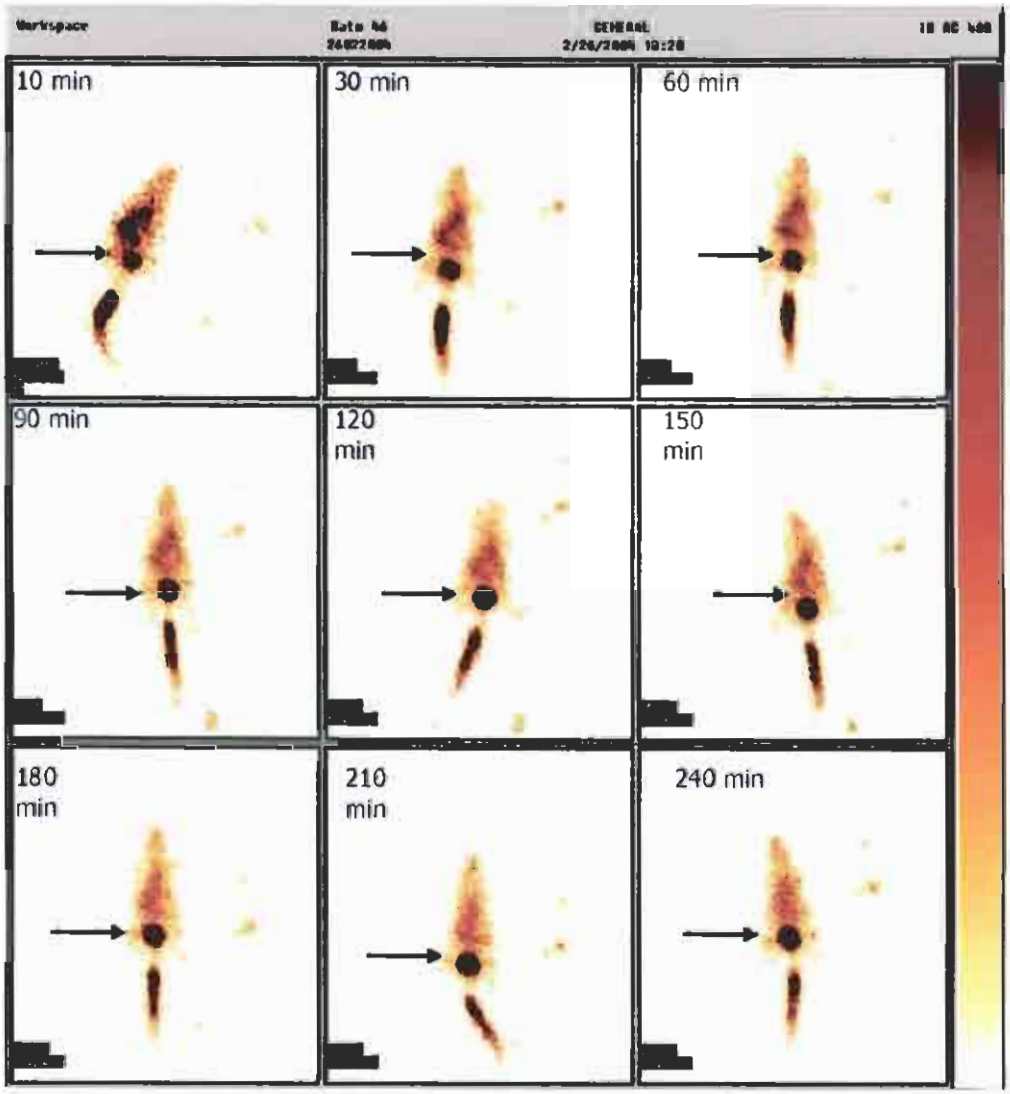

Fig 13-2: Tumour from the POS cell line in a nude mouse scanned at 10 till 240 min p.i. of ^{117m}Sn-PEI-MP (fraction 10-30 kDa)

13.3 Results

Different uptake and wash-out was recorded for the different tumours. Both showed tumour uptake while POS implanted cells retained the activity longer (Fig 13-3 a, b).

13.4 Conclusion

Sn(II)-117m-PEI-MP has potential as a selective bone metastasis and osteosarcoma agent for therapeutic purposes.

a)

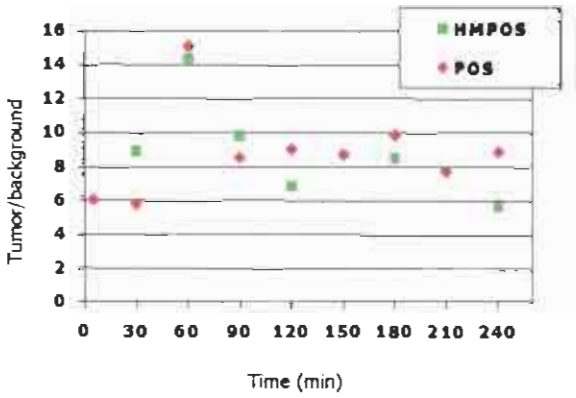

b)

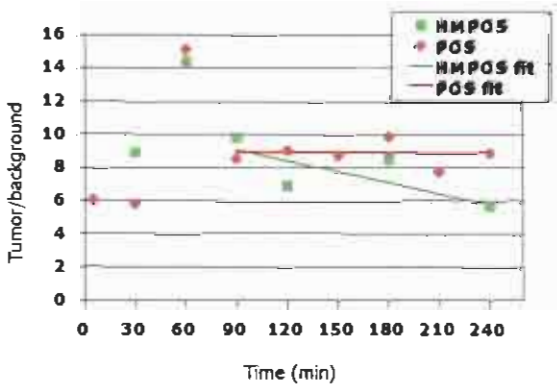

Fig 13-3: (a) Tumour to background ratio of ^{117m}Sn(II)-PEI-MP uptake in POS and HPOS induced tumours (b) Curve fitting of POS and HPOS curves, excluding the uptake phase

13.5 References

1. **DORMEHL, I.C.** et al. 2001. *Drug Res.* 51(1): 258-263.

2. **ZEEVAART, J.R.** et al. 2003. *Nucl. Chem.* 258(1): 83-91

3. **ZEEVAART, J.R.** et al. *Drug Res.* Accepted for publication

Chapter 14 - Discussion

The results following from the investigations presented in chapters 4-13, to a large extent directed the course and progression of the research covered here. In this present chapter the highlights are summarized and additional information not presented in the accompanying papers are shared – information such as clinical application as well as technical spin off's, also information published elsewhere or not yet published, and some results still under scrutiny or in continued research are discussed as work in progress.

14.1 The baboon as a valid experimental animal model

14.1.1 ^{99m}Tc-MDP scintigraphy and bone fracture healing

The radionuclide study described in chapter 4 gives an indication of the degree and extent of operative trauma as well as of the early bone-healing periods in the pre-callus stage (Fig 14-1b) and of bone healing activity in the osteoblastic stage (Fig 14-1d). As seen in the baboon model there was a typical time lapse of 4-6 days before radio activity on the scintigrams relating to bone proliferation was noticeable. This time lapse represents the initial inflammatory stage before new bone formation. Radionuclide uptake on scintigrams was previously showed by Martin to be related to the total regenerative period following a fracture (Martin, 1979). Radioisotope distribution is related to the vascular viability in new bone. In a baseline study of this experiment performed on baboons where bone chips were inserted in the forearm , radioactivity could only be visualized after a time lapse of 3-4 weeks depending on the revascularization of the control material (Mennen *et al.*, 1985). Contrary to radiographic procedures, where the assessment of the bone healing process is quite arbitrary, the radionuclide procedure with the bisphospbonate MDP is a sensitive measure of the processes related to bone healing, and was as such confirmed in this primate study.

Furthermore the profile-evaluation method used uniquely in this radionuclide study allows accurate lesion localization with respect to fixed anatomical points e.g. the elbow and wrist joints. The exact position of the lesion based on the radio-active intensity becomes clear in the later follow-up studies when trauma (i.e. initial inflammatory phase) in the immediate environment had cleared sufficiently. This stage is reached typically on the 7^{th}-10^{th} day, when

it also becomes possible to distinguish fracture radioactivity from 'screw radioactivity', the latter from the fixation plate. Once the activity associated with the line of fracture is determined it is possible to back-track and correlate the early stages of the healing process and thus indicate that the resolution process (i.e. starting at about 21 days) can be linked to a time factor with the initial trauma. This procedure introduces an accuracy of lesion localisation into the nuclear medical study, which would otherwise be difficult. Fig. 14-1 is a schematic representation of normal bone healing based on these studies.

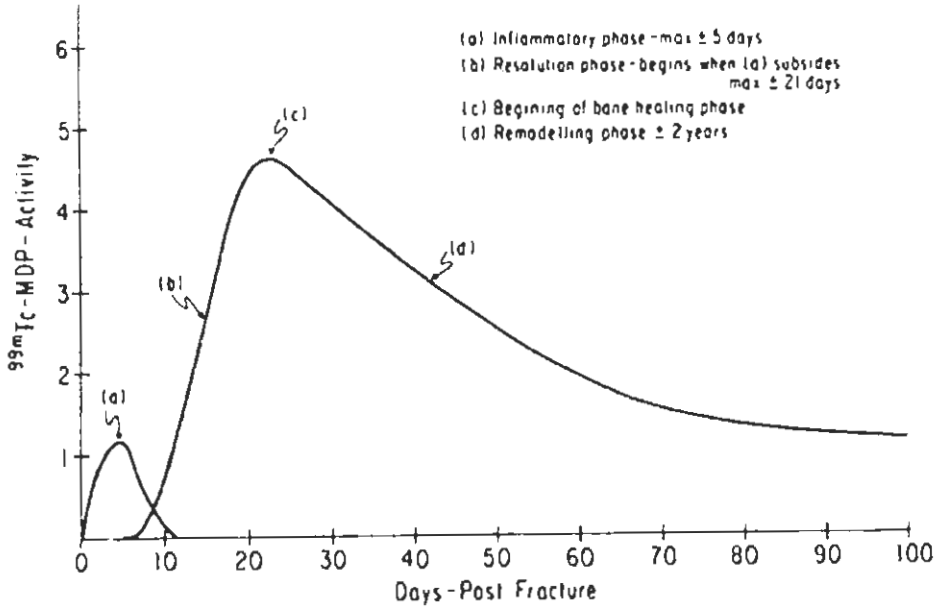

Fig 14-1: Schematic representation of bone healing in a primate model

Nuclear scintigraphy is a useful tool here, based on the profile technique to demonstrate quantitatively (L/N = lesion to normal bone counts) and qualitatively bone healing at any given stage. In practical terms, the clinical application of this technique would require weekly scans between 12-30 days postoperatively in order to demonstrate the radioactivity peak, which is informative in the following way: (i) the higher the peak, the more blood supply to the specific area, and thus more material is available for the healing process (Figs 14-2a and b); (ii) a peak pattern as shown with line (a) in Fig 14-2 indicates a normal bone-fracture healing process; and (iii) a continuous increase of L/N with time during this time interval would indicate that normal bone activity is continuing in an abnormal way, for example in delayed union (Fig 14-2c) or sepsis (Fig 14-2d).

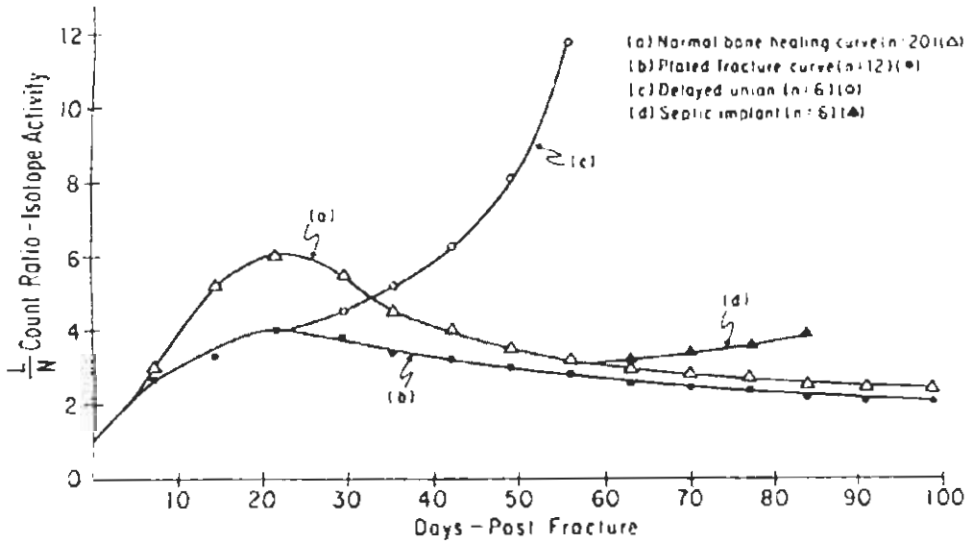

Fig 14-2: ^{99m}Tc-MDP scintigraphy of bone healing in the primate: (a) normal bone-healing curve; (b)plated fracture curve; (c) delayed union; (d) septic union. Note the intense bone healing activity of the normal fracture healing curve

From the ^{99m}Tc-MDP scintigraphic studies of bone fractures the following clinical relevance as far as bone healing is concerned, is deduced: (i) the degree and extent of a lesion to a traumatized bone is determined; (ii) the degree and extent of an operative insult to a bone is shown; (iii) the degree of blood supply to a fracture site and thus the degree of bone-healing activity in the resolution or pre-callus stage is demonstrated by the height of the peak; (iv) the normality of a fracture-healing process is depicted by the shape of the curve; and (v) the time span of the healing process is determined by the duration of technetium activity in a lesion.

Apart therefore from validating the baboon model for its bisphosphonate biochemistry in this investigation clinical relevance also became obvious. In clinical terms, if scans are done at weekly intervals between 12 and 30 days after fracture or postoperatively the pattern of the resulting graph will show much earlier abnormalities in fracture healing (for example delayed or non-union or sepsis) than with conventional radiography. A clinical application would save the patient many unnecessary weeks or months of waiting. For example, non-union of a scaphoid fracture is only detectable on radiography 6-8 weeks after the fracture. Technetium MDP scanning could reduce this time by 50 %.

The results from the studies furthermore contributed to the development of the Mennen plate for fixation in bone fractures (Fig 14-3 a and b)

a)

b)

Fig 14-3 (a) The Mennen clamp-on plate (b) the Mennen clamp-on plate in position on a baboon forearm

14.1.2 Scintigraphic confirmation of appropriate phosphonate pharmacokinetics

Intravenous administered bone-seeking radioisotopic agents distribute via the circulatory system throughout the body while simultaneously accumulating in the bone (Arnold, 1979). The transfer rates of 3.3%/min of the ^{153}Sm-EDTMP from the blood to the bone (Table 5-1) and 2.9%/min from blood to kidney in the baboon study described in chapter 5 resulted in a maximum bone accumulation of 53%, reached after 4 h (Table 5-2). This corresponded with previous results obtained in experimental animals and humans (Goeckler *et al.*, 1987; Turner *et al.*, 1989; Farhanghi *et al.*, 1992; Eary *et al.*, 1993; Bayouth *et al.*, 1994), again confirming that the baboon would be a good model in bone ligand investigation.

From this study a slight washout of ^{153}Sm from the bone with a long half-life of 43, 000 min (Table 5-) was demonstrated. The blood-to-bone transfer rate of ^{166}Ho-EDTMP of 1.3%/min and blood-to-kidney transfer rate of 1.5% is lower than that of ^{153}Sm-EDTMP (Table 5-1), resulting in a maximum accumulation in bone of 45% after 4 h (Table 5-2). There was no washout of ^{166}Ho from bone, resulting in a half-life of infinity (∞) (Table 5-1). Forty-six percent of ^{153}Sm-EDTMP and 54% of ^{166}Ho-EDTMP were excreted in the urine (Table 5-2). The bone-to-background uptake for ^{166}Ho-EDTMP was 69% in comparison to 91% for ^{153}Sm-EDTMP and 95% for ^{99m}Tc-MDP (Fig 5-3).

These results indicate that ^{166}Ho-EDTMP, in comparison to ^{153}Sm-EDTMP, exhibits poorer in vivo biodistribution and pharmacokinetic properties in the baboon model, which contrasts with previous findings in dogs (Appelbaum *et al.*, 1992). A possible reason for the discrepancy between these data and that of Appelbaum *et al.* (Appelbaum *et al.*, 1992) may be related to high plasma citrate levels in the baboon experimental animals. The fact that the ^{166}Ho-EDTMP is a weaker complex (Wagener & Jarvis, 1995) (chapter 5) may account for more transchelation of ^{166}Ho-to-plasma citrate.

Considering the biodistribution and pharmacokinetic imperfections of ^{166}Ho-EDTMP compared to ^{153}Sm-EDTMP, the investigation of a different palliative ^{166}Ho-based bone therapeutic agent with similar biodistribution and pharmacokinetic properties as ^{153}Sm-EDTMP might be an option. The more energetic ß-emissions of ^{166}Ho (with its ~ 8.0 mm max. soft-tissue penetration) could be more efficient for the treatment of large nonossified tumours. These tumours respond poorly to ^{153}Sm-EDTMP owing to the matrix localisation properties of the phosphonates and also due to limited (~3 mm) soft-tissue penetration of the ^{153}Sm ß-emissions (Lattimer *et al.*, 1990 [11]). The half-life of 26.9 h for ^{166}Ho is long enough to eliminate logistic problems, and is sufficient to provide a higher radiation dose rate than ^{153}Sm, which is advantageous for radiotherapeutic treatments (Spencer, 1986; Spencer, 1987; Volkert *et al.*, 1991).

The results in chapter 5 which yielded additional information on holmium's possible use are important. Both ^{153}Sm and ^{166}Ho are lanthanides that easily form EDTMP complexes with a high radiochemical purity. The role of ^{153}Sm-EDTMP is already established and it is confirmed as a therapeutic agent for treatment of painful skeletal metastases. This comparative study of ^{153}Sm-EDTMP and ^{166}Ho-EDTMP in the baboon model reveals, despite

their similar chemical characteristics, a significantly inferior performance of ^{166}Ho-EDTMP with regard to bone localisation, biodistribution and pharmacokinetics. Pursuing clinical trials on humans with ^{166}Ho-EDTMP is therefore perhaps not justified. However, the development of more suitable bone-localising ligand(s) for ^{166}Ho, as for that matter for other radionuclides, should be seriously considered. Furthermore, ^{166}Ho labelled compounds for radionuclide synovectomy and therapy of non osseous tumours do find application (Melichar *et al.*, 2004).

Palliation of bone pain in patients with bone metastases after repeated application of the radioligand as might become necessary was often found to be progressively less effective. The question arises whether EDTMP exerts a blocking function, limiting its access to bone or osseous tumours with successive administration.

Two principle factors lead to the accumulation of radiopharmaceuticals in bone. These are blood flow and extraction efficiency (Garcia & Mettler, 1988). An additional factor to consider is capillary permeability (Garcia & Mettler, 1988). In an important review (Lin, 1996) of bisphosphonates used for senile osteoporosis it was reported that the incubation of the bisphosphonate alendronate with human bone particles resulted in rapid, reversible and saturable bonding. Alendronate is an aminobisphosphonate which has higher antiresorbing activity than the bisphosphonate etidronate which has no amino group (Lin, 1996). EDTMP is a multidentate aminophosphate ligand (Lin, 1996) which localizes in bone by bridging hydroxyapatite (Holmes, 1993) and can therefore be presumed to similarly participate in saturable bonding which could influence the extraction efficiency of the ligand during multiple applications.

A phenomenon of partial blocking indeed appears present in the primate study of chapter 6, with the low EDTMP concentration, as can be seen from the reduced ^{153}Sm-EDTMP uptake in the bone with repeated applications (Fig 14-4). The effect reached statistical significance only after the third application at 13 weeks ($p < 0.02$). Furthermore already at the first application (0 weeks) of the high concentration of EDTMP a lower bone uptake was observed when compared to the lower concentration probably pointing to a blocking phenomenon by the high concentration of the EDTMP. The 0-week values of the high concentration do not show much change with repeated applications. It can be speculated that continual application of EDTMP, especially at high concentration, will lead to reduced calcium serum levels increasing parathyroid hormone concentrations (Lin, 1996;

Percherstorfer *et al.*, 1993) which in turn might trigger osteoblastic activity and some bone remodelling, thus partially offsetting the blocking which was consequently more clearly illustrated at the low EDTMP concentration (Hortobagyi *et al.*, 1984; Cloleman *et al.*, 1988). To avoid a blocking effect during palliative treatment of patients with skeletal metastases the use of the higher concentration EDTMP ligand could be recommended but care should be taken to avoid adverse renal effects.

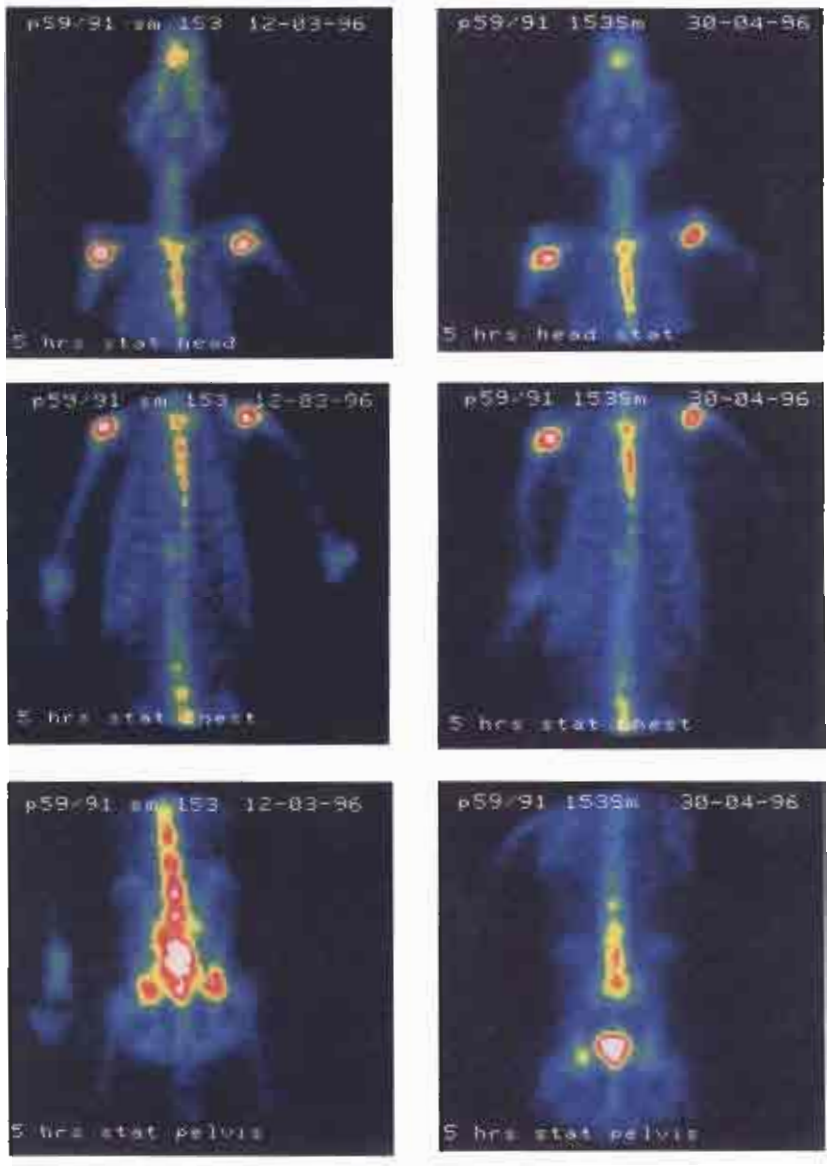

Fig 14-4: Comparative (a) head, (b) chest and (c) pelvic images in the same animal taken at 0 weeks (left) and 6 weeks (right) of administration of ^{153}Sm-EDTMP, already indicating reduced uptake, i.e. a partial blocking effect

14.2 A novel bisphosphonate ligand

14.2.1 The scientific reasoning

The prospects of obtaining new, more effective and more potent medicines have been greatly facilitated by polymer technologies. The use of natural and synthetic polymers as drug delivery vehicles is now well established (Alexander, 2001).

There is also considerable interest in the development of water-soluble polymers to conjugate therapeutic drugs and proteins. While there are other applications for soluble polymers that are currently being examined, conjugation of a bioactive agent to a polymer has been a focus of research for many years and extensively discussed (Godwin *et al.*, 2001).

Conjugation of a proper (i.e., biocompatible) polymer with a drug has become universally accepted, because the polymer confers improved pharmacokinetic characteristics on the original low-molecular-weight active agent (e.g. parent anticancer drug), the latter which has many disadvantages. Such active principles range from cisplatin derivatives to peptides, alkaloids, proteins (e.g., neocarzinostatin), and enzymes (L-asparaginase, xanthine oxidase etc.) (Maeda *et al.*, 2001).

The scope for synthetic polymers in drug delivery applications is exceptionally wide, with a vast array of clinical conditions that require selective targeting of therapeutic agents to particular biological targets (Alexander, 2001).

A key factor in the success of polymer-based cancer therapies is the unique blood vasculature within solid tumours. Compared with the blood vessels in normal tissues, those of growing tumours are frequently more 'leaky' to circulating macromolecules and large particles, allowing them easier access to the tumour's interior. Whereas normally these macromolecules would quickly drain away back to the circulatory system, tumour tissues with lack of a lymphatic system effectively trap them and prevent their escape. This so called enhanced permeability and retention (EPR) effect was discovered in 1986 by Hiroshi Maeda at the University of Kumamoto in Japan, and is a major route to enhanced delivery of

macromolecular cancer therapeutics. Maeda himself exploited the effect in developing Smancs (Maeda *et al.*, 2001; Driscoll, 2000).

In this manner the accumulation and retention of macromolecules and lipidic particles are greatly enhanced in tumour tissue compared with those in normal tissue (Maeda *et al.*, 2001). Plasma residence time (and hence plasma concentration) is the primary driving force for continued tumour accumulation of macromolecules (Duncan *et al.*, 2001). This effect is applicable only to macromolecules and lipidic particles, not to low-molecular-weight compounds, the category to which most drugs in use today belong (Fig 14-5).

The EPR effect is also observed around the periphery of the tumour, i.e., in normal tissues surrounding the tumour, because of the variety of vascular mediators found there. Polymeric drugs may however be cleared more rapidly from normal tissue via lymphatic drainage (Maeda *et al.*, 2001).

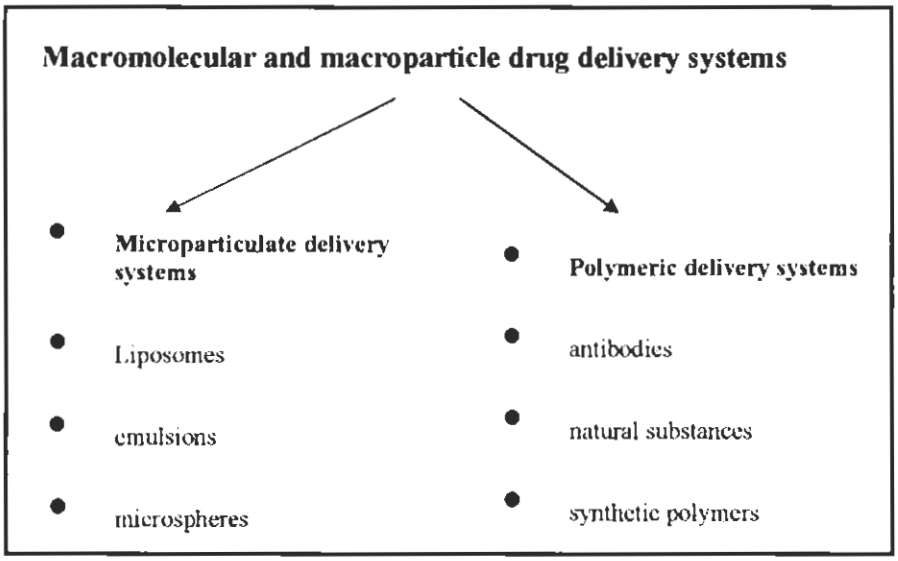

Fig 14-5: Macromolecular and macroparticle drug delivery systems

All of these data seem to indicate that tumour vasculature can be an ideal target for tumour-selective delivery of macromolecular anticancer agents (Maeda *et al.*, 2001).

An ideal pharmaceutical for the treatment of neoplastic and inflammatory (benign) bone disease would be a compound that predominantly accumulates in bone lesions with limited access to normal bone and other organs. Polyethyleneiminomethyl phosphonic acid (PEI-

MP), (the synthesis of which is discussed in chapter 7) is a bone (hydroxyapatite) seeking bisphosphonate, and belongs to the family of compounds of which some are clinically in use for the treatment of various bone pathologies (Fig 14-6) (Lin, 1996). Due to the macromolecular character of PEI-MP allowing selection of different molecular sizes and thus selective accumulation in inflammatory and neoplastic areas (EPR-effect), PEI-MP may exhibit some important advantages above its low-molecular-weight counterparts. Furthermore its affinity for Ca^{2+} (Jarvis *et al.*, 2002) and collagen (Milner, personal communication), may add to PEI-MP being trapped in inflammatory areas and in tumours.

14.2.2 The effect of molecular size and electric charges on the ligand

Molecular sizing of the polymeric PEI-MP can drastically alter its biodistribution and pharmacokinetic properties (Dormehl *et al.*, 2001), and this can be exploited to suit different applications and targeting of specific organs, tissues and pathological affected areas.

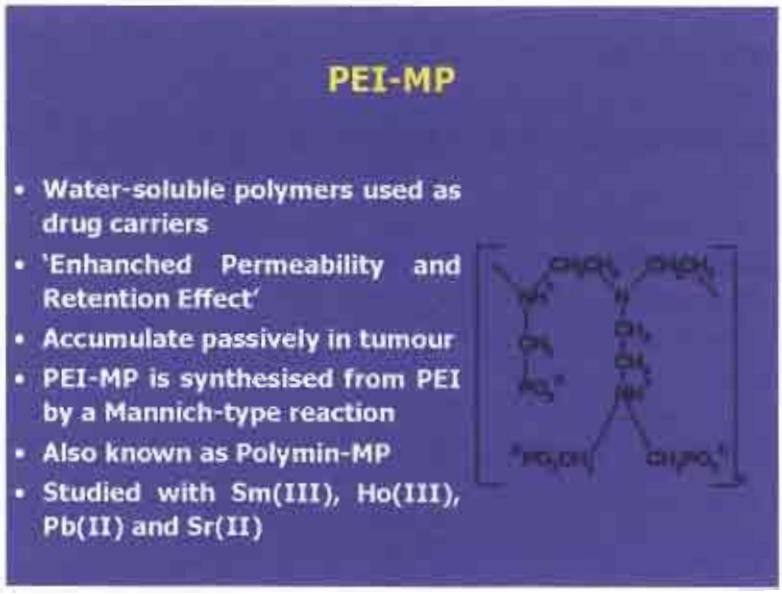

Fig 14-6: Polyethyleneiminomethylphosphonic acid (PEI-MP) – rationale; synthesis, structure.

Due to the ease by which PEI-MP can be labelled with the diagnostic radionuclide ^{99m}Tc (Dormehl *et al.*, 2001) (chapter 7) its pharmacokinetics, including localisation and biodistribution could be scintigraphically studied.

Increasing the sizes of the macromolecules of ^{99m}Tc-labelled PEI-MP resulted in marked changes in their biodistribution (Table 7-2). In normal bone of the primate model there was almost complete exclusion (< 1 %) of the particles larger than 100 kDa. The highest relative skeletal uptake of 18 % was demonstrated by the 10-30 kDa fraction (Table 7-2), but this is still considerably lower than that known for ^{153}Sm-EDTMP (> 50 %) (Zeevaart *et al.*, 2003).

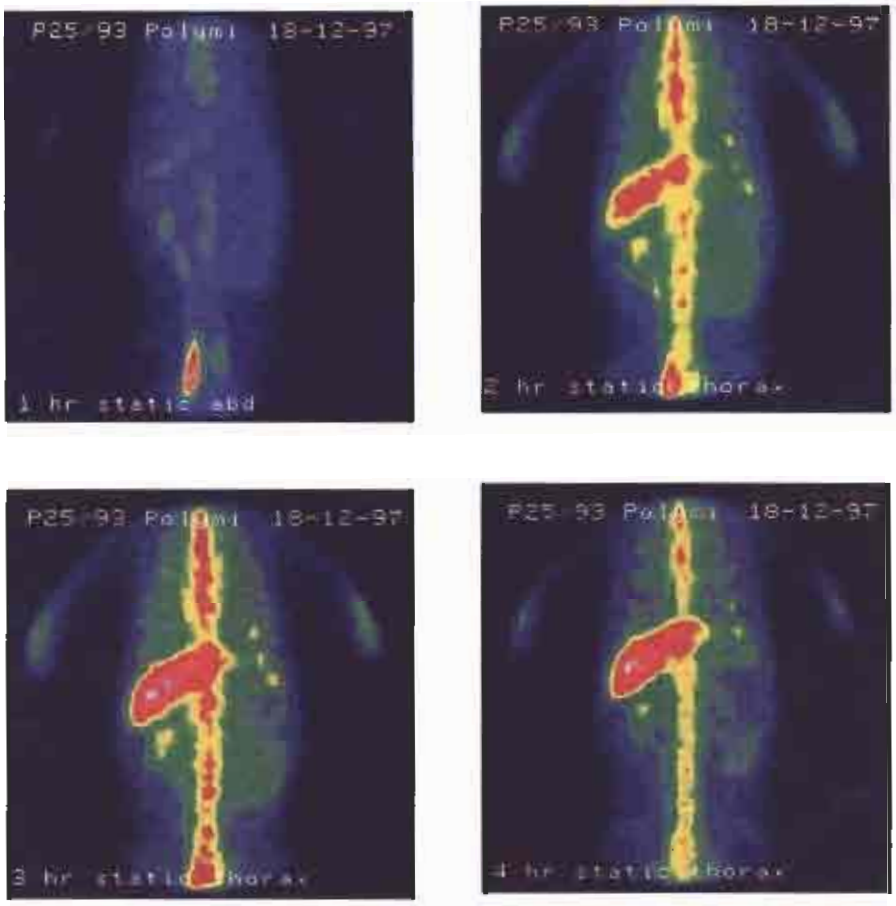

Fig 14-7: Scintigrams at 1-4 hours of the baboon thorax after administration of ^{99m}Tc-PEI-MP (10-30 kDa), showing comparable uptake in bone(spine) and the liver on a scale of brightness relative to the maximum (white and red is maximum radioactivity vs blue as the minimum)(compare Table 7-2)

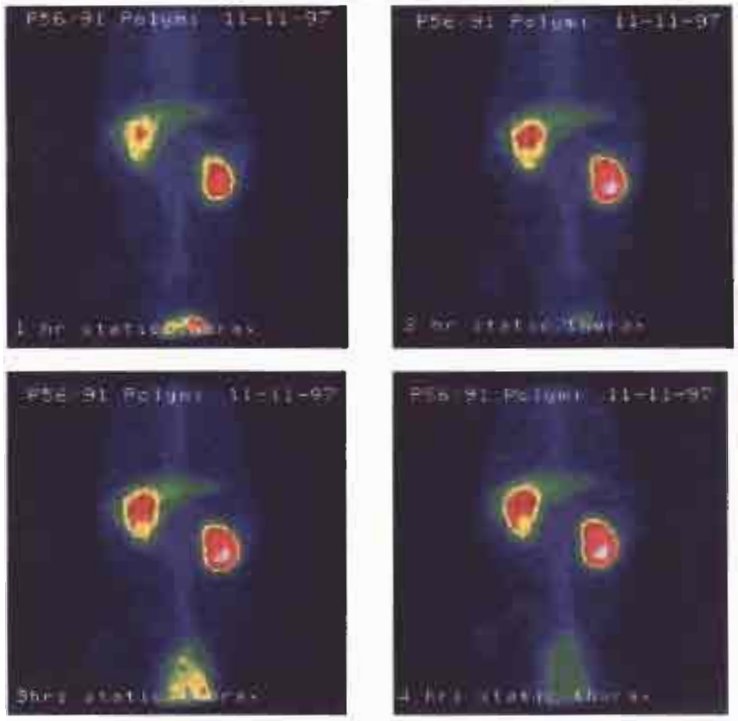

Fig 14-8: Scintigrams at 1-4 hrs of the baboon thorax p.i. of ^{99m}Tc-PEI-MP (30-50 kDa), showing intense activity in the kidneys, with very little in the skeleton (white and red represent high, blue represents low activity).

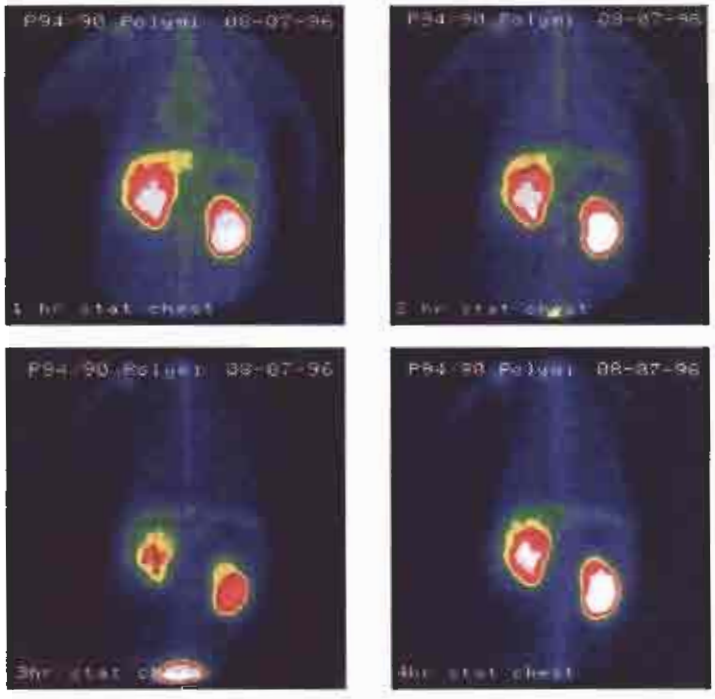

Fig 14-9: Scintigrams at 1-4 hours of the baboon thorax p.i. of ^{99m}Tc-PEI-MP (3-10 kDa) showing intense kidney uptake (white and red represents high, and blue low activity).

This study confirmed successfully the reduced normal bone uptake of ^{99m}Tc-PEI-MP, especially noted for fraction 100-300 kDa. Although the bone uptake value obtained for 10-30 kDa is by comparison more than double that for the other fractions (Table 7-2), some accumulation in bone is necessary in an osseous tumour where it would be beneficial to maximize duration of radiation (Fig 14-7).

To further optimise the molecular size of the macromolecule for its selectivity towards neoplastic and inflammatory diseased areas, potentially harmful kidney and liver uptake should be minimized. This would immediately exclude the fractions with sizes larger than 50 kDa because of liver exposure. Of the smaller fractions, 30-50 kDa and 3-10 kDa seem to leave especially the kidneys vulnerable to radiation exposure (Table 7-2) (Fig 14-8, 14.9).

It seemed that the fraction 10-30 kDa could optimally fit required criteria with relatively low accumulation in normal bone, but with some bone retention indicated. Access into a lesion which depends on the degree of vascular disruption could be fairly early for this fraction because of its relatively small molecular size. The liver and kidney also seemed to enjoy most protection with this fraction (Fig 14-7).

The uptake of 100-300 kDa PEI-MP (chapter 8) in bony lesions, e.g. the osteosarcoma in the Dalmation, which participated in a canine study, was clear from the images with very little normal bone participation. Even better tumour uptake is obtained with the 3-10 kDa fraction ranging from 9: 1 to 11: 1 with respect to normal bone than was obtained with 10-30 kDa (4: 1) (Fig 14-10). This was a preliminary finding during an experimental run on dogs which were intended for conventional treatment for naturally occuring apendicular osteosarcomas.

Differences in the in vivo behaviour of the various size fractions were observed, because of these molecular size variations, but also because of the ionic charges they carried. In the liver, lung and cardiac blood pool the uptake/retention decreased with a decrease in molecular size, with the negatively charged molecules of a particular size throughout tending to higher uptake and slower washout than the positively charged ones. The opposite behaviour was observed in the bone, with higher uptake of the smaller fractions, more so for negatively charged molecules of especially the 30-50 kDa fraction. No uptake or retention of the large negative fraction was observed in the kidney while for the other fractions there was a higher uptake/retention for the positive fractions, even influencing the effect of size (Fig 14-11 a-e).

Charge changes were achieved by passing the macromolecules through different ion-exchange columns (DEAE-Sephadex and CM-Sephadex).

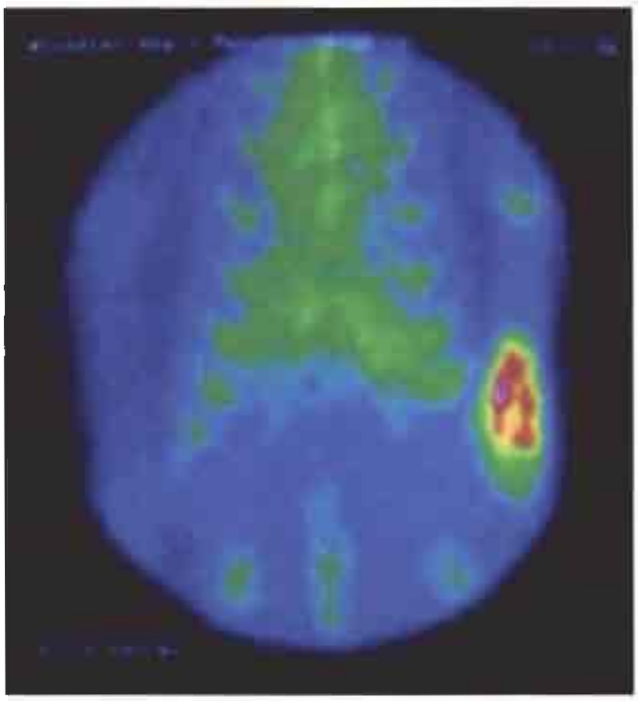

Fig 14-10: High tumour (left forelimb) uptake of the 3-10 kDa fraction of ^{99m}Tc-PEI-MP in a dog with spontaneous osteosarcoma.

These results obtained from a study on dogs (Dormehl *et al.*, 2004) indicate that by manipulation of the molecular size and charge of polymeric delivery vehicles for radionuclides, their in vivo behaviour can be directed e.g. to avoid radiosensitive non-target organs or tissues, which also allows more freedom with increasing therapeutic dosages.

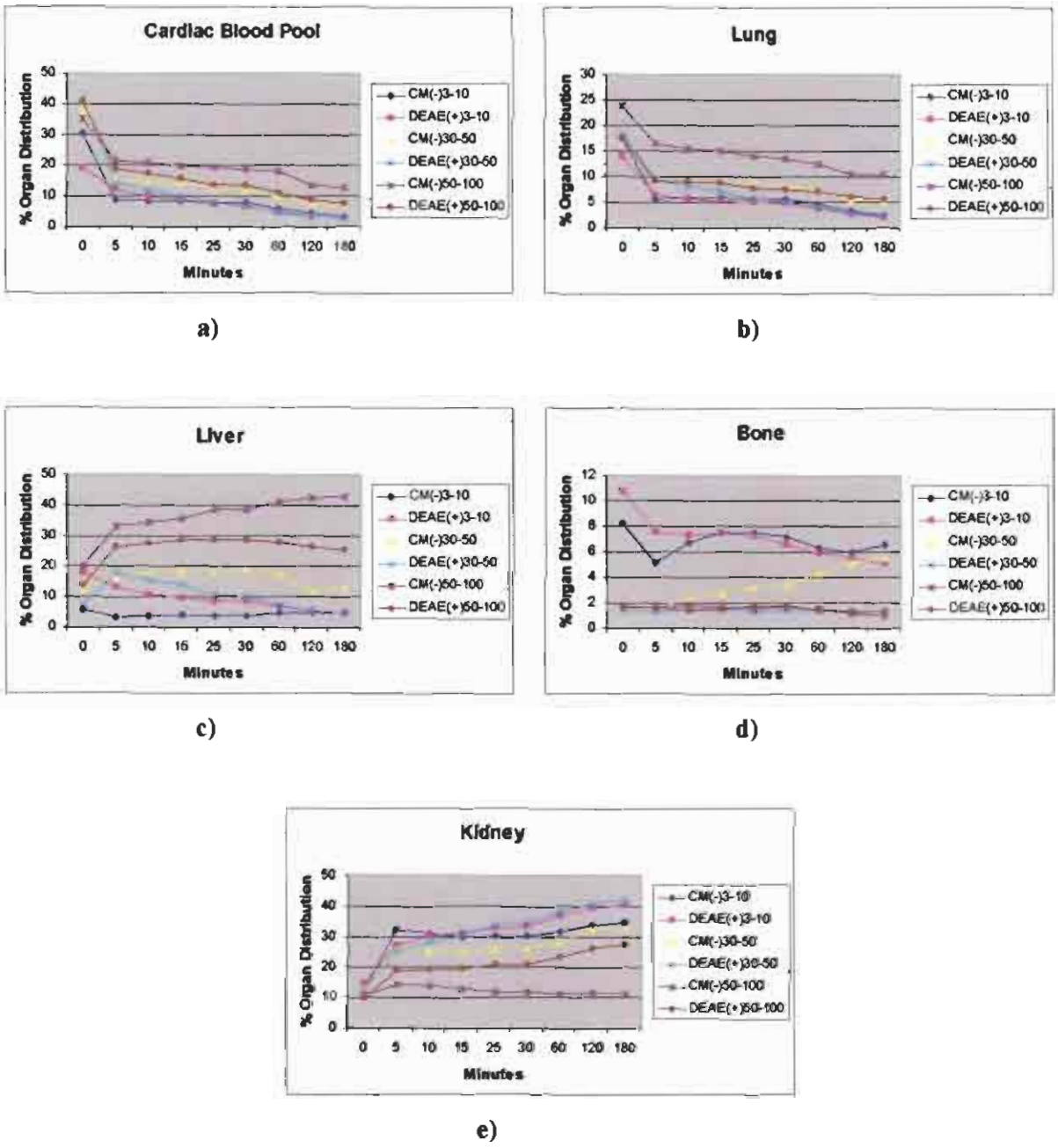

Fig 14-11: Percentage organ distribution curves obtained from dogs of ^{99m}Tc-PEI-MP indicating uptake/washout/retention of the size fractions 3-10, 30-50 and 50-100 kDa, carrying negative (CM), or positive (DEAE) charges in (a) cardiac bloodpool, (b) lung, (c)liver, (d) bone, (e) kidney

14.2.3 Labelling of PEI-MP for therapeutic purpose

14.2.3.1 Metal ion speciation in blood plasma to select potential bone seeking radiopharmaceuticals

The next step, once an optimal size was found, was to label PEI-MP (10-30 kDa) with therapeutic ß-emitting radionuclides such as ^{153}Sm or $^{186/188}$Re, and to investigate pharmacokinetics and therapeutic efficacy of the labelled ligands in osseous tumour bearing animal models.

To evaluate and facilitate informed selection of a therapeutic radionuclide for delivery to metastatic bone tumours by PEI-MP, a blood plasma model for speciation of components in blood plasma was constructed including PEI-MP. Such a blood plasma model, ECCLES (Zeevaart *et al.*, 2003) predicts the speciation of metal ions in plasma, which gives an indication of the capability of the radiopharmaceutical to survive competition for the radionuclide by other blood plasma ligands. This is the first time that a polymer had been included using the ECCLES code (chapter 9).

Therapeutic ß-particle emitting radionuclides under consideration were ^{153}Sm, ^{166}Ho, ^{89}Sr, $^{186/188}$Re, and from previous studies the Auger electron emitter ^{117m}Sn (Zeevaart *et al.*, 2003). A detailed description of the rationale and calculations of chemical speciation in blood plasma can be found in Metal ion Speciation in Blood Plasma as a Tool in Predicting the in vivo Behaviour of Potential Bone-Seeking Radiopharmaceuticals (Zeevaart, 2001).

Blood plasma speciation (computer simulation with ECCLES) as applied in chapter 9 explained the results obtained with ^{153}Sm-EDTMP, ^{166}Ho-EDTMP, and ^{153}Sm-PEI-MP as well as ^{117m}Sn-PEI-MP from in vivo animal studies (chapter 11).

The computer simulation, together with adsorption studies, may now be regarded as screening methods for radioligands before pre-clinical and clinical trials. This research is useful because it allows timeous rejection of such radioligand combinations which do not have good in vivo prospects. In this case it did suggest that ^{117m}Sn(II)-PEI-MP might be an improvement on ^{117m}Sn-DTPA and ^{117m}Sn(II)-HEDP, as PEI-MP was found to be a better carrier of ^{117m}Sn(II)

in blood plasma. The complex redox chemistry of Re makes potentiometry, which is needed for the apparent formation constants to be entered into the model, unreliable for this metal. The chemistry of Re and Tc is however very similar, and ^{99m}Tc-PEI-MP amply demonstrated good in vivo behaviour. This encouraged the investigation of the prospects of $^{186/188}$Re-PEI-MP, and also ^{117m}Sn(II)-PEI-MP as therapeutic radiopharmaceuticals, once proper labelling was reached (chapter 10).

14.2.3.2 In vivo evaluation of ^{117m}Sn(II)-PEI-MP in the normal primate

Initial labelling attempts of PEI-MP with ^{186}Re proved problematic, which delayed its application as a possible radiotherapeutic agent in animal studies. The early successes with ^{117m}Sn(II) labelling of the PEI-MP ligand expedited the primate studies to investigate the in vivo behaviour of ^{117m}Sn(II)-PEI-MP (Yang *et al.*, 2005).

In the search for a cure for metastatic bone cancer, ^{117m}Sn with its conversion electrons and low energy photons (half-life 13.6 days), shows little bone marrow toxicity, providing the opportunity to increase the administered dose (Spencer, 1986) (chapter 11). Selective accumulation in lesions would gain from this advantage.

Furthermore using speciation calculations, it was predicted that the Sn(II)-PEI-MP complex would remain intact in the blood plasma, which was a positive indication for animal experiments to continue.The chemical properties of this labelled compound should be such that an in vivo stability is assured, while the species that predominantly forms in vivo remains charged, since neutral species could lead to colloids with subsequent liver uptake (Zeevaart *et al.*, 2001; Jarvis *et al.*, 2002).

The baboons for the experiments (chapter 11) were subjected to identical experimental procedures except for the mentioned differences in molecular sizes of the injected ^{117m}Sn-PEI-MP and three different size fractions were studied, viz. in the following ranges (1) 3-8 kDa, (2) 8-10 kDa, (3) 10-30 kDa. This last fraction was of special interest, since it ideally suited the characteristics sought for an optimal therapeutic agent as gathered from data on ^{99m}Tc-PEI-MP in primate models (Dormehl *et al.*, 2001).

In comparison to the ^{117m}Sn-PEI-MP 3-8 and 8-10 kDa fractions, the larger 10-30 kDa ^{117m}Sn-PEI-MP exhibits a prolonged retention in all compartments, together with low bone uptake and a reduction in urinary excretion, as can be expected from its larger hydrodynamic volume and its resultant slower diffusion through the endothelium and the decrease in renal excretion rate.

Compared to its ^{99m}Tc-labelled counterpart, the 10-30 kDa ^{117m}Sn-PEI-MP exhibits systemic anomalies regarding its biodistribution, e.g. in the cardiac blood pool and in bone. These anomalies are difficult to explain, but varying the radiolabel of a specific ligand is known on occasion to have changed the biokinetics (see chapter 11). Amongst others it could be suggested that the longer retention in all compartments and lower bone uptake of the ^{117m}Sn-PEI-MP 10-30 kDa fraction originate form it being a larger molecule in comparison to its ^{99m}Tc-counterpart. It must be noted that the latter also contains Sn (not radioactive) of comparable concentrations for redox purposes (Yang *et al.*, 2005). The anomalies between the pharmacokinetics and biodistribution of 10-30 kDa ^{117m}Sn-PEI-MP and ^{99m}Tc-PEI-MP indicate that it cannot simply be assumed that the in vivo behaviour a polymeric ligand complexed with different metal ions will be identical and it therefore cautions that appropriate pre-clinical in vivo experimental work is a prerequisite while *in vitro* studies (such as blood plasma modelling) can assist in reducing the number of animal tests needed.

14.3 Osteosarcoma bearing nude mice and normal Wistar rats

14.3.1 Comparison between pharmacokinetics of ^{99m}Tc- and ^{117m}Sn(II)-PEI-MP

The above in vivo primate study confirmed reduced uptake of ^{117m}Sn-PEI-MP by normal bone and kidneys, especially noted for fractions > 8kDa. Furthermore the theoretical and now proven indications of in vivo stability of Sn(II)-PEI-MP as well as the potential to exploit the EPR effect due to its macromolecular nature, suggest that ^{117m}Sn-PEI-MP can fundamentally be a promising therapeutic radiopharmaceutical for the treatment of malignant bone diseases, pending proper dosimetry, which could be studied in osteosarcoma bearing nude mice.

In turning to rodent studies at this stage to confirm scintigraphically the potential of ^{117m}Sn-PEI-MP (10-30 kDa) as a therapeutic tumour seeker two aspects demanded attention: firstly an appropriate osteosarcoma model should be available, and in addition some normal rodent biodistribution and pharmacokinetic studies, preferably with ^{99m}Tc-PEI-MP and ^{117m}Sn(II)-PEI-MP for rodent control information should be performed.

The choice of normal Wistar rats as controls stemmed from easier scintigraphy for biokinetic information of the larger animals, leading to better statistics (Dormehl *et al.*, 2001). Two groups of six normal rats each were injected with 300-350 mCi of ^{99m}Tc-and ^{117m}Sn-PEI-MP respectively and scintigraphically studied. The target organs for both radiopharmaceuticals were found to be kidney and bladder. From organ counting in a well counter the maximum uptake at 4 hrs was highest for the bladder wall, 18 % ID/g for ^{99m}Tc-PEI-MP, and 8 % ID/g for ^{117m}Sn-PEI-MP.

The delayed retention in the circulation of ^{117m}Sn-PEI-MP vs ^{99m}Tc-PEI-MP seen in this study agrees with the observation in the normal primate studies. The high uptake of ^{117m}Sn-PEI-MP in the bladder wall is disturbing.

The osteosarcoma bearing nude mice (Balb C) were subcutaneously injected with 5 x 10^6 cells cultured from spontaneous canine osteosarcoma; in the one case these cells had high lung metastatic capacity (HPOS), alternatively the cells were without this capacity (POS).

Different uptake and washout of ^{117m}Sn-PEI-MP were recorded from the different cell lines. Both showed tumour uptake, but the tumours from the POS implanted cells retained the activity longer (Fig 13-3 a and b). The tumour to background ratios ranging between 14 and 6 during the period 60-240 min p.i. indicate that ^{117m}Sn(II)-PEI-MP has potential as a selective osteosarcoma therapeutic agent.

14.3.2 Work in progress

The therapeutic efficacy of ^{117m}Sn(II)-PEI-MP for osteosarcoma and more important bone metastasis has yet to be proven. More research is however needed towards a more suitable model for osteosarcoma, preferably from a human osteosarcoma cell line. The alternative of

using ^{186}Re-PEI-MP which meanwhile has been successfully labelled and which would be clinically and logistically easier to use should also be explored. These challenges are presently being addressed in continuing research. It is however certain that the ligand PEI-MP is a adequate carrier of radiotherapeutic nuclides to bone, and because of its flexibility for modification of molecular size most probably also to other areas of neoplastic and inflammatory disease.

The intention however of changing and improving the biokinetics of common polyphosphonates by changes in the complex structures is one extensively being studied by various groups notably the group of Markus Mitterhauser from the Medical University of Vienna (Mitterhauser *et al.*, 2004). Exact mechanisms involved in bone uptake of labelled polyphosphonates is still highly speculative. Possible explanations for the process of uptake range from simple chemisorption onto the osseous surface over incorporation, into the mineralization process to a combination of both. Other factors such as solubility of the complex, calcification of the ligand, transchelation to the bone hydroxyapatite matrix, effects of the radionuclide could also be parameters influencing bone uptake which should be well researched. What seems clear is that binding of bone seekers is irreversible and takes place on the mineral matrix and very little on collagen. It is important that preparation and labelling methods should be well thought through and carefully handled in the laboratory in order to have a scientifically sound and reproducible product.

14.4 References

ALEXANDER, C. 2001. Synthetic polymer systems in drug delivery. *Expert Opin. Emerging Drugs* 6(2): 345-363.

APPELBAUM, F.R., BROWN, P.A., SANDMAIER, B.M., STORB, R., FISHER, D.R., SHULMAN, H.M., GRAHAM, T.C., SCHUENING, F.G., DEEG, H.J., BIANCO, J.A., KETRING, A.R., KAPLAN, D. 1992. Specific marrow ablation before marrow transplantation using an aminophosphonic acid conjugate ^{166}Ho-EDTMP. *Blood* 80: 1608-1613.

ARNOLD, J.S. 1979. Kinetic analysis of bone imaging agents. In: *Principles of Radiopharmacology.* Vol. III (Edited by Colobetti L.G.), PP. 205-223. CRC Press, Boca Raton, FL.

BAYOUTH, J.E., MACEY, D.J., KASI, L.P., FOSELLA, F.V. 1994. Dosimetry and toxicity of samarium-153-EDTMP administered for bone pain due to skeletal metastases. *J. Nucl. Med.* 35: 63-69.

COLEMAN, R.E., MASHITER, G., WHITACKER, K.B. 1988. Bone scan flare predicts successful systemic therapy for bom metastasis. *J. Nucl. Med.* 29: 1354-1359.

DORMEHL, I.C., LOUW, W.K.A., KILIAN, E., SCHNEEWEISS, F.H.A. The importance of molecular size and charge in designing polymeric radiopharmaceuticals to target neoplastic disease in therapy. The 33rd Annual Meeting of the European Society for Radiation Biology, Aug 25-28, 2004, Budapest.

DORMEHL, I.C., LOUW, W.K.A., MILNER, R.J., KILIAN, E., SCHNEEWEISS, F.H.A. 2001. Biodistribution and Pharmacokinetics of variously sized molecular radiolabelled polyethyleneiminomethyl phosphonic acid as a selective bone seeker for therapy in the normal primate model. *Arzneim.-Forsch./Drug Res.* 51: 258-263.

DRISCOLL, R. 2000. Stealth drugs take off. *Chemistry in Britain* 48-49.

DUNCAN, R., CAC-BRETON, S., KEANA, R., MUSILA, R., SAT, Y.N., SATCHI, R., SEARLE, F. 2001. Polymer drug conjugates, PDEPT and PELT: basic principles for design and transfer from the laboratory to clinic. *J. Controlled Release* 74: 135-146.

EARY, J.F., COLLINS, C., STABIN, M., VERNON, C., PETERSDORF, S., BAKER, M., HARTNETT, S., FERENCY, S., ADDISON, S.J., APPELBAUM, F., GORDON, E.E. 1993. Samarium-153-EDTMP biodistribution and dosimetry estimation. *Journal of Nuclear Medicine* 34: 1031-1036.

FARHANGHI, M., HOLMES, R.A., VOLKERT, W.A., LOGAN, K.W., SINGH, A. 1992. Samarium-153-EDTMP: Pharmacokinetic, toxicity and pain response using escalating dose schedule in treatment of metastatic bone cancer. *Journal of Nuclear Medicine* 33: 1451-1458.

GARCIA, J.F., METTLER, F.A. 1988. Radionuclide and bone imaging densitometry, Churchill Livingston, New York

GODWIN, A., BOLINA, K., CLOCHARD, M., DINKAND, E., RANKLIN, S., SIMIC, S., BROCCHINI, S. 2001. New strategies for polymer development in pharmaceutical science – a short review. *J. Pharmacy and Pharmacology* 53: 1175-1184.

GOECKLER, W.F., EDWARDS, B., VOLKERT, W.A., HOLMES, R.A., SIMON, J., WILSON, D. 1987. Skeletal localization of samarium-153-chelates: Potential therapeutic bone agents. *Journal of Nuclear Medicine* 28: 495-504.

HOLMES, R.A. 1993. Radiopharmaceuticals in clinical trials. *Semin. Oncol.* 20: 22-26.

HORTOBAGYI, G.N., LIBSHITZ, H.I., DEABOLD, J.E. 1984. Osseous metastasis of breast cancer: clinical. Biochemical, radiographic, and scintigraphic evaluation of response to therapy. *Cancer* 53: 577-582.

JARVIS, N.V., ZEEVAART, J.R., WAGENER, J.M., LOUW, W.K.A., DORMEHL, I.C., MILNER, R.J., KILIAN, E. 2002. Metal ion speciation in blood plasma incorporating the water-soluble polymer, polyethylenimine functionalised with methylenephophonate groups, in therapeutic radiopharmaceuticals. *Radiochim. Acta* 90: 237-246.

JARVIS, N.V., ZEEVAART, J.R., WAGENER, J.M., LOUW, W.K.A., DORMEHL, I.C., MILNER, R.J., KILIAN, E. 2002. Metal ion speciation in blood plasma incorporating the water-soluble polymer, polyethyleneimine functionalised with methylenephosphonate groups, in therapeutic radiopharmaceuticals. *Radiochim. Acta* 90: 237-246.

LATTIMER, J.C., CORWN, L.A., STAPLETON, J., VOLKERT, W.A., EHRHARDT, G.J., KETRING, A.R., ANDERSON, S.K., SIMON, J., GOECKLER, W.F. 1990. Clinical and clinicopathological response to canine bone tumor patients to treatment with samarium-153-EDTMP. *J. Nucl. Med.* 31: 1316-1325.

LIN, J.H. 1996. Bisphosphonates: a review of their pharmacokinetic properties. *Bone* 18: 75-85.

MAEDA, H., SAWA, T., KONNO, T. 2001. Mechanism of tumour-targeted delivery of macromolecular drugs, including the EPR effect in solid tumour and clinical overview of the prototype polymeric drug SMANCS. *J. Controlled Release* 74: 48-61.

MARTIN, P. 1979. The appearance of bone scans following fractures, including immediate and long-term studies. *J. Nucl. Med.* 20: 1227-1231.

MELICHAR, F., KRIZOVA, V., KROPACEK, M., MIRZAJEVOVS, M. 2004. ^{166}Ho labelled compounds for the radionuclide synovectomy and therapy. *World J. Nucl. Med.* 3: 238.

MENNEN, U., DORMEHL, I.C., GOOSEN, D.J. 1985. Evaluation of the healing process of bone fractures in the non-human primate using sequential ^{99m}Tc-methylene diphosphonate scintigraphy. Suid Afrikaanse Tydskrif vir Chirurgie 23: 98-101. 2.

MILNER, R.J. Personal communication.

MITTERHAUSER, M., TÖGEL, S., WADSAK, W., MIEN, L.K., EIDHERR, H., WIESNER, K., VIERNSTEIN, H., KLETTER, K., DUDCZAK, R. 2004. Binding studies of [^{18}F]-fluoride and phosphonates labelled with [^{111}In], [^{99m}Tc], [^{153}Sm], and [^{188}Re] on bone compartments: a new model for the pre vivo evaluation of bone seekers? *Bone* 34: 835-844.

PERCHERSTORFER, M., SCHILLING, T., JANISCH, S. 1993. Effect of clodronate treatment on bone scintigraphy in metastatic breast cancer. *J. Nucl. Med.* 34(7): 1039-1044.

SPENCER, R.P. 1986. Applied principles of radiopharmaceutical use in therapy. *Nucl. Med. Biol.* 13: 461- 463.

SPENCER. R.P. 1987. Short-lived radionuclides in therapy. *Nucl. Med. Biol.* 14: 537-538.

TURNER, J.H., MARTINDALE, A.A., SORBY, P., HETHERINGTON, E.L., FLEAY, R.F., HOFFMAN, R.F., CLARINGBOLD, P.G. 1989. Samarium-153-EDTMP therapy of disseminated skeletal metastasis. *Eur. J. Nucl. Med.* 15: 784-795.

VOLKERT, W.A., GOECKELER, W.F., EHRHARDT, G.J., KETRING, A.R. 1991. Therapeutic radionuclides: Production and decay property considerations. *Journal of Nuclear Medicine* 32: 174-185.

WAGENER, J.M., JARVIS, N.V. 1995. Complexation of trivalent lanthanides by ethylenediaminetetramethylphosphonate (EDTMP). *S. Afr. J. Chem.* 48: 85-89.

YANG, Y., LOU, S., PU, M., WANG, W., WANG, G., HE, J., LIU, G., BING, W., WEI, H. 2005. Labeling conditions, in vitro properties and biodistributions of various Sn-labeled complexes. *Appl. Radiat. Isot* 62: 597-603.

ZEEVAART, J.R., JARVIS, N.V., LOUW, W.K.A., JACKSON, G.E. 2001. Metal ion speciation in blood plasma incorporating the tetraphosphonate, N,N-dimethylenephosphonate-1-hydroxy-4- aminopropilydenediphosphonate (APDDMP), in therapeutic radiopharmaceuticals. *J. Inorg. Biochem.* 83: 57-65 .

ZEEVAART, J.R., LOUW, W.K.A., JARVIS, N.V., WAGENER, J.M., KOLAR, Z.I., AND CLAESSENS, R.A.M.J. 2003. Speciation studies of SnII in blood plasma incorporating proposed bone-seeking ligands as potential therapeutic radiopharmaceuticals. *J. Radioanal. Nucl. Chem.* 257: 83-91.

ZEEVAART, J.R. PhD-Thesis: Metal ion speciation in bloodplasma as a tool in predicting the in vivo behaviour of potential bone seeking radiopharmaceuticals. 2001. Delft University of Technology, the Netherlands.

Chapter 15- Conclusion

From the research covered in this thesis there is no doubt that the ligand PEI-MP exhibits promising and exciting characteristics for targeted delivery of therapeutic radionuclides to areas of neoplastic bone disease. The flexibility in biodistribution stemming from possibilities of size and charge modification has been illustrated in a non-human primate model. This enables the ideal of organ sparing and thus targeted drug delivery to be achieved.

The groundwork for predictive modelling of appropriate radionuclide-ligand complexes using the ECCLES program for metal ion speciation in blood plasma has successfully been explored and some difficult labelling procedures of the ligand with therapeutic radionuclides have been mastered.

The information following the rodent research confirmed the compliance with conditions for non-toxicity and pyrogenicity, and illustrated the uptake by induced canine osteosarcoma tumours of the radiopharmaceuticals.

The research presented here has only now reached the stage where investigations on the therapeutic efficacy of the various novel radioligands, be it curative or palliative, can be considered in cases of osteosarcoma or metastatic bone disease. This could ideally take place as a controlled clinical trial in dogs with naturally occurring osteosarcoma to the long bones. The merits of this in vivo model have previously extensively been discussed.

Such a study would be extensive and could logistically be quite demanding. Access would be needed to various modalities of expertise – veterinary oncology with accompanying facilities for histopathology, haematology, radiology, diagnostic nuclear medicine, as well as well equipped radiochemistry and radiopharmacy laboratories, and supply lines to therapeutic radionuclides, of which $^{186/188}$Re should initially prove the easier option.

There is reason to believe that the ligand PEI-MP could be useful for drug delivery in general, not only in radiotherapy. The basic requirements for the design of polymer anticancer drug conjugates are that these be biocompatable polymers, i.e.non toxic or immungenic, preferably biodegradable, that they should be able to carry the required payload of drug, able to protect

the drug against premature metabolism in transit, that they should avoid rapid liver uptake (unless this happens to be a target for delivery), should be able to display active or passive (EPR effect) tumour targeting and furthermore, the active drug must be liberated at a rate appropriate to its mechanism of action.

PEI-MP can easily be adapted to also fulfil these functions. By using sub-optimal quantities of phosphonating reagents (formaldehyde and phosphonic acid) in the mannich reaction for the preparation of PEI-MP from polyethyleneimine, methylphosphonate polymers with varying amounts of free amino groups (depending on experimental conditions and drug loading needed), can be obtained. Polymers containing amino groups are amongst the most widely studied and technically useful functional polymers, which is due to the chemical and structural versatility of the amino function. The chemical reactions of amines include those of bases and nucleophiles, two of the fundamental affinities in chemistry (Xie *et al.*, 1996). A variety of compounds, can thus be coupled, directly or with a selection of appropriate linkers to amino groups containing PEI-MP to form many different possible polymer-drug conjugates (Maeda *et al.*, 2001).

The research around PEI-MP can therefore quite possibly in the future be extended to cover a variety of important requirements for targeted drug delivery, not necessarily including radionuclides.

References

MAEDA, H., SAWA, T., KONNO, T. 2001. Mechanism of tumour-targeted delivery of the prototype polymeric drug SMANCS. *J. Controlled Release* 74: 47-61.

XIE, H-Q., BAKER, R., ARSHADY, R. 1996. Amine containing polymers: amine-functionalized polyolefins. p 133-149 in : Desk Reference of Functional Polymers Syntheseses and Applications, R. Arshady, ed. American Chemical Society, Washington, DC.

Appendix 1 – Glossary of Abbreviations and Terms

Å	angström
APD	1-hydroxy-3-amine-propylidene diphophonate
API	transcription factor
BMP	bone morphogenic protein
BMU	basic molecular unit
Bq	Bequerel
C	carbon
Ca	calcium
CM-sephadex	carboxy-methyl-sephadex
CT	computed tomography
CTR	cathode ray tube
d	days
DEAE-sephadex	2-(diethylamino)ethyl-sephadex
ECCLES	Evaluation of Constituent Concentration in Large Equilibrium Systems
ECG	electrocardiograph
EDTMP	ethylenediamine tetramethylenephosphonate
EPR	enhanced permeability and retention
ESTA	equilibrium simulation by titration analysis
eV	electron volt
FGF	fibroblast growth factor
GIT	gastrointestinal tract
h	hours
H	hydrogen ions
HEDP	1-hydroxy-ethylenediphosphonic acid
HMPOS	highly metastazing primary osteosarcoma
Ho	holmium
i.v	intravenously
IGFBP	inhibitory binding proteins

Il	interleukin
ITLC-SG	instant thin layer chromatography
J	joules
kDa	kilo Dalton
keV	kilo electron volt
L	ligand
L/N	lesion to normal
LWL	low-molecular-weight
M	metal ion
MCA	multichannel analyser
mCi	milli Curie
MDP	methylenediphosphonic acid
MeV	million electron volts
min	minute
MIRD	medical internal radiation dosimetry
ml	milliliter
Mo	molybdenum
MRI	magnetic resonance imaging
MW	molecular weight
$Na^{99m}TcO_4$	sodium pertechnetate
NECSA	Nuclear Energy Corporation of SA
NF-κß	nuclear factor- κß; transcription factor
NRC	Nuclear Regulatory Commission
NSAIDS	non steroidal anti inflammatory drug
OPG	osteoprotegerin
P	phosphorus
p.i	post injection
PDGF	platelet derived growth factor
PEI-MP	polyethyleneiminomethylphosphonate
PHA	pulse height analyser
PM	photomultiplier
POS	primary osteosarcoma
PSA	prostate specific antigen
PTH	parathyroid hormone

PYP	pyrophosphoric acid
RANK	receptor activator of nuclear factor κß
RANKL	receptor activator of nuclear factor κß ligand
Re	rhenium
ROI	region of interest
Sm	samarium
Sn	tin
$SnCl_2.2H_2O$	stannous chloride dihydrate
Sr	strontium
Tc	technetium
TGF-β	transforming growth factor-β
TRAPase	tartrate-resistant-acid phosphatase
UPA	urikinase
USP	Unites States Pharmacopeia
viz	namely
VPF	vascular permeability factor
β-emmision	beta emission
μm	micron
$\bar{n}$	average number of protons per ligand in the absence of metal ion
$\bar{Z}$	formation function, the average number of protons bound per metal ion
$\bar{\bar{Z}}_{II}$	formation protonation function, the average number of protons bound per ligand
(n, n')	(neutron, neutron')
(n, γ)	(neutron, gamma)
$^{99m}TcO_4^-$	technetium pertechnetate

Appendix 2 - Reprints

Nucl.-Med. Band XXI Heft 3 1982

A Technique to Evaluate Bone Healing in Non-Human Primates Using Sequential ^{99m}Tc-Methylene Diphosphonate Scintigraphy

From the Institute of Life Sciences, *Atomic Energy Board, Pretoria, the Department of Orthopaedic Surgery*, *H. F. Verwoerd Hospital, Pretoria and the H. A. Grové Animal Research Centre*, *Pretoria, South Africa*

Dormehl, I. C., U. Mennen and D. J. Goosen

(Received: February 5, 1982)

The assessment of bone healing through sequential nuclear medical scintigraphy requires a method of consistent localization of the exact fracture area in each consecutive image as the study progresses. This is difficult when there is surrounding bone activity as in the early stages of trauma, and also if complications should set in. The image profile feature, available from most nuclear medical computer software, facilitates this procedure considerably, as is indicated in the present report on bone healing in baboons. Together with roentgenology and histology a ^{99m}Tc-MDP study was in this way successfully done on the healing of long bone fractures experimentally induced in non-human primates. Different surgical implants were used. The results indicated that ^{99m}Tc-MDP accurately reflects the physiological activity in bone. The time-activity curves obtained are presently being studied together with extensive histology, bearing possible clinical application in mind.

Eine Methode zur Bewertung der Knochenheilung mittels der sequentiellen ^{99m}Tc-MDP Szintigraphie

Die Bewertung der Knochenheilung durch sequentielle nuklearmedizinische Szintigraphie erfordert eine Methode der konsequenten Lokalisierung des genauen Knochenbruchgebietes in jedem aufeinanderfolgenden Bild im Verlaufe der Untersuchung; dies ist bei benachbarter Knochenaktivität, wie im frühen Stadium der Verletzung oder bei Komplikationen schwierig. Das meist in nuklearmedizinischer „software" vorhandene Bildprofilprogramm erleichert dieses Verfahren beträchtlich, wie dieser Bericht über die Knochenheilung bei Pavianen zeigt. Zusammen mit Röntgenologie und Histologie konnte eine ^{99m}Tc-MDP Untersuchung dieser Art erfolgreich zum Studium der Heilung von experimentellen Knochenbrüchen bei nicht-menschlichen Primaten angewendet werden. Verschiedene chirurgische Implantationen wurden vorgenommen. Die Ergebnisse zeigten, daß ^{99m}Tc-MDP die physiologische Aktivität in Knochen genau reflektiert. Derzeit werden die Zeit-Aktivität-Kurven zusammen mit umfassender Histologie im Hinblick auf eine klinische Verwendung untersucht.

This study was performed to devise and assess a sensitive non-invasive method for investigating the healing process of long bones in non-human primates. A specific clinical application in mind is the early detection of non-healing or delayed healing of fractures in the aged.

Important for accurate evaluation is the consistency of the localisation of the fracture site and the region of healthy bone from each scintiscan for the entire study. The present report concerns a technique which seems to be successful for this purpose and is found useful towards the clinical application.

Materials and Methods

Four adult chacma baboons (*Papio ursinus*) were used in the experiment. All four animals were clinically and radiographically normal. They were housed indoors in environmentally controlled rooms for the duration of the experiment and they were fed a balanced commercial diet with water freely available. Eight forearms, i.e. a total of 16 radius and ulna bones were osteotomized with a Gigli saw to create simple standard and controlled fractures. The following internal fixation plates were used:

1. Standard Müller compression plate (Vitalium) with 6 holes, on 1 radius and 1 ulna.
2. Standard Müller compression plate (Vitalium) with 4 holes, on 1 radius and 1 ulna.
3. Sherman plate (stainless steel) 6 holes, on 2 radii and 1 ulna.
4. Sherman plate (stainless steel) 4 holes, on 1 ulna.
5. "Mennen clamp-on plate (stainless steel) on 3 radii and 3 ulnae"*. (Fig. 1).

The Sherman and Mennen plates were protected by above elbow casts of a fibre-glass material (eg. "Scotchcast and Lightcast").

Post-operatively two weekly X-rays of the forearms, lateral and antero-posterior, were taken. X-rays were done on the same day.

* Reference: In press – Journ. of Bone and Joint Surgery.

** Two bones had to be withdrawn from the experiment due to the onset of infection and required additional surgery.

Fig. 1: The Mennen clamp-on plate in position on a cadaver forearm.

but preceding the isotope study. Sections of the osteotomized areas of the radii and ulnae were taken for histology at different times post-operatively from a similar concomitant group. This was accompanied by extensive radionuclide evaluation of the fractures.

The baboons were each intravenously injected with approximately 7 mCi of ^{99m}Tc-MDP (3, 4, 5). In each case scanning of the relevant bones commenced 3 hrs post injection using an Ohio Nuclear (ON 410 Sigma) large field gamma camera. Data were stored on disc for evaluation through an A^2 MDS data processor. The complete study consisted of a pre-operative scan to obtain a baseline image for each bone (Fig. 2) followed by scans at 3 days and again 1 week post-operatively and thereafter at weekly and fortnightly intervals, as the lesions stabilized. To evaluate the degree of bone activity at the site of the fracture, use was made of the image profile facility of the computer software. A profile was chosen along the length of the fractured bone, with a width corresponding to the maximum width of the bone (Figs. 2–5). Such a profile curve represents the distribution of radioactivity along the bone as countrate per channel. A peak is found which represents increased activity across the fracture. This fracture peak can be consistently localized with respect to elbow and wrist activity.

a

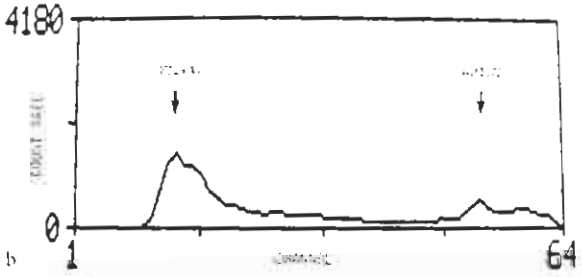

b

Fig. 2a, b: Normal forearm (a) and profile (b); elbow and wrist areas clearly indicated.

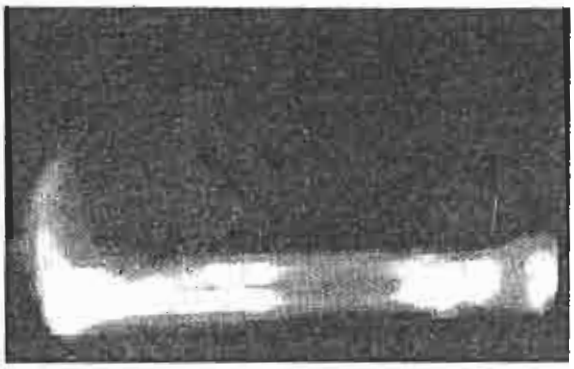

a

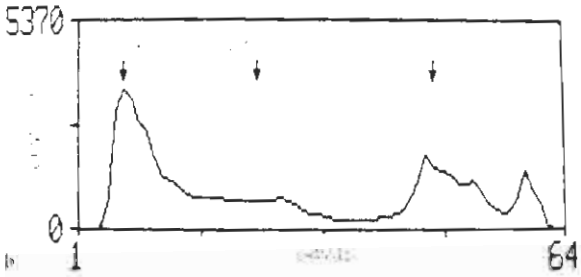

b

Fig. 3a, b: Three days post-operative trauma visible on the profile of the right ulna

The area under this peak is an indication of the total uptake of radioactivity by active bone in the immediate vicinity of the fracture. To obtain the total count across the fracture an integration was performed across the peak and an average countrate/channel (I) was calculated. The same procedure followed across a region of normal bone and an average normal countrate per channel (N) was obtained. The ratio I/N is the factor used to follow bone activity with time in the region of the fracture. An average curve for each of 3 surgical procedures (Mennen, Sherman, Muller) was obtained (Fig. 7) and could be compared to the available histology and X-rays.

Results

A typical pre-operative scan and the subsequent post-operative stages of trauma (at approximately 3 days post operation), early healing (within 3 weeks of the operation) and late healing (after about 6 weeks) are presented in Figs. 2–5, together with their corresponding profiles. The elbow, wrist and fracture areas are marked by arrows. From Figs. 4 and 5a comparison can be drawn between the effects of the Mennen and standard Müller plates on the development of the fracture with time and on the surrounding bone. It is interesting to note the initial spread in the "hot spot" as obtained with a Müller implant in the early stages, with respect to the well defined area of increased radioactivity with a Mennen plate. In the

Nucl.-Med. Band XXI/Heft 3 1982

a

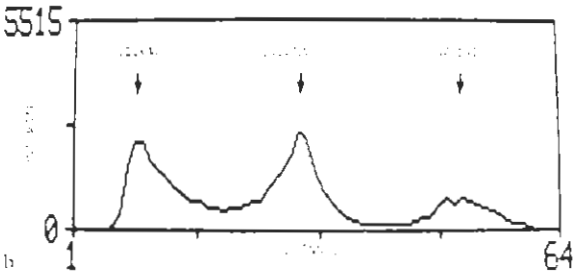

b

Fig. 4a, b. Early healing (inflammatory) stage – 3 weeks post-operative. The profile is of the right ulna. The implant is a Mennen plate.

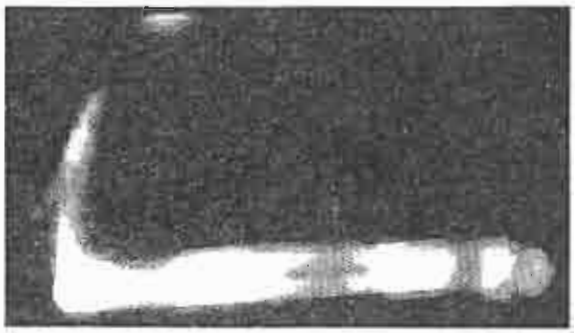

a

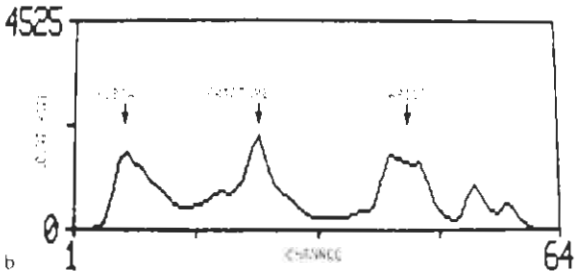

b

Fig. 5a, b. A six weeks post-operative study with a Mennen plate. Profile of left ulna

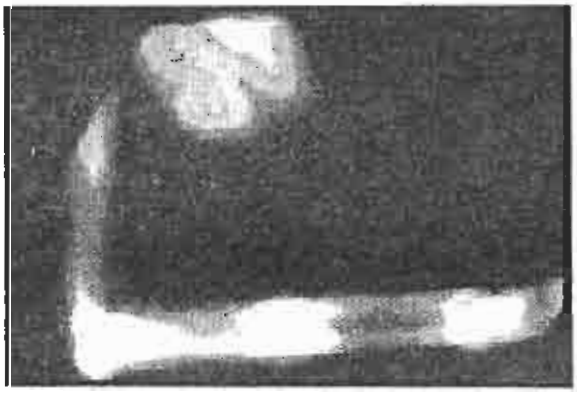

c

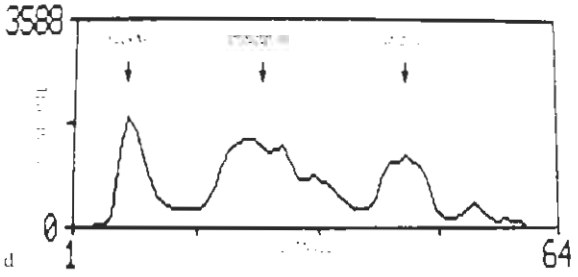

d

Fig. 4c, d. A three week post-operative study with a standard 4-hole Müller plate. The profile is of the right radius.

c

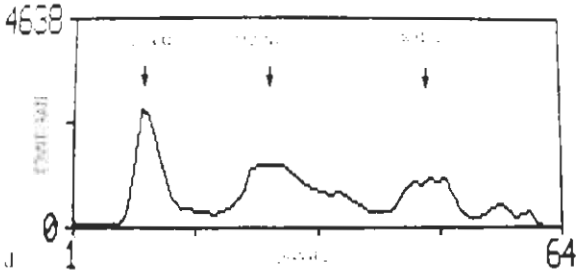

d

Fig. 5c, d. Study of a 4-hole Müller plate – 6 weeks post-operative. Profile of the right radius

Nucl.-Med. Band XXI/Heft 3 1982 107

a

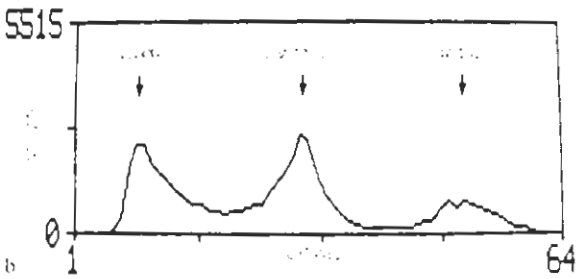

b

Fig. 4a, b. Early healing (inflammatory) stage – 3 weeks post-operative. The profile is of the right ulna. The implant is a Mennen plate.

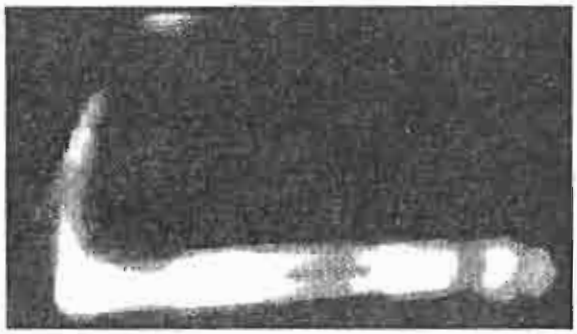

a

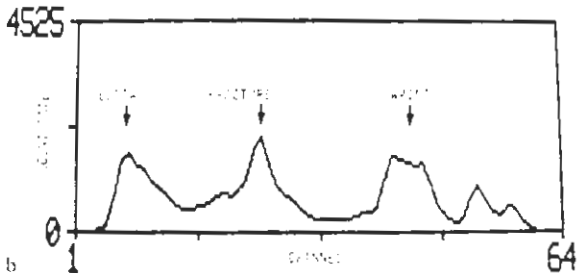

b

Fig. 5a, b: A six weeks post-operative study with a Mennen plate. Profile of left ulna.

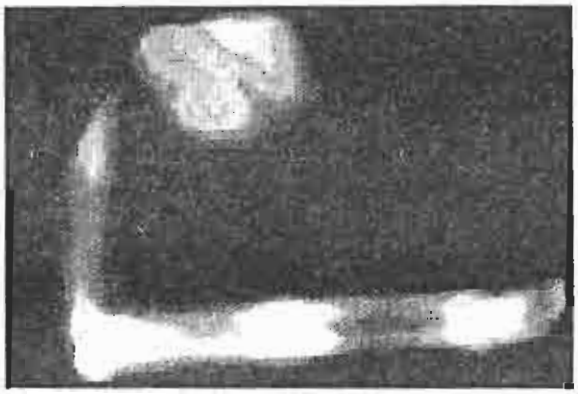

c

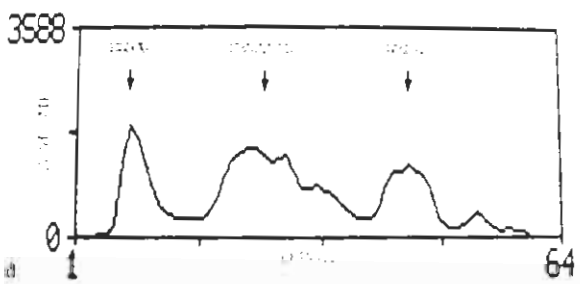

d

Fig. 4c, d: A three week post-operative study with a standard 4-hole Muller plate. The profile is of the right radius.

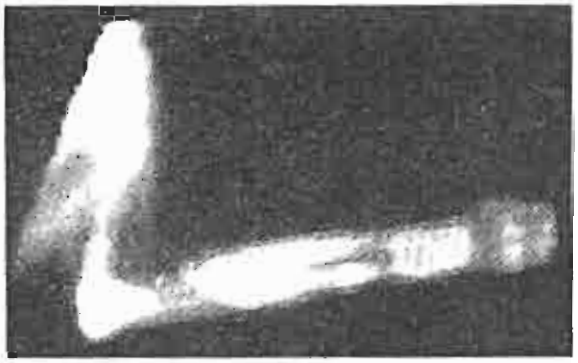

c

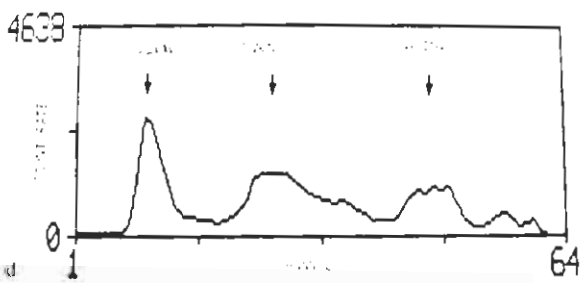

d

Fig. 5c, d. Study of a 4-hole Muller plate – 6 weeks post-operative. Profile of the right radius.

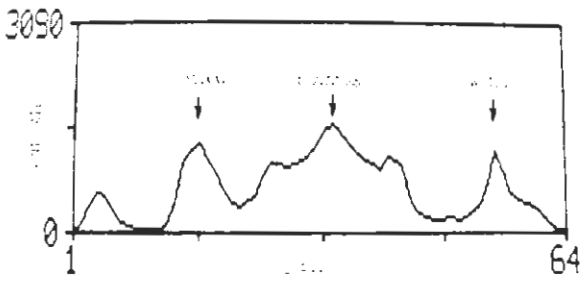

Fig. 6: A typical late study with a Muller plate distinguishing between "fracture" and "screw activity"

late stages the bone activity induced by the screws (Muller plate) can clearly be distinguished from the fracture.

The time-activity curves (L/N vs time) summarize the results. These represent the 3 different implants and show very little difference in time to peak, which turns out to be 3 weeks and the eventual stabilizing time of the lesion, round about 55–60 days. The experimental errors indicated in the time-activity curves were obtained from the statistics of the radioactive countrate and the degradation of the results on applying mathematical procedures.

Roentgenological plates indicate normal bone healing i.e. callus formation in all the studies, but do not reflect any quantifiable indication of the healing process.

Histology on 8 specimens of fracture areas corresponding to different stages of healing demonstrates vascularization of the fracture area and ossification (1).

Discussion

The profile evaluation method used in the radionuclide study allows accurate lesion localization with respect to elbow and wrist. The exact position of the lesion becomes clear in the late studies when trauma in the immediate environment had sufficiently cleared. It is then also possible to distinguish the fracture activity from "screw activity" (Fig. 6). This exact fracture position is then used for the evaluation, also in the early studies. In this way an accuracy otherwise attained with difficulty, is introduced into the nuclear medical study.

The radionuclide study gives an indication of the degree and extent of operative trauma as well as of the early bone healing periods in the pre-callus stage (i.e. inflammatory stage) and of bone healing activity in the bone forming stage (2). It also gives an indication of the duration of the healing process. The radioisotope study shows only vascularized bone. Bone chips which were inserted in a control study were not demonstrated until after 3–4 weeks when vascularization takes place. Contrary to the roentgenological procedure where a shadow of the accumulated healing stages is visualized, the radionuclide study demonstrates very sensitively the bone healing stage as such. Scintigraphically, however, it is not possible to distinguish between the effects of the different implants inserted on the bone fractures. Differences in metal type (e.g. stainless steel, vitalium), thickness and shape as well as biological differences as age (6) of the animal and variation in bone type cannot be corrected for.

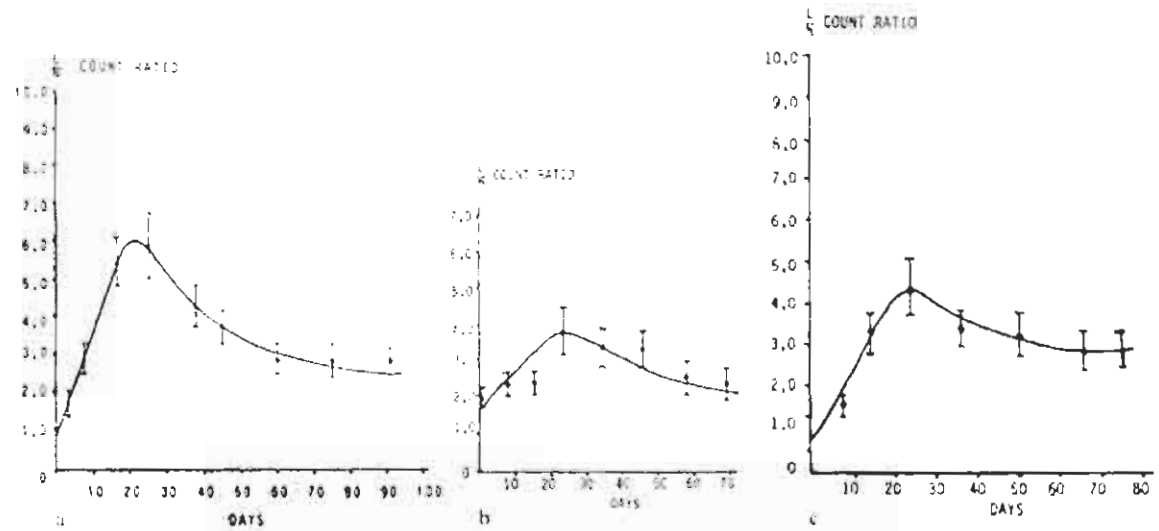

Fig. 7a, b, c: L/N vs time (in days) curves. a Meuneu implant. b Sherman implant. c Muller implant

Histology on 8 specimens of fracture areas corresponding to different stages of healing demonstrates an encouraging relationship with the (L/N) curve.

It therefore seems possible to use nuclear scintigraphy in this manner, as based on the profile technique to demonstrate quantitatively (L/N) and qualitatively bone healing at any given stage. A further study is in progress to extensively correlate the L/N curve with histological change in the long bone of the primate, with eventual clinical application in mind.

References

(1) Greiff, J.: Bone healing in rabbits after compression osteosynthesis: a comparative study between the radiological and histological findings. Injury **10**: 257–267 (1979).

(2) Greiff, J.: Bone healing in rabbits after compression osteosynthesis, studied by Tc-99m (Sn) Polyphosphate Scintimetry and Autoradiology. J. nucl. Med. **22**: 693–698 (1981).

(3) Rudd, T. G., D. R. Allen, and D. E. Hartoch: Tc-99m methylene disphosphonate versus Tc-99m pyrophosphate: biologic and clinical comparison. J. nucl. Med. **18**: 872–876 (1977).

(4) Rudd, T. G., D. R. Allen, and F. D. Smith: Tc-99m labelled methylene disphosphonate and hydroxyethylidine disphosphonate – biologic and clinical comparison. J. nucl. Med. **20**: 821–826 (1979).

(5) Subramanian, G., J. G. McAfee, R. J. Blair et al.: Technetium-99m methylene diphosphonate – a superior agent for skeletal imaging: comparison with other technetium complexes. J. nucl. Med. **16**: 744–755 (1975).

(6) Wilson, M. A.: The effect of age on the quality of bone scans, using Tc-99m pyrophosphonate. Radiology **139**: 703–705 (1981).

(Correspondence: Dr. I. C. Dormehl, Institute of Life Sciences, Atomic Energy Board, Pretoria, South Africa)

Nuclear Medicine & Biology, Vol. 23, pp. 935–940, 1996

ISSN 0969-8051/96/$15.00 + 0.00
PII S0969-8051(96)00117-5

Evaluation of Samarium-153 and Holmium-166-EDTMP in the Normal Baboon Model

W. K. A. Louw,[1] I. C. Dormehl,[2] A. J. van Rensburg,[3] N. Hugo,[2] A. S. Alberts,[3] O. E. Forsyth,[1] G. Beverley,[4] M. A. Sweetlove,[5] J. Marais,[5] M. G. Lötter[5] and A. van Aswegen[5]

[1]ATOMIC ENERGY CORPORATION OF SOUTH AFRICA LIMITED; [2]ASC INSTITUTE FOR LIFE SCIENCES, UNIVERSITY OF PRETORIA; [3]DEPARTMENT OF RADIOTHERAPY, UNIVERSITY OF PRETORIA; [4]H.A GROVE RESEARCH CENTRE, PRETORIA; AND [5]DEPARTMENT OF BIOPHYSICS, FACULTY OF MEDICINE, UNIVERSITY OF THE ORANGE FREE STATE, BLOEMFONTEIN, SOUTH AFRICA

ABSTRACT. Bone-seeking radiopharmaceuticals such as ethylenediaminetetramethylene phosphonate (EDTMP) complexes of samarium-153 and holmium-166 are receiving considerable attention for therapeutic treatment of bone metastases. In this study, using the baboon experimental model, multicompartmental analysis revealed that with regard to pharmacokinetics, biodistribution, and skeletal localisation, ^{166}Ho-EDTMP was significantly inferior to ^{153}Sm-EDTMP and ^{99m}Tc-MDP. A more suitable ^{166}Ho-bone-seeking agent should thus be sought for closer similarity to ^{153}Sm-EDTMP to exploit fully the therapeutic potential of its shorter half-life and more energetic beta radiation. *Copyright © 1996 Elsevier Science Inc.* NUCL MED BIOL 23;8: 935–940, 1996.

KEY WORDS. Samarium-153, Holmium-166, EDTMP, Pharmacokinetics, Baboon model

INTRODUCTION

Radiation teletherapy is effective to control or palliate isolated skeletal metastases. Difficulties associated with its application in multifocal disease together with recent availability of various new bone-seeking radiopharmaceuticals led to renewed interest in treatment with internal radionuclide therapy (9, 11). Although the current treatment objective is primarily for palliative purposes, a potential use in curative therapy should also be investigated (10, 22). Therapeutic success will hinge on many interrelated factors, such as the careful choice of a radionuclide (of which the half-life and radiation emissions dictate its radiobiological effects) linked to a bone-localising agent (of which the biochemical properties dictate its pharmacokinetics and biodistribution) (12, 26, 28).

Radionuclides suitable for therapeutic purposes, but with diverse nuclear properties such as samarium-153 ($t_{1/2}$ 46.7 h; β^- 805[21%]; 702[44%] and 632[34%] keV, max. soft-tissue penetration ~0.3 cm; γ (103 [28%]keV) and holmium-166 ($t_{1/2}$ 26.9 h; β^- 1776 [48%]; and 1840 [51%] keV max. soft-tissue penetration 0.84 cm; γ (81 keV [6.2%] and 1380 [1%] keV) can be considered. These nuclear properties and resultant radiobiological effects may render useful ^{153}Sm- and ^{166}Ho-based radiopharmaceuticals with complementary therapeutic applications (21, 29).

Samarium (Sm) and holmium (Ho) are lanthanides with similar chemical properties. They form stable complexes with bone-seeking phosphonates such as ethylenediamine tetramethylene phosphonic acid (EDTMP). ^{153}Sm-EDTMP has been experimentally investigated in animals and tested in humans for pain palliation of bone metastases (4, 5, 8, 14, 15, 25), while ^{166}Ho-EDTMP and ^{166}Ho-DOTMP (tetraazacyclododecane tetramethylene phosphonic acid) have been evaluated in experimental animals for bone marrow ablation (1, 20). However, more information regarding the pharmacokinetics, biodistribution, and bone localisation of ^{153}Sm-EDTMP and ^{166}Ho-EDTMP is needed before treatment protocols in humans can be concluded. For this purpose extensive in vivo experimentation in animal models cannot be avoided. The use of nonhuman primates such as baboons (*Papio* spp.) is justified in these investigations. The baboon model conforms to many of the required criteria of parallelism (e.g., anatomical, physiological, immunological, and radiobiological) of the human (6, 7, 18).

This investigation concerned the pharmacokinetics, biodistribution, and bone localisation of ^{153}Sm-EDTMP and ^{166}Ho-EDTMP in the normal baboon experimental model, before a clinical trial in humans with metastatic bone cancer was considered. The pharmacokinetics, biodistribution, and bone localisation of ^{153}Sm-EDTMP and, subsequently, also ^{166}Ho-EDTMP were scintigraphically compared with those of ^{99m}Tc-MDP by dynamic and static studies. From these results, together with urine excretion data, compartmental modelling could be done and the in vivo behaviour of ^{153}Sm-EDTMP and ^{166}Ho-EDTMP could be described. These results were also applied to calculate ^{153}Sm- and ^{166}Ho-cumulated activities and absorbed doses in various organs.

MATERIALS AND METHODS

Radionuclides

Both ^{153}Sm and ^{166}Ho were prepared by neutron irradiation of 99% enriched $^{152}Sm_2O_3$ (1.0–2.0 mg, 48 h) and $^{165}Ho_2O_3$ (1.0–2.0 mg, 24 h) in the Safari-1 Research Reactor using a thermal flux of 2.78 × 10^{14} n $cm^{-2}s^{-1}$. Typical specific activities of 272.3 × 10^6 MBq/mmole for $^{153}Sm_2O_3$ and 65.53 × 10^6 MBq/mmole for $^{166}Ho_2O_3$ were obtained. Following irradiation, the oxide targets were dissolved in 0.2 mL HCl (1.0 M for $^{153}Sm_2O_3$ and 2.0 M for $^{166}Ho_2O_3$), diluted to 0.1 M HCl with sterile deionised water and

Address reprint requests to: Dr. W. K. A. Louw, AEC, P3000, P.O. Box 582, Pretoria 0001, South Africa
Received 29 December 1995
Accepted 19 May 1996

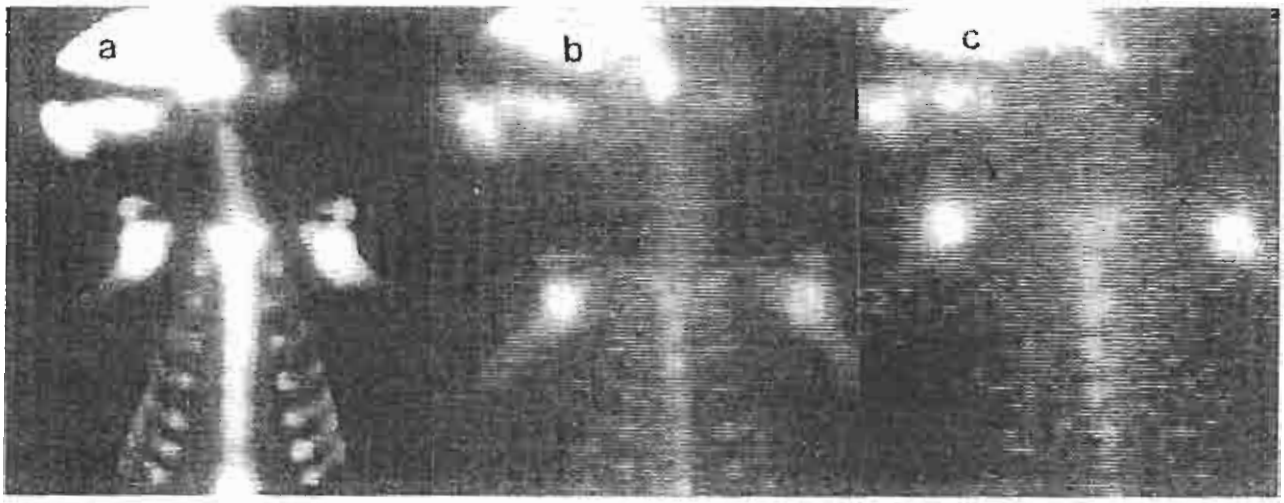

FIG. 1. Typical scintigrams of baboons indicating skeletal localisation of (a) ^{99m}Tc-MDP (185 MBq), (b) ^{153}Sm-EDTMP (111 MBq), and (c) ^{166}Ho-EDTMP (185 MBq) 4 h postinjection.

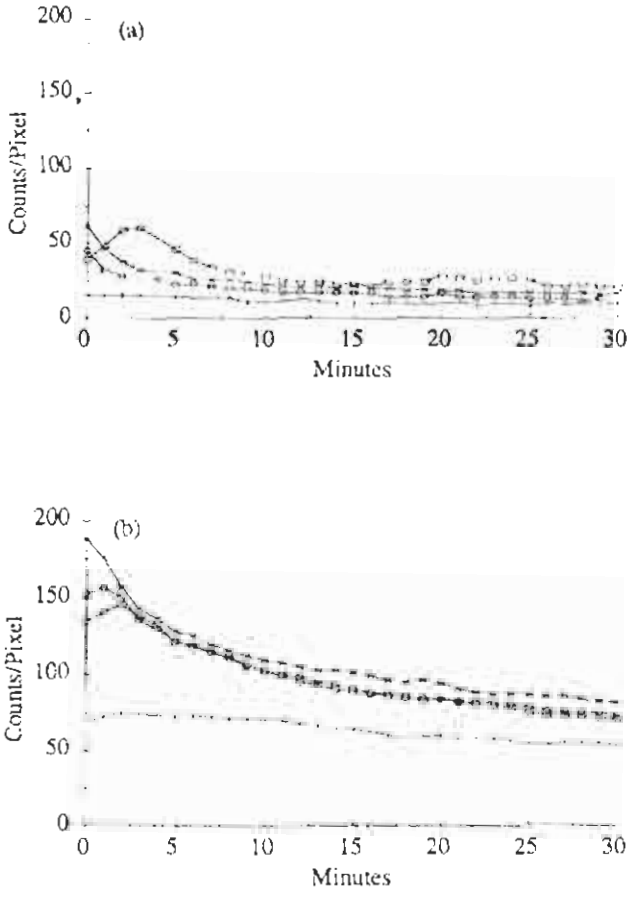

FIG. 2. Time-activity curves (counts/pixel) for the bloodpool (x), liver (⊖), kidney (□), and background (+) obtained from dynamic studies (0 to 30 min postinjection) with 111 MBq ^{153}Sm-EDTMP (a) and 185 MBq ^{166}Ho-EDTMP (b), respectively.

filtered (Millex-GV, 0.22 μm, Millipore Bedford, MA). When necessary a carrier solution $SmCl_3$ was added to obtain a samarium concentration of 2.8 mM and an activity of 1554 MBq/mL 2 days after irradiation. Gamma-ray spectra obtained by counting aliquots of the $^{153}SmCl_3$ and $^{166}HoCl_3$ stock solutions with a Ge(Li)-gamma detector revealed within the $^{153}SmCl_3$ the presence of only ^{152}Eu, ^{154}Eu, and ^{155}Eu. The ^{152}Eu activity at the end of irradiation was less than 6.8×10^{-4}% of ^{153}Sm, while those of ^{154}Eu and ^{155}Eu were $< 4.3 \times 10^{-5}$% and 2.6×10^{-5}%, respectively. The only radionuclide present with ^{166}Ho was ^{153}Sm at an activity of ~0.6% of ^{166}Ho.

The Ligand and Complexing with ^{153}Sm and ^{166}Ho

EDTMP was prepared by the condensation of ethylenediamine, phosphorous acid, and formaldehyde by a modified Mannich reaction in the presence of hydrochloric acid (19). Recrystallisation from water/methanol and water yielded white crystals, m.p. 214°C (lit. m.p. 214°C). Analysis: Found; C, 16.83%; H, 4.62%; N, 6.52%; Calculated for $C_6H_{22}N_2O_{12}P_4$; C, 16.52%; H, 4.62%; N, 6.42%.

The EDTMP reagent was prepared in 10-mL vials by lyophilising 1-mL aliquots of 50 mg/mL EDTMP solution of pH 8.5. The dry product was sealed under nitrogen. Sterility, apyrogenicity, and toxicity were ascertained by standard methods.

For complexing 1-mL aliquots of $^{153}SmCl_3$, alternatively $^{166}HoCl_3$ (containing the prescribed amount of activity and Sm^{3+} or Ho^{3+}) were added to lyophilised EDTMP reagent kits. The solutions were left for 30 min, diluted to 5 mL, and counted, whereafter 3 μL samples were chromatographically analysed. After sealing, the vials containing the final products (pH 7.0–8.0) were sterilised by autoclaving. Radiochemical purity was determined by thin-layer chromatography on cellulose thin-layers (TLC aluminum sheets, cellulose, 0.1 mm, E. Merck, Darmstadt, Germany) using pyridine:ethanol:water (1:2:4) as solvent (25). ^{153}Sm-EDTMP as well as ^{166}Ho-EDTMP was found at R_f 0.75–0.85, and uncomplexed Sm^{3+} and Ho^{3+} remained at the origin. Labelling efficiencies were greater than 97% for both ^{153}Sm-EDTMP and ^{166}Ho-EDTMP.

Blood and Urine Collection After Administration of ^{153}Sm-EDTMP and ^{166}Ho-EDTMP

The animal experimentation was done according to the National Code for the Handling and Use of Animals in Research, Education, Diagnosis and Testing of Drugs and Related Substances in South Africa and approved by the Ethics Committee of the University of Pretoria.

Anaesthesia was induced in healthy, male chacma baboons (*Papio ursinus*) of average weight 27.5 (±2.0) kg with ketamine hydrochloride (Ketalar, Parke Davis, SA, 10 mg/kg) and maintained with pentobarbitone sodium as a solution of 9 mg/mL in Ringer's lactate (Sagatal, Maybaker, SA) at a rate of 30 mL/h in the vena cephalica. A 7F urinary catheter was placed in the urinary bladder to facilitate the collection of urine samples.

Doses of 370 MBq ^{153}Sm-EDTMP (n = 6) and ^{166}Ho-EDTMP (n = 6) were administered. One lyophilised kit containing 50 mg EDTMP was used for each animal. Blood and urine samples were collected at fixed intervals for 4 h. The activity and volume of each sample were measured immediately and registered.

Biodistribution of ^{153}Sm-EDTMP and ^{166}Ho-EDTMP

Twelve healthy male baboons (six each for ^{153}Sm-EDTMP and ^{166}Ho-EDTMP) (average weight 27.5 kg) were used in this study. Anaesthesia in each case was induced with ketamine hydrochloride (10 mL/kg) and maintained as above by an IV administration of pentobarbitone sodium solution.

Scintigraphy was performed (Siemens Orbiter) with the animal positioned in the supine position for planar images. The data acquisition initially involved a view of the thorax, liver, and kidneys and was performed as a dynamic study of 30 × 1-min frames on a countdown bolus injection of 111 MBq ^{153}Sm-EDTMP or 185 MBq ^{166}Ho-EDTMP. Static images of 4-min duration each followed at 2, 3, 4, 5, and 7 h after the injection of the tracer. These images presented the skeletal structure from the skull to the pelvis as two matched images.

From the dynamic study, time-activity curves were obtained for the cardiac, kidney, and liver regions. Regions of interest (ROI) placed on areas of the bony structures of skull, shoulder, sternum, ribs, and pelvis, as well as appropriate muscular background areas (no other organs were at this stage visible) from the static images, rendered relative region-to-muscular background ratios after natural background subtraction and consequently percentage uptake of ^{153}Sm and ^{166}Ho by the bone. This uptake of ^{153}Sm and ^{166}Ho by the bone was compared to ^{99m}Tc-MDP (185 MBq) uptake previously measured similarly in the same animals at the same time intervals but starting 3 h after ^{99m}Tc-MDP administration. Kinetic data from the dynamic studies and data from the static studies were normalised in agreement, with urine activity values expressed as a percentage of the injected activity. Blood sample activity was corrected with estimated blood volume and compared to injected activity to determine percentage blood activity at a specific time. These percentages were used to normalise ROI counts over the left ventricle in the dynamic study. These calibrated data were fitted to a multicompartment model using the Simulation Analysis and Modeling (SAAM-30) software and performed once for each of ^{153}Sm and ^{166}Ho on averaged raw data.

Six compartments were considered—viz. blood, bone, kidney, liver, urinary bladder, and the remainder of the body. Transfer rates, half-lives, and ^{153}Sm and ^{166}Ho-distributions for the different compartments were simulated using the compartmental model.

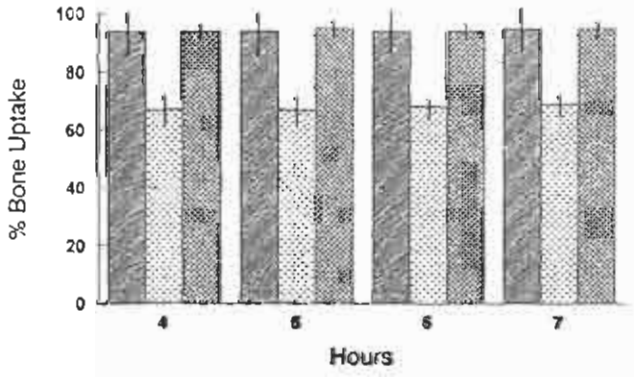

FIG. 3. Percent of bone uptake (region of interest—hip) of 185 MBq ^{99m}Tc-MDP (▨), 185 MBq ^{166}Ho-EDTMP (▤), and 111 MBq ^{153}Sm-EDTMP (■) 4 to 7 h postinjection. SD ranges are indicated.

Dosimetry

The Medical Internal Radiation Dosimetry (MIRD) dose calculation system was used (16). The blood, bone, liver, kidney, urinary bladder content, and rest of the body were selected as source organs for absorbed-dose calculations. Target organs were the ovaries, bone marrow, colon, lung, stomach, urinary bladder wall, breast, liver, oesophagus, thyroid, skin, bone surface, and remainder of the body. The absorbed dose $D(r_k)$ to each target organ k as the sum of the contributions of n source organs h for the radionuclide r was calculated using the following equation:

$$D(r_k) = A_h(0,\infty)S(r_k \leftarrow r_h)F$$

where $A_h(0,\infty)$ is the cumulated activity in source organ h, $S(r_k \leftarrow r_h)$ the mean dose per unit cumulated activity (rad/μCi h), received by target organ k from source organ h and F the conversion factor from rad/μCi to mSv/MBq.

The cumulated activity ($A_h(0,\infty)$) for each source organ and the blood was calculated as the integral of the time-activity curve up to 4 h, plus the integral of the physical decay of the activity at 4 h. Cumulated bladder activity was calculated using only the 0-to-4-h period assuming voiding at 4 h. The total absorbed dose of each target organ k is the sum of the contributions from the n source organs to that specific target organ. The effective dose was calculated according to the latest recommendations of the International Commission on Radiological Protection (13). The effective dose E can be considered as a rough estimate of the comparable whole-body irradiation and was calculated from the formula

$$E = \sum_T W_T \cdot H_T$$

where W_T is the weighting factor for tissue or organ T and H_T is the equivalent dose in tissue T, give in Sv. The equivalent dose H_T was calculated using the formula

$$H_T = \sum_R W_R \cdot D(r_k)_R$$

with W_R the radiation weighting factor (equal to 1 for the radio-

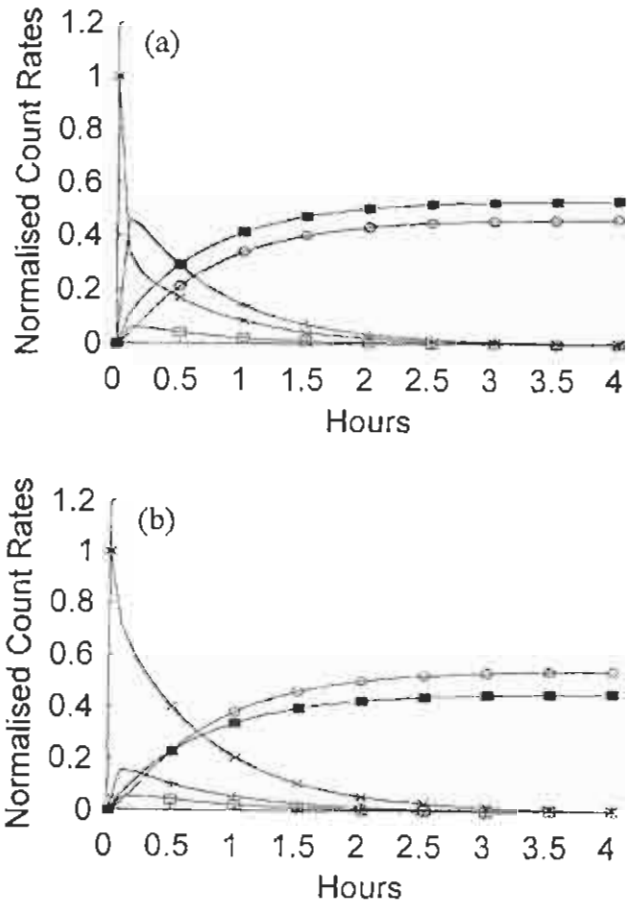

FIG. 4. Compartmental analysis showing fitted curves for the bloodpool (x), urine (⊖), bone (■), kidney (□), and remainder of the body (+) of ^{153}Sm-EDTMP (a) and ^{166}Ho-EDTMP (b).

nuclides under discussion) and $D(\tau_K)_R$ the absorbed dose for the different organs and tissue.

RESULTS

Scintigraphic images of individual representative animals 4 h after injection of 111 MBq ^{153}Sm-EDTMP or 185 MBq ^{166}Ho-EDTMP are shown, respectively, in Fig. 1b, c. These images reveal selective skeletal and little nonosseous tissue accumulation. For qualitative comparison, a typical skeletal image of 185 MBq ^{99m}Tc-MDP uptake previously measured in the same group of animals is presented (Fig. 1a).

Time-activity curves for the bloodpool, liver, kidney, and background obtained from the dynamic studies (0 to 30 min) with ^{153}Sm- and ^{166}Ho-EDTMP are presented in Fig. 2a, b. The resulting tracer uptake in the bone structure, which was measured at 4, 5, 6, and 7 h by static acquisition, produced additional count rate data that are shown as target-to-background ratios in Fig. 3. The uptake ratio of ^{99m}Tc-MDP in the bone is included for comparison.

The above data were used for the compartmental analysis, and the fitted curves from these calculations are shown in Fig. 4 a, b for ^{153}Sm-EDTMP and ^{166}Ho-EDTMP, respectively.

Transfer rates and half-lives for the various organs appear in Table 1 and tracer distribution in Table 2.

The total absorbed dose and effective dose to each target organ appear in Table 3. The effective dose was 0.208 mSv/MBq for ^{153}Sm and 0.293 mSv/MBq for ^{166}Ho.

TABLE 1. Transfer Rates and Half-Lives of Clearance from Various Organs of ^{153}Sm and ^{166}Ho

	Sm-153		HO-166	
Compartment	Transfer Rate (min^{-1})	Half-Life (min)	Transfer Rate (min^{-1})	Half-Life (min)
Blood–Bone	0.033		0.013	
Bone–Blood		43 000		∞
Blood–Liver	0.000016		0.0000002	
Blood–Kidney	0.029		0.015	
Kidney–Urine	0.141		0.167	
Blood–Remainder	0.252		0.067	
Remainder–Blood		4.0		2.5

DISCUSSION

Intravenous administered bone-seeking internal radioisotopic agents distribute via the circulatory system throughout the body while simultaneously accumulating in the bone (2). The transfer rates of 3.3%/min of the ^{153}Sm-EDTMP from the blood to the bone (Table 1) and 2.9%/min from blood to kidney resulted in a maximum bone accumulation of 53% reached after 4 h (Table 2). This corresponded with previous results obtained in experimental animals and humans (3–5, 8, 25).

There is a slight washout of ^{153}Sm from the bone with a long half-life of 43,000 min (Table 1). The blood-to-bone transfer rate of ^{166}Ho-EDTMP of 1.3%/min and blood-to-kidney transfer rate of 1.5% is lower than that of ^{153}Sm-EDTMP (Table 1), resulting in a maximum accumulation of 45% after 4 h (Table 2). There was no washout of ^{166}Ho from bone, resulting in a half-life of infinity (∞) (Table 1). Forty-six percent of ^{153}Sm-EDTMP and 54% of ^{166}Ho-EDTMP were excreted in the urine (Table 2). The bone-to-background (cardiac blood pool) uptake for ^{166}Ho-EDTMP was 69% in comparison to 91% for ^{153}Sm-EDTMP and 95% for ^{99m}Tc-MDP (Fig. 3).

These results indicate that ^{166}Ho-EDTMP, in comparison to ^{153}Sm-EDTMP, exhibits poorer *in vivo* biodistribution and pharmacokinetic properties in the baboon model, which contrasts with previous findings in dogs (1). A possible reason for the discrepancy between these data and that of Appelbaum *et al.* (1) may be related to high plasma citrate levels in the baboon experimental animals. The fact that the ^{166}Ho-EDTMP is a weaker complex than ^{153}Sm-EDTMP (27) may account for more transchelation of ^{166}Ho-to-plasma citrate.

The highest absorbed doses were received by the bone marrow and bone surface for both ^{153}Sm-EDTMP and ^{166}Ho-EDTMP (Table 3). The higher urinary accumulation and higher energy of ^{166}Ho leads to the high radiation dose to the urinary bladder wall.

The count rate/unit activity was higher for ^{166}Ho than for ^{153}Sm (Fig. 2 a, b). This is due to the scatter contribution from the high-energy γ-photon emitted by ^{166}Ho (1.38 MeV), as is also visible on the ^{166}Ho scintigram (Fig. 1c). The effect of the scatter on the percentage distribution was never more than 2%, tending to reduce the skeletal uptake of ^{166}Ho.

TABLE 2. Tracer Distribution of ^{153}Sm and ^{166}Ho

	Maximum %		Time of Max (h)		% at 4 h	
Organ	Sm-153	Ho-166	Sm-153	Ho-166	Sm-153	Ho-166
Bone	53	45	4	4	53	45
Urine	46	54	4	4	46	54
Kidneys	5.8	5.0	0.2	0.2	0	0
Remainder	46	15	0.1	0.1	1	0
Blood	100	100	0	0	0	0.4
Liver	0.03	0		0		0

The total absorbed dose of ^{153}Sm for various target organs as presented in Table 3 corresponds to the calculated values of Logan *et al.* (17). In contrast, the calculated ^{166}Ho bone marrow dose (even if corrections are made for the lower bone uptake in the baboon model) differs considerably from the values for ^{166}Ho-EDTMP obtained by Appelbaum *et al.* (1) in a beagle (dog) model. This discrepancy might be *inter alia* due to their use for S-values for human children, whereas adult human S-values were used for calculating the results in Table 3.

Considering the above biodistribution and pharmacokinetic imperfections of ^{166}Ho-EDTMP compared to ^{153}Sm-EDTMP, the development of a different palliative ^{166}Ho-based bone therapeutic agent with similar biodistribution and pharmacokinetic properties as ^{153}Sm-EDTMP might be a worthwhile approach.

The more energetic β-emissions of ^{166}Ho (with its ~8.0 mm max. soft-tissue penetration) may be more efficient for the treatment of large nonossified tumors. These tumors respond poorly to ^{153}Sm-EDTMP owing to the matrix localisation properties of the phosphonates and limited (~3 mm) soft-tissue penetration of the ^{153}Sm β-emissions (15). Its half-life of 26.9 h is long enough to eliminate logistic problems, but is sufficient to provide a higher radiation dose rate than ^{153}Sm, which is advantageous for radiotherapeutic treatments (23, 24, 26).

CONCLUSIONS

Bone-seeking phosphonate complexes of ^{153}Sm and ^{166}Ho can form complementary therapeutic radiopharmaceutical agents owing to their different physical properties with regard to half-life and beta energies. Both ^{153}Sm and ^{166}Ho are lanthanides that easily form EDTMP complexes with a high radiochemical purity. The role of ^{153}Sm-EDTMP is defined and confirmed as a therapeutic agent for the treatment of painful skeletal metastases. This comparative study of ^{153}Sm-EDTMP and ^{166}Ho-EDTMP in the baboon model reveals, despite their similar chemical characteristics, a significantly inferior performance of ^{166}Ho-EDTMP with regard to bone localisation, biodistribution, and pharmacokinetics. Pursuing clinical trials on humans with ^{166}Ho-EDTMP is perhaps not justified. However, the development of more suitable bone-localising ligand(s) for ^{166}Ho should be seriously considered.

The authors wish to thank Ms Evelyn Watson from Oak Ridge Institute for Science and Education for supplying the data to perform the dose calculations, and the Medical Research Council of South Africa and the National Cancer Association for financial support. Our thanks also go to Erika Oosthuizen for typing the manuscript.

References

1. Appelbaum F. R., Brown P. A., Sandmaier B. M., Storb R., Fisher D. R., Shulman H. M., Graham T. C., Schuening F. G., Deeg H. J., Bianco J. A., Ketring A. R. and Kaplan D. (1992) Specific marrow ablation before marrow transplantation using an aminophosphonic acid conjugate ^{166}Ho-EDTMP. *Blood* 80, 1608–1613.
2. Arnold, J. S. (1979) Kinetic analysis of bone imaging agents. In: *Principles of Radiopharmacology*, Vol. III (Edited by Colombetti L. G.), pp. 205–223. CRC Press, Boca Raton, FL.

TABLE 3. Total Absorbed Dose in mSv/MBq Injected Dose for Variou Target Organs

		Sm-153		HO-166	
Organ	W_t	Dose (mGy/MBq)	Eff. dose (mSv/MBq)	Dose (mGy/MBq)	Eff. dose (mSv/MBq)
Ovaries	0.20	0.007	0.00144	0.003	0.00061
Bone Marrow	0.12	1.240	0.14879	1.565	0.18778
Colon	0.12	0.007	0.00090	0.003	0.00031
Lung	0.12	0.009	0.00110	0.031	0.00368
Stomach	0.12	0.003	0.00041	0.001	0.00018
Urinary Bladder Wall	0.05	0.551	0.02757	1.566	0.07831
Breast	0.05	0.003	0.00016	0.001	0.00007
Liver	0.05	0.007	0.00033	0.010	0.00049
Oesophagus	0.05	0.010	0.00050	0.016	0.00080
Thyroid	0.05	0.006	0.00029	0.012	0.00060
Skin	0.01	0.004	0.00004	0.002	0.00002
Bone Surface	0.01	2.6441	0.02641	1.920	0.01920
Remainder	0.05	0.010	0.00050	0.016	0.00080
Total	1		0.20844		0.29289

W_t is the tissue weighting factor used in the calculation of effective dose

3. Bayouth J. E., Macey D. J., Kasi L. P. and Fosella F. V. (1994) Dosimetry and toxicity of samarium-153-EDTMP administered for bone pain due to skeletal metastases. *J. Nucl. Med.* **35**, 63–69.
4. Eary J. F., Collins C., Stabin M., Vernon C., Petersdorf S., Baker M., Hartwell S., Ferency S., Addison S. J., Appelbaum F. and Gordon E. E. (1993) Samarium-153-EDTMP biodistribution and dosimetry estimation. *J. Nucl. Med.* **34**, 1031–1036.
5. Farhanghi M., Holmes R. A., Volkert W. A., Logan K. W. and Singh A. (1992) Samarium-153-EDTMP: Pharmacokinetic, toxicity and pain response using an escalating dose schedule in treatment of metastatic bone cancer. *J. Nucl. Med.* **33**, 1451–1458.
6. Fridman E. P. and Popova V. N. (1988) Species of the genus *Papio* (*Cercopithecidae*) as subjects of biomedical research: I. Biological basis of experiments on baboons. *J. Med. Primatol.* **17**, 291–307.
7. Fridman E. P. and Popova V. N. (1988) Species of the genus Papio (*Cercopithecidae*, Primates) as subjects of biomedical research: II. Quantitative characteristics of contemporary use of baboon species in medical and biological investigations. *J. Med. Primatol.* **17**, 309–318.
8. Goeckeler W. F., Edwards B., Volkert W. A., Holmes R. A., Simon J. and Wilson D. (1987) Skeletal localization of samarium-153-chelates: Potential therapeutic bone agents. *J. Nucl. Med.* **28**, 495–504.
9. Hoefnagel C. A. (1991) Radionuclide therapy revisited. *Eur. J. Nucl Med.* **18**, 408–431.
10. Holmes R. A. (1992) [^{153}Sm]EDTMP: A potential therapy for bone cancer pain. *Semin. Nucl. Med.* **22**, 41–45.
11. Hosain F. and Spencer R. P. (1992) Radiopharmaceuticals for palliation of metastatic osseous lesions: Biologic and physical background. *Semin. Nucl. Med.* **22**, 11–16.
12. Humm J. L. (1986) Dosimetric aspects of radiolabeled antibodies for tumor therapy. *J. Nucl. Med.* **27**, 1490–1497.
13. International Commission on Radiological Protection (1990) 1990 recommendations of the ICRP. *Ann. ICRP* **21**, 1–201.
14. Lattimer J. C., Corwin L. A., Stapleton J., Volkert W. A., Ehrhardt G. J., Ketring A. R., Hewett J. E., Simon J. and Goeckeler W. F. (1990) Clinical and clinicopathologic effects of samarium-153-EDTMP administered intravenously to normal beagle dogs. *J. Nucl. Med.* **31**, 586–593.
15. Lattimer J. C., Corwin L. A., Stapleton J., Volkert W. A., Ehrhardt G. J., Ketring A. R., Anderson S. K., Simon J. and Goeckeler W. F. (1990) Clinical and clinicopathologic response to canine bone tumor patients to treatment with samarium-153-EDTMP. *J. Nucl. Med.* **31**, 1316–1325.
16. Loewinger R., Budlinger T. F. and Watson E. E. (1991) *MIRD Primer for Absorbed Dose Calculations*, pp. 1–21. Society of Nuclear Medicine, New York.
17. Logan K. W., Volkert W. A. and Holmes R. A. (1987) Radiation dose calculations in persons receiving injection of samarium-153 EDTMP. *J. Nucl. Med.* **28**, 505–509.
18. Louw W. K. A., van Rensburg E. J., Izatt H. and Engelbrecht R. I. (1991) Nucleoid sedimentation analysis of DNA superstructure, γ-radiation-induced damage and repair in human and chacma baboon (*Papio ursinus*) peripheral lymphocytes. *Int. J. Radiat. Biol.* **59**, 951–962.
19. Moedritzer K. and Irani R. R. (1966) The direct synthesis of α-aminomethyl-phosphonic acids: Mannich-type reactions with orthophosphorous acid. *J. Org. Chem.* **31**, 1603–1607.
20. Parks N. J., Kawakami T. G., Avila M. J., White R., Cain G. R., Raaka S. D., Hornuff W., Fisher P., Moore P., Seibert J. A., Garlich J., Simon J. and Champlin R. (1993) Bone marrow transplantation in dogs after radio-ablation with a new Ho-166 amino phosphonic acid bone-seeking agent (DOTMP). *Blood* **82**, 318–325.
21. Rao D. V. and Howell R. W. (1993) Time-dose-fractionation in radioimmunotherapy: Implications for selecting radionuclides. *J. Nucl. Med.* **34**, 1801–1810.
22. Robinson R. G. (1990) Systemic radioisotopic therapy of primary and metastatic bone cancer. *J. Nucl. Med.* **31**, 1326–1327.
23. Spencer R. P. (1986) Applied principles of radiopharmaceutical use in therapy. *Nucl. Med. Biol.* **13**, 461–463.
24. Spencer R. P. (1987) Short-lived radionuclides in therapy. *Nucl. Med. Biol.* **14**, 537–538.
25. Turner J. H., Martindale A. A., Sorby P., Hetherington E. L., Reay R. F., Hoffman R. F. and Claringbold P. G. (1989) Samarium-153 EDTMP therapy of disseminated skeletal metastasis. *Eur. J. Nucl. Med.* **15**, 784–795.
26. Volkert W. A., Goeckeler W. F., Ehrhardt G. J. and Ketring A. R. (1991) Therapeutic radionuclides: Production and decay property considerations. *J. Nucl. Med.* **32**, 174–185.
27. Wagener J. M. and Jarvis N. V. (1995) Complexation of trivalent lanthanides by ethylenediaminetetramethylphosphonate (EDTMP). *S. Afr. J. Chem.* **48**, 85–89.
28. Wessels B. W. and Rogus R. D. (1984) Radionuclide selection and model absorbed dose calculations for radiolabeled tumor associated antibodies. *Med. Phys.* **11**, 638–645.
29. Wheldon T. E. (1993) Radionuclide therapy of cancer: Particle range and therapeutic effectiveness. *Nucl. Med. Commun.* **14**, 408–410.

Sonderdruck / Reprint

Arzneimittel-Forschung/Drug Research
ECV · Editio Cantor Verlag · Aulendorf (Germany)
Arzneim.-Forsch./Drug Res. 48 (I), 4, 408–414 (1998)

Uptake of Ethylenediamine Tetramethylene Phosphonic Acid in Normal Bone after Multiple Applications

A non-human primate study

Irene C. Dormehl[a], Werner K. A. Louw[b], Frank. H. A., Schneeweiss[c], Rowan Milner[d], Gerd Schmitt[c], Ulrich Carl[e], and Sandra A. Croft[a]

AEC Institute for Life Sciences, Medical Faculty[a], University of Pretoria (South Africa), Atomic Energy Corporation of SA Ltd.[b], Pretoria (South Africa), Institute for Medicine, Research Centre Jülich GmbH[c], Jülich (Germany), Veterinary Faculty[d], University of Pretoria (South Africa), and Klinik und Poliklinik für Strahlentherapie und Radiologische Onkologie[e], University of Düsseldorf (Germany)

Summary

Palliation of bone pain in patients with bone metastases has previously been evaluated using ^{153}Sm (samarium) complexed to bone seeking ethylenediamine tetramethylene phosphonic acid (CAS 1429-50-1, EDTMP). Repeated application of the radioligand as needed was found progressively less effective. This study questions whether EDTMP exerts a blocking function, limiting access to bone or osseous tumours with successive administration.

The pharmacokinetics and biodistribution of ^{153}Sm-EDTMP in the normal experimental baboon (n = 6) during three successive applications (6 weekly) each with two different concentrations of EDTMP (0.7 and 1.4 mg/kg b.wt.) were investigated using bone scintigraphy. ^{153}Sm-EDTMP (111 MBq) was injected in each case and monitored for 5 h. Curves of tracer kinetics and bone to background uptake were obtained, also blood and cumulative urine curves. Comparisons were statistically assessed in each group between successive applications and between EDTMP concentrations.

Partial blocking with the low EDTMP concentration reached statistical significance after the third application. The first application of the high EDTMP concentration yielded lower uptake in the bone than did low EDTMP pointing to blocking by the high concentration, but not seen with repeated applications.

Continual application of high concentration EDTMP could lead to a reduced level of calcium in serum and increased parathyroid hormone levels which might trigger osteoblastic activity and bone remodelling. This would partially affect the blocking which was thus more obvious at the low EDTMP concentration.

Zusammenfassung

Aufnahme von Ethylendiamin-tetramethylen-phosphonsäure in gesunde Knochen nach Mehrfachapplikation / Eine Primatenstudie

Bei Patienten mit Knochenmetastasen wurde mit Hilfe von ^{153}Sm (Samarium), komplexiert mit Ethylendiamin-tetramethylen-phosphonsäure (CAS 1429-50-1, EDTMP), die Affinität zu Knochengewebe besitzt, eine palliative Schmerzbehandlung bewirkt. Wiederholte Applikationen des Radioliganden erwiesen sich zunehmend als weniger effektiv. Die vorliegende Studie beschäftigt sich mit den Fragen, ob EDTMP die ^{153}Sm-EDTMP-Inkorporation blockiert oder begrenzt, wenn der Ligand sukzessiv appliziert wird.

Die Pharmakokinetik und die Blutverteilung von ^{153}Sm-EDTMP im gesunden Versuchstier (Pavian) während drei aufeinanderfolgender Applikationen (0,7 und 1,4 mg/kg Körpergewicht) wurden mittels Knochenszintigraphie untersucht. 111 MBq ^{153}Sm-EDTMP wurden jeweils

injiziert und 5 h lang gemessen. Die Kurven für die Tracerkinetik, für die Aufnahme in die Knochen relativ zum Hintergrund, für Blut und den angesammelten Urin wurden ermittelt. Vergleiche zwischen den aufeinanderfolgenden Applikationen und zwischen den beiden EDTMP-Konzentrationen wurden in jeder Gruppe statistisch ausgewertet.
Teilweise Blockierung der ^{153}Sm-EDTMP-Aufnahme durch die niedrigere EDTMP-Konzentration erreichte erst nach der dritten Applikation statistische Signifikanz. Die erste Applikation mit der höheren EDTMP-Konzentration ergab eine geringere Knochenaufnahme als die mit der niedrigeren EDTMP-Konzentration, was auf einen Blockierungseffekt bei der höheren Konzentration hinweist. Bei wiederholten Applikationen wurde das nicht beobachtet. Kontinuierliche Applikation der höheren EDTMP-Konzentration könnte zu einem verminderten Kalzium-Spiegel im Serum und demzufolge zu einem erhöhten Parathormon-Spiegel führen, wodurch osteoblastische Aktivitäten und Knochenwiederaufbau ausgelöst würden.

Key words Bisphosphonate, multiple applications · Bone metastases · Samarium-153, complexed to ethylenediamine tetramethylene phosphonic acid · ^{153}Sm-EDTMP

Arzneim.-Forsch./Drug Res. 48 (I), 408–414 (1998)

1. Introduction

Radiation teletherapy has been found effective to control or palliate isolated skeletal metastases. The therapeutic success in multifocal disease with bone-seeking radiopharmaceuticals will hinge on many interrelated factors, such as the careful choice of the radionuclide (of which the half-life and radiation emissions dictate its radiobiological effect) and on the bone localizing agent (of which the biochemical properties dictate its pharmacokinetics and biodistribution [1, 2, 3]. ^{153}Sm($t_{1/2}$ = 46.7 h; β = 805 keV [21 %]; 702 keV [44 %] and 632 keV [34 %]; max. soft-tissue penetration = 0.3 cm; γ = 103 keV [28 %]) is a radionuclide with nuclear properties suitable for therapeutic purposes. It is furthermore a lanthanide which forms a stable complex with bone-seeking phosphonates such as ethylenediamine tetramethylene phosphonic acid (EDTMP). ^{153}Sm-EDTMP has been experimentally investigated in animals and successfully tested in humans for pain palliation of bone metastases [4–9].

Information regarding the pharmacokinetics, biodistribution and bone localization of ^{153}Sm-EDTMP is needed to direct treatment protocols in humans. Such information has been obtained during extensive in vivo experimentation in non-human primates [9]. Preliminary patient studies, however, have shown that ^{153}Sm-EDTMP progressively loses its palliative effect with repeated administration as it becomes necessary. Dogs with osteosarcoma and treated with ^{153}Sm-EDTMP also showed no improved efficacy after a second administration (own experience). The question arises whether EDTMP exerts a blocking function, limiting access to the bone or osseous tumor with successive administration, or whether radiation damage to the vasculature system disturbs proper access of the radioligand into the tumor.

Bisphosphonates and multidentate phosphonates such as EDTMP are chemically stable and are not significantly metabolized. They are tightly bound to bone matrix and are powerful inhibitors of osteoclast mediated bone resorption [10]. Once taken up by the bone, bisphosphonates are liberated again only when the bone in which it was deposited is resorbed [11]. For example, the half-life of the bisphosphonate alendronate ([4-amino-1-hydroxybutylidene]bisphosphonate) in bone was estimated to be about three years for dogs and ten years for humans [11, 12]. There are also data, although conflicting, that the affinity of radiolabelled bisphosphonates for diagnostic bone imaging is altered in the presence of therapeutically administered bisphosphonates [13].

This investigation concerns the pharmacokinetics, biodistribution and bone localization of ^{153}Sm-EDTMP in the normal baboon experimental model during three successive applications (6-week intervals which resemble the patient protocol) with two different concentrations of EDTMP to possibly confirm its blocking effect.

Such information could assist in optimalizing the ligand as well as possibly lead to improved patient treatment protocols for palliation of painful bone metastases.

2. Materials and methods

2.1. Radiopharmaceutical

Isotopically enriched $^{152}Sm_2O_3$ (> 98 %) targets were irradiated for a maximum time of 50 h and a neutron flux of 1.0×10^{14} cm^{-2} s^{-1} in the Safari-1 Research Reactor. Following irradiation the targets were dissolved in 0.25 ml 0.2 mol/l HCl/mg Sm_2O_3 and diluted to result in a solution which is 0.04 mol/l in HCl, and filtered (0.22 µm).

EDTMP was synthesized in house by W.K.A. Louw. The ^{153}Sm-Ca/Na-EDTMP is prepared by adding one part of the $^{153}SmCl_3$ solution to three parts of 0.22 µm filtered Ca/Na-EDTMP solution (46.6 mg EDTMP × H_2O/ml and 7.05 mg/ml Ca as $Ca(OH)_2$ adjusted to pH 7.9–8.0 with NaOH) to form a solution containing samarium (< 200 µg/ml), EDTMP × H_2O (35 mg/ml), and 53 mg/ml Ca (as $Ca(OH)_2$), pH 7.5–8.0. This solution is then diluted with an appropriate volume of Ca/Na-EDTMP/0.4 mol/l HCl (3 : 1), to yield the individual animal doses containing ≈ 185 MBq ^{153}Sm and 0.7 mg EDTMP/kg b.wt. (low administered EDTMP level), and ≈ 185 MBq ^{153}Sm and 1.4 mg EDTMP/kg b.wt. (for the

high EDTMP level. Terminal sterilization of the product is achieved by steam autoclaving whereafter it is stored frozen to minimize radiolysis. The maximum lapse of time between production and administration was not more than three days.

Complex identity and radiochemical purity was determined by thin-layer chromatography on cellulose thin-layers (TLC aluminium sheets, cellulose (0.1 mm), E. Merck, Darmstadt, Germany), using ammonia (= 25 %): methanol : water (0.1 : 1 : 2) as solvent. ^{153}Sm-EDTMP was found at R_f = 0.75–0.85 and uncomplexed Sm^{3+} remained at the origin. The yield of the complex (always ≥ 99 %) was determined by ion exchange on CM-Sephadex C-25 (Sigma Chemical Co.).

2.2. Biodistribution of ^{153}Sm-EDTMP in the primate model

The animal experimentation was done according to the National Code for the Handling and Use of Animals in Research, Education, Diagnosis and Testing of Drugs and Related Substances in South Africa, and the protocol approved by the authorised Ethics Committee of the University of Pretoria. The animals were obtained from a registered breeder, kept under environmentally controlled conditions and fed fresh fruit and special primate pellets.

Twelve healthy male baboons (Papio ursinus), six each for the low and the high EDTMP concentration (average weight 27.5 kg) were used. Anaesthesia in each case was

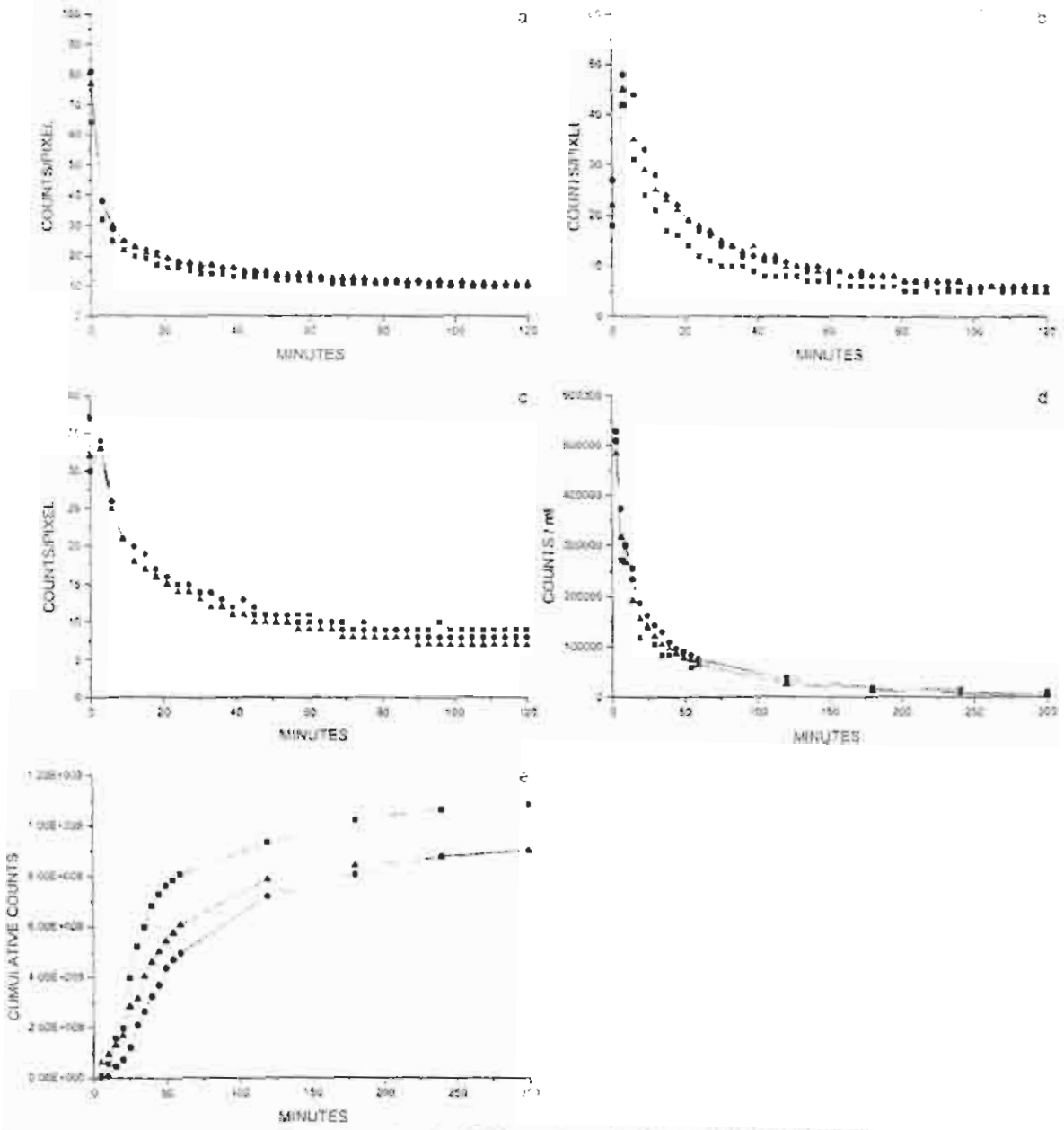

Fig. 1: a–c: Mean (n = 6) time-activity curves from the 2-h dynamic study of the cardiac blood pool *(a)*, kidney *(b)*, and liver *(c)* after the 0-week (■), 6-week (●), and 12-week (▲) applications of ^{153}Sm-EDTMP with low concentration of EDTMP. *d* and *e*: Mean (n = 6) blood clearance *(d)*, and cumulative urine values *(e)* of ^{153}Sm-EDTMP (low concentration) taken over 5 h after 0-week (■), 6-week (●) and 12-week (▲) applications.

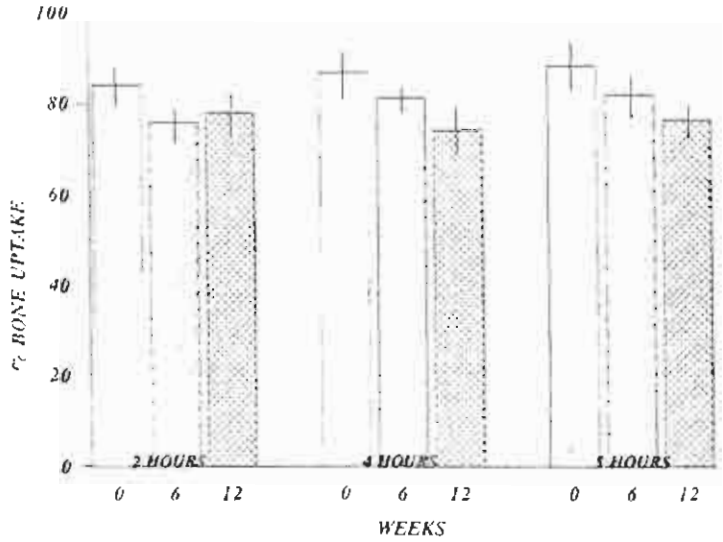

Fig. 2. Histogram of mean percentage bone uptake of ^{153}Sm-EDTMP (low concentration) obtained from 2-h-, 4-h-, and 5-h-static scintigraphy after 0-week (□), 6-week (▨), and 12-week (■) applications

induced with ketamine hydrochloride (10 ml/kg i.m. Ketalar, Parke Davis, S.A.) and maintained by an i.v. administration of pentabarbital sodium solution (9 mg/ml in saline: Sagatal, Maybaker, S.A.) at a rate of 30 ml/h in the vena cephalica from which, contralaterally, blood samples could be drawn. A urinary catheter (foley) was placed in the bladder to facilitate the collection of urine samples. Blood pressure and heart rate were continually monitored as well as blood gases.

Scintigraphy was performed (Siemens Orbiter gamma camera) with the animal in the supine position for planar images. The data acquisition initially involved a view of the thorax, liver and kidneys, and was performed as a dynamic study of 120 × 1 min frames on a count down bolus injection of 111 MBq ^{153}Sm-EDTMP. Static images of 4 min duration each followed at 2, 3, 4 and 5 h after the tracer injection. These images were chosen to present the skeletal structure from the skull to the pelvis as two matched images.

Blood and urine samples were collected at fixed intervals for 5 h, i.e. every 3 min for the first hour and then hourly for blood samples, and urine every 5 min for the first hour, subsequently hourly. The activity and volume of each sample were measured and registered.

From the dynamic study time-activity curves were obtained for the cardiac, kidney and liver regions. ROI (region of interest) placed on areas of the bony structures of skull, shoulder, sternum, ribs and pelvis as well as muscular background areas (no organs were visible at this stage) from the static images rendered relative region to background ratios after background subtraction. Consequently relative uptake of ^{153}Sm by the bone was calculated with bone and background taken as 100 %. Blood clearance and cumulative urine curves were also obtained. After 6 and later 12 weeks the same procedure was repeated for the six baboons in the low EDTMP concentration group.

A similar procedure followed also with three applications for the six baboons in the group receiving high EDTMP concentrations. Comparisons were drawn in each group between the successive applications and also between low and high concentrations. The statistical analysis was performed by Student's t-test for paired variables on a 5 % level of confidance.

3. Results

Time-activity curves for cardiac blood pool, kidney and liver obtained from the dynamic studies (0–120 min) with 0.7 mg ^{153}Sm-EDTMP/kg b.wt. after each of the consecutive tracer applications

Table 1. Mean half-times ($t_{1/2}$) of tracer clearance obtained from the dynamic organ distribution studies, for low and high concentrations of EDTMP after repeated administrations at 0, 6 and 12 weeks.

Low [EDTMP]	$t_{1/2}$ (min)		
	0 week	6 weeks	12 weeks
Cardiac blood pool	3.0 ± 0.5	4.0 ± 0.6	4.0 ± 0.4
Kidney	13.1 ± 4.1	16.3 ± 5.1	18.4 ± 4.2
Liver	12.4 ± 4.1	14.2 ± 5.3	18.6 ± 4.3
Blood samples	6.9 ± 1.4	9.1 ± 2.0	8.3 ± 2.1
High [EDTMP]	0 week	6 weeks	12 weeks
Cardiac blood pool	4.0 ± 0.3	4.0 ± 0.5	4.0 ± 0.3
Kidney	14.4 ± 4.1	14.6 ± 5.5	25.8 ± 7.1*
Liver	15.5 ± 5.3	15.4 ± 5.5	18.1 ± 4.3
Blood samples	8.1 ± 4.5	8.5 ± 3.0	8.1 ± 3.1

* $p < 0.05$.

Table 2. Percentage skeletal uptake of tracer with low and high EDTMP concentration at 2, 3, 4 and 5 h after administration during 0, 6 and 12 weeks repeated studies.

Low [EDTMP]	Percentage uptake in bone (%)		
	0 week	6 weeks	12 weeks
2 h	84.1 ± 4.3	75.8 ± 3.0	78.0 ± 4.6
3 h	82.4 ± 5.1	79.4 ± 5.2	79.5 ± 4.5
4 h	86.7 ± 4.7	81.2 ± 2.5	74.1 ± 5.0*
5 h	88.1 ± 4.4	81.8 ± 3.9	76.2 ± 3.6*
High [EDTMP]	0 week	6 weeks	12 weeks
2 h	75.5 ± 2.6	77.2 ± 5.4	77.2 ± 4.1
3 h	81.4 ± 3.3	79.2 ± 6.2	78.0 ± 5.2
4 h	82.4 ± 2.1	81.0 ± 7.9	80.4 ± 6.4
5 h	84.4 ± 5.3	86.7 ± 5.1	81.9 ± 3.3

* $p < 0.02$.

(time intervals of 0, 6 and 12 weeks) are presented in Fig. 1a, b, and c. No significant differences in the early biokinetics appear from these curves. Consequently the early phase (up to the first 120 min) average washout rates from the cardiac bloodpool, kidneys, liver and whole blood sampling (Fig. 1d) expressed in terms of $t_{1/2}$ of clearance and presented in Table 1 are not statistically significantly different, but show a tendency of slower clearance especially for the kidney, liver and blood with repeated applications. The urine excretion of the tracer after the first application furthermore reached a higher (by 21 %) cumulative value after 5 h than for the second and third applications which in turn did not differ from each other (Fig. 1e). Large standard deviations of the order of 40 % jeopardised statistical validation in this case. Partial renal clearances estimated from the blood curves also did not differ significantly.

The tracer uptake and retention in the bone structure which was measured at 2, 3, 4 and 5 h by static acquisition produced additional count rate data which are shown as percentage bone uptake of the tracer (considering only the skeletal and soft tissue compartments; only these were still visible) at 2, 3, 4 and 5 h (Fig. 2, Table 2). Decreased uptake is seen at 4 and 5 h with consecutive applications – on the average 6.0 % less between the first two applications and likewise (6.3 %) between the second and third injections. Statistical significant differ-

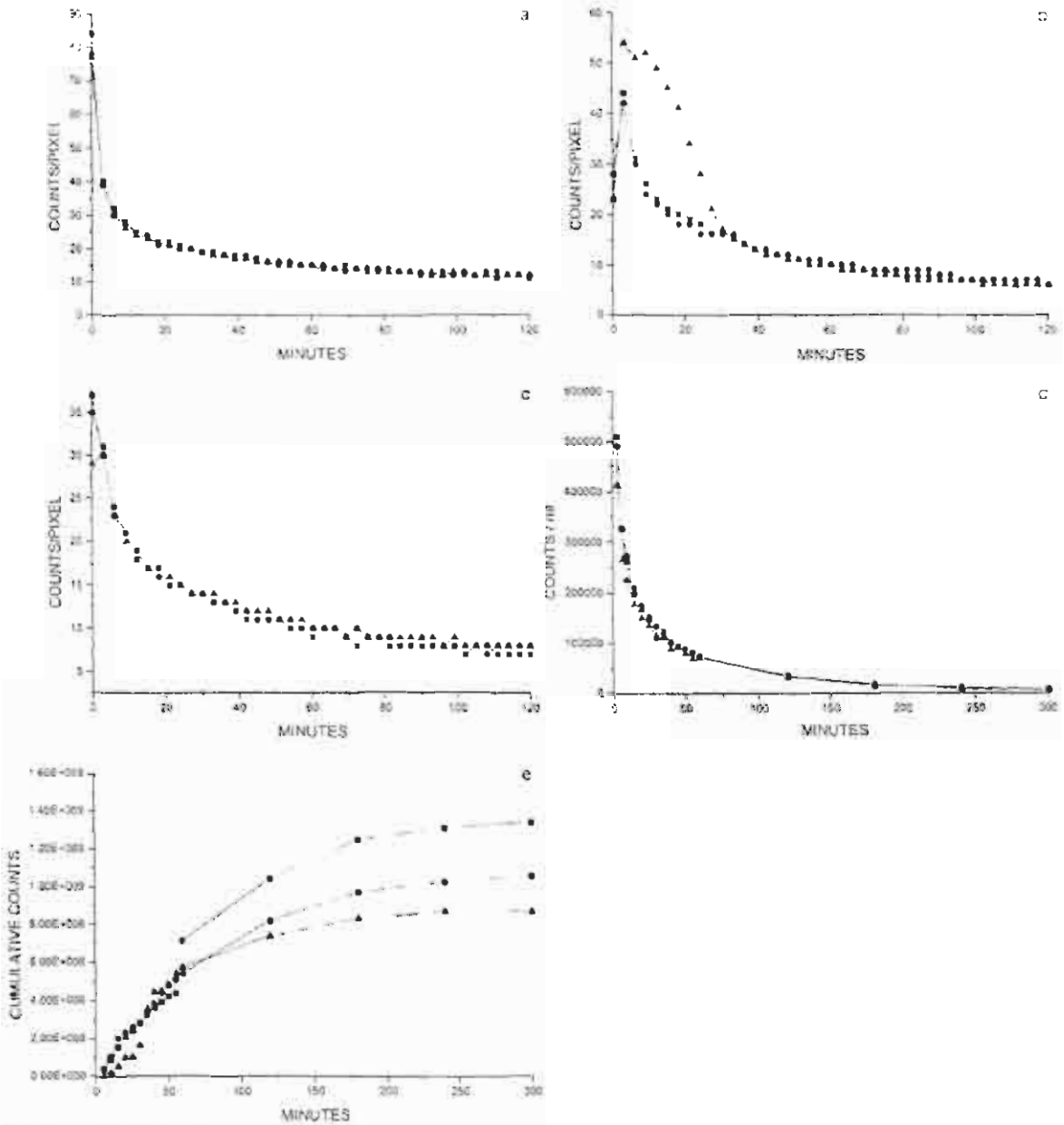

Fig. 3. a–c: Mean (n = 6) time-activity curves from the 2-h dynamic study of cardiac blood pool *(a)*, kidney *(b)*, and liver *(c)* after the 0-week (■), 6-week (●), and 12-week (▲) application of ^{153}Sm-EDTMP with high concentration EDTMP. *d* and *e*: Mean blood clearance *(d)*, and cumulative urine values *(e)* of ^{153}Sm-EDTMP (high concentration) taken over 5 h after 0-week (■), 6-week (●), and 12-week (▲) applications.

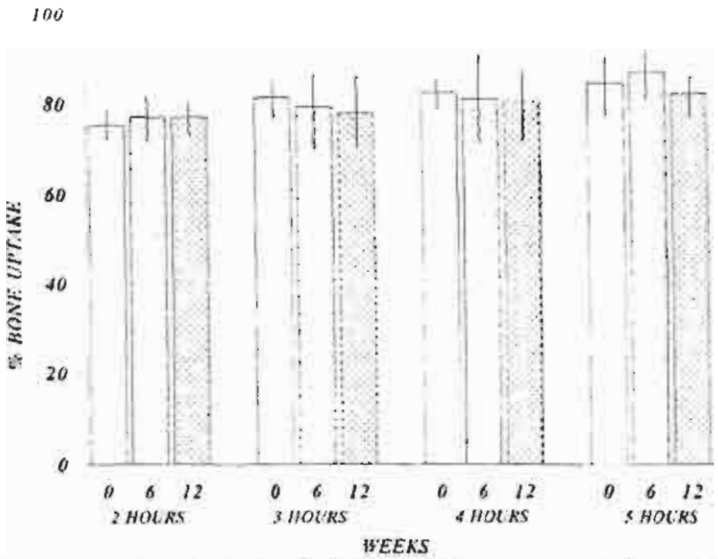

Fig. 4 Histograms of mean percentage bone uptake of ^{153}Sm-EDTMP (high concentration) obtained from 2-h-, 3-h-, 4-h- and 5-h-static scintigraphy after 0-week (□), 6-week (▨), and 12-week (■) applications.

ences are reached between the 0 and 6 week injections at 2 h ($p < 0.05$), but not at 5 h ($0.05 < p < 0.01$) between the 0 and 12 week administrations at 4 and 5 h ($p < 0.02$), but not at 3 h ($0.05 < p < 0.01$). It is at 4 and 5 h that maximum uptake of ^{153}Sm-EDTMP has been proven to occur [9].

In the high EDTMP group of animals which received the 1.4 mg EDTMP/kg b.wt. the time-activity curves of cardiac bloodpool and liver indicated no biokinetic and biodistribution differences between the tracer applications (0, 6 and 12 weeks; Fig. 3a and c). The kidney, however, (Fig. 3b), presented markedly delayed excretion of the tracer at the third application. This is confirmed by the $t_{\frac{1}{2}}$ values for the kidney clearance in Table 1 ($t_{\frac{1}{2}}$ = 25.8 ± 7.1) at the third application ($p < 0.05$). Delayed kidney clearance is also illustrated (Fig. 3e) in the cumulative urine values after 12 weeks, where a clear blocking effect of ^{153}Sm-EDTMP excretion is seen in the first 30 min after the application of the high EDTMP concentration followed by the subsequent sudden increase of tracer clearance.

The blood clearance curves show no differences between the three applications (Fig. 3d and Table 1), and from these the calculated renal clearance values were also not different.

The tracer uptake and retention of the high EDTMP concentration in the bone structure as measured during the static studies at 2, 3, 4 and 5 h show no statistical significant changes between the 0, 6 and 12 weeks administrations (Fig. 4, Table 2). At 0 weeks, however, the tracer with the high concentration of EDTMP indicates reduced uptake with respect to the low concentration ($p > 0.05$). This pattern was not repeated at 6 and 12 weeks (Fig. 2 and 4). The scintigrams (which are not shown here) clearly illustrate reduced skeletal uptake with repeated administration.

4. Discussion

Two principle factors lead to the accumulation of radiopharmaceuticals in bone. These are blood flow and extraction efficiency [14]. An additional factor to consider is capillary permeability [14]. In a recent review [10] of bisphosphonates used for senile osteoporosis it was reported that the incubation of the bisphosphonate alendronate with human bone particles resulted in rapid, reversible and saturable bonding. Alendronate is an aminobisphosphonate which has higher antiresorbing activity than the bisphosphonate etidronate which has no amino group [10]. EDTMP is a multidentate aminophosphonate ligand [10] which localizes in bone by bridging hydroxyapatite [15] and can therefore be presumed to similarly participate in saturable bonding which could influence the extraction efficiency of the ligand during multiple applications.

A phenomenon of partial blocking indeed appears present in this primate study with the low EDTMP concentration, as can be seen from the reduced ^{153}Sm-EDTMP uptake in the bone with repeated applications. The effect reached statistical significance only after the third application ($p < 0.02$). Furthermore already at the first application (0 weeks) of the high concentration of EDTMP a lower bone uptake was observed when compared to the lower concentration probably pointing to a blocking phenomenon by the high concentration of the EDTMP. The 0-week values of the high concentration do not show much change with repeated applications. It can be speculated that continual application of EDTMP, especially at high concentration, will lead to reduced serum calcium levels increasing parathyroid hormone concentrations [10, 13] which in turn might trigger osteoblastic activity and some bone remodelling, thus partially offsetting the blocking which was consequently more clearly illustrated at the low EDTMP concentration [16, 17].

In this study, haemodynamically monitored under controlled anaesthesia and each animal being its own reference, no blood flow changes need to be considered. Early changes in capillary permeability could maybe follow from localized radiation damage to the skeletal microvasculature and could also cause reduction in bone metabolism visible in the subsequent administration [18]. However, the 0 week difference between the low and high EDTMP concentrations ^{153}Sm-EDTMP cannot be attributed to radiation damage effects on bone metabolism, and would seem to negate radiation effects at this stage. So also does the fact that no reduction in uptake is seen for the high EDTMP concentration with multiple applications and the same radioactive dose as with the low EDTMP concentration.

In considering the early biokinetic data it should be noted that renal excretion is the only route of elimination of bisphosphonates. Animal and human studies indicate that systemically administered bisphosphonates are partly taken up by bone and the remainder excreted by the kidneys [10].

The effect of delayed kidney clearance ($t_{1/2}$) seen in this study progressively with multiple administrations of ^{153}Sm-EDTMP and especially pronounced after the third application of the high EDTMP concentration could possibly be explained by a saturable transport mechanism in the kidney by bisphosphonates also seen in rat studies [10, 19]. Compromising the renal excretion as seems the case in this study with multiple ^{153}Sm-EDTMP applications could also explain the general delayed clearance pattern seen in the dynamic studies [15]. However, no significant differences could be found in partial renal clearances calculated from the blood clearance curves.

Bisphosphonates bind preferentially to bones with high turnover rates and their distribution is not homogeneous. The preferential localization of bisphosphonates could be due to the larger exposure of hydroxyapatite at sites prepared for undergoing bone resorption which makes them accessible to the drugs in circulation [20]. Trabecular bone accounts for 80 % of the bone turnover although it represents only 20 % of the skeleton [21]. The near absence of long bones in the ^{153}Sm-EDTMP scintigrams and the high activity in trabecular bone (ribcage, vertebrae, sternum, shoulder and wrist joints) have been found typical of ^{153}Sm-EDTMP [9], ^{153}Re-HEDP (hydroxyethylidenediphosphonate) [22] but to some extent different to the routinely used diagnostic ligand ^{99m}Tc-MDP (methylenediphosphonate). Although all bisphosphonates have similar physicochemical properties, their anti-resorbing activities differ substantially [14]. This could be the reason for the conflicting data on possible impaired sensitivity of radiopharmaceutical bone imaging after previous bisphosphonate therapy [12, 23, 24, 25].

5. Conclusion

The results of the present primate study clearly indicate a blocking effect to the entry of ^{153}Sm-EDTMP into normal bone with repeated applications of the low EDTMP concentration. To avoid this effect during a palliative treatment of patients with skeletal metastases the use of the higher concentration of the EDTMP ligand could be recommended but only on condition that no renal damage takes place. Due to the bone remodelling effect seen here at high EDTMP concentration, its combination with a stronger β-emitter (^{166}Ho) could maybe enhance the palliative effect.

5. References

[1] Wessels, B. W., Rogus, R. D., Med. Phys. **11**, 638 (1984)

[2] Humm, J. L., J. Nucl. Med. **27**, 1490 (1986)

[3] Volkert, W. A., Goeckeler, W. F., Ehrhardt, G. J., J. Nucl. Med. **32**, 174 (1991)

[4] Goeckler, W. F., Edwards, B., Volkert, W. A., J. Nucl. Med. **28**, 494 (1987)

[5] Turner, J. H., Martindale, A. A., Sorby, P., Eur. J. Nucl. Med. **15**, 784 (1989)

[6] Lattimer, J. C., Corvin, L. A., Stapleton, J., J. Nucl. Med. **31**, 586 (1990)

[7] Farbanghi, M., Holmes, R. A., Volkert, W. A., J. Nucl. Med. **33**, 1451 (1992)

[8] Enry, J. F., Collins, C., Stabin, M. J. Nucl. Med. **34**, 1031 (1993)

[9] Louw, W. K. A., Dormehl, I. C., Van Rensburg, A. J., J. Nucl. Med. Biol. **23**, 935 (1996)

[10] Lin, J. H., Bone **18**, 22 (1996)

[11] Lin, S. H., Duggan, D. E., Chen, I. W., Drug Metab. Dispos. **19**, 926 (1991)

[12] Gertz, R. I., Holland, S. D., Kline, W. B., Osteopor. Int. **19**, (1993)

[13] Percherstorfer, M., Schilling, T., Janisch, S., J. Nucl. Med. **34**, 1039 (1993)

[14] Garcia, J. F., Mettler, F. A., Radionuclide and bone imaging and densitometry, Churchill Livingston, New York (1988)

[15] Holmes, R. A., Semin. Oncol. **20**, 22 (1993)

[16] Hortobagyi, G. N., Libshitz, H. I., Deabold, J. E., Cancer **53**, 577 (1984)

[17] Cloleman, R. E., Mashiter, G., Whitaker, K. B., J. Nucl. Med. **29**, 1354 (1988)

[18] Charkes, N. D., Silverman, C., J. Nucl. Med. **33**, 1780 (1992)

[19] Lin, J. H., Chen, I. W., De Luna, F. A., Drug Metab. Dispos. **20**, 608 (1992)

[20] Sahni, M., Guenther, H. L., Fleisch, H., J. Clin. Invest. **91**, 2004 (1993)

[21] Fleisch, H., Stampth **8**, 24 (1993)

[22] Palmedo, H., Bender, H., Schomburg, A., Nucl. Med. **35**, 63 (1996)

[23] Krasnow, A. Z., Collier, B. D., Isitman, A. T., Clin. Nucl. Med. **13**, 264 (1988)

[24] Westmark, K. D., Nagel, J. S., Franceshi, D., N. Engl. J. Med. **323**, 1633 (1990)

[25] Serafini, A. N., Int. J. Rad. Oncol. Biol. Phys. **30**, 1187 (1994)

Acknowledgements

We would like to express our gratitude to the National Cancer Association of South Africa for the funding of this project. Also to the staff of the H. A. Grove Research Centre, thank you for handling and care of the animals.

Correspondence: Prof. Irene C. Dormehl (DSc), AEC Institute for Life Sciences, University of Pretoria, P.O. Box 2034, Pretoria 0001 (South Africa)

Antibiotika · Chemotherapeutika · Virustatika · Zytostatika

Biodistribution and Pharmacokinetics of Variously Sized Molecular Radiolabelled Polyethyleneiminomethyl Phosphonic Acid as a Selective Bone Seeker for Therapy in the Normal Primate Model

Irene C. Dormehl[a], Werner K. A. Louw[b], Rowan J. Milner[a], Elmaré Kilian[a], and Frank H. A. Schneeweiss[c]

AEC (Atomic Energy Corporation) Institute for Life Sciences, University of Pretoria[a], (Republic of South Africa), Atomic Energy Corperation of South Africa Ltd.[b], Pelindaba (Republic of South Africa), and Institut für Medizin, Forschungszentrum Jülich, Jülich (Germany)

Summary

An ideal radiopharmaceutical for the treatment of neoplastic and inflammatory (benign) bone disease would be a radiolabelled compound that predominantly accumulates in bone lesions with limited access to normal bone and other organs. Neoplastic tissue's abnormal blood supply (increased permeability) and lack of lymphatics will selectively accumulate radiolabelled macromolecules. This enhanced permeability and retention effect forms the basis of this study, using various molecular sizes of the radiolabelled macromolecule polyethyleneiminomethyl phosphonic acid (PEI-MP) for increased selectivity of the bone-seeking radiopharmaceutical. PEI-MP was synthesized by condensation of polyethyleneimine, phosphonic acid and formaldehyde, followed by fractionation into different molecular sizes by membrane ultrafiltration. Labelling efficiency to ^{99m}Tc (as radiotracer) was ~ 99 % with complexes stable for 24 h. The pharmacokinetics and biodistribution of various ^{99m}Tc-PEI-MP fractions were investigated using 4 experimental baboons (*Papio ursinus*) per fraction. Scintigraphy was performed on the baboons under general anesthesia of pentobarbital i.v. After an i.v. bolus of ^{99m}Tc-PEI-MP (~ 185 MBq) both dynamic studies (30 × 1 min frames), and static studies (2 min acquisition every hour for 4 h) were done, as well as blood samples and urine collected. From the results macromolecules with sizes ranging between 30–300 kDa were characterized by excessive liver (21 %–57 % retained activity) and kidney (40 % retained activity) uptake and accompanying long residing times ($t_{1/2}$ up to 24 h). The percentage bone uptake averaged at 8 % for these particles excluding sizes 100–300 kDa where very little bone uptake was seen (< 1 %). In this case the blood clearance was also slow ($t_{1/2}$ ~ 2 h). The fraction size 10–30 kDa had comparatively low accumulation and short residence times in the liver and kidneys (resp. 20 %, $t_{1/2}$ = 22 ± 4 min; 17.5 %, $t_{1/2}$ = 20 ± 3 min) and although the bone uptake of 18 % in this case was high, it is still low for a bone-seeking agent. These particles cleared the blood with $t_{1/2}$ = 25 ± 2 min and seemed suitable for labelling with a therapeutic radioisotopic agent.

Key words

- Bone disease, inflammatory, neoplastic
- Polyethyleneiminomethyl phosphonic acid, biodistribution, macromolecules, pharmacokinetics
- Radionuclide therapy
- Technetium ligands

Arzneim.-Forsch./Drug Res. 51 (I), 258–263 (2001)

Arzneim.-Forsch./Drug Res. 51 (I), 258–263 (2001)

Antibiotics · Antiviral Drugs · Chemotherapeutics · Cytostatics

Zusammenfassung

Verteilung und Pharmakokinetik von radioaktiv markierter Polyethylenimino-methylphosphonsäure unterschiedlicher Molekülgröße als selektiver Knochensucher im normalen Primatenmodell

Ein ideales Radiopharmazeutikum für die Behandlung von neoplastischen und entzündlichen (benignen) Knochenkrankheiten stellt eine radioaktiv markierte Verbindung dar, die sich vorwiegend an Knochenläsionen anreichert und zu normalen Knochen und anderen Organen einen möglichst begrenzten Zugang hat. Die anomale Blutversorgung infolge steigender Gefäßpermeabilität sowie das Fehlen lymphatischer Gefäße in neoplastischem Gewebe können eine selektive Akkumulation radioaktiv markierter Makromoleküle bewirken. Diese erhöhte Permeabilität und der Retentionseffekt bilden die Basis für die vorliegende Arbeit, die verschiedene Molekülgrößen des radioaktiv markierten Makromoleküls Polyethylenimino-methylphosphonsäure (PEI-MP) für zunehmende Selektivität des knochensuchenden Radiopharmazeutikums benutzt. PEI-MP wurde durch Kondensation von Polyethylenimino-phosphonsäure mit Formaldehyd synthetisiert. Die Fraktionierung in verschiedene Molekülgrößen erfolgte mittels Membranultrafiltration. Die Markierungseffizienz des Komplexes mit ^{99m}Tc als Radiotracer betrug ca. 99 % bei 24stündiger Stabilität. Die Pharmakokinetik und die Bioverteilung von verschiedenen ^{99m}Tc-PEI-MP-Fraktionen wurde an 4 Pavianen (*Papio ursinus*) pro Fraktion untersucht. Szintigraphische Messungen wurden an den Versuchstieren unter allgemeiner Anästhesie mit Pentobarbital durchgeführt. Nach einem i.v. Bolus von ca. 185 MBq ^{99m}Tc-PEI-MP erfolgten dynamische (30 × 1 min Bilder) und statische Untersuchungen (Akquisition: 2 min Dauer für 4 h). Zusätzlich wurden Blutproben genommen und Urin gesammelt. Die Resultate zeigten, daß Makromoleküle, deren Größe zwischen 30 und 300 kDa lag, durch exzessive Aufnahme in Leber und Nieren (verbleibende Radioaktivität: 21–57 % bzw. 40 %) sowie bei gleichzeitig langer Verweildauer ($t_{1/2}$ bis zu 24 h) charakterisiert waren. Die durchschnittliche prozentuale Aufnahme in die Knochen betrug 8 % für diese Makromoleküle, ausschließlich solcher, deren Größe 100–300 kDa betrug und die eine sehr kleine (< 1 %) Knochenaufnahme zeigten. In diesem Falle war die Blut-Clearance auch langsam ($t_{1/2}$ = 2 h). Die 10–30 kDa-Fraktion zeigte eine relativ niedrige Akkumulation und Verweildauer sowohl in Leber (20 %, $t_{1/2}$ = 22 ± 4 min) als auch in den Nieren (17.5 %, $t_{1/2}$ = 20 ± 3 min). Obwohl die Knochenaufnahme dieser Fraktion mit 15 % hoch erschien, war sie für einen Knochensucher relativ niedrig. Ihre Blut-Clearance betrug 25 ± 2 min und schien daher für eine Markierung mit einem therapeutischen Radioisotop geeignet zu sein.

1. Introduction

A variety of skeletal diseases eg. osseous metastases, various bone tumours and inflammatory skeletal disease such as ankylosing spondylitis, Paget's disease and rheumatoid arthritis result in severe skeletal pain, immobility, anxiety, and severely diminish a patient's quality of life.

Radiation teletherapy is to some extent effective to control or palliate isolated skeletal pain foci from these diseases. Difficulties associated with its application in multifocal disease together with recent commercial availability of various bone-seeking radiopharmaceuticals eg. strontium-89 (^{89}Sr), samarium-153 (^{153}Sm)-ethylenediaminetetramethylene phosphonate and rhenium-186 (^{186}Re)-hydroxyethylidene diphosphonate [1, 2], led to renewed interest in systemic treatment with internal radionuclide therapy. Intravenously administered bone-seeking radioisotopic agents distribute via the circulatory system throughout the body while simultaneously accumulating in the bone. The material not taken up by the bone is efficiently cleared through the kidneys into the bladder [1, 2]. Using this modality all involved osseous sites can be treated simultaneously with limited associated toxicity. Selective absorption into bone and especially into diseased bony areas limits irradiation to normal tissues and increases the therapeutic ratio.

Therapeutic (and also diagnostic) success of a radiopharmaceutical will hinge on many interrelated factors, such as the careful choice of a radionuclide (of which its half-life and radiation emissions dictate its radiobiological effects and its diagnostic image quality), linked to a bone localising agent of which the biochemical properties dictate its pharmacokinetics and biodistribution.

The basic principle for the design of diagnostic and therapeutic radiopharmaceuticals is the incorporation of a suitable radionuclide in an appropriate chemical compound to attain the highest target-to-background concentration ratio. The important concern, especially with therapeutic radiopharmaceuticals, is to maximise the radiation dose to the lesion while minimising that to the remainder of the body, most specifically to the critical organ in this case, the radiosensitive bone marrow.

Bisphosphonates and aminophosphonic acids (eg. ethylenediaminetetramethylene phosphonic acid [EDTMP]) are chemically stable and are not significantly metabolised. They bind tightly to the bone matrix, and once taken up by bone are liberated only when the bone in which it was deposited is resorbed [3].

Particle-emitting radionuclides, eg. β-emitting ^{153}Sm, have been complexed with bisphosphonates and substituted organic amine phosphonic acid derivatives, eg. EDTMP, wherein the nitrogen and phosphorous are interconnected by an alkylene or substituted alkylene group. Certain of these complexes have been shown to be very selective for the skeletal system with very low

soft tissue uptake [4]. The complexes also tend to concentrate in areas of fast growing bone much more readily than in normal bone. The radionuclides used are mostly β-particle emitting, and a high radiation dose is delivered in the area where they are deposited. Thus therapeutic radiation doses can be delivered specifically to calcific tumours. These complexes (eg. ^{153}Sm-ethylenediaminetetramethylene phosphonate) have been found useful in the treatment of such tumours in humans and animals [5–8]. Unfortunately the selectivity towards fast growing bone (tumour areas) is not adequate so as to avoid bone marrow suppression, which limits the radioactivity doses that can be given to a patient, and thus also the therapeutic efficacy of the agent. Any radionuclide that ends up on trabecular bone, or in the inner surface of cortical bone, will deposit energy in the radiosensitive bone marrow [9].

The principal factors that lead to the accumulation of radiopharmaceuticals in bone are blood flow, extraction efficacy and capillary permeability. The discovery that macromolecules and small particles accumulate passively in solid tumour tissue has had enormous implications for improved design of targeted chemotherapy [10, 11]. This phenomenon has been called the "enhanced permeability and retention effect" (EPR-effect) and has been attributed to two main factors: tumour vasculature often displays a disrupted endothelium (i.e. becomes leaky), which allows macromolecular extravasation to a greater extent than seen via most other endothelial barriers, and also a lack of effective lymphatic drainage, leading to macromolecular accumulation. Generally tumour tissues and inflammatory areas are characterised by an increased permeability of capillary endothelial layers to blood-borne macromolecules. Administration of radiolabelled macromolecules thus leads to a selective accumulation of radioactivity in these areas. Furthermore, if these tumours or inflammatory areas are calcified or associated with the bone matrix, the selective retention of the phosphonate containing macromolecule will also be enhanced by its binding to the hydroxyapatite bone matrix. At the same time the normal bone (and especially the radiosensitive red-marrow) is protected by the normal impermeability of their capillary endothelial layers to blood-borne macromolecules (≥ 60 kDa) [12]. Higher and more effective therapeutic doses are thus attainable.

With small molecules (eg. ^{153}Sm-EDTMP) a significant part of the administered radioactivity is eliminated in the kidneys by glomerular filtration. By increasing the molecular weight, glomerular elimination, and thus also the administered dose can be reduced [13].

The biodistribution and pharmacokinetics of various radionuclide complexes were studied in this investigation in the normal chacma baboon *(Papio ursinus)*. These studies were conducted by injecting the ^{99m}Tc complexes of polyethyleneiminomethyl phosphonic acid (PEI-MP) fractions of various molecular sizes into the experimental animals to obtain the gamma ray images of the entire animal at various times up to 4 h after injection. In this manner an optimal molecular size of polymeric macromolecular radioactive compounds can be determined with optimal protection of normal bone, liver and kidney. ^{99m}Tc is in this study used as a tracer isotope to follow the pharmacokinetics, with no therapeutic properties.

2. Materials and methods

2.1. Synthesis of polyethyleneiminomethyl phosphonic acid (PEI-MP)

PEI-MP was prepared by the condensation of polyethyleneimine (PEI), phosphorous acid and formaldehyde by a modified Mannich reaction in the presence of hydrochloric acid [14, 15].

Phosphorous acid (10.36 g) (Riedel-de Haën, Seelze, Germany), was dissolved in 51.3 ml concentrated hydrochloric acid (32 %, pro analysi, E. Merck, Darmstadt, Germany), while stirring and heating to 60 °C. After dropwise addition of 32 % formaldehyde solution (pro analysi, E. Merck), the temperature was raised to 90 °C (refluxing temperature) and a solution of 8.33 g polyethyleneimine (Polymin®, water-free, BASF, Ludwigshafen, Germany) in 40 ml water, was slowly added to the reaction mixture at a rate of 0.3 ml/min. The reaction mixture was continuously purged with argon. When addition of the polyethyleneimine solution was completed, the reaction mixture was stirred under reflux for another hour, then allowed to cool slowly overnight during which the product separated as a viscous oil. After decanting the mother liquid, 50 ml water was added to the oily precipitate which formed a doughy mass upon stirring.

The liquid phase was decanted and the process repeated twice whereafter the doughy material was dissolved in 37 ml of molar sodium carbonate solution to form the water soluble sodium salt of PEI-MP (pH 7.0). After lyophilization 12 g of PEI-MP was obtained.

2.2. Purification and fractionation of PEI-MP

The macromolecule PEI-MP as prepared above, was further purified and fractionated into different macromolecular sized fractions by membrane ultrafiltration using commercially available polyethersulfone membranes. An aqueous solution of sodium PEI-MP was subjected to a sequential ultrafiltration process through a sequence of 300, 100, 50, 30, 10, and 3 kDa ultrafiltration membranes (Filtron Technology Corp., Northborough, MA, USA). The membrane retentates were washed with distilled water to a theoretically calculated purity of 99 %, to yield 3–10, 10–30, 30–50, 50–100, and 100–300 kDa macromolecular sized fractions (see Table 1).

Typical elemental analysis gave a C:N molar ratio of 2.97:1, which on the basis of a empirical formula of a PEI-MP monomer of $C_9H_{18}N_3O_9P_3$, indicates a high level of methylphosphonation, in contrast to PEI with a monomer empirical formula of C_2H_5N and a ratio C:N of 2:1.

2.3. Labelling of PEI-MP with ^{99m}Tc

The ligand PEI-MP was labelled with (as tracer) by adding sodium pertechnetate (up to 50 mCi) to lyophilized kits of the ligand (10 mg) and a reducing agent (stannous chloride dihydrate 0.5 mg) to produce the labelled complex (pH 5.0–5.5).

Arzneim.-Forsch./Drug Res. 51 (I), 258–263 (2001)

Table 1: Percentage yield of PEI-MP fractions obtained by membrane ultrafiltration.

Fraction (kDa)	Percentage yield
< 3	28.1
3–10	7.8
10–30	9.2
30–50	6.4
50–100	32.4
100–300	17.7
> 300	7.8

Table 3: Mean percentage (n = 4) of injected dose of different ^{99m}Tc-PEI-MP fractions excreted through kidneys after 4 h.

Fraction (kDa)	% of injected dose excreted through the kidneys after 4 h
3–10	40.6
10–30	52.8
30–50	62.0
50–100	28.2
100–300	12.2

The radiolabelled complexes were analysed for radiochemical purity using instant thin-layer chromatography on silica gel impregnated glass-fibre sheets as stationary phase and acetone and 0.9 % sodium chloride solutions as mobile phase. The radiochemical purity of the complexes was > 95 %.

2.4. Biodistribution of ^{99m}Tc-PEI-MP

Twenty healthy male baboons, average weight 27.5 kg, were used in the study and received i.v. ^{99m}Tc-PEI-MP of various molecular sizes. All studies were performed after approval by the Ethics Committee of the University of Pretoria, according to the guidelines of the National Code for Animal Use in Research, Education, Diagnosis and Testing of Drugs and Related Substances in South Africa.

The baboons (n = 4 in each group) were subjected to identical experimental procedures except for the mentioned differences in molecular size of the injected ^{99m}Tc-PEI-MP molecules. Five different size fractions (groups) of the PEI-MP macromolecule were studied, viz in the following ranges: (1) 3–10, (2) 10–30, (3) 30–50, (4) 50–100 and (5) 100–300 kDa. Induction of anaesthesia was performed with ketamine hydrochloride (10 mg/kg i.m.). (Ketalar Parke Davis, Cape Town, S.A.), and immediately followed by a maintained controlled infusion of a 6 % sodium pentobarbitone solution (Sagatal Kyron Laboratories Pty. Ltd., Benrose, S.A.) at 30 ml/h. The animal in the supine position under the gamma camera was injected i.v. with a bolus of 185–250 MBq of ^{99m}Tc-PEI-MP and data acquisition started on a count down with a Siemens Orbiter gamma camera (Siemens, Erlangen, Germany) in 64 × 64 word mode performing a 30 min dynamic study (30 × 1 min frames). At 1, 2, 3, and 4 h, and also at 24 h static images of 120 s were acquired.

Blood and urine samples were collected at fixed intervals for 4 h, viz every 3 min for the first hour, then hourly for blood samples, and urine every five min for the first hour, subsequently hourly. The activity and volume of each sample were recorded.

Regions of interest (ROIs) were placed on the images of cardiac blood pool, liver, lung, spleen, kidneys, and spine (the vertebrae) to obtain time-activity curves of the dynamic study. Similarly, data of countrate per pixel for the ROIs, which were decay-corrected, were obtained from the static images. These were normalised to extend the time-activity curves of the dynamic study to 4 h.

Blood clearance and cumulative urine curves were also obtained in all cases so that average relative organ distributions of the retained activity and eventually of the injected dose (i.d.) could be obtained for all ^{99m}Tc-labelled molecular size fractions. These could be compared for optimal distribution characteristics for therapy according to the mentioned criteria. The statistical analysis was performed by Student's t-test for paired variables on a 5 % level of confidence.

3. Results

The mean (n = 4) half-life of retention of the different ^{99m}Tc-PEI-MP fractions are given in Table 2 for various body compartments including the cardiac blood pool. Also in Table 2 is the highest mean percentage uptake (n = 4) of the different fractions during the first 4 h in the various compartments. The mean (n = 4) percentages of injected dose of the different ^{99m}Tc-PEI-MP fractions excreted by the kidney after 4 h post injection are presented in Table 3. Mean time activity curves as a percentage of retained body activity for the different ^{99m}Tc-PEI-MP fractions for the liver and kidney are presented in Fig. 1 and 2, as well as normalised blood clearance curves in Fig. 3.

Table 2: Mean $t_{1/2}$ in min (n = 4) and mean maximum percentage uptake (in the first 4 h) of the various ^{99m}Tc-PEI-MP fractions in the various body compartments of the primate model.

Fraction (kDa)	$t_{1/2}$ (min) and percentage of uptake					
	Cardia blood pool	Liver	Kidney	Lung	Spleen	Bone
3–10	10 ± 1 15 ± 4 %	90 ± 22 16 ± 1 %	> 4 h 30 ± 4 %	10 ± 1.5 8 ± 2 %	75 ± 2 10 ± 1 %	> 2 h 8 ± 1 %
10–30	10 ± 1.5 15 ± 3 %	22 ± 3 20 ± 2 %	20 ± 3 18 ± 4 %	15 ± 3 12.5 ± 4 %	60 ± 9 12.5 ± 1 %	> 4 h 10 ± 1 %
30–50	8 ± 2 10 ± 4 %	68 ± 15 20 ± 2 %	> 4 h 40 ± 5 %	8 ± 2 7.5 ± 2 %	45 ± 8 8 ± 3 %	> 4 h 9 ± 0.5 %
50–100	12 ± 1.5 15 ± 4 %	> 4 h 43 ± 3 %	> 4 h 15 ± 2 %	22 ± 2 9 ± 3 %	> 4 h 8 ± 0.5 %	> 24 h ± 2 h 7 ± 0.5 %
100–300	2 h ± 0.1 h 30 ± 7 %	24 h ± 1.5 h 57 ± 9 %	- -	2.5 h ± 0.5 h 7.5 ± 2 %	> 24 h ± 2 h 5.5 ± 2	- -

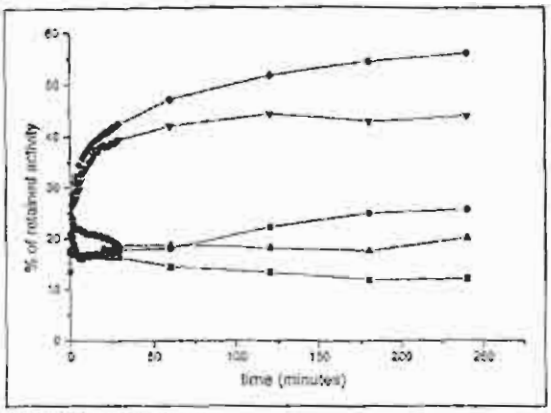

Fig. 1: Percentage of retained body activity for different ^{99m}Tc-PEI-MP fractions in the primate liver. ■ = Fraction 3–10, ● = Fraction 10–30, ▲ = Fraction 30–50, ▼ = Fraction 50–100, ◆ = Fraction 100–300.

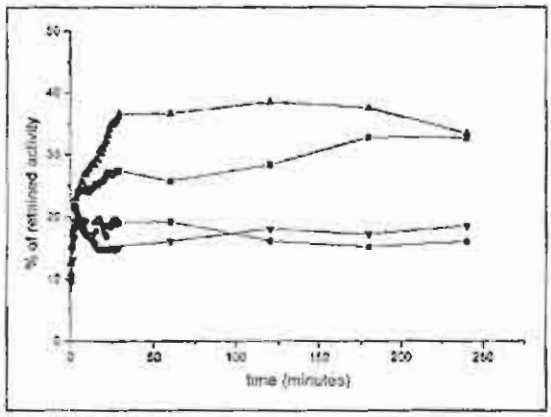

Fig. 2: Mean percentage of retained body activity for different ^{99m}Tc-PEI-MP fractions in the primate kidney. ■ = Fraction 3–10, ● = Fraction 10–30, ▲ = Fraction 30–50, ▼ = Fraction 50–100.

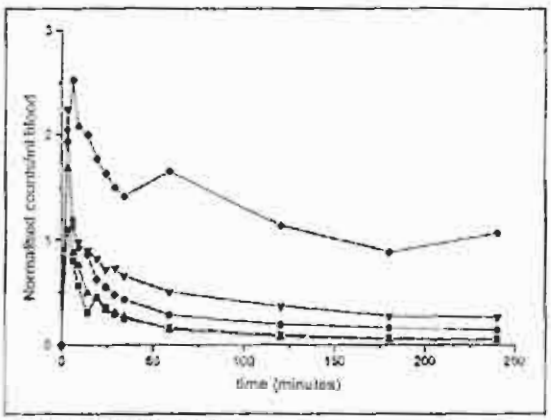

Fig. 3: Normalised blood clearance for different ^{99m}Tc-PEI-MP ■ = Fraction 3–10, ● = Fraction 10–30, ▲ = Fraction 30–50, ▼ = Fraction 50–100, ◆ = Fraction 100–300.

4. Discussion

Increasing the size of the macromolecules of ^{99m}Tc-labelled PEI-MP results in marked changes in their pharmacokinetics and biodistribution (Table 2). In normal bone of the primate model there was almost complete exclusion (< 1 %) of the particles larger than 100 kDa. The highest relative skeletal uptake of 18 % was demonstrated by the 10–30 kDa fraction (Table 2), but this is till considerably lower than that known for ^{153}Sm-EDTMP (> 50 %) [16].

All macromolecules of sizes > 50 kDa experienced an excessively high uptake and prolonged retention by the liver, which would lead to unacceptably high radiation doses eventually from the corresponding therapeutic agents (Fig. 1). A measurable liver accumulation is present for all particle ranges (Table 2), contrary to ^{153}Sm-EDTMP which demonstrates minimal liver uptake (< 0.03 %) [16]. However, the retention time ($t_{1/2}$) of the smaller particles in the liver is short (maximum 90 min for fraction 3–10 kDa (Table 2) and lowest ($p < 0.05$) for 10–30 kDa).

No uptake by the kidney is observed for the PEI-MP fraction 100–300 kDa. For the fraction 50–100 kDa there is kidney uptake which is largely retained at around 15 % of body activity. The fraction 3–10 kDa demonstrates initial high kidney uptake and an increasing percentage of retained activity with time (t > 4 h). This is also the case with fraction 30–50 kDa. The high (> 20 %) initial kidney uptake of fraction 10–30 kDa experiences fast washout within the first 30 min, and is soon reduced to around 50 % of the initial uptake (Fig. 2) which is significantly lower than for the other fractions with molecular size < 50 kDa. Blood clearance ($t_{1/2}$) from the cardiac blood pools was < 15 min, except for fraction 100–300 kDa where there was a prolonged retention of the particles in the circulation ($t_{1/2} \approx 2$ h). The lung clearance rate followed a similar pattern with prolonged retention for fraction 100–300 kDa ($t_{1/2} \approx 2.5$ h). In all other cases $t_{1/2}$ for the lung was < 30 min (Table 2). The percentage uptake and retention for the spleen lies around 10 % for all particle sizes, but $t_{1/2}$ is prolonged for sizes > 50 kDa. Clearance curves obtained from the blood samples (Fig. 3) are found to be multiphasic because of the particle size ranges of each fraction.

The highest percentage of injected dose excreted in the urine at 4 h was found for the fraction 30–50 kDa, followed by 10–30 kDa (62 % vs 52.8 %, respectively) (Table 3). Because urinary excretion of 30–50 kDa PEI-MP is 50 % higher than for 3–10 kDa, and ≈ 7 % higher than for 10–30 kDa, the radiation dose from the retained activity to all organs, except the kidney, can be expected to be lowest for 30–50 kDa PEI-MP. High radiation dose to the kidneys will follow in this case because most of ^{99m}Tc-PEI-MP (30–50 kDa) will be handled by the kidney over a prolonged time interval ($t_{1/2} > 4$ h).

Arzneim.-Forsch./Drug Res. 51 (I), 258–263 (2001)
© ECV · Editio Cantor Verlag, Aulendorf (Germany)

5. Conclusion

This study demonstrated the required reduced normal bone uptake of ^{99m}Tc-PEI-MP, especially noted for fraction 100–300 kDa. Although the value for 10–30 kDa is by comparison more than double that for the other fractions, some retention in bone is necessary such as in an osseous tumour where it would be beneficial to maximise duration of radiation.

To further optimise the molecular size of the macromolecule for its selectivity towards neoplastic and inflammatory diseased areas, potentially harmful kidney and liver uptake should be minimised. This would immediately exclude the fractions with sizes larger than 50 kDa because of liver exposure. Of the smaller fractions, 30–50 and 3–10 kDa seem to leave especially the kidneys vulnerable to radiation exposure (Table 2).

In conclusion it would seem that the fraction 10–30 kDa could optimally fit required criteria with relatively low accumulation in normal bone, but with some bone retention indicated. Access into a lesion which depends on the degree of vascular disruption could be fairly early for this fraction because of its relatively small molecular size. The liver and kidney also seem to enjoy most protection with this fraction.

The next step would be to label PEI-MP (10–30 kDa) with ^{153}Sm or $^{186/188}$Re, and to investigate biodistribution, pharmacokinetics and therapeutic efficacy in osseous tumour bearing animal models.

6. Literature

[1] Lewington, V. J., Cancer therapy using bone-seeking isotopes. Phys. Med. Biol. **41**, 2027 (1996)

[2] Atkins, H. L., Overview of nuclides for bone pain palliation. Appl. Radiat. Isot. **49**, 277 (1998)

[3] Lin, J. H., Biophosphonates: A review of their pharmacokinetic properties. Bone **18**, 75 (1996)

[4] Goeckeler, W. F., Edwards, B., Volkert, W. A. et al., Skeletal localization of Samarium-153 chelates: Potential therapeutic bone agents. J. Nucl. Med. **28**, 495 (1987)

[5] Turner, J. H., Martindale, A. A., Sorby, P. et al., Samarium-153 EDTMP therapy of disseminated skeletal metastasis. Eur. J. Nucl. Med. **15**, 784 (1989)

[6] Alberts, A. S., Smit, B. J., Louw, W. K. A. et al., Dose response relationship and multiple dose efficacy and toxicity of Samarium-153-EDTMP in metastatic cancer to bone. Radiother. Oncol. **43**, 175 (1997)

[7] Lattimer, J. L., Corwin, L. D., Stapleton, J. et al., Clinical and clinopathologic effects of Samarium-153-EDTMP administered intravenously to normal Beagle dogs. J. Nucl. Med. **31**, 586 (1990)

[8] Milner, R. J., Dormehl, I. C., Louw, W. K. A. et al., Targeted radiotherapy with Sm-153-EDTMP in nine cases of canine primary bone tumours. J. S. Afr. Vet. Ass. **69**, 12 (1998)

[9] Van Rensburg, A. J., Alberts, A. S., Louw, W. K. A., Quantifying the radiation dosage to individual skeletal lesions treated with Samarium-153-EDTMP. J. Nucl. Med. **39**, 2110 (1998)

[10] Seymour, L. W., Passive tumor targeting of soluble macromolecules and drug conjugates. Critical Reviews in Therapeutic Drug Carrier Systems. **9**, (1992)

[11] Duncan, R., Dimitrijevic, S., Evagorou, E. G., The role of polymer conjugate in the diagnosis and treatment of cancer. S. T. P. Pharma Sci. **6**, 237 (1996)

[12] Louw, W., Dormehl, I., Milner, R. J. et al., Biodistribution of radiolabelled polymin-mp of different molecular sizes as a selective bone seeker for therapy in animal models. Eur. J. Nucl. Med. **25**, 1167 (1998)

[13] Láznicek, M., Láznicková, A., Budsky, F. et al., Comparison of biological characteristics of EDTMP complexes with ^{99m}Tc, ^{111}In and ^{153}Sm in rats. Appl. Radiat. Isot. **45**, 949 (1994)

[14] Moedritzer, K., Irani, R. R., The direct synthesis of α-amine-methyl-phosphonic acids: Mannich-type reactions with orthophosphorous acid. J. Org. Chem. **31**, 1603 (1966)

[15] Manecke, V. G., Stockhausen, K., Gergs, P., Amphotere Ionenaustauscher (Teil IV). Macromolek. Chemie **128**, 229 (1969)

[16] Louw, W., Dormehl, I. C., Van Rensburg, A. et al., Evaluation of Samarium-153 and Holmium-166-EDTMP in the normal baboon model. Nuc. Med. Biol. **23**, 935 (1996)

Acknowledgements

The authors express their gratitude towards the Pretoria Biomedical Research Centre for the animal care and support services during the experimentation. We are also thankful for partial funding through the German-South African Research agreement.

Correspondence:
Prof. Dr. Irene C. Dormehl,
AEC (Atomic Energy Corporation)
Institute for Life Sciences, University of Pretoria,
P. O. Box 2034, Pretoria 0001
(Republic of South Africa)
E-mail: dormehl@medic.up.ac.za

Editors: Prof. Dr. Hans Georg Classen, Viktor Schramm. Editorial services: Eveline Dangel. Publisher: ECV · Editio Cantor Verlag für Medizin und Naturwissenschaften GmbH, P.O.B. 12 55, 88322 Aulendorf (Germany), Phone (00 49) 0 75 25/94 00, Fax (00 49) 0 75 25/94 01 99; e-mail: redaktion@ecv.de; http://www.ecv.de. Printed by YEBU Druck GmbH, Am Rentele 18, 88427 Bad Schussenried (Germany).

Terms of supply: The journal is published monthly and is supplied by the publisher or via bookstores. Annual subscription rates (VAT included, minimum 12 issues): Germany: print 290.00 €/567.19 DM; print + online 333.50 €/652.37 DM. Outside Germany: print 328.00 €/641.51 DM; print + online 377.20 €/737.74 DM. Postage: Germany 13.10 €/25.62 DM, outside Germany 30.20 €/59.07 DM (air mail 76.00 €/148.64 DM). Price for a single copy (issue) is 29.00 €/56.72 DM plus postage. Please ask for extended network licenses. A subscription remains legally valid unless it is cancelled at 3 months notice for the end of the period of computation. Free specimen copies are supplied by the publisher upon request.
Printed in Germany · ISSN 0004-4172

Proceedings of the Topical Meeting on
"Medical Radiation Physics and Engineering"
Lisbon (Portugal), November 20-22, 2000

Physica Medica - Vol. XVII, Supplement 4, 2001

Optimalisation of Radiolabelled Polymin-MP of Different Molecular Sizes as a Selective Bone Seeker for Therapy in Animal Models

I.C. Dormehl*[1], F.H.A. Schneeweiss[2], W.K.A. Louw[3], R.J. Milner[1], E. Kilian[1]

1. *AEC Institute for Life Sciences, University of Pretoria, Pretoria (RSA)*
2. *Institute of Medicine, Research Centre Juelich (Germany)*
3. *Atomic Energy Corporation, Pelindaba (RSA)*

Abstract

Abnormal blood supply and lack of lymphatics of neoplastic tissue lead to enhanced permeability and retention effects which form the basis of this study using various sizes of the radiolabelled macromolecule polyethyleniminomethyl phosphonic acid (polymin-mp) to increase the selectivity of bone seeking radiopharmaceuticals. Polymin-mp was synthesised and fractionated by membrane ultrafiltration into different molecular sizes, viz. 3-10, 10-30, 30-50, 50-100 and 100-300 kDa. Labelling efficiency to ^{99m}Tc as radiotracer was 99% with complexes stable for 24 hours. The pharmacokinetics and biodistribution of all ^{99m}Tc-polymin fractions were investigated in five experimental baboons per fraction and dogs (n = 5) with naturally occuring appendicular osteosarcomas. Scintigraphy followed a bolus injection of ^{99m}Tc-polymin (185 MBq) to the baboons and data were acquired as 30 × 1 min frames dynamic, and hourly static studies for four hours. Regular blood and urine samples were taken. The dogs underwent static studies of the tumours at four hours p.i. For baboons, the macromolecular size fraction 10–30 kDa had comparatively low accumulation and short residence times in the liver and kidney (resp. 20%, $T_{1/2} = 22 \pm 4$ min; 18%, $T_{1/2} = 20 \pm 3$ min) and although the bone uptake of 18% in this case was comparatively high, it is still low for a bone seeking agent, e.g.40 % for ^{153}Sm-EDTMP. Results from the dogs showed good uptake in the tumour (e.g.1:4, 1:8 and 1:9) with 3-10 kDa but reduced uptake with the larger molecular sizes.

KEYWORDS: Radiopharmaceutical, neoplastic bone diseases, targeted therapy, polyethyleniminomethyl phosphonic acid

1. Introduction

An ideal radiopharmaceutical for treatment of neoplastic and inflammatory bone disease should predominantly accumulate in the bone lesions with limited access to normal bone and other organs. Neoplastic tissue tends to display abnormal blood supply (increased permeability) and lack of lymphatics leading to selective accumulation of macromolecules [1]. These effects of enhanced permeability and retention form the basis of this study: to use various molecular sizes of the radiolabelled macromolecule polyethyleniminomethyl phosphonic acid (polymin-mp) for increased selectivity of the bone seeking radiopharmaceutical, and to investigate the pharmacokinetics and biodistribution in the normal primate model and in dogs with spontaneously occurring appendicular osteosarcomas.

2. Materials and Methods

Polymin-mp was synthesised by the condensation of polyethyleneimine, phosphorous acid and formaldehyde in the presence of hydrochloric acid (modified Mannich reaction) [2]. Then followed fractionation into different molecular sizes by membrane ultrafiltration, viz. 3-10, 10-30, 30-50, 50-100, and 100-300 kDa. Subsequently labelling was performed with ^{99m}Tc as radiotracer. A labelling efficiency of ~ 99% was reached.

For the animal experimentation five experimental baboons (Papio ursinus, ~ 28 kg) per size fraction of the macromolecules were used and dogs (n = 5) with spontaneous appendicular osteosarcomas. All animals received general anaesthesia for the duration of the scintigraphic investigation, i.e., pentobarbitone infusion (Sagatal: 6%, 30 mL/hr). The scintigraphy (Siemens Orbiter tomographic camera) of the baboons were performed after an i.v. bolus injection of ^{99m}Tc-polymin-mp (185 MBq) on a count down for dynamic data acquisition (30 × 1 min frames) followed by static images of 5 minutes every hour for 4 hours. Blood and urine samples were collected every 10 minutes for the first hour and then hourly till the fourth hour. Scintigraphy for the dogs consisted of static images of the tumour and contralateral sites at four hours p.i.

From the time activity curves percentage organ distribution and retention times could be evaluated (Table I) which would allow the calculation of percentage injected dose and dosimetry, when urinary excretion is taken into consideration.

3. Results

The biodistribution in normal primates is described in Table I where the half life times ($T_{1/2}$) of clearance

* Corresponding author: Prof. I.C. Dormehl, Director of AEC Institute for Life Sciences, University of Pretoria, P.O. Box 2034, RSA. E-mail: dormehl@medic.up.ac.za

Table I – Half Life and *highest percentage* of the different ^{99m}Tc-polymin-mp fractions in various organs of the primate model

Fraction	T ½ and *max. %*					
kDa	Cardiac	Liver	Kidney	Lung	Spleen	Bone
3-10	10 ± 1 min	90 ± 22 min	> 4 h	10 ± 1.5 min	75 ± 2 min	> 2 h
	15 ± 4 %	*16 ± 1 %*	*36 ± 4 %*	*8 ± 2 %*	*10 ± 1 %*	*8 ± 1 %*
10-30	10 ± 1.5 min	22 ± 4 min	20 ± 3 min	15 ± 3 min	60 ± 9 min	> 4 h
	15 ± 3 %	*20 ± 2 %*	*18 ± 4 %*	*12.5 ± 4 %*	*12.5 ± 1 %*	*18 ± 1 %*
30-50	6 ± 2 min	60 ± 15 min	> 4 h	8 ± 2 min	45 ± 8 min	> 4 h
	10 ± 4 %	*20 ± 2 %*	*40 ± 5 %*	*7.5 ± 2 %*	*8 ± 3 %*	*9 ± 0.5 %*
50-100	12 ± 1.5 min	> 4 h	> 4 h	22 ± 2 min	> 4 h	> 4 h
	15 ± 4 %	*43 ± 3 %*	*15 ± 2 %*	*9 ± 3 %*	*8 ± 0.5 %*	*7 ± 0.5 %*
100-300	2 h ± 0.05 h	24 h ± 1.5 h	–	2.5 h ± 0.5 h	> 24 h ± 2 h	–
	30 ± 7 %	*52 ± 9 %*	–	*17.5 ± 2 %*	–	–

of various fractions of ^{99m}Tc-polymin-mp and maximum percentage of tracer accumulation in 4 hours are presented.

For the dogs with appendicular osteosarcoma the smaller size fractions of polymin-mp showed higher uptake into the lesions; see Figure 1 where the uptake of ^{99m}Tc-polymin-mp (10-30 kDa) into the lesion reached 4:1 at three hours. This uptake was lower in the two cases (not depicted here) with macromolecular size range of 100-300 kDa, and reached up to 11 : 1 for the size range of 3-10 kDa.

4. Discussion

^{99m}Tc-polymin-mp of various molecular sizes have distinct differences in biokinetics which predominantly pertain to the rate of removal from the cardiac blood pool, i.e., clearance either by involvement of the liver or the kidney or both. Substantial liver and kidney participation (20% and 40% resp. max. uptake) for the fraction 30-50 kDa leads to fast clearance for blood pool ($T_{1/2}$ = 6 min), and fast blood clearance as measured from the blood samples ($T_{1/2}$ = 20 min). Reduced liver and kidney involvement, as with 3-10 kDa and 10-30 kDa leads to delayed cardiac blood clearance (10 min and 25 min resp. for both fractions). The slow although substantial liver participation for 50-100 kDa, and 100-300 kDa lead to long retention in the cardiac blood pool (12 min and 2 hrs resp.), as well as to slow clearance from the blood (45 min and 75 min resp.). The highest normal bone participation, viz. 18%, occurs for the fraction 10-30 kDa, but this is still much lower than the 40%, or higher of EDTMP and other characteristic biphosphonate accumulation in normal bone. This fraction

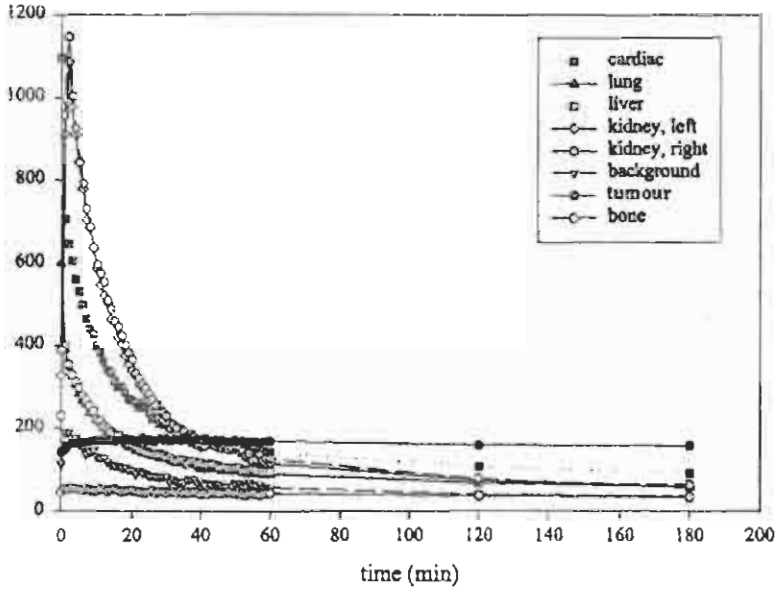

Fig. 1 – Uptake of ^{99m}Tc-polymin-mp (10-30 kDa) into various organs of the Dalmatian as a function of time (1 hr dynamic study and up to 3 hr static study).

Physica Medica - Vol. XVII, Supplement 4, 2001

seems to be the best compromise for low tracer uptake in both liver and kidney. The uptake in bony lesions, e.g. the osteosarcoma in the Dalmatian of 100-300 kDa was clear from the images with very little normal bone participation. Even better tumour uptake is obtained with the 3-10 kDa fraction ranging from 9:1 to 11:1 with respect to normal bone than was obtained with 10-30 kDa (4:1).

5. Conclusion

From the biokinetics and organ distribution of the various polymin-mp fractions the next step would be to label the polymin-mp with either ^{153}Sm or $^{186/188}$Re and to apply the agent for therapeutic purposes in cases of osteosarcoma or bone metastases [3]. It is expected that the organ distribution especially for the $^{186/188}$Re polymin-mp will be similar to that obtained from ^{99m}Tc polymin-mp so that enough data already exist for dosimetric calculation.

REFERENCES

[1] Maeda H, Wu J, Sawa T, Matsumura Y, Hori K. Tumour vascular permeability and EPR effects in macromolecular therapeutics: a review. J Controlled Release 2000; 65; 271-284.

[2] Moedritzer K, Irani RR. The direct synthesis of α-aminomethyl phosphonic acids: Mannich-type reaction with orthophosphorous acid. J Org Chem 1966; 31; 1603-1607.

[3] Park CH. The role of radioisotopes in radiation oncology 1997; 24; 639-654.

Radiochim. Acta 90, 237–246 (2002)

Metal-ion speciation in blood plasma incorporating the water-soluble polymer, polyethyleneimine functionalised with methylenephosphonate groups, in therapeutic radiopharmaceuticals

By Neil V. Jarvis[1], Jan Rijn Zeevaart[1,*], Judith M. Wagener[1], Werner K. A. Louw[1], Irene C. Dormehl[2], Rowan J. Milner[2] and Elmaré Killian[2]

[1] Radiochemistry, South African Nuclear Energy Corporation, PO Box 582, Pretoria 0001, South Africa
[2] Biomedical Research Centre, University of Pretoria, PO Box 2034, Pretoria 0001, South Africa

(Received April 10, 2001; accepted in revised form November 6, 2001)

Therapeutic radiopharmaceuticals / Water-soluble polymers / Bone cancer / Potentiometry / Blood plasma / Formation constants

Summary. A water-soluble polymer, polyethyleneimine functionalised with methylene phosphonate groups (PEI-MP) and labelled with ^{99m}Tc, has shown selective uptake into bone tumours. Apparent formation constants for the complexation of important blood plasma metal-ions and metal-ions of radionuclides used in therapeutic radiopharmaceuticals (excluding Tc) with PEI-MP were measured potentiometrically. These were added to the ECCLES data base in order to construct a blood plasma model for PEI-MP. From this model it could be predicted that the polymer would not deliver the therapeutic radionuclides ^{153}Sm, ^{166}Ho, ^{212}Pb, ^{213}Pb and ^{89}Sr to bone. This was clinically verified for ^{153}Sm. However good uptake of ^{99m}Tc-PEI-MP could be demonstrated in dogs. Due to the similar chemistry of Re as compared to Tc, it can be expected that PEI-MP labelled with ^{186}Re or ^{188}Re could result in effective therapeutic radiopharmaceuticals for bone cancer.

1. Introduction

The use of ^{153}Sm complexed to the octaanion, ethylenediaminetetramethylene-phosphonate (EDTMP), in pain palliation therapy for metastatic bone cancer is well established [1] and has been extensively studied in clinical trials in a number of countries. Studies were undertaken to elucidate the *in vivo* behaviour of ^{153}Sm-EDTMP [2, 3]. The use of the blood plasma model, ECCLES [4], has proved particularly useful and it was found that predictions made by the model were closely comparable to clinical observations.

Improvement of the therapeutic efficacy of bone-seeking radiopharmaceuticals could possibly be achieved using ^{166}Ho ($t_{1/2}$ = 26.9 hr; maximum β-particle energy = 1.86 MeV (3.0×10^{-13} J)) instead of ^{153}Sm ($t_{1/2}$ = 46.75 hr; maximum β-particle energy = 0.81 MeV (1.3×10^{-13} J)). However, experiments using both baboon [2] and rat [5] models showed poor uptake of ^{166}Ho from ^{166}Ho-EDTMP. Blood plasma modelling [2] was able to explain the deficiency of EDTMP in this regard. Thus, a more suitable ligand than EDTMP is needed to deliver a high percentage of injected ^{166}Ho to bone tumours. Attempts with other bisphosphonate ligands have proven to be ineffective [5–8]. The behaviour of these bisphosphonates (used in the treatment of bone diseases [9]) in conjunction with ^{153}Sm and ^{166}Ho could be prognosticated, using ECCLES [4].

Water-soluble polymers as drug carriers have been the subject of research activity for some time [10] and have been studied as potential chemotherapy agents for cancer [11]. The principle behind this approach is that water-soluble macromolecules accumulate passively in solid tumours according to the "Enhanced Permeability and Retention Effect" [12]. This phenomenon is thought to be caused by the production in tumour cells of compounds such as Vascular Permeability Factor (VPF) and Bradykinine that increase vascular permeability of the tumour tissue. Retention is enhanced by the impairment of the lymphatic system in tumour tissue, retarding the removal of macromolecules from tumours. The polymer must therefore be large enough not to be taken up in healthy tissue but not so large as to be trapped in organs such as the liver or kidneys. In this paper it is assumed that this phenomena also applies to secondary metastasis - although the latter has a different physiology.

To extend this approach to therapeutic radiopharmaceuticals, the water-soluble polymer, polyethyleneimine (see Fig. 1) was functionalised with methylenephosphonate groups to make the resulting water-soluble polymer bone-seeking – PEI-MP. Extensive pre-clinical work using ^{99m}Tc-labelled PEI-MP has been done to ascertain the optimum fraction in terms of mass [13]. It has been found that anionic species in the fraction 10 to 30 kDa achieve good tumour uptake with minimal uptake in healthy bone, kidneys or liver. The polymer thus has the potential to selectively deliver a therapeutic radionuclide to tumours.

The object of the research reported in this paper, was to construct a blood plasma model including PEI-MP. This should enable an informed selection of a therapeutic radionuclide for delivery to metastatic bone tumours by PEI-MP. In order to achieve this, apparent formation constants of blood plasma metal-ions as well as radionuclides

* Author for correspondence (E-mail: radchem@aec.co.za).

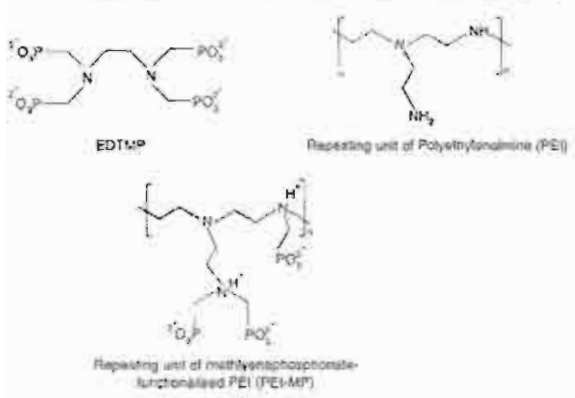

Fig. 1. The ligand EDTMP and polymer repeating units discussed in this paper.

of interest had to be measured. This may be achieved, as was previously done with polyethyleneimine (PEI) [14], by treating the water-soluble polymer as a collection of separate repeating units. Potentiometric titrations, in which the repeating unit is considered to be the ligand, yield data that may be analysed by computer codes such as ESTA [15]. Apparent formation constants are then added to the blood plasma model, ECCLES [4], which predicts the speciation of metal-ions in plasma. This gives an indication of the ability of the radiopharmaceutical to survive competition for the radionuclide by other blood plasma ligands. This approach is novel in so far as polymers having not yet been included in work performed using the ECCLES code. Therapeutic β-particle emitting radionuclides under consideration were ^{153}Sm, ^{166}Ho, ^{89}Sr, ^{186}Re and ^{188}Re. In addition to blood plasma metal-ions, potentiometric titrations involving Sm(III), Ho(III) and Sr(II) were performed. Unfortunately, the complex redox chemistry of Re makes potentiometry with this metal unreliable. Recently, α-emitting radionuclide couples, ^{212}Pb/^{212}Bi and ^{213}Pb/^{213}Bi together with EDTMP have been studied [16] as potential therapeutic radiopharmaceuticals for metastatic bone cancer. In order to predict the *in vivo* behaviour of these radionuclides with PEI-MP, potentiometric titrations were also performed with Pb(II).

2. Experimental

2.1 Synthesis of PEI-MP

Synthesis of the polymer was achieved using a Mannich type reaction as described by Moedritzer and Irani [17]. Phosphorous acid (18.4 g) and concentrated hydrochloric acid (51.3 ml) were added to a reaction vessel equipped with a thermometer, magnetic stirrer bar, dropping funnel and condenser. The reaction was performed under an inert atmosphere of argon. Dissolution of the phosphorous acid was achieved by stirring and heating to 80 °C. The dropping funnel was charged with formaldehyde solution (23.3 ml) which was added dropwise to the reaction mixture. On completion, the temperature was raised to 90 °C (refluxing temperature) and a solution of polyethyleneimine (8.33 g in 40 ml water; Polymin™ Water-Free, a BASF product in which the ratio of primary, secondary and tertiary amine groups is 1 : 1 : 1; see Fig. 1) was slowly added to the reaction mixture at a rate of 0.3 ml/min with the aid of a peristaltic pump. The reaction mixture was continuously purged with argon. On completion of the addition of polyethyleneimine, the mixture was stirred under reflux for an additional hour, then allowed to cool slowly during which the product separated as a viscous oil. After decanting the mother liquor, 50 ml water were added to oil which formed a doughy mass upon stirring.

The liquid phase was decanted and the process repeated twice. The doughy material was dissolved in 37 ml molar sodium carbonate solution to form the water-soluble sodium salt of the PEI-MP. After lyophilisation, 12 g of product were obtained. Microanalysis: Found: C, 23.11; H, 5.98; N, 8.91; Na, 9.86%. Calculated for $C_9H_{22}P_3N_3O_9Na_2{\cdot}H_2O$: C, 22.84; H, 5.11; N, 8.87; Na, 9.72%. Potentiometric titrations to determine protonation constants were used to double-check the purity of the ligand.

To obtain the 10 to 30 kDa fraction, an aqueous solution of sodium PEI-MP was subjected to ultrafiltration through the appropriate membranes (Filtron Technology Corporation). The membrane retentates were washed with distilled water to a theoretically calculated purity of 99% and lypholised.

Due to the scarcity of the 10–30 kDa fraction, the PEI-MP used in potentiometric titrations was not fractionated. However, apparent protonation formation constants were calculated for the 10–30 kDa fraction and found to be practically identical to the unfractionated polymer (see Table 1). This is because the polymer was treated in calculations as a collection of monomeric units. It is thus assumed that the calculation of apparent formation constants by potentiometry is not affected by the molecular size fraction of the polymer.

2.2 Metal-ion solutions

Fresh metal-ion solutions were employed in the titrations. These were made by dissolving reagent grade chloride salts of the metal-ions in distilled water and standardised by complexometric titration using EDTA and a Metrohm Titrino equipped with a copper selective electrode. Where necessary, solutions were acidified to prevent hydrolysis.

2.3 Potentiometry

Potentiometric titrations were performed using a Metrohm Titroprocessor 670 with a Metrohm 665 dosimat and a combination glass electrode (Ag/AgCl reference). The electrode was calibrated regularly using strong acid-base titration data. All titrations were performed under an inert atmosphere of nitrogen and solutions were held at a constant ionic strength of 0.15 mol/l NaCl and a temperature of 25.0 ± 0.1 °C. The titrations were performed beginning at low and ending at high pH, adding 0.10 ml aliquots of 0.050 mol/l NaOH (carbonate-free) in 0.10 mol/l NaCl. Protonation constants were calculated from data obtained from titrations of the ligand in the presence of various hydrochloric acid concentrations. Metal-PEI-MP apparent formation constants were calculated from titration data at five different metal:ligand ratios varying from 2:1 to 1:3. For

Table I. Comparative apparent protonation constants for PEI-MP and Polymin Water-free determined in this study at 25.0 ± 0.1 °C and $I = 150$ mmol dm^{-3} NaCl. Charges on the repeating units have been omitted for simplicity. L represents the repeating unit as in Fig. 1. The protonation formation constants in italics are those calculated for the 10 to 30 kDa fraction of the polymer.

Equilibrium	log*K* PEI-MP	log*K* Polymin Water-free	log*K** Polymin Water-free [14]
$H + L \rightleftharpoons HL$	9.34(1) *(9.47(1))*	9.24(< 1)	9.71
$H + HL \rightleftharpoons H_2L$	7.54(1) *(7.48(1))*	6.60(1)	7.70
$H + H_2L \rightleftharpoons H_3L$	5.95(1) *(5.86(1))*	* Not found	2.64
$H + H_3L \rightleftharpoons H_4L$	3.26(2) *(3.42(2))*	–	–
$3H + 2L \rightleftharpoons H_3L_2$	–	28.93(1)	30.87
$5H + 2L \rightleftharpoons H_5L_2$	–	37.10(2)	41.58
Number of data points	436 *382*	582	–
Hamilton *R*-factor	0.0120 *(0.0114)*	0.00687	–

* The protonation constant is probably < 2 and could thus not be detected within the pH range used in this work;
* Measured at 25.0 ± 0.1 °C and $I = 0.1$ mol dm^{-3} $NaNO_3$.

titrations involving lanthanides, precipitates formed at low pH, as was found for EDTMP [3]. By pH 5, the solutions had cleared and data points from here onwards were used in calculations. Data were analysed by the ESTA [15] library of programmes. During the analysis the previously determined protonation constants were held constant. Hydrolysis constants and pK_w were taken from the literature [18] and held constant during optimisation procedures. The models were tested for plausibility by comparing experimental and calculated formation and deprotonation curves. Formation constants for PEI-MP with Re and Tc were not measured as both can exist in different oxidation states and change between these states easily making it virtually impossible to accurately study the complexes involved by potentiometry.

2.4 Blood plasma modelling

All constants measured in this study were added to the ECCLES database [4]. The concentration of the repeating unit of PEI-MP used in modelling was 8.5×10^{-5} mol/l. This value is representative of actual clinical amounts, and is similar to that previously employed during EDTMP work [2]. The metal ion concentrations employed ranged from 1.0×10^{-8} to 1.8×10^{-6} mol/l which also resembles clinical amounts.

The plasma mobilisation index (p.m.i.) is defined as:

$$\text{p.m.i.} = \frac{\text{total concentration of low-molecular-weight metal complex species in the presence of the drug}}{\text{total concentration of low-molecular-weight metal complexes in normal plasma}}$$

The p.m.i. values give an indication of which metal-ions are mobilised by the added drug. This may be used as a screening method to predict the loss of biologically important metal-ions from blood plasma. Remedial actions such as taking supplementary metal ions may then be followed, if necessary. In this study, p.m.i. values were computed by ECCLES for the blood plasma metal-ions Ca(II), Mg(II), Ni(II) and Zn(II).

2.5 Preparation of ^{153}Sm-PEI-MP

^{153}Sm was prepared by neutron irradiation of 1.0–2.0 mg $^{152}Sm_2O_3$ (99% enriched) for 24 h in the SAFARI-1 reactor at a neutron flux of 1×10^{14} neutron cm^{-2} s^{-1}. Typical specific activities of ~ 4000 MBq/mg of $^{152}Sm_2O_3$ were obtained. Using the necessary shielding, the irradiated oxide was dissolved in 250 µl of 0.2 M HCl solution, diluted to 0.04 M HCl with sterile deionised water and filtered. (Millex-Gv, 0.22 µm, Milipore Bedford, M.A.)

Complexation was achieved by adding 0.3 ml of the ^{153}Sm solution above to 0.9 ml PEI-MP solution (48 mg Na-PEI-MP/ml, pH = 8.0). This was diluted up to 5 ml and sterilized by ultrafiltration (0.22 µm).

Complexation yields were determined by separating the complexed and uncomplexed ^{153}Sm species on a carboxymethyl sephadex cation exchange column [19]. Complexation yields of > 99% were obtained.

2.6 Preparation of ^{99m}Tc-PEI-MP

As is the procedure for ^{99m}Tc-radiopharmaceuticals, lyophilised, labelling kits of the ligand were prepared in advance and stored in a freezer until the day of use. The kits were prepared by mixing 5 µl of a solution containing 250 mg of $SnCl_2 \cdot 2H_2O$ crystals in 0.5 ml HCl(c) with an aqueous PEI-MP solution (48 mg Na-PEI-MP/ml, pH = 8.0) where after the pH was adjusted to 6. This mixture was dispensed into 5 vials and freeze dried. The evacuated vials were stored below 0 °C until used.

The final solutions for injection were prepared by adding 0.3 ml ^{99m}Tc (111 to 185 MBq), obtained from a ^{99}Mo/^{99m}Tc

generator, to the above vials. Radiochemical purity was checked using instant thin-layer chromatography on silica gel impregnated glass-fibre sheets as stationary phase and acetone and 0.9% sodium chloride solutions as mobile phase. Complexation yields of > 99% were recorded.

2.7 Determination of biodistributions in the canine model

Animal experimentation was done according to the National Code for the Handling and Use of Animals in Research, Education, Diagnosis and Testing of Drugs and Related Substances in South Africa, and the protocols approved by the authorised Ethics Committee of the University of Pretoria.

Healthy adult German Shepherd dogs were studied. Anaesthesia in each case was induced via an indwelling catheter (Jelco) with a mixture of ketamine hydrochloride (3 mg/kg, i.v., Ketalar, Parke Davis, S.A.) and medetomidine hydrochloride (0.1 mg/10kg, i.v. Domitor, Novartis, SA) and maintained by an i.v. administration of pentobarbitone sodium solution (20 mg/ml, 10 ml diluted in 200 ml saline, Kyron Laboratories, SA) at a constant rate of 20–30 ml per hour for the first 2 hours and then the infusion was stopped for the last hour. Blood samples were collected via an indwelling catheter placed in the opposite forelimb. A urinary catheter (Foley's) was placed in the bladder to facilitate the collection of urine samples. Arterial blood pressure (Hewlett Packard Life Scope 12) and heart rate were continually monitored by indwelling femoral arterial catheter (Jelco 18G). Oxygen saturation, expired carbon dioxide and respiratory rate were also monitored (Hewlett Packard Life Scope 12) for the duration of the anaesthesia.

Scintigraphy was performed (Siemens Orbiter γ-camera, low energy collimator, energy peak 140 keV, window 15%) for ^{99m}Tc-PEI-MP and ^{153}Sm-PEI-MP (energy peak 103 keV, window 15%). The animals were positioned in the supine position for planar images. Static images of 2 min duration were recorded in 64 × 64 word mode at 1, 2 and 3 hours after a bolus injection of between 111 and 185 MBq of the ^{99m}Tc and ^{153}Sm labelled PEI-MP.

Using these static images the relative region to background ratios were calculated by placing ROI (region of interest) on areas of the cortical bone, liver, kidneys, cardiac blood pool, lungs and muscular background. These values were used to obtain the relative biodistributions.

3. Results and discussion

3.1 Potentiometry

The results of modelling for PEI-MP using the computer programme ESTA [15] are given in Tables 1 and 2. Good fits, indicated by low Hamilton R-factors and standard deviations in $\log\beta$ values, were obtained for all the systems studied. For the parent polymer, PEI, the same model as previously applicable at a different ionic strength, was found to be plausible [14].

For the repeating unit-proton system, pK_a^cs corresponding to protonation of the nitrogen centres functionalised with methylenephosphonate groups could not be calculated as they are probably too high for the potentiometric method used here. Comparisons of pK_a^cs of nitrogens in ligands to which methylenephosphonate groups are successively added are given in Tables 3 and 4. It can be seen that these increase with increasing number of methylenephosphonates presumably due to attractive electrostatic effects. Hence pK_{a1} for ammonia rises from 9.43 to 12.4 and for ethylenediamine from 9.61 to 13.0. For ethylenediamine it can be further seen that pK_{a2} rises from 6.83 to 9.78 as more methylenephosphonate groups are added. The pK_a^cs of the nitrogens become very large and some doubt as to their accuracy is therefore suggested [18]. When modelling the protonation titrations for PEI-MP, it became apparent that two fewer protons then

Table 2. Apparent formation constants for PEI-MP determined in this study at 25.0±0.1 °C and I = 150 mmol dm^{-3} NaCl. Charges on metal-ions, hydroxide, the polymer repeating unit and complexes have been omitted for simplicity. L represents the repeating unit as in Fig. 1.

Equilibrium	log K Ca(II)	log K Mg(II)	log K Sr(II)	log K Ni(II)	log K Zn(II)	log K Pb(II)	log K Sm(III)	log K Ho(III)
Binuclear species								
$2M + L \rightleftharpoons M_2L$	8.81(1)	8.81(2)	7.34(1)	13.61(4)	15.50(5)		16.08(9)	14.73(13)
$M_2L + H \rightleftharpoons M_2(HL)$	8.16(2)	8.01(3)	8.05(2)	6.01(5)	5.59(5)		6.79(13)	5.94(20)
$M_2(HL) + H \rightleftharpoons M_2(H_2L)$		5.76(7)			4.42(3)			
$M_2L + OH \rightleftharpoons M(H_{-1}L)$	3.86(2)	3.94(3)	3.84(2)					
$M_2(H_{-1}L) + OH \rightleftharpoons M_2(H_{-2}L)$		2.87(4)						
Mononuclear species								
$M + L \rightleftharpoons ML$				8.83(2)	10.34(2)	7.51(2)		
$ML + H \rightleftharpoons M(HL)$				7.09(3)	6.45(3)	7.48(2)		
$M(HL) + H \rightleftharpoons M(H_2L)$				5.57(3)	5.33(3)	6.20(2)		
$M(H_2L) + H \rightleftharpoons M(H_3L)$						4.42(3)		
$M + L + OH \rightleftharpoons M(H_{-1}L)$				14.72(3)	16.10(3)	11.70(2)	14.32(5)	12.85(7)
Number of Data points	304	314	327	253	383	300	106	102
Hamilton R-factor (R-limit)	0.0170 (0.00192)	0.0258 (0.00195)	0.0155 (0.00179)	0.0160 (0.00807)	0.0201 (0.00689)	0.0115 (0.00806)	0.0174 (0.0124)	0.0240 (0.0111)

Table 3. Comparison of protonation constants for methylenephosphonate functionalised ammonia ligands [17]. All data were measured at 25 °C and 0.1 M ionic strength.

Ligand	pK_{a6}	pK_{a5}	pK_{a4}	pK_{a3}	pK_{a2}	pK_{a1}
NH_3						9.43
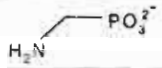					5.40	10.06
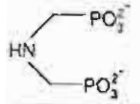			0.9	5.04	6.08	10.79
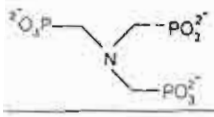	1.08	4.62		5.99	7.30	(12.4)

Table 4. Comparison of protonation constants for methylenephosphonate functionalised ethylenediamine ligands [17]. All data were measured at 25 °C and 0.1 M ionic strength except for PEI-MP at 25 °C and 0.15 M ionic strength.

Ligand	pK_{a8}	pK_{a7}	pK_{a6}	pK_{a5}	pK_{a4}	pK_{a3}
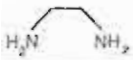					6.83	9.61
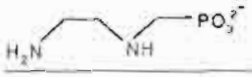				4.85	7.35	10.3
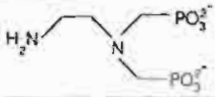			4.10	6.34	8.41	10.85
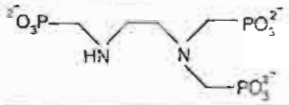		3.03	5.48	6.70	8.76	10.9
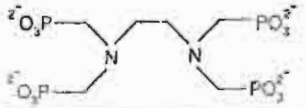	3.02	5.17	6.42	7.94	9.78	13.0
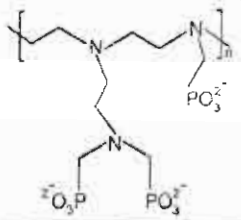	3.26	5.95	7.54	9.34	Not found[a]	Not found[a]

a: The value is probably too high to be determined by the experimental setup used in this work.

expected were dissociating in the pH band 2–11. It is therefore assumed that these protonation constants must exceed 11 and correspond to the protonation of the two nitrogen centres functionalised with methylenephosphonate groups. The first pK_a that could be calculated must correspond to the unfunctionalised tertiary nitrogen. This is supported by the results obtained for the parent polymer, where pK_{a1}, corresponding to the protonation of this nitrogen, was found to be almost identical (see Table 1). The rest of the pK_a's are for the protonation of methylenephosphonate groups and are in good agreement with results obtained for similar ligands (see Table 4).

For metal-ligand systems, a typical example of the approach used in model selection and validation is shown in Fig. 2. In this diagram, the curves for the calculated and experimental deprotonation function, $\overline{Q}$ (the average number of protons released on complexation per metal-ion), for the Ca(II)-PEI-MP system are shown. The dashed curve is $\overline{n}$, the protonation state of the repeating unit in the absence of the metal-ion. Interpretation of these curves assists greatly in model selection. In the example shown, $\overline{Q}$ rises to 0.5 for all titrations meaning that one proton is being released on complexation for every two metal-ions. At pH between 6 and 7, $\overline{n}$ is approximately 2. Hence, in the absence of

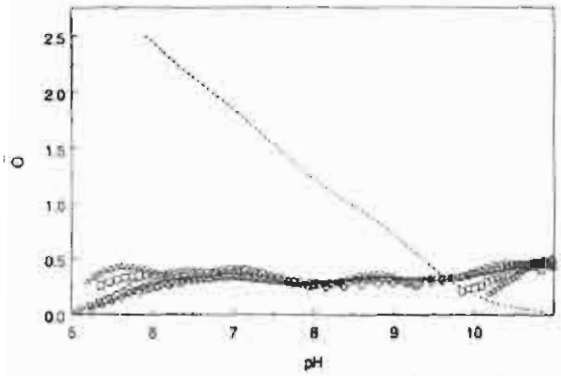

Fig. 2. Experimental (points) and modelled (lines) deprotonation ($\bar{Q}$) curves for Ca(II) complexation by the repeating unit of PEI-MP. The dashed line is the $\bar{n}$ curve and represents the protonation state of the ligand in the absence of the metal-ion. The five separate titrations are represented by: (○) 0.000852 mol dm^{-3} Ca(II), 0.00869 mol dm^{-3} repeating unit of PEI-MP and 0.00997 mol dm^{-3} HCl; (□) 0.000852 mol dm^{-3} Ca(II), 0.00174 mol dm^{-3} repeating unit of PEI-MP and 0.00997 mol dm^{-3} HCl; (△) 0.000852 mol dm^{-3} Ca(II), 0.00261 mol dm^{-3} repeating unit of PEI-MP and 0.00989 mol dm^{-3} HCl; (◇) 0.00128 mol dm^{-3} Ca(II), 0.00100 mol dm^{-3} repeating unit of PEI-MP and 0.0102 mol dm^{-3} HCl and (▽) 0.00170 mol dm^{-3} Ca(II), 0.00100 mol dm^{-3} repeating unit of PEI-MP and 0.00101 mol dm^{-3} HCl; *versus* 0.0500 mol dm^{-3} NaOH in 0.010 mol dm^{-3} NaCl. All solutions were at 25 °C and 0.15 mol dm^{-3} NaCl or 0.15 mol dm^{-3} total ionic strength.

the metal-ion the repeating unit would be of the form H_2L. In the presence of metal-ions, one proton is lost per two metal-ions. Therefore the predominant species present in this pH range would be $M_2(HL)$ as found in the model and illustrated in the species distribution curve (Fig. 3). Similar reasoning can be used to arrive at the M_2L species in the region of pH 9. Above pH 10, $\bar{Q}$ rises above $\bar{n}$. This indicates that the glass electrode detects more free protons in the system than expected from the repeating unit. These come from either deprotonation of coordinated water or a nitrogen centre. Comparing the constant obtained for the formation of the $M_2(H_{-1}L)$ species with the first hydrolysis constant for Ca(II) would indicate that the latter is more likely. A similar deprotonation reaction is observed

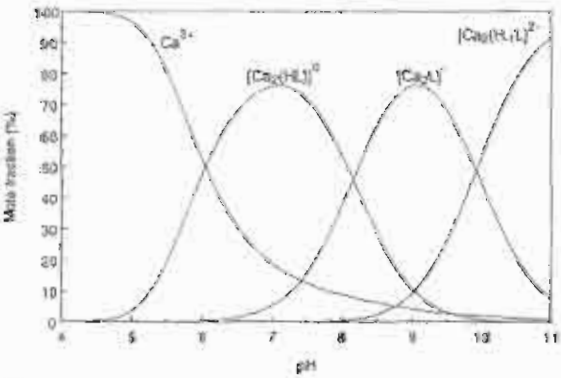

Fig. 3. Species distribution curves for Ca(II) complexation by PEI-MP at 25 °C and 0.15 mol dm^{-3} as calculated from the formation constants in Table 2. Concentrations used were 0.000852 mol dm^{-3} Ca(II) and 0.00174 mol dm^{-3} repeating unit of PEI-MP.

for Mg(II) and Sr(II) with constants remarkably close to that of Ca(II).

The presence of dinuclear species is similar to that found for other phosphonate ligands previously studied [5–8]. In this case it is expected that one repeating unit could accommodate two metal-ions at the two methylenephosphonate functionalised nitrogen centres.

The formation function (not shown here), $\bar{Z}$ (the average number of repeating units per metal-ion), rises to 0.5 which corroborates the model of one repeating unit per two metal-ions. At low free repeating unit concentration, "backfanning" occurs indicating that hydrolysis or deprotonation of the repeating unit to a greater extent than expected, is occurring. This is in agreement with the deprotonation function information.

The protonation constant for the M_2L species lies between pK_{a1} and pK_{a2}. It is therefore likely that the nitrogen centre -not functionalised with methylenephosphonate groups- is being protonated. Similarly, for Mg(II), the complex is protonated at the same nitrogen after which successive protonation of methylenephosphonate groups occurs.

The formation constants for the M_2L species for the alkaline earth metals are in the expected order Sr(II) < Ca(II). However, the constant for Mg(II) is equal to that of Ca(II). This is unexpected as Mg(II) is a harder metal-ion. An explanation could be that, as found with EDTMP, stability is less than expected due to steric hindrance derived from a number of negatively charged oxygen donor groups having to "fit" around the small Mg(II) ion.

For the transition metal-ions, Ni(II) and Zn(II), it was found that the composition of the complexes was strongly dependent on the ratio of repeating unit to metal used

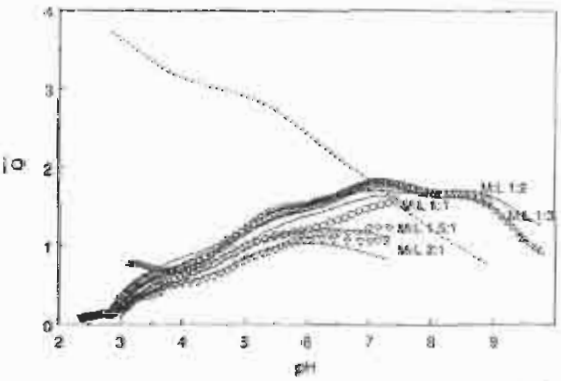

Fig. 4. Experimental (points) and modelled (lines) deprotonation ($\bar{Q}$) curves for Zn(II) complexation by the repeating unit of PEI-MP. The dashed line is the $\bar{n}$ curve and represents the protonation state of the ligand in the absence of the metal-ion. The five separate titrations are represented by: (○) 0.000100 mol dm^{-3} Zn(II), 0.00100 mol dm^{-3} repeating unit of PEI-MP and 0.00998 mol dm^{-3} HCl; (□) 0.00100 mol dm^{-3} Zn(II), 0.00201 mol dm^{-3} repeating unit of PEI-MP and 0.00977 mol dm^{-3} HCl; (△) 0.000100 mol dm^{-3} Zn(II), 0.00301 mol dm^{-3} repeating unit of PEI-MP and 0.00971 mol dm^{-3} HCl; (◇) 0.0020 mol dm^{-3} Zn(II), 0.00100 mol dm^{-3} repeating unit of PEI-MP and 0.0102 mol dm^{-3} HCl and (▽) 0.00150 mol dm^{-3} Zn(II), 0.00100 mol dm^{-3} repeating unit of PEI-MP and 0.00101 mol dm^{-3} HCl; *versus* 0.0500 mol dm^{-3} NaOH in 0.010 mol dm^{-3} NaCl. All solutions were at 25 °C and 0.15 mol dm^{-3} NaCl or 0.15 mol dm^{-3} total ionic strength.

and is reflected in the deprotonation curves for Zn(II) complexation in Fig. 4. At the highest metal : ligand ratio (2 : 1), the curve flattens off at just above 0.5 at low pH indicating that complexes are formed predominantly in the ratio 2 : 1. For this titration, sensible data points end at about pH = 7 as the free ligand concentration becomes zero under these conditions. At pH = 4, $\overline{Q}$ has risen to about 0.5 for this titration whereas $\overline{n}$ is at 3. Therefore, in the absence of the metal-ion, the ligand would be in the form H_3L. In the presence of the metal-ion, one proton is lost per two metal-ions. Hence the species predominating at this pH value should be $Zn_2(H_2L)$. As pH increases to 7, $\overline{Q} = 1$ and $\overline{n} = 2$. Hence the predominating species should be Zn_2L. As the concentration of repeating unit in relation to the metal-ion increases so the curves show inflections at 1.0 and 1.5. Therefore both mononuclear and dinuclear complexes are formed. At higher ligand : metal ratios, monomuclear species predominate.

For Ni(II) and Zn(II) it is presumed that the ML species is formed by complexation of the metal-ions by the nitrogen centre functionalised with two methylenephosphonate groups. The M_2L species must therefore be formed by complexation by the nitrogen centre functionalised with one methylenephosphonate group of the second metal-ion. It is difficult to speculate regarding the role of the unfunctionalised nitrogen centre in complexation.

Protonation of the Ni(II) and Zn(II) complexes takes place at phosphonate centres and not at the unfunctionalised nitrogen centre. This may be seen by comparison of the protonation constants for the complexes with those of the repeating unit.

For Pb(II), deprotonation curves rise to 1.0 for all titrations (Fig. 5). This is an indication that only mononuclear complexes are formed with the repeating unit which is perhaps due to the large ionic radius of the Pb(II) ion (1.2 Å)

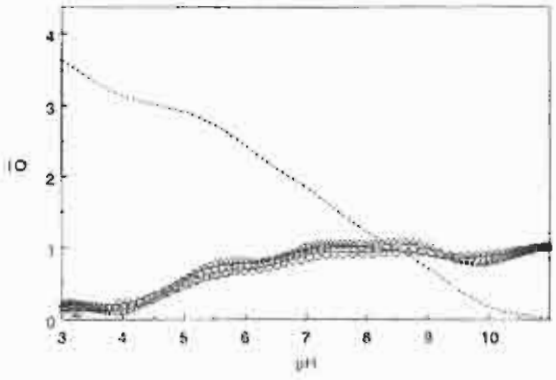

Fig. 5. Experimental (points) and modelled (lines) deprotonation ($\overline{Q}$) curves for Pb(II) complexation by the repeating unit of PEI-MP. The dashed line is the $\overline{n}$ curve and represents the protonation state of the ligand in the absence of the metal-ion. The three separate titrations are represented by: (○) 0.000871 mol dm^{-3} Ca(II), 0.00100 mol dm^{-3} repeating unit of PEI-MP and 0.0101 mol dm^{-3} HCl; (□) 0.000871 mol dm^{-3} Pb(II), 0.00140 mol dm^{-3} repeating unit of PEI-MP and 0.0100 mol dm^{-3} HCl and (△) 0.000871 mol dm^{-3} Pb(II), 0.00200 mol dm^{-3} repeating unit of PEI-MP and 0.00996 mol dm^{-3} HCl; *versus* 0.0500 mol dm^{-3} NaOH in 0.010 mol dm^{-3} NaCl. All solutions were at 25 °C and 0.15 mol dm^{-3} NaCl or 0.15 mol dm^{-3} total ionic strength

making it sterically difficult for the repeating unit to accommodate two metal-ions.

The Pb(II), Zn(II) and Ni(II) models contain "hydrolysis" species. Here, the extra proton detected by the electrode could originate from coordinated water or the ligand. Inspection of the hydrolysis constants for these three metal-ions indicates that the latter is more likely. Therefore deprotonation of one of the functionalised nitrogens takes place.

For the lanthanides, Sm(III) and Ho(III), models containing mononuclear and dinuclear species were found – as was found for Ni(II) and Zn(II). The Ho(III) complexes are generally less stable than those of Sm(III) – as was found for EDTMP [3]. The expected order due to the lanthanide contraction is reversed, presumbuly due to steric effects caused by the large number of negatively charged oxygen donors having to "fit" around the smaller Ho(III) ion.

3.2 *In vivo* speciation calculated by ECCLES

The speciation of the repeating unit of PEI-MP in normal blood plasma is given in Table 5. As has previously been found with bisphosphonates and aminomethylenephosphonates [2, 5, 6, 8], the repeating unit has a strong affinity for Ca(II) and Mg(II). The p.m.i. curves, however, indicate that little mobilisation of the blood plasma metal-ions, Ca(II), Mg(II), Zn(II) and Ni(II) occurs at the likely clinical concentration of PEI-MP in blood plasma (Fig. 6). This is an encouraging result as side-effects due to mobilisation of blood plasma metal-ions can be predicted to be negligible.

For Pb(II) and Sr(II), no difference in speciation for these two metal-ions in the absence or the presence of PEI-MP could be discerned by ECCLES. Therefore, PEI-MP will be unable to compete *in vivo* for these metal-ions above the ligands cysteinate and phosphate which respectively strongly complex these metal-ions in blood plasma. Hence it is unlikely that the polymer will be able to deliver therapeutic radioisotopes of these metal-ions to bone tumours.

The speciation of Sm(III) and Ho(III) in the presence of PEI-MP in blood plasma is presented in Table 6. Transferrin was not included as kinetics of complexation for lanthanides is slow and would probably not occur before bone localization. From this result it is clear that no Sm(III) or Ho(III)

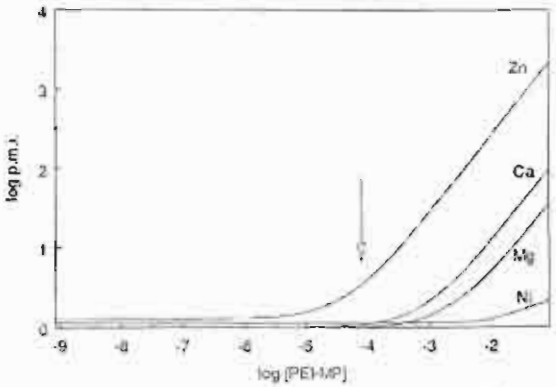

Fig. 6. Plasma mobilisation index (p.m.i.) curves for blood plasma metal-ions *versus* PEI-MP concentration. The arrow indicates a typical PEI-MP concentration used clinically.

Table 5. Speciation of PEI-MP in normal blood plasma as calculated by ECCLES. L = repeating unit of PEI-MP as illustrated in Fig. 1.

Species	Mol %
$[Ca_2(HL)]^+$	70.6
$[Ca_2L]^0$	12.2
$[Mg_2(HL)]^+$	10.6
$[Mg_2L]^0$	2.7
H_2L^{2-}	1.8
HL^{3-}	1.3
$[Mg_2(H_2L)]^{3+}$	0.2
$[Ca_2(H_{-1}L)]^-$	0.1

Table 6. Speciation of Sm(III) and Ho(III) in the presence of PEI-MP in blood plasma.

Species	Mol % Sm(III)	Mol % Ho(III)
$[LnCit(OH)]^-$	66.4	69.9
$[LnCit(OH)_2]^{2-}$	26.1	19.8
$[LnCit]^0$	3.0	4.2
$[LnSla]^{2+}$	1.8	3.3
$[Ln(CO_3)]^+$	0.8	0.6

Where Cit = citrate and Sla = salicylate.

remains bound to PEI-MP in blood plasma. Citrate competes favorably for the lanthanides and thus the distribution of the lanthanides in blood plasma is almost exclusively determined by their affinity for and complexation to citrate.

The main reason for the poor retention of Sm(III) or Ho(III) by PEI-MP in blood plasma lies in its affinity for Ca(II). 82.8% of the ligand is bound to Ca(II) rather than Ln(III). This means that almost all of the lanthanide ion is available to complex to citrate. Therefore, results from the animal test with ^{153}Sm-PEI-MP should be comparable with results for ^{153}Sm-Citrate. The only species to be considered for liver uptake is $[SmCit]^0$ (neutral species at low concentrations form fine precipitates or colloids) which is only present in a small percentage at physiological pH.

3.3 Animal studies

Tables 7 and 8 present the calculated biodistribution achieved for ^{99m}Tc-PEI-MP and ^{153}Sm-PEI-MP as studied in canine subjects. In interpreting the *in vivo* results it is important to note that the values presented here are comparisons of the activity measured (counted pixels) in a defined area in the different organs. These values were then normalized between the organs and expressed as a percentage biodistribution, which has no correlation with the percentage of injected dose but rather to percentage of retained activity in the body. Organs with no or low uptake were ignored. Furthermore, it must be kept in mind that only the distribution of the radionuclide entity of the complex is observed which is not necessarily the same as the radionuclide-ligand complex that has been administered, due to possibilities of *in vivo* transchelators.

If the results for the two radionuclides are compared for the 10–30 kDa section of the polymer, it follows that, at three hours after injection, the relative bone uptake for ^{153}Sm is 7% while for ^{99m}Tc it is 12%. For ^{153}Sm the uptake is especially low (this is as predicted that no Sm(III) remains complexed to PEI-MP – the bone seeker) especially after three hours. ^{99m}Tc in the pertechnetate form stays bound to PEI-MP during the tests as free pertechnetate would have been demonstrated in thyroid uptake. No difference in the background and excretion rate (presented by the kidney uptake) for ^{99m}Tc-PEI-MP and ^{153}Sm-EDTMP were recorded. However the blood pool and liver uptake are both higher for ^{153}Sm than for ^{99m}Tc indicating that ^{153}Sm is distributed throughout the whole body – an indication that it is no longer complexed by the polymer.

These results agree with those predicted by the blood plasma model. Although the latter predicted that no Sm(III) would stay complexed to PEI-MP, a low bone uptake could still be foreseen as citrate is metabolized by all parts of the body including the bone. The distribution of ^{153}Sm throughout the body of the canine subjects corresponds with this prediction. This reasoning is further justified by the recording of higher bone uptake of ^{153}Sm-PEI-MP in 'trabecular' (growing) bone where there is higher metabolic activity [13].

As the biodistribution for ^{153}Sm-PEI-MP can therefore be estimated with that of ^{153}Sm-citrate the liver uptake (expressed as a liver to bone ratio) is lower than expected, if compared with animal studies using ^{153}Sm-citrate [20–22]. A possible explanation for this apparent discrepancy can be found in the pH sensitive speciation of Sm(III)-Citrate. The pH of the injected formulation (bolus) contributes to the liver uptake as set out in Appendix A.

Table 7. Biodistribution of intravenously administered ^{99m}Tc-PEI-MP (10–30 kDa) in dogs (*three dogs studied*), as % retained activity.

	Cortical Bone	Liver	Kidneys	Cardiac blood pool	Lung	Background
1 h	10 ± 1	21 ± 2	22 ± 1	20 ± 2	17 ± 1	10 ± 1
2 h	11 ± 1	21 ± 2	21 ± 1	20 ± 2	17 ± 1	10 ± 1
3 h	12 ± 1	21 ± 2	19 ± 1	20 ± 2	18 ± 0.5	10 ± 1

Table 8. Biodistribution of intravenously administered ^{153}Sm-PEI-MP (10–30 kDa) in dogs (*four dogs studied*), as % retained activity

	Cortical Bone	Liver	Kidneys	Cardiac blood pool	Lung	Background
1 h	7 ± 1	24 ± 3	19 ± 2	23 ± 2	16 ± 1	11 ± 1
2 h	7 ± 1	28 ± 6	18 ± 3	22 ± 1	14 ± 2	10 ± 1
3 h	7 ± 2	30 ± 6	18 ± 3	21 ± 1	14 ± 2	10 ± 1

For ^{153}Sm-PEI-MP which was prepared at pH = 7.8, the neutral M_2L species forms to a small extent (9%) while M_2LOH (63%) and MLOH (28%) account for the complexation of most of the ^{153}Sm in the bolus. At first, Sm(III) is complexed to PEI-MP in the injected bolus. As it passes the bone the complex is absorbed due to PEI-MP's phosphonate moiety, at first resulting in a higher than expected bone uptake. As time passes the complex reaches equilibrium with the blood plasma and citrate competes for the Sm(III) and once equilibrium is achieved, complexes all the injected Sm(III). As only a small amount of $[SmCit]^0$ colloid is present, a low liver uptake is recorded. As other Sm(III)-Citrate species distribute through the body, they are absorbed on the basis of metabolic activity of citrate in all organs including the liver, bone, muscle and blood. The decline in bone uptake with time as well as the higher uptake in trabecular bone [13] can both be explained by this mechanism. Although Sm(III)-phosphate-albumin ternary complexes will also contribute towards liver uptake [23] evidence for the formation of this species only exists after longer periods (22 h) and is presumed to have little effect in the 3 h study for ^{153}Sm-PEI-MP.

4. Conclusions

A water soluble polymer was successfully included in the ECCLES model for blood plasma. Prognostications made by the programme could be verified by clinical observations. The anionic fraction of the 10–30 kDa range of the polymer can be prognosticated to poorly deliver the therapeutic radionuclides ^{153}Sm, ^{166}Ho, ^{212}Pb, ^{213}Pb and ^{89}Sr to bone. This was clinically verified for ^{153}Sm. Better, although not good, uptake of ^{99m}Tc-PEI-MP could be demonstrated in dogs. This confirms that the ligand tends to have less leakage from healthy vascular tissue into healthy bone than other bisphosphonate ligands. This could result in increased leakage from disrupted vascular tissue into lesions, with a resulting increased lesion to normal ratio if it is complexed by a radionuclide that is able to remain coordinated to PEI-MP in blood plasma. Due to the similar chemistry of Re as compared to Tc, it can be expected that PEI-MP labelled with ^{186}Re or ^{188}Re could result in effective therapeutic radiopharmaceuticals for bone cancer. In addition, speciation calculations illustrated the importance of pH in an intravenously administered preparation.

Acknowledgement. The authors thank the South African Nuclear Energy Corporation, NECSA, for permission to publish this work.

Appendix

Speciation calculations involving Sm(III)-citrate. If the results achieved with ^{153}Sm-Citrate in the literature are analysed we find the following. Durbin *et al.* [24] showed that citrate complexed with transition lanthanides (for example Sm(III)) localises mainly in the liver and to a lesser extent in bone tissue. O'Mara *et al.* [25] confirmed this and proposed that the found reticuloendithelial (liver, spleen and lungs) accumulation could by ascribed to colloid formation. No proposal was made as to the identity of the colloid. Later work by Woolfenden *et al.* [20], Turner *et al.* [21] and Tse *et al.* [22] all register high liver uptake (although not identical) in different animal types. Turner and coworkers [21] identified a Sm-Na-CO_3 species as being responsible for the colloid formation.

From these animal studies [20–22] the following can be noted on the biodistribution of ^{153}Sm-Citrate. The pH of the injected radiopharmaceutical is of great importance. With the help of speciation calculations (Table 9) it can be shown that at pH values lower than employed in this study, the speciation of Sm(III)-Citrate changes dramatically. It is important to compare the neutral $[SmCit]^0$ species (which would be likely to form precipitates or colloids) and the total of other species (which are all soluble) at different pH values. The neutral $[SmCit]^0$ species is more prevalent at lower pH values. (At pH = 5, 82.1% is in the form of $[SmCit]^0$ and at this pH forms the colloids used for radiation synovectomy [26, 27], which will be irreversibly filtered by the liver if injected intravenously [28]). Although one can argue that blood plasma will buffer and adjust an injected bolus of

Table 9. Species distribution of Sm(III) citrate at various pH values.

pH	% $[SmCit]$ (neutral)	% $[SmCitOH]^-$	% $[SmCit(OH)_2]^{2-}$	% $[SmCit_2]^{3-}$
5	82.1	7.1	–	8.5
5.5	66.5	17.5	–	15.3
6	42.6	40.6	0.7	15.9
6.5	22.3	64.4	3.4	9.8
7	8.7	75.3	11.9	4.0
7.4	3.1	68.2	27.6	1.5

Table 10. The ratio of liver to bone uptake 24 hrs after injection in various animals.

	Woolfenden *et al.* [19]	Turner *et al.* [20]	Tse *et al.* [21]
pH	5–6	6–7	6.5
Liver : Bone	19.5	16.3[b]	10.3[a,b]
Type of Tumor	V-2 Carcinoma	B16 Melanoma	Dunning R3327-H
Animal	Rabbits	C-57 black mice	Copenhagen-Fisher rats

a: Publication data incomplete – estimated ratio presented;
b: Ratio Ligand: Metal-ion = 80 : 1 compared to 50 : 1 for the others.

pH = 6, to pH = 7.4, this will require some time. The liver and reticuloendothelial cells should irreversibly filter all colloids present in the injected bolus. If the above literature results are compared according to the pH of the injected dose there appears to be a correlation (Table 10). The trend of lower pH, higher liver uptake is followed for all three sets of results.

Other aspects to note are the concentration of injected therapeutic preparations (higher than the concentrations used in the blood plasma model although instant mixing is assumed) and the formation of ternary complexes [23]. Both these aspects are kinetically controlled. In reality the injected bolus is pumped speedily through the body and is exchanged with organs while being diluted to the equilibrium conditions. On the other hand, evidence for the formation of the Sm(III)-phosphate-albumin ternary complexes (which will also contribute towards liver uptake [23]) only exists after longer periods (22 h). Although the values reported in Table 10 are for results gathered after 24 h, the corresponding 6 h liver to bone ratio values are even higher: 20.9 and 27.7 for Turner [21] *et al.* and Tse *et al.* [22] respectively. It is therefore assumed that the existence of ternary complexes does not explain high liver uptake shortly after administration.

Liver uptake (Table 10) was expressed as a ratio of the liver to bone uptake using as input the percentage of injected dose per gram of organ for both the liver and bone. As only relative organ uptake values are available for PEI-MP a direct comparison with these results is impossible but from Table 8 it is clear that the liver:bone ratio will be significantly lower for PEI-MP.

References

1. USA Food and Drug Administration approval for ^{153}Sm-EDTMP (™Quadramet) granted during March (1997).
2. Jarvis, N. V., Wagener, J. M., Jackson, G. E.: J. Chem. Soc., Dalton Trans. 1411 (1995).
3. Wagener, J. M., Jarvis, N. V.: S. Afr. J. Chem. **48**, 85 (1995).
4. May, P. M., Williams, D. R., Linder, P. W.: J. Chem. Soc., Dalton Trans. 588 (1977).
5. Zeevaart, J. R., Jarvis, N. V., Louw, W. K. A., Jackson, G. E., Cukrowsky, I., Mouton, C. J.: J. Inorg. Biochem. **73**, 265 (1999).
6. Zeevaart, J. R., Jarvis, N. V., Cukrowski, I., Jackson, G. E.: S. Afr. J. Chem. **50**, 189 (1997).
7. Cukrowski, I., Zeevaart, J. R., Jarvis N. V.: Anal. Chim. Acta **379**, 217 (1999).
8. Zeevaart, J. R., Jarvis, N. V., Louw, W. K. A., Jackson, G. E.: J. Inorg. Biochem. **83**, 57 (2001).
9. Bijvoet, O. L. M., Fleisch, H. A., Canfield, R. E., Russell, R. G. G. (Eds.): *Bisphosphonate on Bones*. Elsevier, Amsterdam (1995).
10. Duncan, R., Kopeček, J.: Adv. Polym. Sci. **57**, 51 (1984).
11. Soyez, H., Schacht, E.: Pharmaceutical Technology Europe. November (1999) p. 50.
12. Seymour, L. W.: CRC Crit. Rev. Ther. Drug Carrier Syst. **9**, 249 (1992).
13. Dormehl, I. C., Louw, W. K. A., Milner, R. J., Kilian, E., Schneeweiss, F. H. A.: Drug Res. **51**, 258 (2001).
14. Jarvis, N. V., Wagener, J. M.: Talanta **42**, 219 (1995).
15. May, P. M., Murray, K.: Talanta **35**, 927 (1988) and references therein.
16. Hassfjell, S. P., Hoff, P., Bruland, Ø. S., Alstad J.: J. Labelled Compd. Radiopharm. **34**, 717 (1994).
17. Moeditzer, K., Irani, R. R.: J. Org. Chem. **31**, 1603 (1966).
18. Martell, A. E., Smith R. M.: *Critical Stability Constants*. Vols. 3 and 6, Plenum, New York (1977 and 1989) and references therein.
19. Goeckeler, W. F., Edwards, B., Volkert, W. A., Holmes, R. A., Simon, J., Wilson, D.: J. Nucl. Med. **28**, 176 (1987).
20. Woolfenden, J. M., Hall, J. N., Barber, H. B., Wacks, M. E.: Int. J. Nucl Med. Biol. **10**, 251 (1983).
21. Turner, J. H., Martindale, A. A., de Witt, G. C., Webb, J., Sorby, P., Boyd, R. E.: Eur. J. Nucl. Med. **13**, 432 (1987).
22. Tse, J. W., Wiebe, L. I., Noujaim, A. A.: Nucl. Med. Biol. **16**, 17 (1989).
23. Neumaier B., Rösch F.: Radiochim. Acta **84**, 201 (1999).
24. Durbin, P. W., Asing, C. W., Johnston, M. E., Hamilton, J. G., Williams, M. H.: USAEC Report. ORINS-1 (1956) p. 171.
25. O'Mara, R. E., McAfee, J. G., Subramanian, G.: J. Nucl. Med. **10**, 49 (1968).
26. Ferro-Flores, G., García-Salinas, L., Pedraza-López, M., González-Zavala, M. A., Tendilla, J. I., López-Gómez, M. A.: J. Radioanal. Nucl. Chem. **222**, 93 (1997).
27. Prabhkar, G., Joshi, S. H., Ranganatha, D. K., Umamaheswari, S., Ananthakrishnan, M., Ramamoorthy, N.: Nucl. Med. Biol. **27**, 353 (2000).
28. Neves, M.: personal communication.

tions to patient care and the investigation findings. Differentiation between normal changes of ageing and deficits due to disease processes must be made. Increased life expectancy is accompanied by a greater prevalence of degenerative diseases such as heart disease, diabetes, hypertension and osteoarthritis all of which affect the outcome of the nuclear medicine investigation. Depression is a frequent and debilitating emotional problem of the aged person. Symptoms of depression in the elderly are often mistaken for dementia. These symptoms are not part of the normal ageing process but rather a disease process and these patients are frequently seen for diagnostic examination.

Conclusion: As health care professionals, we need to guard against 'ageism', i.e. the prejudiced attitude towards the elderly. Given that the elderly are the fastest growing segment of the population, the nuclear medicine practitioner needs to tailor his or her practice to suit the needs of the geriatric patient.

5. Current directions in radiopharmaceutical research – a personal view

S.J. Mather
Cancer Research UK, London, UK

People undertake research in radiopharmacy for many different reasons. Those who work in the pharmaceutical industry follow defined development strategies with the ultimate aim of registering a new product and generating money for the company. This review is concerned mostly with the work that is carried out at academic institutions where intellectual, rather than financial, stimuli are more common. The most successful research projects are normally those which seek to solve a particular clinical problem. This provides the necessary focus to the project as well as giving the researchers the ultimate satisfaction of seeing their endeavours put to good use. With the improvements in competing modalities such as spiral CT, Doppler echo and spectroscopic MRI for the determination of locality and perfusion of disease, there is an increasing need for nuclear medicine to concentrate on its unique ability to perform functional assessment of tissues and, in particular, to try and assess intracellular as well as extracellular changes. Recent developments in the field of targeted radionuclide therapy have also given a fresh impetus to work in this area.

The main areas of current radiopharmaceutical research can be summarized as

- infection imaging,
- cancer imaging,
- cancer therapy,
- neuro-receptor imaging,
- radiopharmaceutical chemistry.

Infection imaging is perhaps the most prolific area for radiopharmaceutical development and a survey of the literature would surely result in dozens of potentially 'useful' new products but few, if any, have stood the test of time. The main challenges in infection imaging are the ability to distinguish true infection from sterile inflammatory processes and the need for a universal detector of inflammation to replace the use of radiolabelled white cells. In cancer the diagnostic applications of nuclear medicine have moved away from early screening and primary diagnosis towards secondary staging and subsequent individual tailoring of patient therapies. As new expensive biological therapeutic possibilities become available then ways of identifying those patients who will benefit from such treatment will become essential.

For the first time in many years new therapeutic radiopharmaceuticals such as labelled anti-CD20 antibodies in lymphoma, radiolabelled octreotide analogues in neuroendocrine disease and radiolabelled phosphonates for bone metastases are proving to have real clinical utility. This has stimulated further research into other therapeutic applications and even the use of 'new' radionuclides such as the beta emitter ^{177}Lu and alpha emitters such as ^{213}Bi.

The challenge in neuroreceptor imaging is to translate the successes of the PET field into SPECT tracers. Although a number of ^{99m}Tc labelled ligands which bind to receptors *in vitro* have been developed, their application *in vivo* continues to be limited by the low brain uptake caused by the sub-optimal physico-chemical properties of these compounds.

Progress in radiopharmaceutical chemistry, such as the development of the aqueous route to the tricarbonyl ^{99m}Tc precursor continue to produce new complexes with novel properties which will provide new avenues for clinical exploitation in years to come.

6. ^{117m}Sn and ^{186}Re radiolabelling of polyethyleneiminomethyl phosphonic acid (PEI-MP), a potential selective therapeutic bone tumour seeker

W.K.A. Louw,[1]* J.R. Zeevaart,[1] Z.I. Kolar,[2] I.C. Dormehl,[3] J.M. Wagener,[1] R.J. Milner,[4] E. Killian[3] and F.H.A. Schneeweiss[5]
[1]*Department of Radiochemistry, NECSA, P.O. Box 582, Pretoria 0001, South Africa;* [2]*Interfaculty Reactor Institute, Delft University of Technology, Delft, the Netherlands;* [3]*AEC Institute for Life Sciences, University of Pretoria, Pretoria, South Africa;* [4]*Department of Small Animal Clinical Studies, College of Veterinary Medicine, University of Florida, USA; and* [5]*Institut für Medizin, Forschungszentrum, Jülich GmbH, Germany*
*Corresponding author

Introduction: An ideal radiopharmaceutical for the diagnosis and/or treatment of neoplastic and inflam-

matory (benign) bone diseases would be a radiolabelled compound that predominantly accumulates in bone lesions with limited access to normal bone and other organs. Water soluble polymers are under development as vehicles for systemic drug delivery due to the enhanced permeability and retention effect whereby neoplastic tissue selectively accumulates macromolecules. In previous studies, the ^{99m}Tc-PEI-MP 10–30 kDa fraction showed promising biodistribution and pharmacokinetic properties in primates and dogs, as well as good tumour localization in dogs with natural osteosarcomas. Metal-ion speciation studies, however, predicted that the polymer would not deliver therapeutic radionuclides such as ^{153}Sm to bone, but that ^{117m}Sn[1] will remain bound to PEI-MP in blood plasma. The purpose of this study was therefore to evaluate the labelling of 10–30 kDa PEI-MP with ^{117m}Sn and ^{186}Re, both radionuclides with proven therapeutic properties.

Materials and methods: PEI-MP was synthesized by condensation of polyethylenimine, phosphonic acid and formaldehyde. The 10–30 kDa fraction was prepared using membrane ultrafiltration techniques. ^{117m}Sn was prepared by the ^{117}Sn(n,n')^{117m}Sn reaction in the HFR-Petten reactor, the Netherlands. The irradiated metal was dissolved in 10 M HCl at 60°C under Ar and diluted to 3.3 M with water. PEI-MP (10–30 kDa, 100 mg) was dissolved in 1.2 ml water and 0.2 ml 10 M NaOH. To this an aliquot containing 2.6 mg Sn was added and the pH adjusted to 6.0. Radiochemical purity was determined by chromatography on ITLC-SG (ethanol) and cellulose thin layers (1 M citrate, pH 7.0). ^{186}Re was prepared by the ^{185}Re(n,γ)^{186}Re reaction in the SAFARI-1 reactor, Pelindaba, Pretoria, South Africa. The irradiated metal was dissolved in 10% H_2O_2, evaporated to dryness (80°C), whereafter an aliquot containing 25 μg Re was added to a PEI-MP freeze dried labelling kit (10 mg Na-PEI-MP; 0.5 mg $SnCl_2{\cdot}2H_2O$) at a pH of 1.0. After incubation at ±90°C (30 min) the pH was ajusted to 6.0. Radiochemical purity was determined by chromatography on ITLC-SG (ethanol) and cellulose ITLC (1.0 M citrate, pH 7.0).

Results: Both ^{117m}Sn-PEI-MP and ^{186}Re-PEI-MP gave radiochemical purities ≥98% with <1.0% colloids. For ^{117m}Re-PEI-MP the respective percentages were the same for 1 week while those for ^{186}Re-PEI-MP stayed the same for 48 h.

Conclusions: These results indicate that PEI-MP can be labelled successfully with radioisotopes that have proven therapeutic properties. The next step would be to investigate their biodistribution, pharmacokinetics and therapeutic efficacy in animals bearing osseous tumours.

7. Stabilization of fractionated HMPAO kits after labelling with ^{99m}Tc

S.M.A. Siddig,[1]* S.M. Rubow[2] and A. Ellmann[2]
[1]Institute of Nuclear Medicine and Molecular Biology, University of Gezira, Wad Medani, Sudan, and [2]Dept Nuclear Medicine, Tygerberg Hospital and Stellenbosch University, South Africa
*Corresponding author

Introduction: The two main disadvantages of ^{99m}Tc labelled hexamethylpropyleneamine oxime (HMPAO) are its instability after labelling with ^{99m}Tc, and the high cost of the kit. The latter problem is solved in many institutions by fractionating and freezing the kit. It has been reported that the addition of methylene blue enhanced the stability of the lipophilic ^{99m}Tc-HMPAO complex for up to 3 h after reconstitution, using an intact kit (not fractionated). No description of stabilization of a fractionated kit could be found.

Aim: This study evaluated the stabilization of fractionated HMPAO kits, with special attention to the concentration of methylene blue required.

Materials and methods: HMPAO kits were fractionated by addition of 6 ml nitrogen-purged saline solution and subdivision into 0.5 ml aliquots. The fractions were stored at −20°C. A 10 mg·ml^{-1} stock solution of methylene blue in water for injection was prepared. Just before use, 0.5 ml of methylene blue solution was added to 4.5 ml of 0.003 M phosphate buffered saline. Fractionated kits were reconstituted with 400–2100 MBq freshly eluted [^{99m}Tc]-pertechnetate. Methylene blue/buffer solution at varying concentrations was added within 5 min. The three-strip paper and thin-layer chromatography method recommended by Nycomed-Amersham was used to evaluate labelling efficiency. Chromatography was done at 10 min after labelling and repeated at intervals for up to 6 h.

Results: The labelling efficiency was found to be more than 80% (84.2%±1.9%) up to 4 h after labelling when 0.7 ml of buffered methylene blue solution was added to fractionated kits labelled in a volume of 2.5 ml (final MB concentration 0.22 mg·ml^{-1}, total volume 3.2 ml). At a final methylene blue concentration of 0.17 mg·ml^{-1}, the labelling efficiency remained above 80% at 4 h with activities up to 1300 MBq ^{99m}Tc, but deteriorated to 78.2% at 4 h when 2100 MBq ^{99m}Tc was added to the kit. The labelling efficiency of fractionated kits without stabilization deteriorated to below 80% within 1 h (73.5%±5.8%).

Conclusion: It is possible to stabilize fractionated HMPAO kits using a concentration of 0.22 mg·ml^{-1} methylene blue in a final kit volume of 3.2 ml. This could provide an affordable radiopharmaceutical for ictal SPECT imaging.

Biodistribution and Pharmacokinetics of Variously Molecular Sized ^{117m}Sn(II)-Polyethyleneiminomethyl Phosphonate Complexes in the Normal Primate Model as Potential Selective Therapeutic Bone Agents

Jan R. Zeevaart[a], Werner K. A. Louw[a], Zvonimir I. Kolar[b], Elmaré Killian[c], Frederika E. Jansen van Rensburg[c], and Irene C. Dormehl[c]

Radiochemistry, South African Nuclear Energy Corporation (NECSA)[a], Pretoria (South Africa), Department of Radiochemistry, Interfaculty Reactor Institute, Delft University of Technology [b], Delft (The Netherlands), AEC Institute for Life Sciences, University of Pretoria[c], Pretoria (South Africa)

Summary

In the search for a cure for metastatic bone cancer, ^{117m}Sn with its conversion electrons and low energy photons both of discrete energies shows little bone marrow toxicity, providing the opportunity to increase the administered dose. Selective accumulation in lesions would capitalise on this advantage. The 10-30 kDa fraction of the water-soluble polymer polyethyleneimine, functionalised with methyl phosphonate groups (PEI-MP) and labelled with ^{99m}Tc, has shown selective uptake into bone tumours. Furthermore using speciation calculations it was predicted that the Sn(II)-PEI-MP complex would remain intact in the blood plasma. Because of this positive indication animal experiments were carried out to test this prediction. This paper relates the labelling, biodistribution and pharmacokinetics of various fractions of ^{117m}Sn-(II) PEI-MP in the normal primate model, and points to promising therapeutic possibilities.

Key words

- Bone therapeutics
- Polyethyleneiminomethyl phosphonate, ^{117m}Sn (II) labelled
- Polymer, enhanced permeability and retention effect

Arzneim.-Forsch./Drug Res. 54, No. 6, 340–347 (2004)

Zusammenfassung

Verteilung und Pharmakokinetik von ^{117m}Sn(II)-Polyethyleniminomethyl-Phosphonat-Komplexen unterschiedlicher Molekulargröße im normalen Primatenmodell als potentielle selektive Knochentherapeutika

Bei der Suche nach einer kurativen Behandlung gegen metastasierenden Knochenkrebs zeigte Sn-117m mit seinen Konversionselektronen geringe Knochenmarktoxizität. Dies ermöglicht eine Erhöhung der verabreichten Dosis, was zu

einer gewünschten Kumulierung am Ort der Läsionen führt. Die 10–30 kDa-Fraktion des wasserlöslichen Polymers Polyethylenimin, das Methylphosphonat-Gruppen enthält (PEI-MP) und mit Tc-99m markiert wurde, zeigte selektive Aufnahme in die Knochentumoren. Anhand spezieller Berechnungen wurde die Voraussage getroffen, daß der Sn(II)-PEI-MP-Komplex im Blutplasma intakt bleibt. Zur Überprüfung dieser Voraussage wurden entsprechende Tierversuche durchgeführt.

In der vorliegenden Arbeit wird über die Markierung, Verteilung und Pharmakokinetik verschiedener Fraktionen der Sn-117m-PEI-MPs im normalen Primatenmodell berichtet, wobei vielversprechende Ergebnisse im Hinblick auf eine therapeutische Verwendung erzielt werden konnten.

1. Introduction

In principle, internal radionuclide therapy (IRT) works by the delivery of large radiation doses to the targeted diseased tissues while sparing normal tissues. Ideally 100 % target localization of the radiopharmaceutical is the aim, but in practice this has hardly been attained, and is a major disadvantage of clinically established IRT agents. This lack of selectivity causes systemic radiotoxicity to radiosensitive tissues/organs, which limits the applied doses with resulting low palliative or curative rates [1, 2].

In recent years there has been an increasing awareness that the lack of selectivity of low molecular weight antitumour drugs could be related to their pharmacokinetic properties, i.e. their short half-life in the bloodstream and their rapid diffusion throughout the body resulting in an essentially even tissue accessibility [3].

Therefore, one approach to alter the pharmacokinetic behaviour and to overcome the radiotoxicity of IRT agents to normal tissues is to attach the appropriate therapeutic radionuclide to a water-soluble macromolecule, such as the polymers presently under investigation. These form chemically stable in vivo vehicles for systemic drug delivery due to the enhanced permeability and retention (ERP) effect whereby neoplastic tissue selectively accumulates macromolecules [3, 4, 5].

This strategy can also be applied by labelling the macromolecular bone tumour seeker

PEI-MP = $(CH_2CH_2N(CH_2CH_2NH)_x(CH_2CH_2N)_y(CH_2CH_2NH)_z)_n$

with an appropriate therapeutic radionuclide. The chemical properties of this labelled compound should be such that an in vivo stability can be assured while the species that predominantly forms in vivo is charged, as neutral species could form colloids with subsequent liver uptake [6, 7].

In previous studies, the macromolecular 10–30 kDa PEI-MP (polyethyleneimine functionalised with methyl phosphonate groups) labelled with ^{99m}Tc (a diagnostic radionuclide) showed promising biodistribution and pharmacokinetic properties (viz. localisation in bony tissue, and fast renal clearance) for normal primates and dogs [8], as well as good tumour localization in dogs with naturally occurring osteosarcoma [9]. Metal-ion speciation studies, however, predicted that the polymer would not deliver the therapeutic radionuclides ^{153}Sm, ^{166}Ho, ^{212}Pb, ^{203}Pb and ^{89}Sr to bone. These studies were also clinically verified for ^{153}Sm [7]. Additional speciation studies with Sn(II) predicted that it will remain bound to PEI-MP in blood plasma and therefore will exhibit only slight reticuloendothelial uptake [10]. Blood plasma modelling can also be used to predict the speciation of complexes at elevated levels of Ca(II) which characterises sites of metastasis where high bone turnover occurs [11]. PEI-MP is furthermore easy to complex with Sn(II) that contains ^{117m}Sn (half-life = 13.60 days), a low energy electrons and photons emitting radionuclide with proven therapeutic properties [12, 13].

The biodistribution and pharmacokinetics of variously molecular sized [^{117m}Sn(II)] Sn(II)-PEI-MP (to be abbreviated as ^{117m}Sn-PEI-MP) complexes (up to 30 kDa) were studied in this exploratory investigation using scintigraphy as well as blood and urine sampling for radioactivity determination in the normal chacma baboon (Papio ursinus) in order to assess their possible usefulness as optimal therapeutic agents. The choice of Sn(II) instead of Sn(IV) is debated elsewhere [10] and therefore great care was taken with these experiments to ensure that a Sn(II) complex is injected.

2. Materials and methods

2.1. Polyethyleneiminomethyl phosphonic acid (PEI-MP)

PEI-MP was prepared, fractionated (based on molecular size and not molar mass) and characterised as described previously [8].

2.2. Preparation of ^{117m}Sn (II) PEI-MP and the determination of its radiochemical purity

^{117m}Sn(II)-PEI-MP was prepared according to a similar procedure as described previously [10].

The radionuclide ^{117m}Sn was produced by fast neutron irradiation of tin metal – enriched in ^{117}Sn to 92% – according to the nuclear reaction ^{117}Sn (n,n') ^{117m}Sn. The irradiation of 8.6 mg targets were performed in the High Flux research nuclear reactor at Petten (The Netherlands) at a neutron flux of about 10^{14} cm^{-2} s^{-1} and took 21 days followed by a decay period of 4 days and subsequent shipping to South Africa. The specific activity achieved on the day of preparation (7 days after end of irradiation) was 2 mCi ^{117m}Sn/mg Sn. Using the necessary shielding, the irradiated metal was dissolved in 1 ml of concentrated HCl solution at 60 °C under Ar over a period of 1 h and was diluted with 2 ml water. In a separate vial 100 mg (211

μmol, as expressed for the monomer which has a molar mass of 473.2 g/mol) of PEI-MP (typically the 10–30 kDa fraction) was dissolved in 1.2 ml water and 0.2 ml 10 mol dm^{-3} NaOH using a small magnetic stirrer bar. To this an aliquot of the ^{117m}Sn-labelled $SnCl_2$ solution (strongly acidic) containing 2.6 mg (22 μmol) Sn was added. After addition the pH is gradually adjusted to pH = 6 with a 1 mol dm^{-3} NaOH solution while being heated and stirred [10].

The radiochemical purity was checked chromatographically. Five μl of this solution was spotted on ITLC-SG (silica gel impregnated glass fibre sheets, Gelman Sciences Inc., Ann Arbor, MI, USA) and cellulose (TLC aluminium sheets, cellulose 0.1 mm, E. Merck, Darmstadt, Germany) chromatograms and developed in ethanol and 1 mol dm^{-3} citrate (pH = 7.0), respectively. After scanning the chromatograms with a radiation sensitive scanner, the first showed that ≥ 98 % of the activity remained at the origin, indicating that less than 2 % unbound Sn(II) was present. The chromatograms developed in 1 mol dm^{-3} citrate showed ≥ 99 % of the activity on the solvent front, indicating less than 1 % colloidal species remaining at the origin. The chromatograms were repeated daily and after one week the respective percentages were the same. This indicated that the complex is stable and almost no colloids are formed.

For verification purposes the radiochemical purity was also checked at pH = 7.4 and found to be 99.2 % and 97 %, respectively, but the formulation at pH = 6 was preferred as it would help to prevent oxidation of Sn(II). All the above solutions were prepared with de-aerated water and kept under Ar. For the ITLC-SG chromatograms ethanol proved to be a more effective developer than acetone because $SnCl_2$ is more soluble in ethanol and moves to the front.

In both cases a negative control was also performed. Free Sn(II) (in the form of $SnCl_2$ in HCl) was spotted on ITLC-SG and developed with ethanol. The result was that > 85 % of the activity moved with the solvent front. Sn(II)-colloids were made by adjusting the solution above to pH 9. After spotting on cellulose and development in citrate > 98 % of activity was found in the lower part of the chromatogram (R_f 0–0.5). These negative controls confirmed that the selected chromatographic material and mobile phase are able to determine colloids as well as free Sn(II).

2.3. Biodistribution and pharmacokinetics of ^{117m}Sn-PEI-MP

Five normal male baboons, average weight 27.5 kg, were used in the study and received i.v. ^{117m}Sn-PEI-MP of various molecular sizes. All studies were performed after approval by the Ethics Committee of the University of Pretoria, according to the guidelines of the National Code for Animal Use in Research, Education, Diagnosis and Testing of Drugs and Related Substances in South Africa.

The baboons were subjected to identical experimental procedures except for the mentioned differences in molecular sizes of the injected ^{117m}Sn-PEI-MP. Three different size fractions were studied, viz. in the following ranges (1) 3–8 kDa (number of experiments n = 1), (2) 8–10 kDa (n = 1), (3) 10–30 kDa (n = 3). This last fraction was of special interest, since it ideally suited the characteristics sought for an optimal therapeutic agent as gathered from data on ^{99m}Tc-PEI-MP in primate models [8].

Induction of anaesthesia was performed with ketamine hydrochloride (10 mg/kg i.m.; Ketalar, Parke Davis, Cape Town, S.A.), and immediately followed by a maintained controlled infusion of a 6 % sodium pentobarbital solution (Sagatal, Kyron Laboratories Pty. Ltd., Benrose, S.A.) at 30 ml/h. The animal in the supine position under the gamma camera was injected i.v. with a ± 4 ml bolus containing 111–148 MBq of ^{117m}Sn-PEI-MP (± 2.3 mg Sn and ± 90 mg PEI-MP formulated at pH 6 to prevent premature oxidation of Sn(II)) and data acquisition started on a count down with a Siemens Orbiter large view gamma camera equipped with a collimator, low energy, high resolution (Siemens, Erlangen, Germany) in 64 × 64 word mode performing a 60 min dynamic study (60 × 1 min frames). At 1, 2 and 3 h, and in some cases at 24 h static images of 120 s were acquired.

Blood and urine samples were collected at fixed intervals for 3 h, viz. every 3 min for the first h, then hourly for blood samples, and for the urine every 5 min for the first h, subsequently hourly. The activity and volume of each sample, and cumulative urine volumes were recorded.

Regions of interest (ROIs) were placed on the images of cardiac blood pool, liver, lung, spleen, kidneys, and bone (cortical and trabecular) to obtain time-activity curves for these compartments from the dynamic study. Similarly, data of count-rate per pixel for the ROIs, which were decay-corrected, were obtained from the static images. These were normalised, according to acquisition protocol, to extend the time-activity curves of the dynamic study to 3 h from which $t_{1/2}$, the halftime of clearance, could be calculated.

Blood clearance and cumulative urine curves were also obtained in all cases so that relative organ distributions of the retained activity and eventually of the injected dose (i.d.) could be obtained for all ^{117m}Sn labelled molecular size fractions. These could be compared for optimal distribution characteristics for therapy according to the mentioned criteria.

2.4. Blood plasma modelling

The ECCLES (Evaluation of Constituent Concentrations for Large Equilibrium Studies) program was used for speciation calculations in this paper. The ECCLES database was previously updated to include all formation constants for Sn(II) [10]. To simulate areas of higher or lower calcification the free Ca(II) concentration in blood plasma model was manipulated as to achieve 0.1, 10 and 100 fold Ca(II) levels.

3. Results

None of the animals showed any adverse effects from the labelled fractions at any time during the study and thereafter.

Scintigraphic images of individual representative animals after injection of the various ^{117m}Sn-PEI-MP fractions are shown. Fig. 1 presents the thorax images at 1, 2, 3 and 24 h after injection of the 10–30 kDa fraction. Liver uptake is visible as well as high blood pool activity while only low bone uptake is present even at 24 h. This is confirmed from the mean time activity curves (T-A-C) (Fig. 2) up to 3 h after injection. Fig. 3 presents the mean (n = 3) blood clearance curve for the same set of animals and confirms continuing high blood pool activity even from 1 h onwards. However, after 24 h most of the activity is cleared as can be seen in the scintigraphic image, extreme right in Fig. 1. Accumulative urinary excretion of activity is shown as percentage of injected dose (i.d.) in Fig. 4.

Arzneim.-Forsch./Drug Res. 54, No. 6, 340–347 (2004)

Fig. 1: Scintigraphic images of the thorax at 1, 2, 3 and 24 h (from left to right) p.i. of ^{117m}Sn-PEI-MP, fraction 10–30 kDa.

Fig. 5 presents scintigraphic images (head, thorax and abdominal/pelvic area) of the baboon injected with the 3–8 kDa fraction of ^{117m}Sn-PEI-MP, 3 h after administration. Note the reduced liver uptake while the blood clearance of ^{117m}Sn-PEI-MP for this fraction is much faster (Fig. 7). However, most significant is the high cortical bone uptake (Fig. 6). The accumulative urine curve indicates continuing excretion of the activity (Fig. 8). Little retention of activity in the bladder is visible after 3 h (Fig. 5). The results are summarized in Table 1 which represents the mean $t_{1/2}$ of clearance and mean maximum percentage retained body activity between 2 and 3 h p.i. of the 10–30 kDa fractions of ^{117m}Sn-PEI-MP as well as individual corresponding values for the other fractions. For comparison, ^{99m}Tc-PEI-MP fractions taken from a previous study [8] are included together with cumulative urinary excretion as percentage i.d. and $t_{1/2}$ of blood clearance from blood sampling. Results from blood plasma modelling are presented in Table 2 and 3.

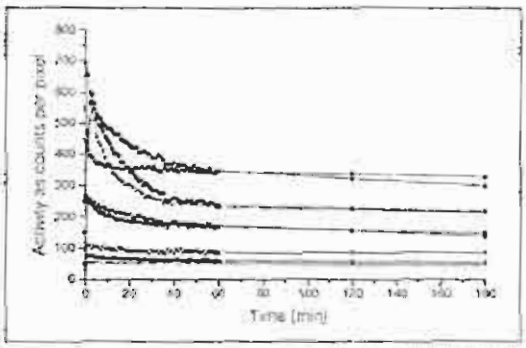

Fig. 2: Mean time activity curves (n=3), fraction 10–30 kDa, for cardiac blood pool (■), lung (●), liver (▲), spleen (▼), left kidney (◆), right kidney (✦), shoulder (✖), arm (✲) and background (bottom curve) vs. time in min.

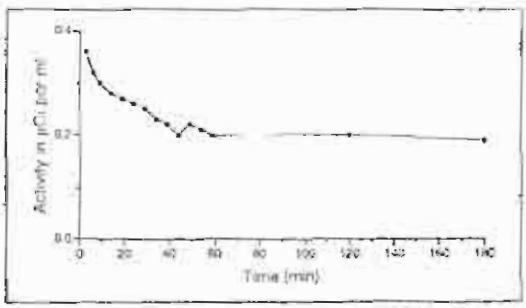

Fig. 3: Mean blood clearance curve (n = 3), normalised to injected dose, for the 10–30 kDa fraction vs. time in min.

4. Discussion

Due to limited and costly availability of ^{117m}Sn and because the blood plasma model indicated that positive results were to be expected with ^{117m}Sn-PEI-MP [10], only a small number of animal tests were needed to confirm the predictions. As a follow up on previous ^{99m}Tc-PEI-MP studies [8] it was decided to carry out a limited number of tests on non-human primates, viz. baboons, that are best suited for this explorative study as they answer many of the criteria of parallelism to the human. Because the ^{99m}Tc-PEI-MP, 10–30 kDa fraction gave the best biodistribution and kinetics with small

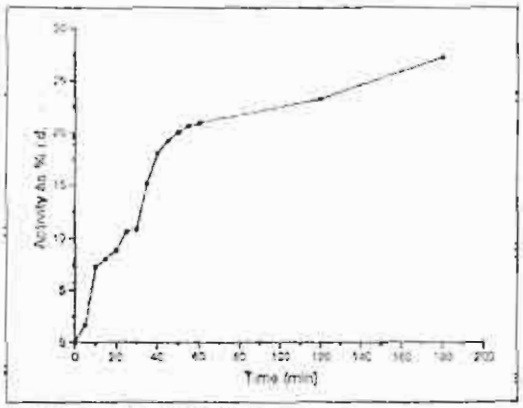

Fig. 4: Mean cumulative urinary excretion curve (n = 3) for fraction 10–30 kDa as a percentage of i.d. (injected dose).

Fig. 5: Scintigraphic images of the head, thorax and pelvic area (from left to right), 3 h p.i. of ^{117m}Sn-PEI-MP, fraction 3–8 kDa.

inter-animal variations per fraction [8], three animals were chosen for investigation with the ^{117m}Sn-PEI-MP 10–30 kDa fraction, while only one animal/fraction was investigated with the 3–8 and 8–10 kDa fractions. These single-animal experiments gave some useful information, but naturally presented statistics shortcomings. The lack of a visible spleen compartment in the 3–8 kDa fraction animal was due to gastric bloat. This fraction yielded a fast clearance from all compartments ($t_{1/2}$),

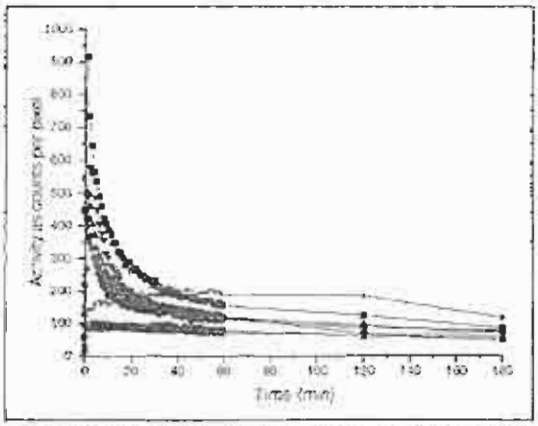

Fig. 6: Individual time activity curves, fraction 3–8 kDa, for cardiac blood pool (■), lung (●), liver (▲), left kidney (▼), right kidney (◆), shoulder (+), arm (✖), background (*) vs. time in min.

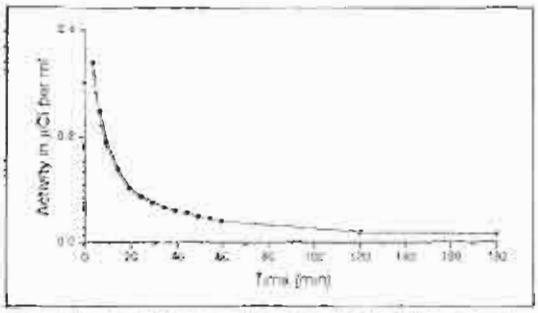

Fig. 7: Individual blood clearance curve for the 3–8 kDa fraction.

except from bone, where it accumulates, as is known of a phosphonate [14]. (Table 1)

In comparison with the ^{99m}Tc-PEI-MP (3–10 kDa fraction), the significant differences for the 3–8 kDa fraction reside in the kidney ($t_{1/2}$ and max % uptake) and bone (max % uptake). The contribution of some larger molecules in the 3–10 kDa vs. the 3–8 kDa fraction could be a reason for lower accessibility to normal bone in the former case. An estimation of 11 % uptake for the non-visualised spleen in the animal injected with the 3–8 kDa fraction of ^{117m}Sn PEI MP was made after comparing the 3–10 kDa ^{99m}Tc-PEI-MP complex.

The ^{117m}Sn-PEI-MP complex with smallest molar size behaves as if the ligand is a monomer phosphonate ligand, e.g. as ^{153}Sm-EDTMP [14] however with considerably lower bone uptake for ^{117m}Sn-PEI-MP. The complex remains intact in the blood plasma long enough for the ^{117m}Sn to reach the target, the bone (in Table 1 the cortical bone), because it is small enough to escape from the circulation and small enough to avoid trapping by the liver.

The baboon which received the 8–10 kDa ^{117m}Sn-PEI-MP fraction had only one functioning kidney, which could have influenced the clearance rates from

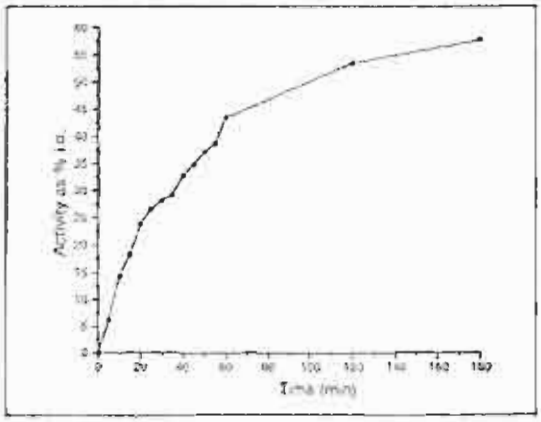

Fig. 8: Individual cumulative urinary excretion curve for fraction 3–8 kDa as a percentage of i.d. (injected dose).

Arzneim.-Forsch./Drug Res. 54, No. 6, 340–347 (2004)

Table 1: Mean $t_{1/2}$ in min and mean maximum % uptake between 2 and 3 h p.i. of ^{117m}Sn-PEI-MP fraction 10–30 kDa, and ^{99m}Tc-PEI-MP fractions in various body compartments of the primate with corresponding individual values for fractions 3–8 and 8–10. Cumulative urinary excretion is presented as % i.d. (% of injected dose) and $t_{1/2}$ of blood clearance in min.

Fraction kDa and ^{117m}Sn	Maximum % uptake and $t_{1/2}$ (min)						Urine (%)	Blood $t_{1/2}$ (min)
	Cardiac blood pool	Liver	Kidney	Lung	Spleen	Cortical bone		
3–8 (n = 1)	17 (8 min)	13 (10 min)	13 (12 min)	13 (12 min)	11 (estimation)	22 (> 4 h)	55	12
8–10 (n = 1)	22 (22 min)	24 (> 4 h)	13 (10 min)	16 (> 4 h)	10 (> 4 h)	5 (> 4 h)	25	20
10–30 (n = 3)	24 ± 2.7 (44 ± 12 min)	23 ± 1 (>4 h)	15 ± 1.1 (30 ± 6 min)	11 ± 1.4 (> 120 min)	10 ± 1.3 (> 4 h)	5 ± 1.3 (> 4 h)	40	5
^{99m}Tc								
3–10 (n = 4)	15 ± 4 (10 ± 1 min)	16 ± 1 (98 ± 22 min)	30 ± 4 (> 4 h)	8 ± 2 (10 ± 1.5 min)	10 ± 1 (75 ± 2 min)	8 ± 1 (> 4 h)	49.0	5
10–30 (n = 4)	15 ± 3 (10 ± 1.5 min)	20 ± 2 (22 ± 3 min)	18 ± 4 (20 ± 3 min)	13 ± 4 (15 ± 3 min)	13 ± 1 (60 ± 9 min)	18 ± 1 (> 4 h)	52.5	6

Background compartment not included in table.

most compartments and explain the low (25 %) excretion in the urine. The drastic reduction in bone uptake from the 8–10 kDa fraction and upwards may be because the critical molecular weight above which diffusion becomes restricted in continuous endothelium is about 5 kDa [15].

Statistically, the results of the 10–30 kDa ^{117m}Sn-PEI-MP fraction (n = 3) can be regarded as the most useful. The small inter-animal deviations throughout, which were also observed previously with 10–30 kDa ^{99m}Tc-PEI-MP [8], point to the consistency of the in vivo behaviour of this fraction. In comparison to the ^{117m}Sn-PEI-MP 3–8 and 8–10 kDa fractions, the larger 10–30 kDa ^{117m}Sn-PEI-MP exhibits a prolonged retention in all compartments, together with low bone uptake and a reduction in urine excretion, as can be expected from its larger hydrodynamic volume and its resultant slower diffusion through the endothelium as well as a decrease in renal excretion rate.

The fact that the ^{117m}Sn bound to the 10–30 kDa fraction remains in the blood plasma in healthy animals (see Table 1 and Fig. 4) can be explained by two possibilities, one that the ^{117m}Sn-PEI-MP, as complex remains bound in blood plasma but this particular size of the polymer complex is too big to escape from intact vasculature while a significant portion is trapped by the liver. In this case the complex between the polymer, a phosphonate and therefore a bone-seeker, and the ^{117m}Sn(II) remains in the blood pool and can only escape from circulation to accumulate in the bone, if the vasculature is damaged. A low bone-uptake follows as well as completed renal excretion after 24 h. This is confirmed in Fig. 1 and 2.

The alternative is that the ^{117m}Sn dissociates from the complex and attaches to other blood plasma ligands like histidinate or remains as $^{117m}Sn(OH)_2$. Therefore the biodistribution observed could not be that of the ^{117m}Sn-PEI-MP complex but of some other species also taken up by the liver and excreted slowly. In such a process some of the ^{117m}Sn would inevitably have been trapped in the red blood cells as it is known that $Sn_3(PO_4)_2$ (which is always part of the red-blood-cell kit administered before ^{99m}Tc [16] itself) is trapped inside the red blood cells where it reduces the Tc(VII). It was, however found in this study that, even after 3 h p.i. > 99 % of the activity was in the serum. It therefore seemed unlikely that the ^{117m}Sn-PEI-MP complex had dissociated.

Table 2: Species distribution (in percentage) of PEI-MP in normal blood plasma at normal, elevated and reduced Ca(II) levels.

	Normal Ca(II) levels	Ca(II) × 10	Ca(II) × 100	Ca(II) × 0.1
Ca_2LH	68	84	85	3
Ca_2L	12	15	15	0.5
Mg_2LH	10			57
Sn_2LOH	3	1		3
Mg_2L	2.5			14
LH_2	2			10
LH	1			7
Sn_2LOH_2	1	0.3		1

L = PEI-MP

Table 3: Species distribution (in percentage) of Sn(II) in normal blood plasma incorporating the ligand PEI-MP at normal, elevated and reduced Ca(II) levels, respectively.

	Normal Ca(II) levels	Ca(II) × 10	Ca(II) × 100	Ca(II) × 0.1
M_2(PEI-MP)(OH)	57	16	0.4	61
M_2(PEI-MP)$(OH)_2$	26	7	0.2	29
M(His)OH	7	31	29	3
$M(OH)_2$	5	23	43	2
M(Cys)	3	15	21	1.5
M(His)	0.5	2	2	0.3
M(PEI-MP)	0.5			0.5

M = Sn (II), His = histidinate and Cys = cysteinate.

area. Ultimate prove of the preferential location of the complex in the tumour should follow from studies on osteosarcoma bearing animal models.

5. Conclusion

It is easy to synthesize PEI-MP, purify and fractionate it into variously sized fractions which can readily be labelled with ^{117m}Sn to obtain a labelled product of high radiochemical purity and in vitro stability. This in vivo study confirmed the demand for reduced uptake of ^{117m}Sn-PEI-MP by normal bone and kidneys, especially noted for fractions > 8kDa. Furthermore the theoretical and now proven indications of in vivo stability of Sn(II)-PEI-MP as well as the potential to exploit the EPR effect due to its macromolecular nature, suggest that ^{117m}Sn-PEI-MP can fundamentally be a promising therapeutic radiopharmaceutical for the treatment of malignant bone diseases, pending proper dosimetry. The anomalies between the pharmacokinetis and biodistribution of 10–30 kDa ^{117m}Sn-PEI-MP and ^{99m}Tc-PEI-MP indicate that it cannot simply be assumed that the in vivo behaviour a polymeric ligand complexed with different metal ions will be identical and therefore cautions that appropriate pre-clinical in vivo experimental work is a prerequisite while in vitro studies including blood plasma modelling can assist in reducing the number of animal tests needed.

6. Literature

[1] Volkert, W. A., Hoffman, T. J., Therapeutic radiopharmaceuticals. Chem. Rev. **99**, 2269 (1999)

[2] Ercan, M. T., Caglar, M., Therapeutic radiopharmaceuticals. Curr. Pharm. Design **6**, 1085 (2000)

[3] Kratz, F., Schütte, M. T., Anticancer metal complexes and tumour targeting strategies. Cancer J. **11**, 60 (1998)

[4] Maeda, H., Wu, J., Sawa, T. et al., Tumor vascular permeability and the EPR effect in macromolecular therapeutics: a review. J. Controlled Release **65**, 271 (2000)

[5] Seymour, L. W., Passive tumor targeting of soluble macromolecules and drug conjugates. Crit. Rev. Ther. Drug Carrier Systems **9**, 135 (1992)

[6] Zeevaart, J. R., Jarvis, N. V., Louw, W. K. A. et al., Metal-ion speciation in blood plasma incorporating the tetraphosphonate, N,N-dimethylenephosphonate-1-hydroxy-4-aminopropylidenediphosphonate (APDDMP), in therapeutic radiopharmaceuticals. J. Inorg. Biochem. **83**, 57 (2001)

[7] Jarvis, N. V., Zeevaart, J. R., Wagener, J. M. et al., Metal-ion speciation in blood plasma incorporating the water-soluble polymer, polyethyleneimine functionalised with methylenephosphonate groups, in therapeutic radiopharmaceuticals. Radiochim. Acta **90**, 237 (2002)

[8] Dormehl, I. C., Louw, W. K. A., Milner, R. J. et al., Biodistribution and Pharmacokinetics of variously sized molecular radiolabelled polyethyleneiminomethyl phosphonic acid as a selective bone seeker for therapy in the normal primate model. Arzneim.-Forsch./Drug Res. **51 (I)**, 258 (2001)

[9] Dormehl, I. C., Schneerwiese, E. H. A., Louw, W. K. A. et al., Optimalisation of radiolabelled polymin-MP of different molecular sizes as a selective bone seeker for therapy in animal models. Proceedings of the Medical Radiation Physics and Engineering Conference (MeRPE 2000), Lisbon, Portugal, Nov. 2000

[10] Zeevaart, J. R., Louw, W. K. A., Kolar, Z. I. et al., A thermodynamic approach (using speciation studies) towards the evaluation and design of bone-seeking radiopharmaceuticals as illustrated for ^{117m}Sn(II)-PEI-MP. J. Radioanal. Nucl. Chem. **257**, 83 (2003)

[11] Jarvis, N. V., Wagener, J. M., Jackson, G. E., Metal-ion speciation in blood plasma as a tool for elucidating the in vivo behaviour of radiopharmaceuticals containing ^{153}Sm and ^{166}Ho. J. Chem. Soc. Dalton Trans. 1411 (1993)

[12] Atkins, H. L., Mausner, L. F., Srivastava, S. C. et al., Tin-117m(4+)-DTPA for palliation of pain from osseous metastases: a pilot study. J. Nucl. Med. **36**, 725 (1995)

[13] Bouchet, L. G., Bolch, W. E., Goddu, S. M. et al., Considerations in the selection of radiopharmaceuticals for palliation of bone pain from metastatic osseous lesions. J. Nucl. Med. **41**, 682 (2000)

[14] Louw, W. K. A., Dormehl, I. C., van Rensburg, A. J. et al., Evaluation of Sm-153 and Ho-166-EDTMP in the normal baboon model. Nucl. Med. Biol. **23**, 935 (1996)

[15] Peters, A. M., Jamar, F., The importance of endothelium and interstitial fluid in nuclear medicine. Eur. J. Nucl. Med. **25**, 801 (1998)

[16] Saha, G.B., Fundamentals of nuclear pharmacy, pp. 118-119, Springer Verlag, New York (1997)

[17] Claessens, R. A. M. J., Kolar, Z. I., Affinity of tin(II) and tin(III) diphosphonates for hydroxyapatite: an experimental and model study. Langmuir **16**, 1360 (2000)

[18] Zeevaart, J. R., Metal-ion speciation in blood plasma as a tool in predicting the in vivo behaviour of potential bone-seeking radiopharmaceuticals. PhD thesis, pp. 153–156, Delft University Press, Delft (2001)

[19] Schwartz, Z., Shani, J., Soskolne, W.A. et al., Uptake and biodistribution of technetium-99m-MDP during rat tibial bone repair. J. Nucl. Med. **34**, 104 (1993)

Acknowledgements

This work was supported in part by a grant from the Volkswagen Stiftung, Hannover (Germany). The authors thank the South African Nuclear Energy Corporation for permission to publish this work and Prof. J. J. M. de Goeij (IRI, Delft, The Netherlands) for helpful discussions.

Correspondence:
Dr. Jan Rijn Zeevaart,
South African Nuclear Energy
Corporation (NECSA),
P. O. Box 582, Pretoria, 0001
(South Africa)
E-mail: zeevaart@necsa.co.za

3.6

Imaging of nAchReceptors with the PET-Receptorligand 2-^{18}F-A85380: Automated Synthesis, In-Vitro and In-Vivo Evaluation in Alzheimer's Disease

J. Schmaljohann[1,2], M. Minnerop[1], S. Gabilke[2], D. Grünbach[3], F. Jessen[4], M. Reichardt[3], U. Wüllner[1]
[1]Dept. of Neurology, [2]Dept. of Nuclear Medicine, [3]Depart. of Pharmaceutical Chemistry, [4]Depart. of Psychiatry, University of Bonn, Germany

Aim: PET is an important tool for the in-vivo investigation of the functional status of the different receptors in brain, especially valuable for the early diagnosis of neurodegenerative disorders. Labelling nicotinic Acetylcholin-Receptors (nAchR) with 2-^{18}F-A85380, a ligand with high affinity to nAchR's subtyp α4b2, enables the visualization of the nAchR in vivo. In our work, we investigated the potential of this PET-tracer for its clinical use by automating the synthesis of the 2-^{18}F-A85380 and the in vitro and in vivo evaluation for Alzheimer's disease (AD) in human.
Methods: The synthesis of 2-^{18}F-A85380 with 2-^{18}NMe$_3$ (N-BOC)-A-85380 as precursor was established in an automatic synthesis module for in vivo PET investigations. In-vitro experiments with sections of occipital cortex, entorhinal cortex and thalamus of patients with AD and healthy controls were incubated with 2-^{18}F-A85380, followed by measuring the distribution of the tracer by means of phosphor imaging. The sections were stained with HE to determine the ROI's in the brain regions. Initial PET-investigations of patients with AD and healthy control will be presented.
Results: Up to 10 GBq 2-^{18}F-A85380 could be reproducible produced in the automatic synthesis module with an uncorrected yield of 30 % (80 min from EOB up to final product formulation). The specific activity of the final product was >300 GBq / µmol and the radiochemical purity of >96 % was sufficient for human use. Incubation of brain sections with 2-^{18}F-A85380 showed a 2.5 times higher uptake in the thalamus than in cortical regions. In brain sections of the AD group thalamus and occipital cortex showed a reduced tracer uptake of app. 36 % of binding of control brain. In our first human PET studies this decrease in uptake was observed likewise. Additionally, in comparison to healthy control lower 2-^{18}F-A85380 concentrations were measured in putamen and caudate of AD patients.
Conclusions: The automated synthesis of 2-^{18}F-A85380 allows safe production and sufficient yield for clinical application. In vitro human binding data with 2-^{18}F-A85380 show the labeling of human nAchR's with distinctly reduced binding in thalamus and occipital cortex of Alzheimer's disease brain sections. First results of human PET studies identify 2-^{18}F-A85380 as a potential diagnostic tool in Alzheimer's disease.

3.7

Routine Preparation of [^{11}C]Flumazenil Using Direct HPLC Purification

Andreas Krssak[1], Wolfgang Wadsak[1,2,3], Oliver Langer[1], Susanne Asenbaum[1,4], Kurt Kletter[1], Robert Dudczak[1,3]
Departments of [1]Nuclear Medicine, [2]Inorganic Chemistry, [3]Clinical Pharmacology and [4]Neurology, University of Vienna, Austria; [5]Ludwig-Boltzmann-Institute for Nuclear Medicine, Vienna, Austria

Aim: During the last years, the relevance of [^{11}C]flumazenil ([^{11}C]FMZ) in neurological investigations such as epilepsy or Alzheimer's disease is rising. The major problem with the preparation of [^{11}C]FMZ was the separation of the product from residual solvents and precursor. Common preparations include preparative HPLC and subsequent distillation or solid phase extraction. We developed a preparative HPLC-set up using an injectable mobile phase solution circumventing the need for any further purification.
Methods: [^{11}C]FMZ is produced from [^{11}C]methyl iodide and N-desmethylflumazenil, the precursor, in presence of KF (potassium fluoride) immobilised on Al_2O_3 as a phase transfer catalyst in acetonitrile. The product solution was filtered in a collecting vial. The filter was washed with water to increase the yield and the combined solutions were transfered onto a preparative HPLC column (stationary phase: Nucleosil 100-7, RP-18, 7µm, 250 x 16mm; mobile phase: 0.01M phosphoric acid/ethanol 50/50 (v/v); 6mL/min). The retention times of product and precursor were 10-11min and 8-9min, respectively. The cutted fraction was diluted with 6mL 21mM phosphate buffered saline solution and sterile filtrated.
Results: Overall synthesis time was <30 minutes (12 minutes for the preparation of the [^{11}C]methyl iodide, 3 minutes for the conversion into [^{11}C]FMZ and <15 minutes for purification and formulation). So far, typical yields were 4GBq (not decay corrected) of the ready to inject radiopharmaceutical (starting activities: 45-55GBq). The radiochemical purity was always higher than 99% determined by analytical radio-HPLC. The amount of the precursor in the injected volume was always <5µg. pH was 6.8-7.5 and osmolality was 250-310mosmol/kg.
Conclusion: The presented synthesis of [^{11}C]FMZ using direct HPLC purification is a reliable and fast method for the routine preparation of this widely-used PET-tracer with excellent purity.

Radiopharmaceutical Sciences III; Infection

5.2

^{117m}Sn and ^{186}Re radiolabelling of Polyethyleneiminomethyl Phosphonic Acid (PEI-MP), Followed by In Vivo Targeting of Induced Osteosarcoma in Nude Mice

I. Dormehl[1], W. Louw[2], J. Zeevaart[2], Z. Ketz[3], F. Botelho[4], J. Wagener[5], S. Hübner[6], A. Abrunhosa[4], C. Gomes[4], L. Nisiello[4], F. Schweinfurth[6], J. de Lima[1]
[1]MEC Institute of Life Sciences, University of Pretoria, South Africa, [2]NECSA, Pretoria, South Africa, [3]RCI, Delft University of Technology, The Netherlands, [4]IBILI, University of Coimbra, Portugal, [5]College of Veterinary Medicine, University of Florida, USA, [6]Forschungszentrum Juelich, Germany

Aim: Water-soluble polymers are under development as vehicles for systemic drug delivery due to the effect of enhanced permeability and retention whereby neoplastic tissue selectively accumulates macromolecules. The 10-30 kDa fraction of the polymer ^{99m}Tc-PEI-MP previously presented promising biodistribution and pharmacokinetics in primates and dogs and good tumour location in natural canine osteosarcoma. The purpose of this study was therefore to evaluate the labelling of 10-30 kDa PEI-MP with ^{117m}Sn and ^{186}Re, both nuclides with proven therapeutic properties and subsequently to confirm scintigraphically the potential of ^{117m}Sn-PEI-MP as a selective therapeutic bone tumour seeker in BALB C nude mice with induced canine osteosarcoma.
Methods: ^{117m}Sn metal was dissolved in 10 M HCL at 60 °C under Ar and diluted to 3.3 M with water. PEI-MP (10-30 kDa, 100 mg) was dissolved in 1.2 ml water and 0.2 ml 10 M NaOH. An aliquot containing 2.6 mg Sn was added and the pH adjusted to 6.0. ^{186}Re metal was dissolved in 10 % H_2O_2, evaporated to dryness (80 °C), whereafter an aliquot containing 25 µg Re was added to a PEI-MP freeze-dried labelling kit: (10 mg Na-PEI-MP; 0.5 mg $SnCl_2.2H_2O$) at a pH of 1.0. After incubation at ± 90 °C (30 min) the pH was adjusted to 6.0. BALB C nude mice were subcutaneously injected with 5 M cells, cultured from spontaneous canine osteosarcoma.

and with high lung metastatic capacity (HPOS). At 4 weeks the tumour bearing mice were injected 75 µCi ^{117m}Sn-PEI-MP and scintigraphy was performed. Organ and tumour counting in a well counter followed.

Results: Both ^{117m}Sn-PEI-MP and ^{186}Re-PEI-MP gave radiochemical purities >98% with <1.0% colloids. For ^{117m}Sn-PEI-MP the respective percentages were constant for one week,while those for 186Re-PEI-MP stayed the same for 48h. Tumour to background uptake within the period of 30-210 min post injection was around 8.0-6.0. Normal bone could not be visualized,but cartilage had similar uptake as the tumour.

Conclusion: These results indicate that PEI-MP can be labelled successfully with radioisotopes that have proven therapeutic properties.The bone tumour targeting properties of ^{117m}Sn-PEI-MP were also confirmed.

5.3

A New Model for the Pre-Viva Evaluation of Bone Seekers?

Stefan Vögele[1,2], Markus Mitterhauser[1,2,4], Wolfgang Wadsak[1,2,3], Leonhard-Kay Mien[1,2], Harald Eidherr[1,2], Helmut Viernstein[2], Kurt Kletter[1], Robert Dudczak[1,3]
Departments of [1]Nuclear Medicine, [2]Pharmaceutic Technology and Biopharmaceutics, [3]Inorganic Chemistry University of Vienna, Austria; [4]Hospital Pharmacy of the General Hospital of Vienna, Austria; [5]Ludwig-Boltzmann-Institute for Nuclear Medicine, Vienna, Austria;

Introduction: Although the first radioactive-labelled bone tracers were already introduced in the early 70s, mechanisms involved in uptake and integration into the bone matrix still remain speculative. The present work aimed to establish a new method to evaluate the influence of various factors on the uptake as well as the potential as a model for future bone seeking agents.

Methods: To a vial containing 0.25-15mg hydroxyapatite (HA) or amorphous calcium phosphate (ACP) 3mL of Hanks' Balanced Salt Solution were added. The tube was sealed and swayed in a thermostatic chamber at 37°C for 24 hours. Then, 0.3µmol of radioactive-labelled diphosphonate or 40-60MBq of 18F-fluoride solution were added. Subsequently, the tube was placed in the water bath for incubation (10, 30, 60 and 120 min, 37°C) and homogenated. An aliquot of 50µL of this suspension was added to 2mL of physiological saline. From this diluted suspension 3 aliquots of 50µL were taken and placed in tubes for gamma-counting. The rest was filtered (Millex-FG®, 0.22µm), and 3 aliquots of 50µL were taken from the filtrate. Finally, the radioactivity of the 6 tubes was measured in a gamma-counter and the percentage of irreversibly bound radioactivity was calculated.

Results: The influence of incubation time, amount of matrix, preparation method, type and concentration of ligand and carrier was determined. Kinetic uptake experiments revealed a continuous increase over time for ^{99m}Tc-MDP on various amounts of matrix (3mg HA: 44.82% at 10min to 71.66% at 120min) as well as for ^{18}F-fluoride (3mg HA: 38.73% at 10min to 67.8% at 120min). After an incubation period of 120min the studies on HA yielded the following order: ^{99m}Tc-EDTMP (8.9%)<^{186}Re/Re-EDTMP <^{99m}Tc/11µlRe-EDTMP<^{99m}Tc/In-EDTMP<^{99m}Tc/15µlRe-EDTMP <n.c.a^{186}Re-EDTMP<^{111}In/ReEDTMP<^{111}In-EDTMP<^{153}In/In-EDTMP<^{99m}Tc-DPD<^{99m}Tc/80µlRe-EDTMP<^{99m}Tc-EDTMP "-boiled"<^{99m}Tc/150µlRe-EDTMP<^{153}Sm-EDTMP<^{99m}Tc/11µl Re-EDTMP "boiled"<^{18}F-fluoride<^{99m}Tc-MDP (71.6%). Reincubation experiments demonstrated that bone tracers are not adhesively bound on the crystal surfaces but incorporated.

Conclusion: The described procedure is a rapid and feasible method to examine the adsorption of radiolabelled substances on bone components. Additionally, there is evidence that - based on our findings - it may be possible to establish a pre-vivo model to predict the in-vivo behaviour of new bone seekers.

5.5

Evaluation of the In Vitro Binding of [^{18}F]Ciprofloxacin to Bacteria

O. Langer[1], M. Zeitlinger[1], M. Mitterhauser[2], M. Brunner[1], U. Müller[1], W. Wadsak[2], K. Kletter[2], C. Joukhadar[1], M. Müller[1]
Departments of [1]Clinical Pharmacology, Division of Clinical Pharmacokinetics and [2]Nuclear Medicine, Vienna University Medical School, Austria

Aim: A complex of the fluoroquinolone antibiotic ciprofloxacin with technetium-99m (Infecton®, Draximage Inc.) has previously been proposed as an infection imaging agent for single-photon emission tomography (SPET). In our laboratory ciprofloxacin has been labelled with the positron emitter fluorine-18. The aim of the present work was to investigate *in vitro* the mechanism of [^{18}F] ciprofloxacin binding to bacterial cells.

Methods: Bacterial suspensions (1 x 10^6 colony forming units per ml) in phosphate buffer (3 ml, pH 7.0) were incubated for 10 min at 37°C with [^{18}F]ciprofloxacin (50-200 kBq or approximately 50-200 ng). Bacteria were separated from the incubation medium by centrifugation and washed with ice cold phosphate buffer. Radioactivity retention was measured in a gamma counter.

Results: Binding of [^{18}F]ciprofloxacin to *Escherichia coli* ATCC 25922 amounted to 55±2 ng (n=9) retained [^{18}F]ciprofloxacin per µg/ml [^{18}F]ciprofloxacin in the incubation medium, which is an about 18-fold higher bacterial concentration than in the buffer. Bacterial binding of [^{18}F]ciprofloxacin was rapid and unaffected by variation of the incubation time from 3 to 120 min. Bacterial binding appeared to be linear and non-saturable over a concentration range of ciprofloxacin of 0.05 to 50 µg/ml. Incubation of [^{18}F]ciprofloxacin-loaded bacterial cell pellets with fresh phosphate buffer resulted in a rapid efflux of radioactivity (about 90% within 10 min) indicating reversibility of binding. Addition of the efflux pump inhibitor carbonyl cyanide-*m*-chlorophenylhydrazone (CCCP, 100 µM) to the incubation buffer caused a 21±1% (*n*=3) increase in bacterial binding compared to the control experiment without CCCP, which indicated intracellular binding of [^{18}F]ciprofloxacin. Binding of [^{18}F]ciprofloxacin to clinical isolates of *E. coli* with different *in vitro* susceptibility to ciprofloxacin (minimum inhibitory concentrations ranged from <0.025 to >16 µg/ml) appeared to be similar.

Conclusions: [^{18}F]Ciprofloxacin is rapidly taken up *in vitro* by *E. coli* bacterial strains including those that are resistant to ciprofloxacin. The employed binding assay was not able to distinguish specific binding to bacterial type II topoisomerase enzymes from non-specific bacterial binding. Additional *in vitro* and *in vivo* evaluation models are needed for assessing the usefulness of [^{18}F] ciprofloxacin for the *in vivo* imaging of bacterial infections with positron emission tomography (PET).

5.6

Detection of Infections in Nuclear Medicine Practice Using 99m-Tc Fab' Antigranulocyte Fragments (Leukoscan): Our Experience

M. Focan[1], G. Tartaglione[1], E. Rubini[2]
[1]Department of Nuclear Medicine, Cristo Re Hospital, Rome, Italy; [2]Department of Emergency, Cristo Re Hospital, Rome Italy

Aim of the study was to asses the diagnostic utility of Fab' antigranulocyte fragments -99mTc (Leukoscan) for detection of suspected orthopaedic and vascular infections by means of triphasic scintigraphy in clinical practice.

Methods: From december 2000 to august 2003 , 44 patients (22 male, 22 female) suspected of infections underwent triphasic scintigraphy. After a 7 days antibiotic therapy interruption, a dose of Leukoscan 99mTc (Byk-Gulden) 555 MBq , diluted in 2 ml of saline solution, via disposable intravenous cannula, was in-

Radiochemical yield was 85 ± 5%, and radiochemical purity was >95%.
Biodistribution studies in mice showed penetration and accumulation in the brain (2.5 % ID/g at 20 min p.i. in brain, 0.5% ID/g at 20 min p.i. in blood).
CONCLUSION: Biodistribution studies in mice showed that [123I]-(1-(5-iodo-2-methoxyphenethyl)piperidin-4-yl)(4-fluorophenyl)methanone could be a suitable agent for in vivo imaging of the 5HT2A-receptor. Regional distribution and displacement studies in rabbits are further needed to demonstrate specific binding to 5HT2A-receptors in the brain.

O7

Synthesis of the receptorligand [^{131}I]-3-iodocytisine for in-vivo imaging of the nAChRs

Aysel Oezbolat* , Lenka Munoz** , Stefan Guhlke* , Ullrich Wuellner*** , Hans-Juergen Biersack* , Daniela Guendisch** , Joern Schmaljohann ****
*Dept. of Nuclear Medicine,**Dept. of Pharmaceutical Chemistry,***Dept. of Neurology,
****Depts. of Nuclear Medicine and Neurology, Germany

AIM : In vivo labelling of the nicotinic acetylcholine receptors (nAChRs) could be a useful tool for early diagnosis an evaluating therapies of neurodegenerative disorders. Relatively few data are available on physiological functions of nAChRs and their potential role in neurological diseases. 3-Iodocytisin displays a high affinity for neuronal nAChRs and subtype selectivity for α4β2. Thus for the radiolabelled analogue a high potential can be expected for its clinical use in the diagnostic of neurodegenerative disorders.
METHODS : The n.c.a. iodination was carried out by four standard methods for electrophilic substitution (chloramine-T, iodogen, nitric acid, thallium(III)trifluoroacetate). TFA, acetic acid and phosphate buffer were used as solvents. Except for the iodogen and nitric acid the oxidation agent (in 200µl solvent) was added to 8.5µmol (-)-cytisine and iodine-131 in 300µl solvent. The reactions were stopped and an aliquot was analyzed by HPLC.
RESULTS : All investigated oxidation agents enabled the [^{131}I]iodination of (-)-cytisine preferring the highly activated position 3. The rcy were obtained using iodogen in pH 1 buffer (78%). [^{131}I]-(-)-3-Iodocytisine was built as labelling side product with minor amounts (1.7% chloramine-T, 5% iodogen). No side products were observed using nitric acid or thallium(III)trifluoroacetate with rcy of 49% and 60%, respectively. A SepPak-purification method is under investigation.
CONCLUSION : For the first time iodine-131 labelling of (-)-cytisine was succeeded selectively at position 3. Due to exclusively built product [^{131}I]-(-)-3-iodocytisine we prefer the demetallation method with thallium. Sufficient yields and the radiochemical purity of [$^{123/131}$I]-(-)-3-iodocytisine allow (1) the labelling of the majority of nAChRs in the human brain, (2) a comparison with [^{18}F]-2-F-A85380 and (3) the evaluation of nAChR ligands as a potential diagnostic tool in neurodegenerative disorders.

O8

Comparison of tumor uptake in different types of osteosarcoma mice as studied with the potential bone-seeking radiopharmaceutical, Sn(II)-^{117}m-PEI-MP

Jan Rijn Zeevaart* , Werner Louw* , Judith Wagener* , Filomena Botelho** , Celia Gomes** , Antero Abrunhosa** , Luiz Metello** , Zvonko Kolar*** , Irene Dormehl****
*Radiochemistry, Necsa, South Africa
**Biophysics Department, IBILI, Faculty of Medicine, University of Coimbra, Portugal
***Radiochemistry, Interfaculty Reactor Institute, Delft University of Technology, the Netherlands
****AEC Institute for Lifesciences, University of Pretoria, South Africa

AIM : In the search for a cure for metastatic bone cancer, Sn-117m with its conversion electrons of discrete energies shows little bone marrow toxicity, providing the opportunity to increase the administered dose. Selective accumulation in lesions would capitalise on this advantage. The 10-30 kDa fraction of the water-soluble polymer polyethyleneimine, functionalised with methylene phosphonate groups (PEI-MP) and labelled with Tc-99m, has proved a promising agent for selective uptake into bone tumours [1]. From speciation calculations using the ECCLES database it was predicted [2] that Sn(II) will stay bound to the polymer in blood plasma and therefore should deliver the therapeutic radionuclide Sn(II)-^{117}m to the bone with only a slight reticuloendothelial uptake. As this was the first blood plasma model that has been compiled for Sn(II), predictions about the behaviour of Sn(II)-^{117}m-PEI-MP in blood plasma were verified with primate tests [3]. The biodistribution studies on these healthy animals confirmed these predictions.
METHOD: To test the tumour selectiveness, tests in nude balb C mice containing canine osteosarcomas were carried out. HMPOS (fast growing but not per se metastising) and POS (slower growing but metastasing) cells were implanted and the results compared with each other.
RESULTS : Different uptake and wash-out was recorded for the different tumours. Both showed tumour uptake while POS implanted cells retained the activity longer.
CONCLUSION : Sn(II)-^{117}m-PEI-MP has potential as a selective bone metastasis agent.

O9

Production of a ^{68}Ge/^{68}Ga Generator

Behrouz Shirazi Tirani*
*Nuclear Research Center for Agriculture and Medicine, Atomic Energy Organization of Iran

AIM : Gallium-68 is a radioisotope with a half life of 68 min. As it has a specific decay mode, it is a positron emitter and hence, it is popularly used in nuclear medicine. The

Letters of Consent

Geschäftsbereich
Sicherheit und Strahlenschutz
Leiter: Dr. Ralf Hille
Forschungszentrum Jülich
in der Helmholtz-Gemeinschaft

Forschungszentrum Jülich GmbH · GS · 52425 Jülich
Fracht-/Paketanschrift: Leo-Brandt-Straße · 52428 Jülich

Professor HA Koeleman
Dean: Fac. of Health Sciences
North West University
Potchefstroom

• Ihr Ansprechpartner: Dr. F.H.A. Schneeweiss
• Bei Antwort bitte angeben:
• Telefon: 02461 61- 5573
• Telefax: 02461 61- 4110
• E-Mail: f.schneeweiss@fz-juelich.de

Jülich, 29 April 2005

Dear Prof. Koeleman,

Prof. Dormehl and myself have been involved in collaborative research since 1995. During this time I participated in research projects which she led. I thus became the co-author of a number of publications and congress presentations which followed from the research.

We discussed the possibility of submitting these research results for a PhD study. I am of the opinion that the research and the results which were previously peer reviewed and successfully published comply with the requirements for a PhD degree in view of their unique international contributions. I therefore agree that these results which followed from my collaboration may be used for Prof. Dormehl's intended PhD degree.

Yours sincerely,

(Dr. F.H.A. Schneeweiss)

Nuclear Technology – a division of Necsa

PO Box 582
Pretoria 0001
South Africa

+27 12 305 5706
+27 12 305 5944

zeevaart@necsa.co.za
www.necsa.co.za

necsa
We're in your world
NUCLEAR TECHNOLOGY

Dept. Radiochemistry

Date 6 May 2005
Ref. No.

Professor HA Koeleman,
Dean:Fac. of Health Sciences,
North West University,
Potchefstroom

Dear Prof.Koeleman,

Prof Dormehl and I have been involved in collaborative research since 1999. During this time I participated in joint research projects which her. The results were reported in the form of publications and congress presentations which we co-authored.

We discussed the possibility to submit these research results for a PhD study. I am of the opinion that the research and the results which were previously peer reviewed and successfully published comply with the requirements for a PhD degree in view of the international standard attained. I therefore agree that these results which followed from my collaboration be used for the intended PhD degree of Prof. Dormehl.

Yours sincerely,

Jan Rijn Zeevaart
PhD (Delft)
Head: Radiochemistry
NECSA

University of Pretoria
Faculty of Medicine
AEC - Institute for Life Sciences
P.O. Box 2034
Pretoria 0001

Enq. : Prof. I. Dormehl
Tel. : 012-319 2675
Fax. : 012-319 2557
E-mail : dormehl@medic.up.ac.za

Professor H.A. Koeleman
Dean: Faculty of Health Sciences
North West University
Potchefstroom

Dear Prof. Koeleman,

Prof Dormehl and myself have been involved in collaborative research since 1980. During this time I participated in research projects which she was leading. I thus became co-author to publications and congress presentations which followed from this research. I am of the opinion that the research and the results which were previously peer reviewed and successfully published comply with the requirements for a PhD degree in view of the unique international contributions. I therefore agree that these results which followed with my collaboration be used for the intended PhD degree of Prof. Dormehl.

Yours sincerely,

UNIVERSITY OF
FLORIDA

College of Veterinary Medicine
Department of Small Animal Clinical Sciences

Post Office Box 100126
Gainesville, Florida 32610-0126
(352) 392-4700, ext. 5700
Fax. (352) 392-6125
www.vetmed.ufl.edu/sacs

4/28/2005

Professor HA Koeleman,

Dean: Faculty of Health Sciences,

North West University,

Potchefstroom

Dear Prof.Koeleman,

I have known Prof Dormehl since 1996 and during my time at the University of Pretoria and Florida, I have been involved in collaborative research with her. During this time I participated in research projects which she was the principal investigator and leader of the research team. I thus became co-author to numerous publications and congress presentations which followed from the research.

We discussed the possibility of submitting these research results for a PhD study. I am of the opinion that the research and the results which were previously peer reviewed and successfully published comply with the requirements for a PhD degree in view of the unique international contributions. I therefore agree that these results which followed with my collaboration be used for the intended PhD degree of Prof. Dormehl. It is both and honor and a privilege to know her.

Yours sincerely,

Dr Rowan Milner BVSc MMed Vet (Med) Dip ECVIM

Assistant Professor

Dept. Small Animal Clinical Sciences

College of Veterinary Medicine, University of Florida

PO Box 100126 Gainesville 32610-0126,

e-mail: rmilnerr@mail.vetmed.ufl.edu